La queue de l'aire tegmentale ventrale : définition anatomo-moléculaire, implication dans la réponse aux stimuli aversifs et influence sur la voie nigrostriée

Fanny Faivre

UNIVERSITE DE STRASBOURG

Ecole doctorale des Sciences de la Vie et de la Santé

Thèse présentée par :

Fanny Faivre
Soutenue le 27 septembre 2018

Pour obtenir le grade de : Docteur de l'Université de Strasbourg
Spécialité : Neurosciences

La queue de l'aire tegmentale ventrale : définition anatomo-moléculaire, implication dans la réponse aux stimuli aversifs et influence sur la voie nigrostriée

---

Thèse dirigée par :

M. Michel Barrot	Directeur de recherche – CNRS UPR 3212, Strasbourg
RAPPORTEURS :	
M. Philippe De Deurwaerdère	Professeur –Université de Bordeaux, CNRS UMR 5287
Mme Nathalie Thiriet	Maître de Conférence – Université de Poitiers, INSERM U 1084
EXAMINATEUR :	
Mme Katia Befort	Chargée de recherche – CNRS UMR 7364

« Le but n’est pas toujours placé pour être atteint,
mais pour servir de point de mire »
Joseph Joubert

REMERCIEMENTS

En premier lieu, je tiens à remercier les membres de mon jury, le Professeur Philippe de Deurwaerdère, les docteurs Nathalie Thiriet et Katia Befort pour avoir accepté d'évaluer ce travail de thèse.

Je tiens surtout à remercier mon directeur de thèse, le docteur Michel Barrot. Merci d'avoir cru en moi quand je me suis présentée devant vous avec mon M1 de Besançon dans la poche alors qu'on ne pariait pas vraiment sur moi. Merci également de m'avoir fait grandir scientifiquement et de m'avoir permis d'aller au bout de ce travail de thèse.

Je tiens également à remercier le Professeur Marie-José Freund-Mercier pour sa gentillesse, ses encouragements, ses conseils et ses nombreuses relectures de rapport. Au docteur Ipek Yalcin-Christmann, merci pour tes messages d'encouragements, pour tes conseils et surtout pour montrer qu'une femme peut être à la fois mère et scientifique accomplie, tu es un grand exemple pour moi et j'espère que tu continueras ton chemin avec autant de réussite. C'est une grande fierté pour moi de t'avoir côtoyée. Aux docteurs Pierre Veinante et Sylvain Hugel, merci pour vos conseils tant neuroanatomiques que phylogénétiques, j'ai beaucoup appris à vos côtés. Merci au docteur Dominique Massotte pour ses conseils en immuno, en confocal et le soutien qu'elle a pu m'apporter tout au long de ces années de thèse. Je voudrais également remercier le docteur Perrine Inquimbert pour les discussions scientifiques ou non autour d'un café ou d'un repas. Tu m'as été d'un grand soutien au moment de la rédaction de cette thèse. J'aimerais également remercier le « double médecin » Eric Salvat pour sa gentillesse et son sourire communicatif. J'espère que nous aurons l'occasion de nous revoir.

Je tiens à remercier vivement le docteur Jennifer Kaufling pour l'aide qu'elle m'a apporté à la fin de cette thèse et ses nombreux conseils. Je te souhaite une belle carrière scientifique, qui sera riche en publication je n'en doute pas. Tels ces irréductibles Gaulois, nous devons continuer à faire vivre la tVTA ! Au docteur Pierre-Eric Lutz, merci pour ton aide sur la partie RNAseq, tout cela reste du chinois pour moi mais je te remercie d'avoir essayé de me faire comprendre tout ça.

A ma petite famille du laboratoire, tout d'abord Betty, merci d'avoir été une petite maman pour moi, de m'avoir épaulée, soutenue alors même que tu doutais de mes

capacités à survivre à tout cela. Je te serai éternellement reconnaissante pour tout ce que tu m'as apporté ici et je te souhaite une très belle (future) retraite avec tes « petits ».

A mes géniaux voisins de bureau, Léa, Baptiste et Xavier, merci pour vos sourires, vos blagues (pas) toujours très drôles, votre gentillesse et merci Baptiste pour avoir assouvi ma passion des mots fléchés en me fournissant un 20 minutes quotidiennement. A mon petit Flo, merci d'avoir su me redonner le sourire quand les expériences foiraient et merci pour toutes ses soirées partagées. Je te souhaite une très belle continuation à Bordeaux et j'espère que tu donneras de tes nouvelles de temps en temps !

For Anil, thank you for your help in my experiments, I wish you a nice end of thesis and hope that you'll have a lot of good publications.

For Alessandro, thank you for your kindness and your help. I wish you the best for the rest of you career.

Merci enfin au reste de l'équipe, pour les discussions scientifiques ou non et pour votre gentillesse: Müzeyyen, Han, Muris, Alice, Lyes, Quentin et Jiahao.

A mes collègues, qui sont devenues bien plus que des collègues désormais… Tout d'abord Clémentine. Merci pour ton sourire, ton humour et ta gentillesse. Cela a été un honneur pour moi que de t'avoir côtoyée durant ma thèse, tant scientifiquement que nail-artement. Tu es une personne formidable et, je n'en doute pas, une future grande scientifique. Je tiens à remercier Mélanie, tu m'as, toi aussi tellement apportée. Merci pour ton soutien sans faille quand je doutais de tout, de m'avoir aidée à survivre à cette fin de thèse et merci d'avoir eu suffisamment confiance en moi pour me partager ton petit secret.

A ma petite Steph, tu vois nous avons survécu à tout cela ! Merci d'avoir été un soutien, un pilier durant cette rédaction de thèse. C'est avec fierté et une pointe d'émotion que je peux dire que tu es désormais une amie et j'espère que nous aurons de nouvelles occasions de partager des pizzas au Barbut'O !

C'est avec émotion que j'en viens à vous...

A mes amis, Zaza, Manu, Ju, Chou. Que de chemin parcouru depuis la fac… Vous êtes mes plus belles rencontres et je ne vous remercierai jamais assez pour tout ce que

vous avez fait pour moi. J'espère que nous vivrons encore de longues années les uns avec les autres. Je vous aime. C'est ici la fin de la looser team, place aux winner !

A mes parents, il n'y aura jamais de mots assez forts pour vous remercier pour tous les sacrifices et les encouragements que vous m'avez donnés. Merci d'avoir su me relever après mes échecs, d'avoir soutenu tous mes choix et d'avoir été à mes côtés à chaque instant, j'espère que vous êtes fiers de moi.

A ma famille, Papy, Mamie, mes oncles et tantes… J'ai tellement de chance d'avoir une famille comme la nôtre. Vous êtes tous d'un grand soutien et je ne vous remercierai jamais assez pour toute l'aide que vous m'avez apportée. On ne peut pas rêver mieux comme famille que la nôtre et j'espère que nous vivrons encore de beaux moments tous ensemble. Nous ne nous le disons pas souvent mais je vous aime de tout mon cœur.

Enfin, vient le moment de parler de toi, mon mari. Je n'ai pas été facile durant cette thèse et pourtant tu as toujours su m'épauler, me remonter le moral, me porter à bout de bras. Merci d'être l'homme que tu es, ce travail est en partie le tien. Place maintenant à de nouveaux projets ensemble… Je t'aime.

PUBLICATIONS & COMMUNICATIONS

Publications liées aux travaux de thèse :

Response of the tail of the ventral tegmental area to aversive stimuli.

Sánchez-Catalán MJ*, **Faivre F***, Yalcin I, Muller MA, Massotte D, Majchrzak M, Barrot M. (*co-premier auteur)

Neuropsychopharmacology (2017) 42:638-648

Anatomo-molecular definition of the tail of the ventral tegmental area in the rat.

Faivre F, Fillinger C, Kaufling J, Sandu C, Maduna T, Thahouly T, Daniel D, Deschatrettes E, Plassard D, Thibault-Carpentier C, Zwiller J, DiLeone R, Romieu P, Veinante P, Massotte D, Lutz PE, Barrot M.

En préparation

Influence of a lesion of the tail of the ventral tegmental area in a rat model of Parkinson's disease.

Faivre F*, Sánchez-Catalán MJ*, Dovero S, Bido S, Joshi A, Bezard E, Barrot M. (* co-premier auteur)

En préparation

The hidden side of Parkinson's disease: studying pain, anxiety and depression in animal models.

Faivre F, Joshi A, Bezard E, Barrot M.

Neuroscience & Biobehavioral Reviews, sous presse

The tail of the ventral tegmental area / rostromedial tegmental nucleus: a ten-year story.

Faivre F & Barrot M.

Revue en préparation

Communications affichées :

Re-definition of a recently discovered midbrain structures: the tVTA (tail of ventral tegmental area) or RMTg (rostromedial tegmental nucleus).

Faivre F, Veinante P, Barrot M.

Congrès MAPS, From Maps to Circuits: Models and Mechanisms for Generating Neural Connections, Strasbourg, France, Février 2015.

422.22 Reconsidering the definition of the tVTA (tail of ventral tegmental area) or RMTg (rostromedial tegmental nucleus).

Faivre F, Fillinger C, Daniel D, Kaufling J, Deschatrettes E, Plassard D, Romieu P, Zwiller J, Lutz PE, Sandu C, Thibault-Carpentier C, Massotte D, Veinante P, Barrot M.

47th Annual Meeting of the Society for Neurosciences, Washington DC, USA. Novembre 2017.

422.23 The tail of the ventral tegmental area: aversive drugs, painful stimuli, stressful stimuli, opioid withdrawal and conditioned taste aversion.

Barrot M, **Faivre F**, Yalcin I, Muller MA, Massotte D, Majchrzak M, Sánchez-Catalán MJ.

47th Annual Meeting of the Society for Neurosciences, Washington DC, USA. Novembre 2017.

Influence of the tail of the ventral tegmental area on symptoms of Parkinson's disease.

Faivre F, Sánchez-Catalán MJ, Dovero S, Bido S, Joshi A, Bezard E, Barrot M.

Advances in neurodevelopmental and neurodegenerative disorders, Strasbourg, France. Juin 2018

Communications orales :

Influence of the tail of the ventral tegmental area on symptoms of Parkinson's disease.

Journée fédérative des Neurosciences, Doctoneuro/Neuropole, 20 avril 2018, Strasbourg

Financement de la thèse :

Ma thèse a été financée par un contrat doctoral de l'Université de Strasbourg (concours Ecole Doctorale Vie & Santé, Université de Strasbourg) du 01/10/2014 au 30/09/2017. J'ai ensuite obtenu un financement de fin de thèse par la Fondation pour la Recherche Médicale pour la période du 01/10/2017 au 30/09/2018.

Bourse et prix obtenus :

- Bourse du Neuropôle de Strasbourg couvrant les frais de participation au 47ème congrès de la Society for Neuroscience à Washington (USA), Novembre 2017
- 1er prix « Blitz », journée fédérative des Neurosciences de Strasbourg, Avril 2018

ABREVIATIONS

ARN : acide ribonucléique

aVTA : aire tegmentale ventrale rostrale ou antérieure

BDA : biotine dextran amine

CB1 : récepteur aux cannabinoïdes de type 1

CNO : clozapine-N-oxide

CTb : sous-unité β de la toxine cholérique

DA : neurone dopaminergique

DBS : stimulation cérébrale profonde

dMAM : région mammilaire dorsale

DREADD : Designer Receptor Exclusively Activated by Designer Drug

FG : FluoroGold®

GABA : acide gamma-aminobutyrique

GAD : acide glumatique décarboxylase

GPCR : récepteur couplé aux protéines G

hMR : récepteur muscarinique humain

IRM : imagerie à résonnance magnétique

LiCL : chlorure de lithium

LHb : habénula latérale

LPS : lipopolyssacharide

MOPR : récepteur μ des opioïdes

PHA-L : leucoagglutinine de *Phaseolus vulgaris*

pVTA : aire tegmentale ventrale caudale ou postérieure

RMTg : noyau rostromédial du tegmentum

SNc : substance noire *pars compacta*

TH : tyrosine hydroxylase

tVTA : queue de l'aire tegmentale ventrale

VGLUT2 : transporteur vésiculaire du glutamate de type 2

VTA : aire tegmentale ventrale

SOMMAIRE

INTRODUCTION

A. Historique du projet de thèse

J'ai commencé à travailler sur la queue de l'aire tegmentale ventrale (tVTA) en 2014 lors de mon stage de 2ème année de Master dans l'équipe « Neuroanatomie, Douleur et Psychopathologies » dirigée par le Docteur Michel Barrot. Le but de départ était alors de définir, chez la souris, les contours de cette structure découverte en 2009 chez le rat.

Les deux premières études publiées concernant cette structure font état, chez le rat, d'un groupe de neurones situés postérieurement à l'aire tegmentale ventrale (VTA) et riches en glutamate décarboxylase, enzyme de synthèse du neurotransmetteur GABA. La première étude a mis en évidence la tVTA par une approche immunohistochimique utilisant des marqueurs de l'activation neuronale : les facteurs de transcription de la famille Fos. Une exposition aiguë à une drogue psychostimulante entraîne la production transitoire de c-Fos et FosB dans la tVTA mais une exposition chronique à cette drogue entraîne la production d'une forme tronquée de FosB, la protéine ΔFosB (Perrotti et al., 2005). Alors que l'expression des autres protéines de la famille Fos montre une certaine tolérance suite à l'exposition répétée à ces drogues, la forme tronquée de FosB, disposant d'une demi-vie plus longue, semble être en lien avec des changements plus durables (Nestler et al., 2001). La structure, dont les contours ont ainsi été définis, est alors nommée « queue de la VTA ».

Parallèlement à cette étude immunohistochimique, une équipe Américaine réalise une étude fonctionnelle mettant en évidence une structure « latérale au noyau du raphé médian et caudale à la VTA influençant les comportements d'immobilité et d'autres réponses aversives passives via ses projections en direction des neurones dopaminergiques du mésencéphale » chez le rat (Jhou, 2005). Cette étude a été le point de départ d'une étude neuroanatomique utilisant la sous-unité β de la toxine cholérique (CTb) comme traceur rétrograde injecté dans la VTA. Cette équipe montre alors que 74% des cellules CTb positives dans cette nouvelle structure sont des neurones GABAergiques et que ces cellules sont également Fos positives après injection de D-amphétamine. Ils nommeront cette structure « noyau rostromédial du tegmentum (RMTg) » (Jhou et al., 2009b).

Le but de mon stage était donc, dans une autre espèce très utilisée en recherche, la souris, de pouvoir généraliser cette définition. Mais devant la difficulté à obtenir des résultats concluants concernant la souris et devant le nombre grandissant d'équipes travaillant sur le sujet, nous avons décidé de changer l'orientation du projet et de réaliser une re-définition de la tVTA dans le but d'en offrir une définition complète et unitaire.

A. Une définition neurochimique

B. Une définition hodologique

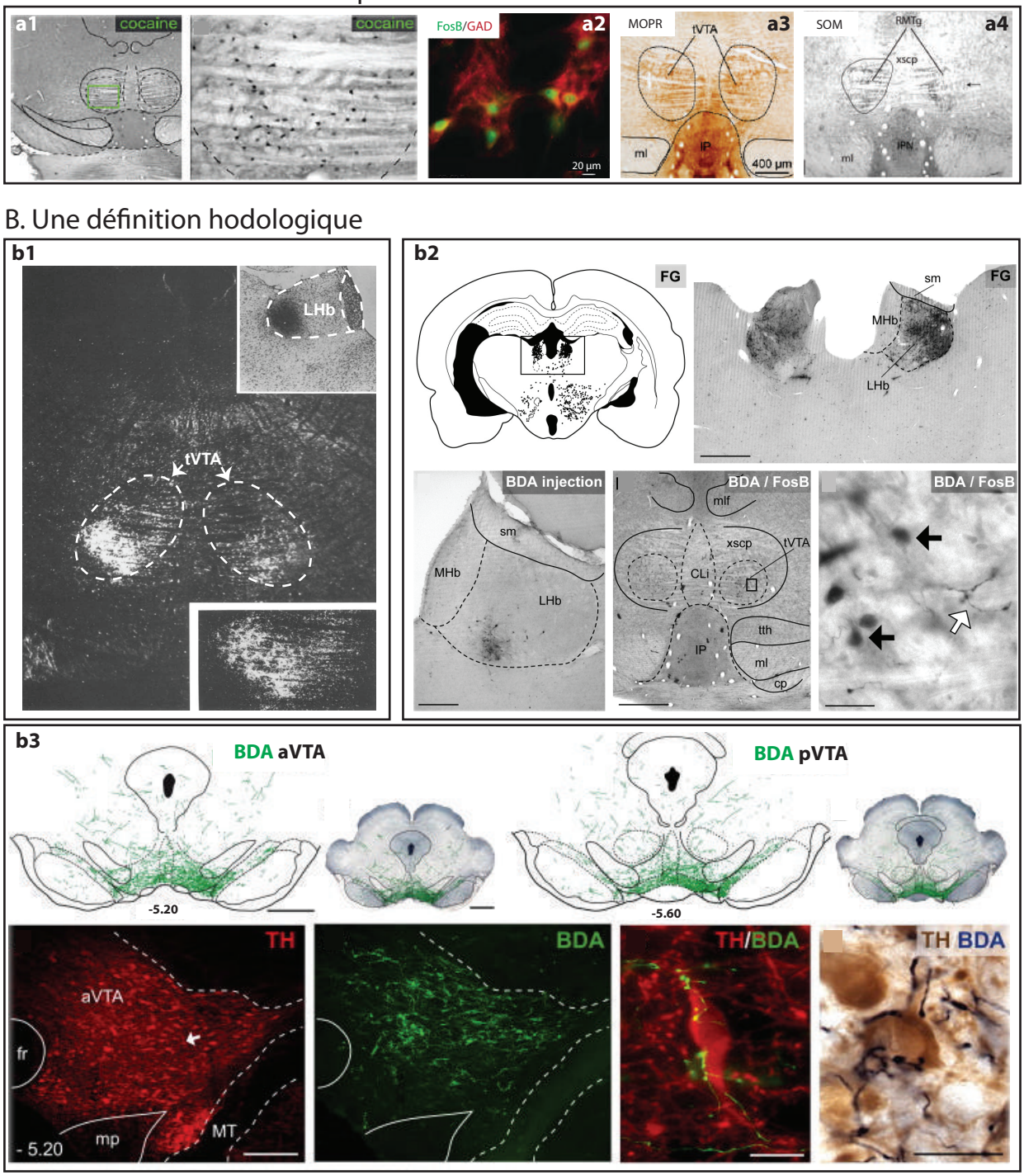

Figure 1. Les définitions neurochimiques et hodologiques de la tVTA. (A) Plusieurs marqueurs neurochimiques ont permis de visualiser les contours de la tVTA. (a1) Une injection aigue de cocaïne (20 mg/kg) entraîne l'expression du facteur de transcription FosB/ΔFosB dans la tVTA (Kaufling et al, 2010), cette induction se situant majoritairement dans des neurones exprimant l'enzyme de synthèse du GABA (Kaufling et al., 2010b) (a2). (a3) La tVTA est également riche en récepteur µ des opioïdes (Jalabert et al., 2011) et présente une forte immunoréactivité pour la somatostatine (Jhou et al., 2009b) (a4). (B) La tVTA reçoit des informations provenant des la LHb et projette sur les neurones dopaminergiques de la VTA et de la SNc. (b1) La première visualisation de la tVTA comme efférence de la LHb date de 1979. Après injection d'un traceur antérograde, des fibres issues de la LHb se retrouvent dans la région qui a été définie depuis comme étant la tVTA (Herkenham and Nauta, 1979). (b2) Des cellules FG+ sont présentes dans la LHb après injection de FluoroGold® dans la tVTA comme le montre la reconstruction (en haut à gauche) et la photo (en haut à droite) prise dans cette région. Réciproquement, des injections de Biotine Dextran Amine, un traceur antérograde, dans la LHb, entraîne l'apparition de fibres BDA+ (flèche blanche) dans la zone dont les contours sont définis par la présence d'un marquage FosB/ΔFosB après injection de cocaïne (flèches noires) (Kaufling et al., 2009). (b3) Projections de la tVTA dans la VTA et la SNc. Ces projections sont représentées à deux niveaux d'antéro-postériorité différents. Les fibres BDA+ issues de la tVTA contactent des neurones dopaminergiques dans la VTA (Kaufling et al., 2010a). Des boutons synaptiques sont visibles au niveau des contacts entre les fibres BDA+ et les corps cellulaires de la VTA. La 3e photographie montre un grossissement de la cellule marquée par une flèche dans la photo en bas à gauche.

B. La queue de l'aire tegmentale ventrale

b1. Contexte bibliographique : plusieurs définitions d'une même structure.

La tVTA est recrutée par de nombreuses substances psychoactives comme la cocaïne (Perrotti et al., 2005; Geisler et al., 2008; Kaufling et al., 2010b, 2010a), les amphétamines (Colussi-Mas et al., 2007) et la nicotine (Pang et al., 1993) et par des substances non addictives comme le modafinil (Scammell et al., 2000). Ces substances entraînent l'apparition d'un marquage Fos local, permettant une délimitation facile de la tVTA. D'autres immunomarquages ont montré l'enrichissement en GAD67 (Olson and Nestler, 2007), la présence d'une forte densité de récepteurs μ des opioïdes (Jhou et al., 2009b), ou une forte immunoréactivité pour la somatostatine (Figure 1A) (Jhou et al., 2009b) et des études de séquençage de l'ARN messager ont mis en évidence la présence de l'ARN messager de la prépronociceptine (données non publiées). Enfin, des études montrent que la tVTA est inclue dans un groupe de structures du mésencéphale immunoréactives pour le récepteur couplé aux protéines G GPR-151 (Broms et al., 2015) et que ses projections à la VTA présentent un marquage au récepteur CB1 aux cannabinoïdes (Melis et al., 2014).

D'autres équipes se basent sur la forte connexion entre l'habénula latérale (LHb), la tVTA et les neurones dopaminergiques du mésencéphale pour établir leurs études neuroanatomiques et fonctionnelles de cette structure. Les connexions de la LHb avec la tVTA ont été mises en évidence par des études de traçage (Figure 1B) et ont permis de voir se multiplier les études sur le rôle de la tVTA dans l'aversion et les comportements d'évitement (Jhou et al., 2009a; Stamatakis and Stuber, 2012; Brown and Shepard, 2013). Des expériences d'électrophysiologie *in vivo* ont mis en évidence le contrôle inhibiteur exercé par la tVTA sur les neurones dopaminergiques de la VTA (Lecca et al., 2011; Kaufling and Aston-Jones, 2015). Enfin des études fonctionnelles ont permis de visualiser l'équivalent de la tVTA chez le primate (Hong et al., 2011). C'est dans ce contexte que nous avons entrepris de réaliser une revue exhaustive des connaissances sur la tVTA.

Cette section présente une revue détaillée de la littérature concernant la tVTA. Trois points essentiels peuvent en être extraits : 1) la tVTA dispose de diverses définitions tant neurochimiques qu'hodologiques, 2) la tVTA a un rôle dans les comportements de type aversifs, 3) la tVTA intervient dans le contrôle de la voie nigrostriée. Les deux premiers points seront abordés ci-après et le troisième point sera plus développé dans la section suivante.

b2. The tail of the ventral tegmental area / rostromedial tegmental nucleus: a ten-year story

THE TAIL OF THE VENTRAL TEGMENTAL AREA / THE ROSTROMEDIAL TEGMENTAL NUCLEUS: A TEN-YEAR STORY

FANNY FAIVRE [a,b] AND MICHEL BARROT [a*]

[a] Centre National de la Recherche Scientifique, Université de Strasbourg, Institut des Neurosciences Cellulaires et Intégratives, F-67000 Strasbourg, France

* Corresponding author at: Institut des Neurosciences Cellulaires et Intégratives, 5 rue Blaise Pascal, F-67000 Strasbourg, France

E-mail address: mbarrot@inci-cnrs.unistra.fr

Abstract

The tail of the ventral tegmental area (tVTA) or rostromedial tegmental nucleus (RMTg) is a GABAergic structure described following the observation of a local FosB/ΔFosB induction after psychostimulant administration. Anatomically, this structure receives input from a wide variety of regions from the telencephalon to the pons and projects mainly to the midbrain dopamine neurons of the ventral tegmental area (VTA) and the substantia nigra *pars compacta* (SNc). Connectivity studies led to identify specific tVTA/RMTg-related pathways, including a lateral habenula (LHb)– tVTA/RMTg – VTA pathway. Functionally, the tVTA/RMTg has been implicated in responses to drugs of abuse, in aversion and avoidance behaviors and in the control of the nigrostriatal pathway. Ten years after the articles reporting its connectivity, the present review presents the actual state-of-the-art concerning the tVTA/RMTg neurochemistry, connectivity and functions.

Keywords: tail of the ventral tegmental area, rostromedial tegmental nucleus, lateral habenula, ventral tegmental area, substantia nigra *pars compacta*, dopamine, drugs of abuse, aversion, reward prediction error, nigrostriatal pathway.

1. INTRODUCTION

The tail of the ventral tegmental area (tVTA) also known as the rostromedial tegmental nucleus (RMTg) is a mesencephalon structure that was described in the rat brain based on anatomical and functional experiments during the first decade of this century (Jhou et al., 2009a, 2009b; Kaufling et al., 2009). However, evidence exists for prior observations of the region now known as tVTA/RMTg (Herkenham and Nauta, 1979; Pang et al., 1993; Scammell et al., 2000). Due to the close proximity of its rostral part with the ventral tegmental area (VTA), the tVTA/RMTg was often considered as part of it (Pang et al., 1993; Rotllant et al., 2010; Scammell et al., 2000), and some functional studies referring to the posterior VTA may in fact concern the tVTA/RMTg (Sanchez-Catalan et al., 2014).

The VTA is mostly constituted of dopamine neurons (65%) but also contain GABAergic (30%) and glutamatergic neurons (5%) (Yetnikoff et al., 2014). Dopamine neurons are in majority in the middle third, their relative density decreasing in the anterior part and in the most posterior part (Olson et al., 2005). This last part, enriched in GABAergic neurons, is now considered as a full-fledged structure. Anatomically, the tVTA/RMTg is in part inserted within the area of passing fibers from the superior cerebellar peduncle (Colussi-Mas et al., 2007) and is, in its rostral tiers, embedded in the paranigral nucleus of the VTA, just above the medial extremity of the medial lemniscus (Geisler et al., 2008) and nearby the interpeduncular nucleus. The tVTA/RMTg receives widespread inputs from the cortex to the pons, and projects to a more restricted array of structures, mostly in the midbrain. Functionally, the tVTA/RMTg has been implicated in the response to drugs of abuse, in the response to aversive stimuli, in reward prediction error, and in the control of nigrostriatal pathway.

The present review aims at providing an overall overview of the literature concerning the neurochemistry, the connectivity and the functions related to this structure described 10 years ago.

1.1. Before the real discovery

While most studies on the tVTA/RMTg started with the 2009 reports (Jhou et al., 2009a, 2009b; Kaufling et al., 2009), there are some older evidence in the literature supporting the existence of this brain region. Herkenham and Nauta (Herkenham and Nauta, 1979) were the first ones to observe something corresponding to what will be referred to as the tVTA/RMTg 30 years later. They saw, after injection of tritiated amino-acids into the lateral habenula (LHb),

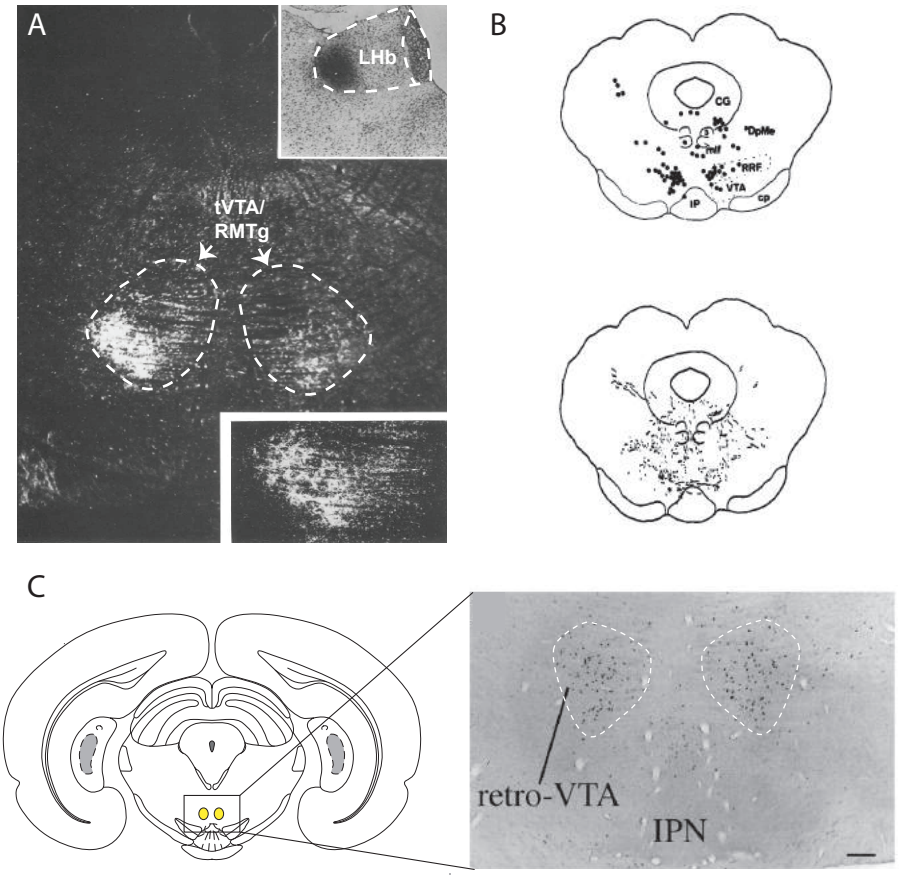

Figure 2. Before the definition of the tVTA/RMTg, some evidence already highlighted the existence of this brain region. (A) By injecting tritiated amino-acids into the lateral habenula (LHb), Herkenham and Nauta showed a dense and localized staining within the area of decussating fibers of the superior cerebellar peduncle, mostly ipsilateral to the injection site (Herkenham and Nauta, 1979). (B) By using an anterograde tracer, Araki and collaborators showed a mesencephalopontine area with fibers and terminals issued from the LHb, which also likely corresponds to what is now defined as the tVTA/RMTg (Araki et al., 1988). (C) The administration of modafinil increases c-Fos expression in a caudal region of the VTA that the researchers referred to as “retro-ventral tegmental area” (Scammel et al., 2000).

a dense and localized staining within the area of decussating fibers of the superior cerebellar peduncle, mostly ipsilateral to the injection site (Fig. 2A). Almost 10 years after this first publication, one of the reconstructed figures in another study using an anterograde tracer showed a mesencephalopontine area with fibers and terminals issued from the LHb (Araki et al., 1988), which also likely corresponds to what is now defined as the tVTA/RMTg (Fig. 2B). Functionally, Pang and colleagues (Pang et al., 1993) showed that a sub-cutaneous injections of nicotine produced an increase in c-Fos mostly in non-dopaminergic neurons in the most caudal part of the VTA. Similarly, the administration of modafinil leads to increased c-Fos expression in a caudal region of the VTA that the researchers referred to as "retro-ventral tegmental area" (Scammell et al., 2000) (Fig. 2C). A first description of the tVTA was made by Perrotti and colleagues (Perrotti et al., 2005), by showing that chronic cocaine or amphetamine administration, but not morphine, led to increased FosB/ΔFosB specifically in the posterior region of the VTA, naming this group of cells "tail of the VTA". The same name was also used by Ikemoto to define a group of cell visible following Nissl staining and containing low density of TH-positive cells (Ikemoto, 2007). In parallel, Jhou published a communication about a midbrain structure enriched in GABA neurons, lateral to the median raphe nucleus and caudal to the VTA and that influences freezing and other passive aversive responses via projections to midbrain DA neurons (Jhou, 2005), which later on was defined as RMTg. In the rat, this population of GABAergic neurons observed by various groups starts around -6.00 mm from the bregma (Olson and Nestler, 2007) and sends projections to the dopaminergic neurons of the VTA (Colussi-Mas et al., 2007; Geisler et al., 2008) and the substantia nigra *pars compacta* (SNc) (Ferreira et al., 2008).

1.2. Two names for one structure

In 2009, 2 different studies were published in parallel, defining the tVTA/RMTg in the rat. In the first article, a cocaine-induced FosB/ΔFosB induction was observed in a GABAergic structure partly embedded within the caudal VTA and shifted dorsally to become inserted, in its most posterior part, within the fibers of the superior cerebellar peduncle. This structure had inputs mostly similar to the VTA ones and was named tVTA (Kaufling et al., 2009). In parallel, another team discovered a new structure of the reticular formation that was activated by footshocks and interconnected the LHb and the VTA, and named it RMTg (Jhou et al., 2009a). The two names are still used to designate this structure and evidence suggests that they refer the same structure. Although ten years have passed since these first observations, there is still

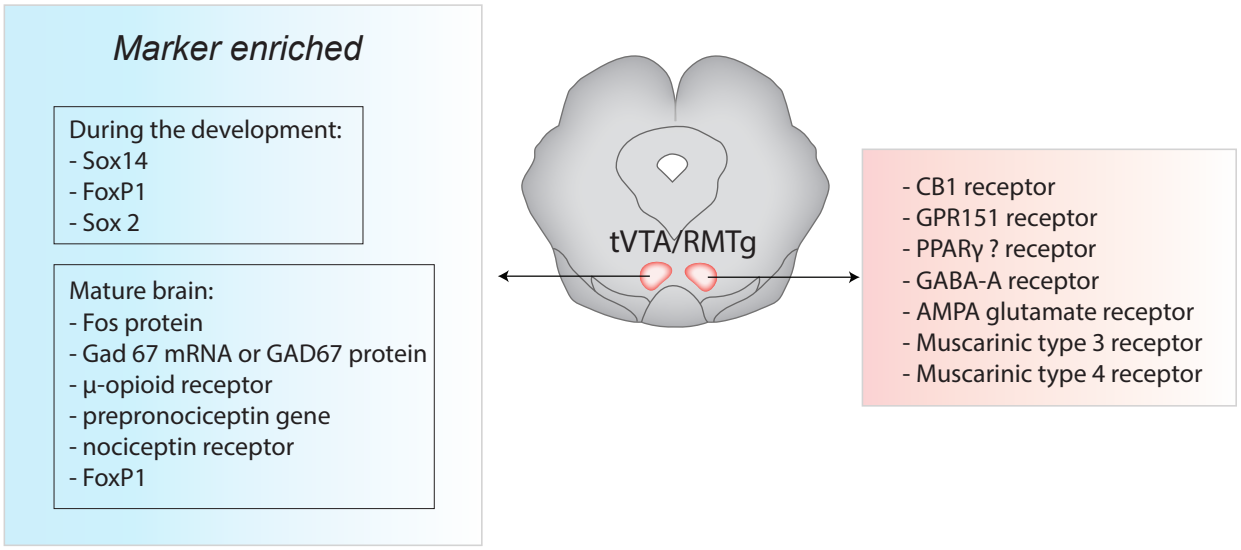

Figure 3. The tVTA/RMTg is enriched in different molecular markers that can be used to highlight its boundaries. During the development, precursors of GABA neurons of the tVTA/RMTg express specific progenitors such as Sox14, FoxP1 and Sox2. In the mature brain, Fos activation, Gad67, μ-opioid receptor, prepronociceptin gene, nociceptin receptor and FoxP1 also distinguish the tVTA/RMTg from surrounding regions.

no mention of this structure in atlases. However, for its posterior part, this cell cluster would be partly located in the region designated as the "interstitial nucleus of the decussation of the superior cerebellum peduncle" in the rat atlas (Paxinos and Watson, 2014).

2. NEUROCHEMISTRY OF THE tVTA/RMTg

In the rat, Fos induction following psychostimulant administration initially allowed to distinguish the tVTA/RMTg from the VTA (Perrotti et al., 2005) and is an easy way to highlight the tVTA/RMTg boundaries in this species (Jhou et al., 2009b; Kaufling et al., 2009) (Fig. 3) (For more details concerning Fos response to drugs, see sections IV). This induction concerns both the c-Fos and FosB/ΔFosB proteins. It appears almost exclusively in neurons that do not express tyrosine hydroxylase, but rather express glutamate decarboxylase (Kaufling et al., 2009, 2010a; Olson and Nestler, 2007; Perrotti et al., 2005; Rotllant et al., 2010). Indeed, 92% of the neurons expressing FosB after acute or chronic cocaine treatment are GABA ones (Perrotti et al., 2005).

Neurochemical studies of the tVTA/RMTg confirmed that this structure is mostly constituted of GABA neurons, as shown by immunohistochemistry (Brinschwitz et al., 2010; Jhou et al., 2009a; Kaufling et al., 2010a, 2010b; Kaufling and Aston-Jones, 2015; Olson et al., 2005; Perrotti et al., 2005; Rotllant et al., 2010; Wasserman et al., 2013, 2016) and by *in situ* hybridization (Brinschwitz et al., 2010; Gao et al., 2018; Jhou et al., 2009b) for glutamate decarboxylase-67, both in rats (Brinschwitz et al., 2010, 2010; Gao et al., 2018; Jhou et al., 2009a, 2009b, Kaufling et al., 2010a, 2010b; Kaufling and Aston-Jones, 2015; Olson et al., 2005; Perrotti et al., 2005; Rotllant et al., 2010) and in mice (Wasserman et al., 2013, 2016). The few tyrosine-hydroxylase positive neurons that are present in the tVTA-RMTg do not exceed 10% of the total neuronal population (Zhao-Shea et al., 2011).

Beside the GABAergic nature of the tVTA/RMTg, other markers were found to be enriched in this structure. For example, the μ-opioid receptors are also densely expressed in the rat (Jalabert et al., 2011; Jhou et al., 2009b, 2012; Kaufling and Aston-Jones, 2015; Yetnikoff et al., 2015) and the mouse (Wasserman et al., 2016) tVTA/RMTg. A somatostatin labelling was also evidenced by immunohistochemistry, mostly in the medial part of the structure (Jhou et al., 2009b). Finally, it has been showed that the tVTA/RMTg may be distinguish from the surrounding structures by detecting the prepronociceptin gene by *in situ* hybridization in rat (Jhou et al., 2009b, 2012) (but illustrations of staining are not provided in these articles), or the nociceptin receptor by immunohistochemistry in mice (Wasserman et al., 2016) (Fig. 3).

Beside these enriched markers, various receptors and other proteins have been found to be present in the tVTA/RMTg, using either morphological or functional approaches. Thus, type 1 cannabinoid receptors were found on the tVTA/RMTg GABA afferents to VTA dopamine neurons using electrophysiological (Barrot et al., 2016; Lecca et al., 2012; Melis et al., 2014) approaches. By immunohistochemistry, it has been shown that the glutamatergic neurons projecting from the LHb to the tVTA/RMTg express the highly conserved GPR151 receptors, both in mice and rats (Broms et al., 2015). PPARγ (peroxisome proliferator-activated receptor γ) immunoreactivity has also been observed in the posterior VTA and in the tVTA/RMTg, but it did not co-localized with GABA cells in the tVTA/RMTg (de Guglielmo et al., 2015). Functionally, the local delivery of various agonists and antagonists provided evidence for a presence of: GABA-A receptors (muscimol, biccuculine) (Lavezzi et al., 2015), AMPA glutamate receptors (AMPA) (Fu et al., 2016b), and muscarinic type 3 receptors (4-DAMP) (Steidl et al., 2017). By immunohistochemistry, the presence of the muscarinic type 3 as well as type 4 receptors was also confirmed in mice, around tVTA-RMTg neurons expressing μ-opioid receptors (Wasserman et al., 2016) (Fig. 3).

Beside reports in adult animals, developmental studies conducted in mice highlighted the existence of specific precursors leading to the GABA neurons of the tVTA/RMTg (Achim et al., 2013; Lahti et al., 2016; Polter et al., 2018). Using knock-out mice, it has been shown that *Tal2* and *Gata2* genes are necessary for the differentiation of the GABAergic neurons of the tVTA/RMTg (Achim et al., 2013; Lahti et al., 2016). During the development, tVTA/RMTg neurons express *Sox14*, FoxP1 and Sox2 (Lahti et al., 2016), and FoxP1 was also found in the mature mouse brain (Lahti et al., 2016; Polter et al., 2018). Interestingly, in adult mice, FoxP1 was found to co-localized with the few tVTA-RMTg FosB-positive neurons in mice treated with a high dose of metamphetamine (Lahti et al., 2016) (Fig. 3).

3. CONNECTIVITY OF THE tVTA

3.1. Inputs (Fig. 4A)

Afferents to the tVTA/RMTg were first studied by using retrograde tracers such as the FluoroGold® or the β subunit of the choleric toxin (Jhou et al., 2009b; Kaufling et al., 2009). The afferent connection pattern of the tVTA/RMTg extents from the rostral part of the frontal cortex to the medulla (Jhou et al., 2009b). From the telencephalon, the tVTA/RMTg receive inputs from various cortical areas such as the frontal associative cortex, the prelimbic and

infralimbic cortices, the dorsal peduncular cortex, the cingulate cortex, the dorsal peduncular regions of the prefrontal cortex and the agranular insular cortex. Some retrograde labelled cells were also found in the lateral and medial septum, in the nucleus of the horizontal limb of diagonal band, in the ventral striatum and more precisely the shell of the nucleus accumbens, as well as the ventral pallidum and in parts of the extended amygdala (the substantia innominata, the ventral and medial part of the bed nucleus of the stria terminalis and the interstitial nucleus of the posterior limb of the anterior commissure). From diencephalic structures, tVTA/RMTg receives strong inputs from the thalamus/epithalamus, especially the lateral habenula, and also inputs from various hypothalamic nuclei and subthalamic nuclei. Finally, the tVTA/RMTg receives information from the mesencephalon and the pons, including from the VTA, the SNc, the periacqueducal gray and various raphe nuclei and tegmental nuclei. While most connections are ipsilateral or bilateral, a few ones are contralateral, as for example the deep mesencephalic nuclei, the prerubral field, the red nucleus, the retrorubral field and the deep layers of the superior colliculus. In the pons, inputs arise from the pontomedullary reticular formation, the pedunculopontine tegmental nucleus, the laterodorsal tegmental nucleus and the dorsomedial tegmental area (Jhou et al., 2009b; Kaufling et al., 2009).

Among this variety of inputs, one structure attracted attention and has been particularly studied, in relation to its strong implication in behavioral responses: the LHb (see chapter IV for more details). This dense LHb to tVTA/RMTg projection mostly arises from the lateral part of the LHb (Petzel et al., 2017), and has been confirmed by many anatomical studies, both in rats (Araki et al., 1988; Balcita-Pedicino et al., 2011; Brinschwitz et al., 2010; Gonçalves et al., 2012; Herkenham and Nauta, 1979; Jhou et al., 2009b; Kaufling et al., 2009; Poller et al., 2013) and in mice (Lammel et al., 2012; Quina et al., 2015). This projection is mostly ispsilateral (Balcita-Pedicino et al., 2011; Jhou et al., 2009b; Petzel et al., 2017; Quina et al., 2015), and displays some topographical organization. Indeed, *Phaseolus vulgaris* leurcoagglutinin injections into the lateral-most part of the LHb produces labeling in lateral parts of the tVTA/RMTg (Jhou et al., 2009b). Outputs from the LHb to the tVTA/RMTg are mostly glutamatergic (Brinschwitz et al., 2010), include GPR151-positive neurons (Broms et al., 2015), and electron microscopy evidenced that axons are both myelinated and unmyelinated (Balcita-Pedicino et al., 2011). Lastly, electrical stimulation of the LHb enhances the spiking activity of half of the tVTA/RMTg neurons (Lecca et al., 2011), and the optogenetic stimulation of the LHb to tVTA/RMTg terminals was found to promote active, passive and conditioned avoidance in mice (Stamatakis and Stuber, 2012). Interestingly, an equivalent of this LHb-tVTA/RMTg projection seems to also exist in lampreys (Robertson et al., 2014; Stephenson-

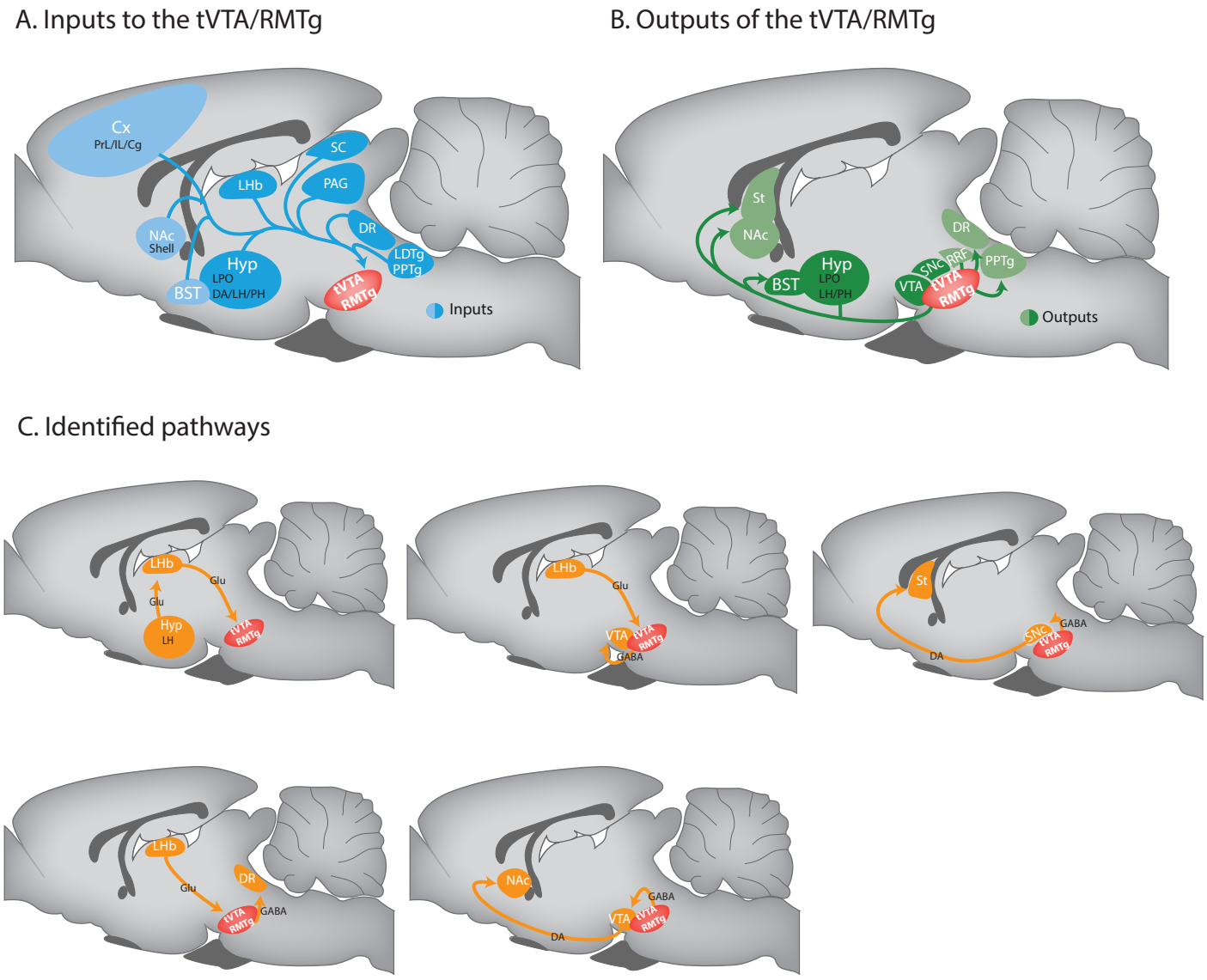

Figure 4. Connectivity of the tVTA/RMTg. (A) The tVTA/RMTg receives afferents from various cerebral structures including the several cortices (Cx), the nucleus accumbens (NAc), the lateral habenula (LHb), various hypothalamic nuclei (Hyp), the bed nucleus of the stria terminalis (BST), the superior colliculus (SC), the periaqueductal gray (PAG), the dorsal raphe (DR), the laterodorsal tegmentum (LDTg) and the pedunculopontine tegmental nucleus (PPTg). The light blue correspond to minor afferents, the dark blue to major afferents. (B) The tVTA/RMTg efferents are more restricted and include the dorsal and ventral striatum (St, NAc), the bed nucleus of the stria terminalis (BST), various hypothalamic nuclei (Hyp), the midbrain dopamine neurons of the ventral tegmental area and the substantia nigra pars compacta (VTA, SNc) the retrorubral field (RRF), the dorsal raphe (DR) and the pedunculopontine tegmental nucleus (PPTg). The light green correspond to minor efferents, the dark green to major ones. (C) The tVTA/RMTg is involved in pathways either as starting point, relay or end point. As a starting point, the tVTA/RMTg is a component of the tVTA/RMTg-VTA-NAc and of the tVTA/RMTg-SNc-dorsal striatum pathways. The tVTA/RMTg is a relay between the LHb and the VTA and between the LHb and the DR. Finally the tVTA/RMTg is the end point of the lateral hypothalamic area (LH)-LHb-tVTA/RMTg pathway.

Jones et al., 2012). Indeed, a dorsal mammillary region, equivalent of the tVTA/RMTg in rodents, receives input from the homolog LHb and projects to dopamine neurons (Robertson et al., 2014; Stephenson-Jones et al., 2012).

3.2. Outputs (Fig. 4B)

Using anterograde tracers (Köbbert et al., 2000), such as the plant lectin *Phaseolus vulgaris* leucoagglutinin or the Biotin Dextran Amine, efferent connections from the tVTA/RMTg were mapped (Jhou et al., 2009b; Kaufling et al., 2010a). These efferent connections extend from the rostral pole of the frontal cortex to the medulla. The tVTA/RMTg projects modestly to the orbitofrontal cortex and to the dorsal hippocampus, and sparsely to the striatal complex (and more specifically to the medial part of the dorsal striatum and the rostral part of the nucleus accumbens), to the ventral pallidum and to some structures belonging to the extended amygdala: the interstitial nucleus of the posterior limb of the anterior commissure, the substantia innominata and the bed nucleus of the stria terminalis. In the diencephalon, tVTA/RMTg fibers form a continuum from the lateral preoptic area to the lateral and posterior hypothalamus. In the brainstem, strong labelling was found in the periacqueducal gray, the VTA, the SNc, the retrorubral field, the median and dorsal raphe nuclei (observation that was confirmed later using PhaL injections into the tVTA/RMTg (Sego et al., 2014)), the deep mesencephalic nucleus, the locus coeruleus, the deep cerebellar nuclei and the pontine and medullary reticular formation (Jhou et al., 2009b; Kaufling et al., 2010a).

However, projections from the tVTA/RMTg to the midbrain dopamine neurons are the densest (Gonçalves et al., 2012; Jhou et al., 2009b; Kaufling et al., 2010a). It is evidenced by using anterograde tracers delivered into the tVTA/RMTg (Jalabert et al., 2011; Jhou et al., 2009b, 2009a; Kaufling et al., 2010a) and by using retrograde tracers injected into the VTA (Colussi-Mas et al., 2007; Geisler et al., 2008; Gonçalves et al., 2012; Jalabert et al., 2011; Mahler and Aston-Jones, 2012; Melis et al., 2014). This connection is predominantly ipsilateral, even if it also includes a strong contralateral component. Fibers from the tVTA/RMTg to the VTA/SNc show apposition on tyrosine hydroxylase-immunoreactive neurons (Balcita-Pedicino et al., 2011; Bourdy et al., 2014; Jhou et al., 2009a). Electron microscopy confirmed the presence of t-VTA/RMTg-VTA (Balcita-Pedicino et al., 2011) and tVTA/RMTg-SNc (Bourdy et al., 2014) symmetric synapses, the majority of tVTA/RMTg axons being unmyelinated and including either small-diameter intervaricose segments or vesicle-containing boutons (Balcita-Pedicino et al., 2011). The tVTA/RMTg cells projecting to the VTA are negative for tyrosine

hydroxylase and choline acetyltransferase, and at least 2/3 of them are GABAergic (Kaufling et al., 2010a).

Electrophysiological studies confirm anatomical data, highlighting the strong influence that tVTA/RMTg neurons exert on midbrain dopamine neurons. *Ex vivo*, electrical or optogenetic stimulation of the tVTA/RMTg neurons induces inhibitory post-synaptic currents in VTA dopamine neurons (Matsui and Williams, 2011). *In vivo*, electrical or optogenetic stimulation of the tVTA/RMTg inhibits midbrain dopamine neurons of the VTA (Kaufling and Aston-Jones, 2015; Lecca et al., 2011, 2012) and the SNc (Bourdy et al., 2014). Conversely, *in vivo* inhibition of the tVTA/RMTg by application of muscimol increases the firing and the bursting rate of midbrain dopamine neurons, in the VTA (Jalabert et al., 2011; Kaufling and Aston-Jones, 2015) and in the SNc (Bourdy et al., 2014). tVTA/RMTg synapses onto midbrain dopamine neurons likely co-release GABA and glycine as synaptic currents originating from this structure were reduced by strychnine (*i.e.* an antagonist of the glycine receptors) (Polter et al., 2018). The comparative study of plasticity at the tVTA/RMTg synapses and at synapses between VTA GABA cells and dopamine cells, highlighted that the latter can display a cyclic GMP-dependent long term potentiation which is not the case for the former (Polter et al., 2018), further supporting the hypothesis and developmental evidence that tVTA/RMTg GABA cells differ from VTA GABA cells.

Finally, behavioral evidence also support the link between the tVTA/RMTg and SNc dopamine neurons. Indeed, lesion of the tVTA/RMTg modify the rotation bias behavior induced by a D-amphetamine injection in animals with SNc unilateral lesion and this lesion also improves both motor coordination and motor skill learning in a rotarod test (Bourdy et al., 2014).

3.3. Identified pathways (Fig. 4C)

Efforts were made to identify specific some tri-structure pathways involving the tVTA/RMTg, either as starting point, relay or end point.

A double tracing study evidenced a pathway from the lateral hypothalamic area to the LHb and then to the tVTA/RMTg (Poller et al., 2013). Indeed, it has been showed that LHb neurons projecting to the tVTA/RMTg are densely targeted by afferents from the lateral hypothalamic area, both projections of this pathway being glutamatergic (Poller et al., 2013).

Most data, however, presently concern pathways with the tVTA/RMTg as relay structure. It is the case of a pathway between the LHb, the tVTA/RMTg and the dorsal raphe. The

connection between the tVTA/RMTg and the dorsal raphe is GABAergic, and preferentially targets a subdivision of the dorsal raphe that is poor in serotonin neurons and enriched in glutamatergic neurons (Sego et al., 2014). The other identified pathway with tVTA/RMTg as relay is the most studied one: the LHb-tVTA/RMTg-VTA pathway.

Direct projections from the LHb to the VTA have been evidenced using tract-tracing (Araki et al., 1988; Herkenham and Nauta, 1979; Kim, 2009), these projections being glutamatergic ones (Aizawa et al., 2012; Geisler et al., 2007; Matsuda and Fujimura, 1992). However, the stimulation of the LHb or of the fasciculus retroflexus (*i.e.* the fiber pathway containing most of the habenular efferents) strong inhibits midbrain dopamine neurons of the VTA and the SNc, which is suppressed by a lesion of the fasciculus retroflexus (Brown et al., 2017; Christoph et al., 1986; Ji and Shepard, 2007; Matsumoto and Hikosaka, 2007). In monkeys, LHb neurons and VTA dopamine neurons show opposite encoding of negative reward signals (Matsumoto and Hikosaka, 2007). These data suggested that a relay may exist between the LHb and the VTA. Evidence now supports that the tVTA/RMTg is this relay. Indeed, the density of LHb synaptic input to the tVTA/RMTg is almost seven times greater than the one to the VTA (Balcita-Pedicino et al., 2011). Moreover, the LHb neurons projecting to the tVTA/RMTg and to the VTA are non-overlapping in the rat (Li et al., 2011) and the mouse (Maroteaux and Mameli, 2012); and tVTA/RMTg receives most of its inputs from subnuclei belonging to the lateral part of the LHb, whereas the VTA is mainly innervated by subnuclei of the medial part of the LHb (Gonçalves et al., 2012). A chemical stimulation of the LHb by the glutamate transporter inhibitor dihydrokainic acid leads to c-Fos expression in the tVTA/RMTg (Cui et al., 2014). Finally, the lesion of the tVTA/RMTg reduces both the number of inhibited VTA neurons and the duration of inhibition following LHb stimulation (Brown et al., 2017). Conversely, a D4 mediated negative feedback from the VTA to the tVTA/RMTg, with LHb as relay, has also been evidenced (Good et al., 2013).

With tVTA/RMTg as starting point of the study, double tracing experiments validated the expected tVTA/RMTg-VTA-nucleus accumbens pathway (Kaufling et al., 2010a) and the tVTA/RMTg-SNc-dorsal striatum one (Bourdy et al., 2014).

4. FUNCTIONAL INSIGHTS

4.1. Response to psychostimulant drugs (Table 1)

Table 1 Response of the tVTA/RMTg to drugs.

	Species	Administration	Dose	Marker	Induction	Ref.
Cocaine						
	Rat	Acute, i.p.	5-40 mg/kg	FosB/ΔFosB	Yes	Kaufling et al., 2009; 2010a; 2010b
		Chronic, i.p.	15 mg/kg, twice a day for 14 days			Perrotti et al., 2005
		Self-adm.	0.5 mg/kg/injection, 4h/jour			Perrotti et al., 2005
		Self-adm.	0.125 mg final dose	c-Fos, FosB		Navailles et al., 2015
		Acute, i.p.	10 mg/kg	c-Fos		Jhou et al., 2013
		Self-adm.	0.5 mg/kg/injection, 2h/day, 6 days			Geisler et al., 2008; Jhou et al., 2009b
		Self-adm.	0.5 mg/kg/inj, 2h/day, 1 and 6 days			Zahm et al., 2010
		Investigator adm.	0.5 mg/kg/inj, 2h/day, 1 and 6 days			Zahm et al., 2010
		Self-adm.	0.25 mg/kg/inj, 2h/session, 10 days	*c-fos*, ISH		Gao et al., 2018
D-amphetamine						
	Rat	Acute, i.p.	1 mg/kg	FosB/ΔFosB	Yes	Kaufling et al., 2010b
		Chronic, i.p.	4 mg/kg, once daily, 4 days			Perrotti et al., 2005
		Acute, s.c.	5 mg/kg	c-Fos		Colussi-Mas et al., 2007
		Acute, s.c.	1.5 or 5 mg/kg			Rotllant et al., 2010
		Acute, s.c.	4 mg/kg			Matsui and William, 2011
	Mice	Acute, i.p.	5 mg/kg			Quina et al., 2015
Methamphetamine						
	Rat	Acute, i.p.	10 mg/kg	c-Fos	Yes	Jhou et al., 2009b; Lecca et al., 2011; Lavezzi et al., 2012
		Acute yoked delivery	0.1 mg/kg/inj, 2h session			Cornish et al., 2012
		Self-adm.	0.1 mg/kg/inj, 2h/day, 3 weeks			Cornish et al., 2012
	Neonatal rats	Acute, s.c.	10 mg/kg			Brown and Shepard, 2016
MDMA						
	Rat	Acute, i.p.	5 mg/kg	FosB/ΔFosB	Yes	Kaufling et al., 2010b
Methylphenidate						
	Rat	Acute, i.p.	10 mg/kg	FosB/ΔFosB	Yes	Kaufling et al., 2010b
Caffeine						
	Rat	Acute, i.p.	10 to 100 mg/kg	FosB/ΔFosB	Yes	Kaufling et al., 2010b
Morphine						
	Rat	Acute, s.c.	10, 50 mg/kg	FosB/ΔFosB	No	Kaufling et al., 2010b
		Chronic, s.c.	Escalating, twice a day, 10 days			Perrotti et al., 2005
		Chronic, pellet	75 mg			Perrotti et al., 2005
Cannabinoids						
	Rat	Acute, i.p.	3 mg/kg	FosB/ΔFosB	No	Kaufling et al., 2010b
GHB						
	Rat	Acute, i.p.	1 g/kg	FosB/ΔFosB	No	Kaufling et al., 2010b
Ethanol						
	Rat	Acute, i.p.	1.5, 5 g/kg	FosB/ΔFosB	No	Kaufling et al., 2010b
Ketamine						
	Rat	Acute, i.p.	50 mg/kg	FosB/ΔFosB	No	Kaufling et al., 2010b
Nicotine						
	Rat	Acute, s.c.	0.4, 1.4 mg/kg	c-Fos	Yes	Pang et al., 1993
PCP						
	Rat	Acute, i.p.	3, 10 mg/kg	FosB/ΔFosB	No	Kaufling et al., 2010b
Modafinil						
	Rat	Acute, i.p.	75 to 100 mg/kg	Fos	Yes	Scammel et al., 2000

Adm., administration; GHB, gamma-hydroxybutyric acid; i.p., intraperitoneal; MDMA, 3,4-methylenedioxy-N-methylamphetamine, PCP, phencyclidine; s.c., subcutaneous

As evoked in previous sections, boundaries of the tVTA/RMTg were first observed following immunohistochemical detection of Fos transcription factors, such as c-Fos and FosB, following exposure to psychostimulants. Indeed, acute (Jhou et al., 2013; Kaufling et al., 2009, 2010a, 2010b) or self- administered (Gao et al., 2018; Geisler et al., 2008; Jhou et al., 2009b; Navailles et al., 2015; Perrotti et al., 2005; Zahm et al., 2010) cocaine increases Fos expression locally. Chronic psychostimulant treatment also produces a truncated and long-lasting form of FosB: ΔFosB. Indeed, chronic cocaine administration induces a strong ΔFosB expression in the tVTA/RMTg (Perrotti et al., 2005), that remains detectable up to 12 days. Acutely, FosB/ΔFosB is detectable within 30 minutes post injection, reaching a peak around 3 hours and remaining detectable 4 days after (Kaufling et al., 2010b). Dose-response study indicates that 20 mg/kg of cocaine is necessary to induce the maximal recruitment of tVTA/RMTg cells (Kaufling et al., 2010b). The Fos induction also depends on the number of cocaine exposures, as 6 self-administration sessions lead to higher Fos density than a single session (Zahm et al., 2010). Conversely, this Fos induction is not affected by the method of administration, as cocaine self-administration or experimenter-administration does not change the amount of Fos induction in the tVTA/RMTg (Geisler et al., 2008). It may however affect the location of expression within the tVTA/RMTg, with more rostral expression after investigator-administration compared to self-administration (Zahm et al., 2010).

Beside the response to cocaine, Fos induction was also observed for D-amphetamine in rats (Colussi-Mas et al., 2007; Kaufling et al., 2010b; Matsui and Williams, 2011; Perrotti et al., 2005; Quina et al., 2015; Rotllant et al., 2010) and mice (Quina et al., 2015), for metamphetamine in adult (Brown and Shepard, 2016; Cornish et al., 2012; Jhou et al., 2009b; Lavezzi et al., 2012; Lecca et al., 2011) and neonatal rats (Brown and Shepard, 2016), and for methylphenidate and 3,4-methylenedioxy-N-methylamphetamine (MDMA) (Kaufling et al., 2010b) (Table 2). This Fos induction seems to be dependent on the psychostimulant properties of the drugs, and is also observed at high dose with modafinil (*i.e.* a treatment for excessive sleepness) (Scammell et al., 2000); whereas ethanol, γ-hydroxybutyric acid sodium (GHB), morphine, ketamine, phencyclidine hydrochloride (PCP) or Δ^9-tetrahydrocannabinol (THC) do not induce Fos proteins in the tVTA/RMTg (Kaufling et al., 2010b). Moreover, this recruitment seems to be dopamine dependent as the administration of a dopamine transporter inhibitor (GBR12909), but not of a noradrenaline (reboxetine) or serotonine (fluoxetine) transporter, can induce Fos in the tVTA/RMTg (Kaufling et al., 2010b).

In vivo, an acute cocaine injection may induce a transient depression of the firing rate of the tVTA/RMTg neurons (Lecca et al., 2011), but this observation remains to be confirmed.

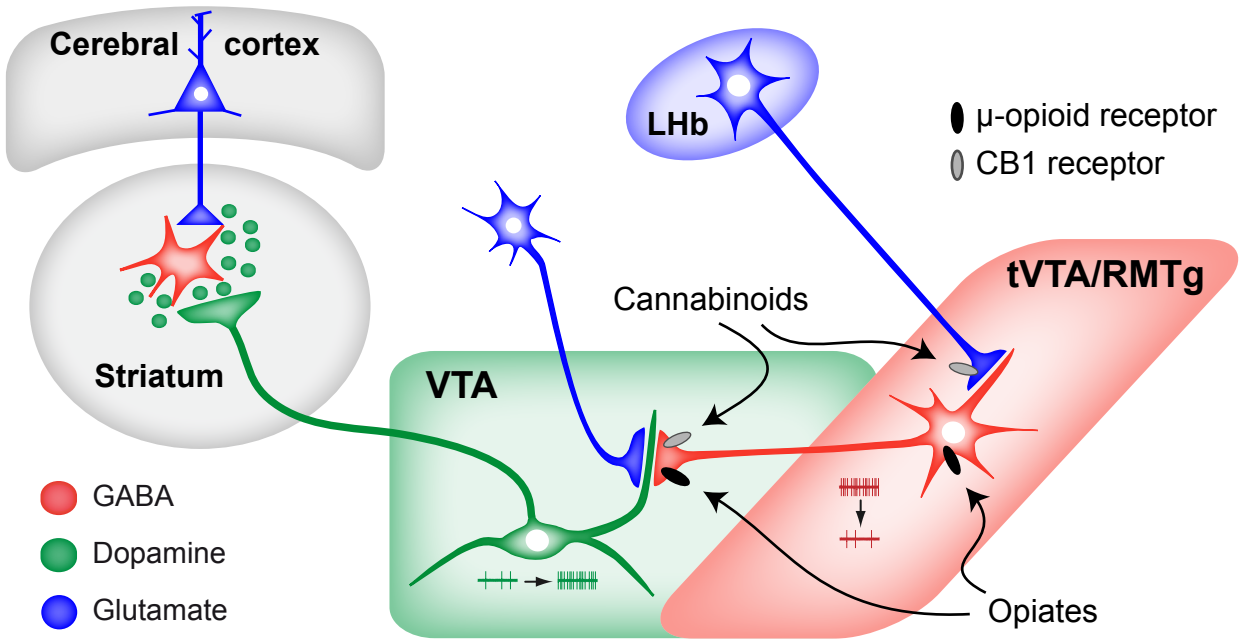

Figure 5. The tVTA/RMTg as a target for disinhibition of dopamine systems. The tVTA/RMTg inhibits the activity of the dopamine neurons. Opiates and cannabinoids can recruit dopamine cells (in green) by controlling the inhibitory brake exerted by the tVTA/RMTg (in red). This disinhibition model requires concomitant glutamate input (in blue) on dopamine cells (Barrot et al., 2016).

In mice, cocaine administration significantly increases AMPA receptor-mediated excitatory postsynaptic current amplitude at the LHb-tVTA/RMTg synapse, but not at the LHb-VTA one (Maroteaux and Mameli, 2012; Meye et al., 2015). This cocaine exposure also increases the AMPA/NMDA ratio at the LHb-tVTA/RMTg synapse. Cocaine induces this synaptic potentiation by increasing the GluA1-containing rectifying AMPAR content at excitatory synapses (Maroteaux and Mameli, 2012; Meye et al., 2015).

Behaviorally, the tVTA/RMTg contributes to cocaine-induced aversion. In a runway operant paradigm, the pharmacological activation of the tVTA/RMTg by S-AMPA induces a conditioned place aversion for cocaine, whereas the lesion of the structure by quinolinic acid or its optogenetic inactivation abolishes the cocaine-induced avoidance behavior (Jhou et al., 2013). Moreover, activation of the tVTA/RMTg favors extinction of cocaine self-administration, whereas the inactivation of this region increases the overall lever pressing in cocaine seeking rats (Huff and LaLumiere, 2015). This influence is somewhat specific to cocaine, as it is not observed in a food-seeking experiment (Huff and LaLumiere, 2015).

4.2. Response to opioids

Contrary to psychostimulant drugs, acute or chronic morphine exposure does not induce Fos proteins in the tVTA/RMTg (Kaufling et al., 2010b; Perrotti et al., 2005), which did not exclude that this brain region may contribute to opioid response. Indeed, the μ-opioid receptors are expressed by tVTA/RMTg neurons (Jalabert et al., 2011; Jhou et al., 2009b, 2012; Kaufling and Aston-Jones, 2015; Wasserman et al., 2016; Yetnikoff et al., 2015), and systemic (Kaufling and Aston-Jones, 2015; Lecca et al., 2011) or local (Jalabert et al., 2011) morphine administration strongly decreases the *in vivo* spontaneous firing rate of these neurons. Similarly, *ex vivo*, the application of morphine, $[Met]^5$ enkephalin or DAMGO (a μ-opioid receptor selective agonist) hyperpolarizes tVTA/RMTg neurons (Lecca et al., 2011; Matsui et al., 2014; Matsui and Williams, 2011), whereas agonists of the δ and κ opioid receptors fail to do so (Matsui and Williams, 2011).

The inhibitory action of opioids on tVTA/RMTg activity contributes to the response of dopamine cells to these drugs. In the 1990s, a disinhibition model has been proposed to explain the recruitment of dopamine system by opioids. In this model, morphine indirectly recruits dopamine neurons by removing the inhibitory drive exerted by neighboring GABA neurons (Johnson and North, 1992). This model has now been updated to include the tVTA/RMTg as main GABA relay mediating these effects (Bourdy and Barrot, 2012) (Figure 5). Indeed, *ex*

vivo recordings indicate that the tVTA/RMTg is the main opioid-sensitive inhibitory input to dopamine neurons, compared to the nucleus accumbens one or the intra-VTA one (Matsui et al., 2014). Accordingly, the *in vivo* tVTA/RMTg inhibition by muscimol blocks the capacity of intra-VTA morphine to recruit dopamine neurons (Jalabert et al., 2011), and morphine (through activation of μ-opioid receptors) can also shorten the duration of tVTA/RMTg-evoked inhibition of dopamine neurons (Lecca et al., 2012). Similar conclusion was reached by *ex vivo* studies, as electrical (de Guglielmo et al., 2015; Lecca et al., 2012; Matsui and Williams, 2011) and optogenetic (Matsui and Williams, 2011) stimulations of the tVTA/RMTg evokes opioid-sensitive inhibitory post-synaptic currents in dopamine neurons.

Behavioral studies further support a role for the tVTA/RMTg in responses to opioids. Indeed, in rats, intra-tVTA/RMTg delivery of the μ-opioid receptor agonist endomorphin-1 can support self-administration and induce conditioned place preference (Jhou et al., 2012). Similarly, in mice, the optogenetic stimulation of tVTA/RMTg neurons expressing μ-opioid receptors induces real time place preference (Siuda et al., 2015). Morphine-induced locomotion is also impacted by manipulation of the tVTA/RMTg. Indeed, overexpression of M5 muscarinic acetylcholine receptors in the tVTA/RMTg reduces morphine-induced locomotion (Wasserman et al., 2013), while local atropine (a muscarinic antagonist) or a M3 specific antagonist (4-DAMP) increases it (Steidl et al., 2017). Clozapine-N-oxide administration to recruit the inhibitory DREADD M4D, a modified muscarinic receptor, expressed into the mouse tVTA/RMTg, increases morphine-induced-locomotion, while recruitment of the locally expressed excitatory DREADD M3D blocks it (Wasserman et al., 2016).

The tVTA/RMTg also contributes to the response to sustained exposure to opioids. Thus, a microinjections of pioglitazone (*i.e.* ligand of the peroxisome proliferator-activated receptor PPARγ) into the tVTA/RMTg reduces heroin self-administration in rats (de Guglielmo et al., 2015). In mice exposed to chronic morphine by the use of osmotic pump, a partial tolerance of μ-opioid receptors has been observed in the tVTA/RMTg (Matsui et al., 2014). On the other hand, in rats under protracted morphine withdrawal, tVTA/RMTg neurons are still responsive to morphine while it is no more the case for dopamine neurons (Kaufling and Aston-Jones, 2015). This deficit in dopamine response has in fact been related to a deficit in tonic glutamatergic inputs to VTA dopamine neurons (Kaufling and Aston-Jones, 2015). Finally, naloxone-precipitated opiate withdrawal induces c-Fos in tVTA/RMTg neurons, but mostly in those that are not expressing μ-opioid receptors suggesting it is likely a network effect (Sánchez-Catalán et al., 2017). However, lesion of the tVTA/RMTg has no impact on physical signs of naloxone-precipitated opiate withdrawal (Sánchez-Catalán et al., 2017).

4.3. Nicotine, cannabinoid and alcohol

In rats, nicotine has been proposed to induce Fos proteins in non-dopaminergic cells from the most posterior part of the VTA (Kaufling et al., 2010b; Pang et al., 1993), which may correspond to the rostral part of the tVTA/RMTg. However, this has not been confirmed yet by other studies, and, in mice, rewarding doses of nicotine failed to induce Fos in this brain region (Zhao-Shea et al., 2011). Nevertheless, nicotine increases the *in vivo* firing rate of tVTA/RMTg neurons (Lecca et al., 2011) and, *ex vivo*, increases excitatory post synaptic current amplitude (Lecca et al., 2011). This excitatory influence on tVTA/RMTg neurons is mediated by α7-containing nicotinic receptors, as the α7 antagonist methyllycaconitine blocks the nicotine-induced excitatory post synaptic current amplitude potentiation (Lecca et al., 2011). However, nicotine fails to modify the duration of tVTA/RMTg-induced inhibition of the VTA dopamine neuronal firing (Lecca et al., 2012).

Cannabinoid receptors 1 are expressed on tVTA/RMTg GABA afferents to the VTA (Melis et al., 2014). In rats, the intravenous administration of the cannabinoid receptors 1 agonist WIN55212-2 produces a long-lasting decrease in the discharge frequencies of tVTA/RMTg neurons (Lecca et al., 2011), and *ex vivo* this agonist reduces the probability of GABA release by the tVTA/RMTg (Lecca et al., 2012). Interestingly, the tVTA/RMTg control of dopamine neurons also contributes to the male/female differences in cannabinoid responses of Lister Hooded rats. In this strain, females are more vulnerable than males to cannabinoid self-administration and this difference can be explained by the fact that an activation of the tVTA/RMTg induces a shorter inhibition of VTA dopamine neurons in females than in males. This difference has been related to the presence in female Lister Hooded rats of a tonic 2-arachidonoylglycerol signaling which can inhibit the tVTA/RMTg-VTA terminals (Melis et al., 2013).

The tVTA/RMTg seems to have also a role in signaling alcohol aversive properties. Indeed, in a sucrose conditioned taste aversion induced by ethanol, cFos expression is present in the LHb and the tVTA/RMTg (Glover et al., 2016). An influence of the tVTA/RMTg on the reward/aversion balance of alcohol is further supported by data in Sardinian rats (Melis et al., 2014). In alcohol-preferring Sardinian rats, the inhibition of VTA dopamine neurons induced by tVTA/RMTg stimulation is shorter; whereas in alcohol-non preferring rats, alcohol increases the activity of tVTA/RMTg neurons and prolongs the duration of VTA dopamine neurons inhibition (Melis et al., 2014). Further supporting these data, the lesion of the tVTA/RMTg

Table 2 Response of the tVTA/RMTg to aversive conditions

Stimulus	Species	Marker	Induction	Ref.
Foot-shock, 4x, 0.5 mA, 0.5 s	Rat	c-Fos	Yes	Jhou et al., 2009a
Foot-shock, 4x, 0.5 mA, 0.5 s			Yes	Brown and Shepard, 2013
Foot-shock, 120x, 0.8 mA, 5-15 s			Yes	Brown and Shepard, 2013
Foot-shock, 5x, 0.5 mA, 0.8s			Yes	Sanchez-Catalan et al., 2017
Shock-paired tone, 20 s, 1 kHz,			Yes	Jhou et al., 2009a
Shock-paired tone, 15s, 4 kHz			Yes	Sanchez-Catalan et al., 2017
Foot-shock, 1x, 0.5 mA, 0.8 s			No	Sanchez-Catalan et al., 2017
Foot-shock, 1x, 0.8 mA, 0.8 s			No	Sanchez-Catalan et al., 2017
Foot-shock, 1x, 0.5 mA, 4 s			No	Sanchez-Catalan et al., 2017
Single tone, 3000 Hz, 1 s	Rat	c-Fos	No	Sanchez-Catalan et al., 2017
B-carboline	Rat	c-Fos	Yes, few	Sanchez-Catalan et al., 2017
LiCl	Rat	c-Fos	No	Sanchez-Catalan et al., 2017
LPS	Rat	c-Fos	No	Sanchez-Catalan et al., 2017
Naloxone	Rat	c-Fos	No	Sanchez-Catalan et al., 2017
Restraint stress, 1h/day, 10days	Rat	FosB/ΔFosB	No	Perrotti et al., 2015
Restraint stress, 1h		c-Fos	No	Sanchez-Catalan et al., 2017
Forced swim test	Rat	c-Fos	No	Sanchez-Catalan et al., 2017
Painful stimuli				
Inflammatory pain (carrageenan)	Rat	c-Fos	No	Sanchez-Catalan et al., 2017
Neuropathic pain (sciatic nerve compression)			No	Sanchez-Catalan et al., 2017
Predator odor (cat, fox)	Rat	c-Fos	No	Sanchez-Catalan et al., 2017
Precipitated opiate withdrawal	Rat	c-Fos	Yes	Sanchez-Catalan et al., 2017

LiCL, lithium chloride; LPS, lipopolyssacharide

increases intake and preference for ethanol, but not for sucrose, increases the conditioned place preference induced by ethanol and slows down the extinction process of alcohol seeking (Fu et al., 2016a; Sheth et al., 2016). Similarly, muscimol infusion into the tVTA/RMTg increases consumption and preference for ethanol as well as alcohol seeking behaviors, while AMPA stimulation of the tVTA/RMTg leads to opposite consequences (Fu et al., 2016b).

4.4. Avoidance behavior (Table 2)

The LHb is implicated in the response of aversive stimuli and reward prediction error (Matsumoto and Hikosaka, 2007). As a relay between the LHb and the VTA, the tVTA/RMTg seems to influence avoidance responses to aversive stimuli.

Both repetitive footshocks and shock-predictive cues markedly increase Fos expression in the center of the tVTA/RMTg, referred to as "core", with a 5-fold increase compared to unshocked rats (Jhou et al., 2009a). The tVTA/RMTg periphery shows similar results but with less Fos-positive neurons (Jhou et al., 2009a). This Fos expression in the tVTA/RMTg is visible for low (4 or 5 shocks at 0.5 mA, Table 2) and high intensities repetitive footshocks (120 shocks at 0.8 mA, Table 2) (Brown and Shepard, 2013; Jhou et al., 2009a), but it requires repetition of the shocks as a single footshock, even at high intensity, cannot induce Fos in the tVTA/RMTg (Sánchez-Catalán et al., 2017). Interestingly, the lesion of the fasciculus retroflexus suppresses Fos expression consecutive to low, but not high, intensity footshocks, suggesting a role for non-habenular inputs during exposure to highly aversive stimuli (Brown and Shepard, 2013).

Beside Fos expression after footshocks, a variety of other aversive stimuli has been tested, including chemical, stressful and nociceptive stimuli. The anxiogenic drug β-carboline induces relatively few Fos expression compared with the response to amphetamine (Sánchez-Catalán et al., 2017). Conversely, neither lithium chloride, naloxone at high dose nor lipopolysaccharide injections induced Fos in the tVTA/RMTg (Sánchez-Catalán et al., 2017). Similarly, aversive situations such as forced swim test or chronic and restraint stress do not recruit Fos in the tVTA/RMTg (Perrotti et al., 2005; Sánchez-Catalán et al., 2017). While it has been observed that paw pinching may stimulate almost ¾ of the tVTA/RMTg neurons (Lecca et al., 2011, 2012), painful stimuli such as inflammatory or neuropathic pain do not induce Fos locally (Sánchez-Catalán et al., 2017). While the tVTA/RMTg lesion reduces freezing behavior after predator odor exposure and increases the number of entries in the open arms of an elevated plus maze, indicating that such lesion can decrease fear responses (Jhou et al., 2009a), a predator

odor (trimehylthiazoline (fox odor), or cat odor) does not induce Fos in the tVTA/RMTg (Sánchez-Catalán et al., 2017).

Beside its rewarding properties, cocaine also displays aversive effects that persist longer that the rewarding ones. In a runway operant paradigm, in which animals have to reach the end of an alley to receive cocaine, prior studies found that cocaine progressively increases the latency to reach the goal compartment as well as alternations between approach and retreat behaviors (Geist and Ettenberg, 1997). Both the excitotoxic lesion and the optogenetic inhibition of the tVTA/RMTg, as well as the electrolytic lesion of the fasciculus retroflexus, prevent the development of conditioned avoidance to the goal compartment (Jhou et al., 2013), showing that the tVTA/RMTg is critical for the aversive properties of cocaine.

Finally, in mice, optogenetic stimulation of the LHb induces conditioned place avoidance by recruiting both dopamine neurons and tVTA/RMTg GABA neurons (Lammel et al., 2012). Moreover, stimulation of the LHb to tVTA/RMTg terminals promotes passive and conditioned avoidance behaviors and decreases the positive reinforcement to sucrose solution (Stamatakis and Stuber, 2012). Similarly, the pharmacological stimulation of the tVTA/RMTg by S-AMPA also induces conditioned place avoidance (Jhou et al., 2013).

4.5. Nociception and pain

First evidence linking the tVTA/RMTg and pain processing was provided by a study showing that endomorphin-1 or muscimol infusions into the tVTA/RMTg reduced the pain score in the second phase of the formalin test (Jhou et al., 2013). In a context of more sustained pain, such as sciatic nerve-related neuropathic pain induced using the spared nerve injury model, the capacity of tVTA/RMTg to inhibit dopamine cells is impaired (Sagheddu et al., 2015). While these findings are supportive of an impact of pain on the tVTA/RMTg, and of the tVTA/RMTg on pain responses, models of inflammatory or neuropathic pain do not induce Fos proteins in this brain region (Sánchez-Catalán et al., 2017).

4.6. Reward-related responses and reward prediction error

In the rat (Jhou et al., 2009a) and in the mouse (Tian et al., 2016), part of the tVTA/RMTg neurons can respond to rewarding or aversive stimuli and to their associated predictive cues and/or to reward omission. In this context, the LHb-tVTA/RMTg pathway has been shown in the rat to play a critical role in promoting negative reward prediction error in Pavlovian

conditioning (Laurent et al., 2017). Similar conclusions were also reached in non-human primate studies. Indeed, monkey putative tVTA/RMTg neurons are excited by the prediction of an absence of reward and inhibited by a prediction of reward (Hong et al., 2011). This encoding by the tVTA/RMTg is similar to the LHb one, and opposite to the dopamine one that appears around 20 msec later (Hong et al., 2011; Tian et al., 2016). Whereas electrophysiological recordings converge in implicating the tVTA/RMTg in reward prediction error, an imaging study in human failed to evidence a structure that may correspond to the tVTA/RMTg while studying error-related functional connectivity of the habenula (Ide and Li, 2011).

The tVTA/RMTg also contributes to punished inhibition of reward seeking. Indeed, the excitotoxic lesion of the tVTA/RMTg impairs the ability of footshocks to suppress operant responding for food. The optogenetic inhibition of tVTA/RMTg-VTA terminals also leads to resistance to punishment when this inhibition accompanies shock delivery (Vento et al., 2017).

In a probabilistic discounting task in which rats choose between a small but certain reward and a large but risky one, the inactivation of the LHb abolishes discernible choice bias. Similar results are obtained with tVTA/RMTg inactivation, indicating that subjective decision biases are mediated by the LHb-tVTA/RMTg pathway that in turn control dopamine neurons (Stopper and Floresco, 2014; Vento et al., 2017). Conversely, a stimulation of either the LHb or the tVTA/RMTg that is time-locked to the delivery of one of the rewards induces a behavioral toward the alternative option (Stopper et al., 2014).

4.7. Implication of the LHb-tVTA/RMTg pathway in motivation and depression

While neither forced swimming (Sánchez-Catalán et al., 2017) nor antidepressant drugs, such as fluoxetine, venlafaxine, nortriptyline or reboxetine, induce Fos in the tVTA/RMTg (Kaufling et al., 2010b), anatomical data and some experimental evidence relate the tVTA/RMTg with motivation and depressive-like behaviors. Indeed, the LHb is a main input to the tVTA/RMTg and has been linked to depression both in animal models and in humans (Knowland and Lim, 2018; Proulx et al., 2014; Sartorius et al., 2010). In animal studies, a stimulation of the LHb-tVTA/RMTg promotes avoidance responses (Stamatakis and Stuber, 2012), increases the immobility time in a forced swim test and reduces the effort to gain palatable food in a progressive ratio operant task (Proulx et al., 2018). Low intensity deep brain stimulation of the tVTA/RMTg also significantly decreases rat's food intake (Melse et al., 2016). Shocks provided according to a procedure usually leading to learned helplessness lead to Fos induction in the tVTA/RMTg (Brown and Shepard, 2013); and in this model of

depression the excitotoxic lesions of the tVTA/RMTg decreased the number of escape failures, while the electrical stimulation of the LHb increased escape failures (Elmer et al., 2018).

4.8. Control of the nigrostriatal pathway and motor activity

Immunohistochemical, electrophysiological and behavioral evidence highlight a tVTA/RMTg-SNc pathway that can contribute to motor control. Indeed, the tVTA/RMTg has dense axon fibers and terminals in the SNc (Ferreira et al., 2008; Jhou et al., 2009a, 2009b; Kaufling et al., 2010a), and the tVTA/RMTg fibers make apposition to TH-expressing neurons of the SNc (Bourdy et al., 2014; Jhou et al., 2009a). Moreover, electrical stimulation or chemical activation of the tVTA/RMTg decreases SNc dopamine neuron firing rate, while muscimol inhibition of the tVTA/RMTg leads to opposite effect (Bourdy et al., 2014). Following SNc unilateral lesion, rats with a concomitant unilateral tVTA/RMTg lesion shows an absence of the rotation bias induced by amphetamine administration (Bourdy et al., 2014). Moreover, a bilateral lesion of the tVTA/RMTg enhances motor performance and motor skill learning in a rotarod task (Bourdy et al., 2014), without inducing significant locomotor hyperactivity *per se* (Bourdy et al., 2014; Jhou et al., 2009a). On the other hand, chemical inactivation of the tVTA/RMTg with muscimol (Huff and LaLumiere, 2015; Lavezzi et al., 2015) or with co-infusion of muscimol and the GABA-B agonist baclofen (Huff and LaLumiere, 2015) produces robust locomotor activation (Huff and LaLumiere, 2015; Lavezzi et al., 2015). Conversely, bilateral infusion of the GABA-A antagonist bicucculine into the tVTA/RMTg blocks the locomotion induced by a disinhibition of the lateral preoptic area as well as the conditioned locomotion induced by chronic amphetamine administration (Lavezzi et al., 2015). Similarly, lesion of the μ-opioid receptor expressing cells in the tVTA/RMTg by the use of dermorphin-saporin increases the mean total ambulation without modifying the basal locomotor activity of the rats (Fu et al., 2016a).

4.9. The tVTA/RMTg and sleep regulation

VTA dopamine neurons contribute to arousal maintenance in animals (Oishi et al., 2017; Wisor et al., 2001) and humans (Saper et al., 2010). A recent study implicated the tVTA/RMTg in sleep regulation. Indeed, the DREADD activation of this structure promotes non-rapid eye movement sleep, with increased slow-wave activity, whereas the neurotoxic lesion of the tVTA/RMTg lead to opposite consequences (Yang et al., 2018). Moreover, rats with bilateral

ibotenic acid lesion of the tVTA/RMTg show reduced sleep homeostasis after sleep deprivation (Yang et al., 2018).

5. CONCLUSION

The tVTA/RMTg, whose connectivity was described in the rat brain in 2009, is now well characterized. Enriched in glutamate decarboxylase-67, it is the major brake of midbrain dopamine neurons. Expressing μ-opioid receptors, cannabinoid receptor 1 and being responsive to drugs acting on dopamine reuptake, it has a role in response to opiates, cannabinoids and psychostimulants. Acting as a relay between the LHb and midbrain dopamine neurons, it plays a role in reward-prediction error and in avoidance behaviors. Recent studies started to highlight new functions influenced by the tVTA/RMTg, demonstrating the importance to push forward the effort to improve our knowledge of this structure and its functions. Moreover, the recent discovery of specific precursors of its GABA neurons in mice may pave the way for phylogenetic studies to highlight the tVTA/RMTg across species.

6. ACKNOWLEDGEMENTS

This work was supported by the Centre National de la Recherche Scientifique [contracts UPR3212 and UMR5293], the University of Strasbourg, the Agence Nationale de la Recherche [ANR-15-CE37-0005-02; Euridol ANR-17-EURE-0022], the Fondation pour la Recherche Médicale [FDT20170437322], and by the NARSAD distinguish investigator grant from the Brain and Behavior Research Foundation [24220].

7. CONFLICT OF INTEREST STATEMENT

The authors declare no conflict of interest.

8. REFERENCES

Achim, K., Peltopuro, P., Lahti, L., Tsai, H.-H., Zachariah, A., Astrand, M., Salminen, M., Rowitch, D., Partanen, J., 2013. The role of Tal2 and Tal1 in the differentiation of midbrain GABAergic neuron precursors. Biol. Open 2, 990–997.

Aizawa, H., Kobayashi, M., Tanaka, S., Fukai, T., Okamoto, H., 2012. Molecular characterization of the subnuclei in rat habenula. J. Comp. Neurol. 520, 4051–4066.

Araki, M., McGeer, P.L., Kimura, H., 1988. The efferent projections of the rat lateral habenular nucleus revealed by the PHA-L anterograde tracing method. Brain Res. 441, 319–330.

Balcita-Pedicino, J.J., Omelchenko, N., Bell, R., Sesack, S.R., 2011. The inhibitory influence of the lateral habenula on midbrain dopamine cells: ultrastructural evidence for indirect mediation via the rostromedial mesopontine tegmental nucleus. J. Comp. Neurol. 519, 1143–1164.

Barrot, M., Georges, F., Veinante, P., 2016. Chapter25. The Tail of the Ventral Tegmental Area/ Rostromedial Tegmental Nucleus: A Modulator of Midbrain Dopamine Systems, in: Handbook of Basal Ganglia Structure and Function. Academic Press, pp. 495–511.

Bourdy, R., Barrot, M., 2012. A new control center for dopaminergic systems: pulling the VTA by the tail. Trends Neurosci. 35, 681–690.

Bourdy, R., Sánchez-Catalán, M.-J., Kaufling, J., Balcita-Pedicino, J.J., Freund-Mercier, M.-J., Veinante, P., Sesack, S.R., Georges, F., Barrot, M., 2014. Control of the nigrostriatal dopamine neuron activity and motor function by the tail of the ventral tegmental area. Neuropsychopharmacology 39, 2788–2798.

Brinschwitz, K., Dittgen, A., Madai, V.I., Lommel, R., Geisler, S., Veh, R.W., 2010. Glutamatergic axons from the lateral habenula mainly terminate on GABAergic neurons of the ventral midbrain. Neuroscience 168, 463–476.

Broms, J., Antolin-Fontes, B., Tingström, A., Ibañez-Tallon, I., 2015. Conserved expression of the GPR151 receptor in habenular axonal projections of vertebrates. J. Comp. Neurol. 523, 359–380.

Brown, P.L., Palacorolla, H., Brady, D., Riegger, K., Elmer, G.I., Shepard, P.D., 2017. Habenula-Induced Inhibition of Midbrain Dopamine Neurons Is Diminished by Lesions of the Rostromedial Tegmental Nucleus. J. Neurosci. 37, 217–225.

Brown, P.L., Shepard, P.D., 2016. Functional evidence for a direct excitatory projection from the lateral habenula to the ventral tegmental area in the rat. J. Neurophysiol. 116, 1161–1174.

Brown, P.L., Shepard, P.D., 2013. Lesions of the fasciculus retroflexus alter footshock-induced cFos expression in the mesopontine rostromedial tegmental area of rats. PloS One 8, e60678.

Christoph, G.R., Leonzio, R.J., Wilcox, K.S., 1986. Stimulation of the lateral habenula inhibits dopamine-containing neurons in the substantia nigra and ventral tegmental area of the rat. J. Neurosci. 6, 613–619.

Colussi-Mas, J., Geisler, S., Zimmer, L., Zahm, D.S., Bérod, A., 2007. Activation of afferents to the ventral tegmental area in response to acute amphetamine: a double-labelling study. Eur. J. Neurosci. 26, 1011–1025.

Cornish, J.L., Hunt, G.E., Robins, L., McGregor, I.S., 2012. Regional c-Fos and FosB/ΔFosB expression associated with chronic methamphetamine self-administration and methamphetamine-seeking behavior in rats. Neuroscience 206, 100–114.

Cui, W., Mizukami, H., Yanagisawa, M., Aida, T., Nomura, M., Isomura, Y., Takayanagi, R., Ozawa, K., Tanaka, K., Aizawa, H., 2014. Glial dysfunction in the mouse habenula causes depressive-like behaviors and sleep disturbance. J. Neurosci. 34, 16273–16285.

de Guglielmo, G., Melis, M., De Luca, M.A., Kallupi, M., Li, H.W., Niswender, K., Giordano, A., Senzacqua, M., Somaini, L., Cippitelli, A., Gaitanaris, G., Demopulos, G., Damadzic, R., Tapocik, J., Heilig, M., Ciccocioppo, R., 2015. PPARc activation attenuates opioid consumption and modulates mesolimbic dopamine transmission. Neuropsychopharmacology 40, 1052.

Elmer, G.I., Palacorolla, H., Mayo, C.L., Brown, P.L., Jhou, T.C., Brady, D., Shepard, P.D., 2018. The rostromedial tegmental nucleus modulates the development of stress-induced helpless behavior. Behav. Brain Res.

Ferreira, J.G.P., Del-Fava, F., Hasue, R.H., Shammah-Lagnado, S.J., 2008. Organization of ventral tegmental area projections to the ventral tegmental area-nigral complex in the rat. Neuroscience 153, 196–213.

Fu, R., Chen, X., Zuo, W., Li, J., Kang, S., Zhou, L.-H., Siegel, A., Bekker, A., Ye, J.-H., 2016a. Ablation of μ opioid receptor-expressing GABA neurons in rostromedial tegmental nucleus increases ethanol consumption and regulates ethanol-related behaviors. Neuropharmacology 107, 58–67.

Fu, R., Zuo, W., Gregor, D., Li, J., Grech, D., Ye, J.-H., 2016b. Pharmacological Manipulation of the Rostromedial Tegmental Nucleus Changes Voluntary and Operant Ethanol Self-Administration in Rats. Alcohol. Clin. Exp. Res. 40, 572–582.

Gao, P., Groenewegen, H.J., Vanderschuren, L.J.M.J., Voorn, P., 2018. Heterogeneous neuronal activity in the lateral habenula after short- and long-term cocaine self-administration in rats. Eur. J. Neurosci. 47, 83–94. https://doi.org/10.1111/ejn.13780

Geisler, S., Derst, C., Veh, R.W., Zahm, D.S., 2007. Glutamatergic afferents of the ventral tegmental area in the rat. J. Neurosci. 27, 5730–5743.

Geisler, S., Marinelli, M., Degarmo, B., Becker, M.L., Freiman, A.J., Beales, M., Meredith, G.E., Zahm, D.S., 2008. Prominent activation of brainstem and pallidal afferents of the ventral tegmental area by cocaine. Neuropsychopharmacology 33, 2688–2700.

Geist, T.D., Ettenberg, A., 1997. Concurrent positive and negative goalbox events produce runway behaviors comparable to those of cocaine-reinforced rats. Pharmacol. Biochem. Behav. 57, 145–150.

Glover, E.J., McDougle, M.J., Siegel, G.S., Jhou, T.C., Chandler, L.J., 2016. Role for the Rostromedial Tegmental Nucleus in Signaling the Aversive Properties of Alcohol. Alcohol. Clin. Exp. Res. 40, 1651–1661.

Gonçalves, L., Sego, C., Metzger, M., 2012. Differential projections from the lateral habenula to the rostromedial tegmental nucleus and ventral tegmental area in the rat. J. Comp. Neurol. 520, 1278–1300.

Good, C.H., Wang, H., Chen, Y.-H., Mejias-Aponte, C.A., Hoffman, A.F., Lupica, C.R., 2013. Dopamine D4 receptor excitation of lateral habenula neurons via multiple cellular mechanisms. J. Neurosci. 33, 16853–16864.

Herkenham, M., Nauta, W.J., 1979. Efferent connections of the habenular nuclei in the rat. J. Comp. Neurol. 187, 19–47.

Hong, S., Jhou, T.C., Smith, M., Saleem, K.S., Hikosaka, O., 2011. Negative reward signals from the lateral habenula to dopamine neurons are mediated by rostromedial tegmental nucleus in primates. J. Neurosci. 31, 11457–11471.

Huff, M.L., LaLumiere, R.T., 2015. The rostromedial tegmental nucleus modulates behavioral inhibition following cocaine self-administration in rats. Neuropsychopharmacology 40, 861–873.

Ide, J.S., Li, C.-S.R., 2011. Error-related functional connectivity of the habenula in humans. Front. Hum. Neurosci. 5, 25.

Ikemoto, S., 2007. Dopamine reward circuitry: two projection systems from the ventral midbrain to the nucleus accumbens-olfactory tubercle complex. Brain Res. Rev. 56, 27–78.

Jalabert, M., Bourdy, R., Courtin, J., Veinante, P., Manzoni, O.J., Barrot, M., Georges, F., 2011. Neuronal circuits underlying acute morphine action on dopamine neurons. Proc. Natl. Acad. Sci. U. S. A. 108, 16446–16450. h

Jhou, T., 2005. Neural mechanisms of freezing and passive aversive behaviors. J. Comp. Neurol. 493, 111–114.

Jhou, T.C., Fields, H.L., Baxter, M.G., Saper, C.B., Holland, P.C., 2009a. The rostromedial tegmental nucleus (RMTg), a GABAergic afferent to midbrain dopamine neurons, encodes aversive stimuli and inhibits motor responses. Neuron 61, 786–800.

Jhou, T.C., Geisler, S., Marinelli, M., Degarmo, B.A., Zahm, D.S., 2009b. The mesopontine rostromedial tegmental nucleus: A structure targeted by the lateral habenula that projects to the ventral tegmental area of Tsai and substantia nigra compacta. J. Comp. Neurol. 513, 566–596.

Jhou, T.C., Good, C.H., Rowley, C.S., Xu, S.-P., Wang, H., Burnham, N.W., Hoffman, A.F., Lupica, C.R., Ikemoto, S., 2013. Cocaine drives aversive conditioning via delayed activation of dopamine-responsive habenular and midbrain pathways. J. Neurosci. 33, 7501–7512.

Jhou, T.C., Xu, S.-P., Lee, M.R., Gallen, C.L., Ikemoto, S., 2012. Mapping of reinforcing and analgesic effects of the mu opioid agonist endomorphin-1 in the ventral midbrain of the rat. Psychopharmacology (Berl.) 224, 303–312.

Ji, H., Shepard, P.D., 2007. Lateral habenula stimulation inhibits rat midbrain dopamine neurons through a GABA(A) receptor-mediated mechanism. J. Neurosci. 27, 6923–6930.

Johnson, S.W., North, R.A., 1992. Opioids excite dopamine neurons by hyperpolarization of local interneurons. J. Neurosci. 12, 483–488.

Kaufling, J., Aston-Jones, G., 2015. Persistent Adaptations in Afferents to Ventral Tegmental Dopamine Neurons after Opiate Withdrawal. J. Neurosci. 35, 10290–10303.

Kaufling, J., Veinante, P., Pawlowski, S.A., Freund-Mercier, M.-J., Barrot, M., 2010a. gamma-Aminobutyric acid cells with cocaine-induced DeltaFosB in the ventral tegmental area innervate mesolimbic neurons. Biol. Psychiatry 67, 88–92.

Kaufling, J., Veinante, P., Pawlowski, S.A., Freund-Mercier, M.-J., Barrot, M., 2009. Afferents to the GABAergic tail of the ventral tegmental area in the rat. J. Comp. Neurol. 513, 597–621.

Kaufling, J., Waltisperger, E., Bourdy, R., Valera, A., Veinante, P., Freund-Mercier, M.-J., Barrot, M., 2010b. Pharmacological recruitment of the GABAergic tail of the ventral tegmental area by acute drug exposure. Br. J. Pharmacol. 161, 1677–1691.

Kim, U., 2009. Topographic commissural and descending projections of the habenula in the rat. J. Comp. Neurol. 513, 173–187.

Knowland, D., Lim, B.K., 2018. Circuit-based frameworks of depressive behaviors: The role of reward circuitry and beyond. Pharmacol. Biochem. Behav. In press.

Köbbert, C., Apps, R., Bechmann, I., Lanciego, J.L., Mey, J., Thanos, S., 2000. Current concepts in neuroanatomical tracing. Prog. Neurobiol. 62, 327–351.

Lahti, L., Haugas, M., Tikker, L., Airavaara, M., Voutilainen, M.H., Anttila, J., Kumar, S., Inkinen, C., Salminen, M., Partanen, J., 2016. Differentiation and molecular heterogeneity of inhibitory and excitatory neurons associated with midbrain dopaminergic nuclei. Dev. Camb. Engl. 143, 516–529.

Lammel, S., Lim, B.K., Ran, C., Huang, K.W., Betley, M.J., Tye, K.M., Deisseroth, K., Malenka, R.C., 2012. Input-specific control of reward and aversion in the ventral tegmental area. Nature 491, 212–217.

Laurent, V., Wong, F.L., Balleine, B.W., 2017. The Lateral Habenula and Its Input to the Rostromedial Tegmental Nucleus Mediates Outcome-Specific Conditioned Inhibition. J. Neurosci. 37, 10932–10942.

Lavezzi, H.N., Parsley, K.P., Zahm, D.S., 2015. Modulation of locomotor activation by the rostromedial tegmental nucleus. Neuropsychopharmacology 40, 676–687.

Lavezzi, H.N., Parsley, K.P., Zahm, D.S., 2012. Mesopontine rostromedial tegmental nucleus neurons projecting to the dorsal raphe and pedunculopontine tegmental nucleus: psychostimulant-elicited Fos expression and collateralization. Brain Struct. Funct. 217, 719–734.

Lecca, S., Melis, M., Luchicchi, A., Ennas, M.G., Castelli, M.P., Muntoni, A.L., Pistis, M., 2011. Effects of drugs of abuse on putative rostromedial tegmental neurons, inhibitory afferents to midbrain dopamine cells. Neuropsychopharmacology 36, 589–602.

Lecca, S., Melis, M., Luchicchi, A., Muntoni, A.L., Pistis, M., 2012. Inhibitory inputs from rostromedial tegmental neurons regulate spontaneous activity of midbrain dopamine cells and their responses to drugs of abuse. Neuropsychopharmacology 37, 1164–1176.

Li, B., Piriz, J., Mirrione, M., Chung, C., Proulx, C.D., Schulz, D., Henn, F., Malinow, R., 2011. Synaptic potentiation onto habenula neurons in the learned helplessness model of depression. Nature 470, 535–539.

Mahler, S.V., Aston-Jones, G.S., 2012. Fos activation of selective afferents to ventral tegmental area during cue-induced reinstatement of cocaine seeking in rats. J. Neurosci. 32, 13309–13326.

Maroteaux, M., Mameli, M., 2012. Cocaine evokes projection-specific synaptic plasticity of lateral habenula neurons. J. Neurosci. 32, 12641–12646.

Matsuda, Y., Fujimura, K., 1992. Action of habenular efferents on ventral tegmental area neurons studied in vitro. Brain Res. Bull. 28, 743–749.

Matsui, A., Jarvie, B.C., Robinson, B.G., Hentges, S.T., Williams, J.T., 2014. Separate GABA afferents to dopamine neurons mediate acute action of opioids, development of tolerance, and expression of withdrawal. Neuron 82, 1346–1356.

Matsui, A., Williams, J.T., 2011. Opioid-sensitive GABA inputs from rostromedial tegmental nucleus synapse onto midbrain dopamine neurons. J. Neurosci. 31, 17729–17735.

Matsumoto, M., Hikosaka, O., 2007. Lateral habenula as a source of negative reward signals in dopamine neurons. Nature 447, 1111–1115.

Melis, M., De Felice, M., Lecca, S., Fattore, L., Pistis, M., 2013. Sex-specific tonic 2-arachidonoylglycerol signaling at inhibitory inputs onto dopamine neurons of Lister Hooded rats. Front. Integr. Neurosci. 7, 93.

Melis, M., Sagheddu, C., De Felice, M., Casti, A., Madeddu, C., Spiga, S., Muntoni, A.L., Mackie, K., Marsicano, G., Colombo, G., Castelli, M.P., Pistis, M., 2014. Enhanced endocannabinoid-mediated modulation of rostromedial tegmental nucleus drive onto dopamine neurons in Sardinian alcohol-preferring rats. J. Neurosci. 34, 12716–12724.

Melse, M., Temel, Y., Tan, S.K., Jahanshahi, A., 2016. Deep brain stimulation of the rostromedial tegmental nucleus: An unanticipated, selective effect on food intake. Brain Res. Bull. 127, 23–28.

Meye, F.J., Valentinova, K., Lecca, S., Marion-Poll, L., Maroteaux, M.J., Musardo, S., Moutkine, I., Gardoni, F., Huganir, R.L., Georges, F., Mameli, M., 2015. Cocaine-evoked negative symptoms require AMPA receptor trafficking in the lateral habenula. Nat. Neurosci. 18, 376–378.

Navailles, S., Guillem, K., Vouillac-Mendoza, C., Ahmed, S.H., 2015. Coordinated Recruitment of Cortical-Subcortical Circuits and Ascending Dopamine and Serotonin Neurons During Inhibitory Control of Cocaine Seeking in Rats. Cereb. Cortex 991 25, 3167–3181.

Oishi, Y., Suzuki, Y., Takahashi, K., Yonezawa, T., Kanda, T., Takata, Y., Cherasse, Y., Lazarus, M., 2017. Activation of ventral tegmental area dopamine neurons produces wakefulness through dopamine D2-like receptors in mice. Brain Struct. Funct. 222, 2907–2915.

Olson, V.G., Nestler, E.J., 2007. Topographical organization of GABAergic neurons within the ventral tegmental area of the rat. Synap. 61, 87–95.

Olson, V.G., Zabetian, C.P., Bolanos, C.A., Edwards, S., Barrot, M., Eisch, A.J., Hughes, T., Self, D.W., Neve, R.L., Nestler, E.J., 2005. Regulation of drug reward by cAMP response element-binding protein: evidence for two functionally distinct subregions of the ventral tegmental area. J. Neurosci. 25, 5553–5562.

Pang, Y., Kiba, H., Jayaraman, A., 1993. Acute nicotine injections induce c-fos mostly in non-dopaminergic neurons of the midbrain of the rat. Brain Res. Mol. 20, 162–170.

Paxinos, G., Watson, C., 2014. The Rat Brain in Stereotaxic Coordinates. Academic Press.

Perrotti, L.I., Bolaños, C.A., Choi, K.-H., Russo, S.J., Edwards, S., Ulery, P.G., Wallace, D.L., Self, D.W., Nestler, E.J., Barrot, M., 2005. DeltaFosB accumulates in a GABAergic cell population in the posterior tail of the ventral tegmental area after psychostimulant treatment. Eur. J. Neurosci. 21, 2817–2824.

Petzel, A., Bernard, R., Poller, W.C., Veh, R.W., 2017. Anterior and posterior parts of the rat ventral tegmental area and the rostromedial tegmental nucleus receive topographically distinct afferents from the lateral habenular complex. J. Comp. Neurol. 525, 2310–2327.

Poller, W.C., Madai, V.I., Bernard, R., Laube, G., Veh, R.W., 2013. A glutamatergic projection from the lateral hypothalamus targets VTA-projecting neurons in the lateral habenula of the rat. Brain Res. 1507, 45–60.

Polter, A.M., Barcomb, K., Tsuda, A.C., Kauer, J.A., 2018. Synaptic function and plasticity in identified inhibitory inputs onto VTA dopamine neurons. Eur. J. Neurosci.

Proulx, C.D., Aronson, S., Milivojevic, D., Molina, C., Loi, A., Monk, B., Shabel, S.J., Malinow, R., 2018. A neural pathway controlling motivation to exert effort. Proc. Natl. Acad. Sci. U. S. A. 115, 5792–5797.

Proulx, C.D., Hikosaka, O., Malinow, R., 2014. Reward processing by the lateral habenula in normal and depressive behaviors. Nat. Neurosci. 17, 1146–1152.

Quina, L.A., Tempest, L., Ng, L., Harris, J.A., Ferguson, S., Jhou, T.C., Turner, E.E., 2015. Efferent pathways of the mouse lateral habenula. J. Comp. Neurol. 523, 32–60.

Robertson, B., Kardamakis, A., Capantini, L., Pérez-Fernández, J., Suryanarayana, S.M., Wallén, P., Stephenson-Jones, M., Grillner, S., 2014. The lamprey blueprint of the mammalian nervous system. Prog. Brain Res. 212, 337–349.

Rotllant, D., Márquez, C., Nadal, R., Armario, A., 2010. The brain pattern of c-fos induction by two doses of amphetamine suggests different brain processing pathways and minor contribution of behavioural traits. Neuroscience 168, 691–705.

Sagheddu, C., Aroni, S., De Felice, M., Lecca, S., Luchicchi, A., Melis, M., Muntoni, A.L., Romano, R., Palazzo, E., Guida, F., Maione, S., Pistis, M., 2015. Enhanced serotonin and mesolimbic dopamine transmissions in a rat model of neuropathic pain. Neuropharmacology 97, 383–393.

Sánchez-Catalán, M.-J., Faivre, F., Yalcin, I., Muller, M.-A., Massotte, D., Majchrzak, M., Barrot, M., 2017. Response of the Tail of the Ventral Tegmental Area to Aversive Stimuli. Neuropsychopharmacology 42, 638–648.

Sanchez-Catalan, M.J., Kaufling, J., Georges, F., Veinante, P., Barrot, M., 2014. The antero-posterior heterogeneity of the ventral tegmental area. Neuroscience 282, 198–216.

Saper, C.B., Fuller, P.M., Pedersen, N.P., Lu, J., Scammell, T.E., 2010. Sleep state switching. Neuron 68, 1023–1042.

Sartorius, A., Kiening, K.L., Kirsch, P., von Gall, C.C., Haberkorn, U., Unterberg, A.W., Henn, F.A., Meyer-Lindenberg, A., 2010. Remission of major depression under deep brain stimulation of the lateral habenula in a therapy-refractory patient. Biol. Psychiatry 67, e9–e11.

Scammell, T.E., Estabrooke, I.V., McCarthy, M.T., Chemelli, R.M., Yanagisawa, M., Miller, M.S., Saper, C.B., 2000. Hypothalamic arousal regions are activated during modafinil-induced wakefulness. J. Neurosci. 20, 8620–8628.

Sego, C., Gonçalves, L., Lima, L., Furigo, I.C., Donato, J., Metzger, M., 2014. Lateral habenula and the rostromedial tegmental nucleus innervate neurochemically distinct subdivisions of the dorsal raphe nucleus in the rat. J. Comp. Neurol. 522, 1454–1484.

Sheth, C., Furlong, T.M., Keefe, K.A., Taha, S.A., 2016. Lesion of the rostromedial tegmental nucleus increases voluntary ethanol consumption and accelerates extinction of ethanol-induced conditioned taste aversion. Psychopharmacology (Berl.) 233, 3737–3749.

Siuda, E.R., Copits, B.A., Schmidt, M.J., Baird, M.A., Al-Hasani, R., Planer, W.J., Funderburk, S.C., McCall, J.G., Gereau, R.W., Bruchas, M.R., 2015. Spatiotemporal control of opioid signaling and behavior. Neuron 86, 923–935.

Stamatakis, A.M., Stuber, G.D., 2012. Activation of lateral habenula inputs to the ventral midbrain promotes behavioral avoidance. Nat. Neurosci. 15, 1105–1107.

Steidl, S., Dhillon, E.S., Sharma, N., Ludwig, J., 2017. Muscarinic cholinergic receptor antagonists in the VTA and RMTg have opposite effects on morphine-induced locomotion in mice. Behav. Brain Res. 323, 111–116.

Stephenson-Jones, M., Floros, O., Robertson, B., Grillner, S., 2012. Evolutionary conservation of the habenular nuclei and their circuitry controlling the dopamine and 5-hydroxytryptophan (5-HT) systems. Proc. Natl. Acad. Sci. U. S. A. 109, E164-173.

Stopper, C.M., Floresco, S.B., 2014. What's better for me? Fundamental role for lateral habenula in promoting subjective decision biases. Nat. Neurosci. 17, 33–35.

Stopper, C.M., Tse, M.T.L., Montes, D.R., Wiedman, C.R., Floresco, S.B., 2014. Overriding phasic dopamine signals redirects action selection during risk/reward decision making. Neuron 84, 177–189.

Tian, J., Huang, R., Cohen, J.Y., Osakada, F., Kobak, D., Machens, C.K., Callaway, E.M., Uchida, N., Watabe-Uchida, M., 2016. Distributed and Mixed Information in Monosynaptic Inputs to Dopamine Neurons. Neuron 91, 1374–1389.

Vento, P.J., Burnham, N.W., Rowley, C.S., Jhou, T.C., 2017. Learning From One's Mistakes: A Dual Role for the Rostromedial Tegmental Nucleus in the Encoding and Expression of Punished Reward Seeking. Biol. Psychiatry 81, 1041–1049.

Wasserman, D.I., Tan, J.M.J., Kim, J.C., Yeomans, J.S., 2016. Muscarinic control of rostromedial tegmental nucleus GABA neurons and morphine-induced locomotion. Eur. J. Neurosci. 44, 1761–1770.

Wasserman, D.I., Wang, H.G., Rashid, A.J., Josselyn, S.A., Yeomans, J.S., 2013. Cholinergic control of morphine-induced locomotion in rostromedial tegmental nucleus versus ventral tegmental area sites. Eur. J. Neurosci. 38, 2774–2785.

Wisor, J.P., Nishino, S., Sora, I., Uhl, G.H., Mignot, E., Edgar, D.M., 2001. Dopaminergic role in stimulant-induced wakefulness. J. Neurosci. 21, 1787–1794.

Yang, S.-R., Hu, Z.-Z., Luo, Y.-J., Zhao, Y.-N., Sun, H.-X., Yin, D., Wang, C.-Y., Yan, Y.-D., Wang, D.-R., Yuan, X.-S., Ye, C.-B., Guo, W., Qu, W.-M., Cherasse, Y., Lazarus, M., Ding, Y.-Q., Huang, Z.-L., 2018. The rostromedial tegmental nucleus is essential for non-rapid eye movement sleep. PLoS Biol. 16, e2002909. In press.

Yetnikoff, L., Cheng, A.Y., Lavezzi, H.N., Parsley, K.P., Zahm, D.S., 2015. Sources of input to the rostromedial tegmental nucleus, ventral tegmental area, and lateral habenula compared: A study in rat. J. Comp. Neurol. 523, 2426–2456.

Yetnikoff, L., Lavezzi, H.N., Reichard, R.A., Zahm, D.S., 2014. An update on the connections of the ventral mesencephalic dopaminergic complex. Neuroscience 282, 23–48.

Zahm, D.S., Becker, M.L., Freiman, A.J., Strauch, S., Degarmo, B., Geisler, S., Meredith, G.E., Marinelli, M., 2010. Fos after single and repeated self-administration of cocaine and saline in the rat: emphasis on the Basal forebrain and recalibration of expression. Neuropsychopharmacology 35, 445–463.

Zhao-Shea, R., Liu, L., Soll, L.G., Improgo, M.R., Meyers, E.E., McIntosh, J.M., Grady, S.R., Marks, M.J., Gardner, P.D., Tapper, A.R., 2011. Nicotine-mediated activation of dopaminergic neurons in distinct regions of the ventral tegmental area. Neuropsychopharmacology 36, 1021–1032.

Stimulus	Marqueur d'activation	Induction ?	Référence
Choc électrique aux pattes, 4x, 0,5 mA, 0,5 s	c-Fos	Oui	(Jhou et al., 2009a)
Choc électrique aux pattes, 4x, 0,5 mA, 0,5 s	c-Fos	Oui	(Brown and Shepard, 2013)
Choc électrique aux pattes, 120x, 0.8 mA, 0,5 s	c-Fos	Oui	(Brown and Shepard, 2013)
Son (stimulus conditionnel)	c-Fos	Oui	(Jhou et al., 2009a)
Stress de contention répété (1h/jour, 10 jours)	FosB/ΔFosB	Non	(Perrotti et al., 2005)
Stress de contention ; aigu	c-Fos	Non	(Barrot et al., 2015)
Test de la nage forcée	c-Fos	Non	(Barrot et al., 2015)
Odeur de prédateur (chat)	c-Fos	Non	(Barrot et al., 2015)
Odeur de prédateur (triméthylthiazoline)	c-Fos	Non	(Barrot et al., 2015)
Carragénine intra-plantaire (douleur inflammatoire)	c-Fos	Non	(Barrot et al., 2015)
Compression du nerf sciatique (douleur neuropathique)	c-Fos	Non	(Barrot et al., 2015)
LiCl	c-Fos	Non	(Barrot et al., 2015)
Lipopolyssacharide	c-Fos	Non	(Barrot et al., 2015)

Table 3. Réponse de la tVTA à des stimuli aversifs (*adapté de Barrot et al, 2017*). Etat des connaissances fin 2015

b3. Implication de la tVTA dans la réponse aux stimuli aversifs

La LHb est impliquée dans la détection des erreurs de prédiction de récompense. Dans une étude réalisée chez le primate, les chercheurs ont montré que les neurones de la LHb étaient excités par des signaux signalant une absence de récompense et inhibés par ceux prédisant une récompense. De manière intéressante, ils ont montré que les neurones dopaminergiques du mésencéphale répondaient de manière inverse et que la stimulation de la LHb entraînait une inhibition des neurones dopaminergiques (Matsumoto and Hikosaka, 2007). Une étude similaire a montré que la tVTA répondait de manière identique à la LHb dans le traitement de ces informations récompensantes et qu'elle était donc un relai potentiel entre la LHb et les neurones dopaminergiques du mésencéphale (Hong et al., 2011). La stimulation optogénétique des terminaisons de la LHb dans la tVTA entraîne, chez la souris, l'apparition de comportements d'évitement passif, actif et conditionné (Stamatakis and Stuber, 2012) et la stimulation pharmacologique de la tVTA chez le rat produit une aversion de place conditionnée (Jhou et al., 2013). Cette structure présente une réponse moléculaire (induction du facteur de transcription c-Fos) à un stimulus aversif imprévisible comme un choc électrique (Table 3) (Jhou et al., 2009a; Brown and Shepard, 2013) et la lésion excitotoxique de la tVTA supprime le comportement d'immobilité du rat dans un test de peur conditionnée, les réponses comportementales d'immobilité face à une odeur de prédateur, les comportements de type anxio-dépressifs dans le test du labyrinthe en croix-surélevé (Jhou et al., 2009a) et les comportements d'évitement induits par la cocaïne (Jhou et al., 2013) (Table 3).

Il était donc important d'explorer la réponse de la tVTA à différents stimulus aversifs en utilisant comme contrôle positif la production de c-Fos en réponse à la D-amphétamine. Les premières expériences avaient déjà été réalisées par Maria-José Sanchez-Catalan lors de mon arrivée en thèse et le manuscrit avait été soumis à *Neuropsychopharmacology*. J'ai donc pu être incluse dans ce projet en réalisant les expériences complémentaires demandées par les reviewers. Cette étude a conduit à la publication de mon premier article en tant que co-premier auteur.

A. Vérification neurochimique

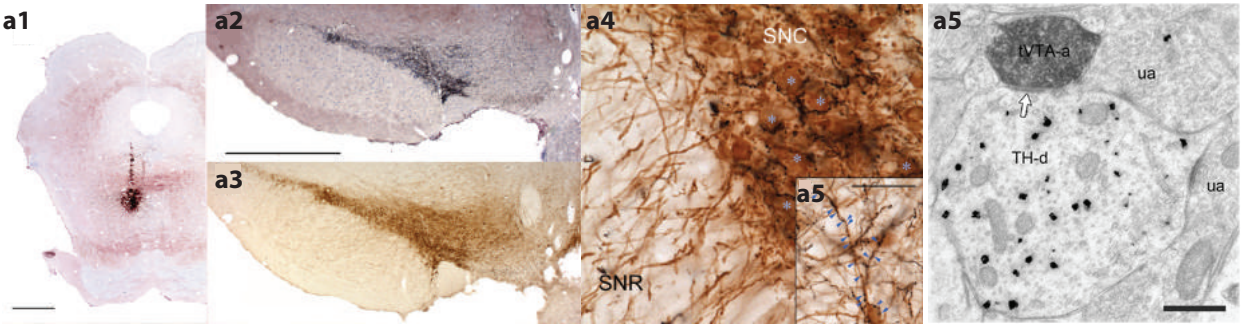

B. Vérification électrophysiologique

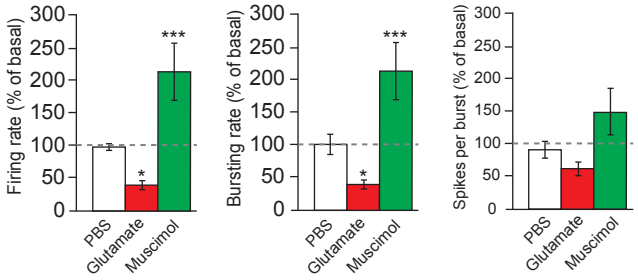

C. Vérification comportementale

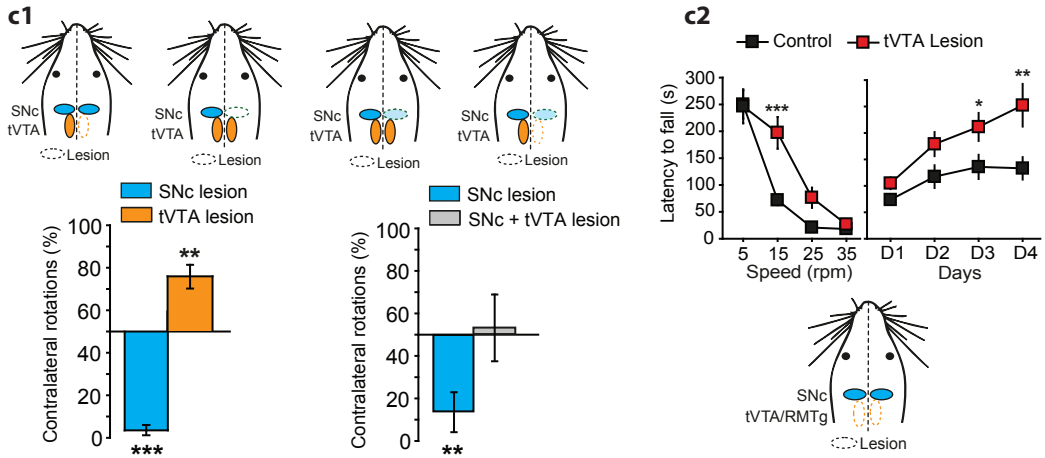

Figure 6. La tVTA dans le contrôle de la voie nigro-striée. (A) Une injection de BDA dans la tVTA (a1) produit un marquage axonal dans les neurones dopaminergiques de la SNc (a2 et a3). A plus fort grossissement (a4), il est possible de voir que les fibres issues de la tVTA contactent les neurones de la SNc (a5) (Jhou et al., 2009a). En microscopie électronique (a5), les axones terminaux de la tVTA (tVTA-a) forment des synapses (flèche) au niveau des dendrites de neurones de la SNc (TH-d) (Bourdy et al, 2014). (B) Conséquences d'une inhibition (muscimol, vert) ou d'une activation (glutamate, rouge) de la tVTA sur les neurones dopaminergiques de la SNc (Bourdy et al., 2014). (C) (c1) Une lésion unilatérale de la SNc (bleu) entraîne un biais de rotation ispilatéral alors que la lésion unilatérale de la tVTA (orange) entraîne un biais de rotation controlatéral, après administration de D-amphétamine. Chez des rats avec une lésion unilatérale partielle de la SNc, une co-lésion de la tVTA ispilatérale compense le biais de rotation induit par la D-amphétamine. (c2) Après une lésion bilatérale de la tVTA, les performances motrices et l'apprentissage moteur des rats dans un test de rotarod sont améliorés (Bourdy et al., 2014).

C. La tVTA dans le contrôle des fonctions motrices

c1. Contexte bibliographique

Les neurones dopaminergiques du mésencéphale sont impliqués dans de nombreuses pathologies psychiatriques et neurologiques. La destruction de ces neurones dans la maladie de Parkinson entraîne l'apparition des symptômes moteurs caractéristiques de cette maladie. Notre équipe a montré que la tVTA, par les projections qu'elle envoie en direction des neurones de la VTA et de la substance noire *pars compacta* (SNc) (Jhou et al., 2009a) (Figure 6A), permet le contrôle des fonctions motrices (Bourdy et al., 2014).

Dans l'article du Docteur Romain Bourdy, doctorant me précédant sur ce sujet, il a été montré qu'une inhibition de la tVTA par du muscimol augmente l'activité des neurones de la SNc et qu'à l'inverse son activation par du glutamate inhibe les neurones de la SNc (Figure 6B). De plus, l'ablation de la tVTA permet, dans un modèle de lésion unilatérale de la SNc, de compenser le biais de rotation induit par une injection de D-amphétamine (Bourdy et al., 2014). Une autre expérience a mis en évidence que cette ablation entraînait une augmentation des performances motrices des rats soumis au test du rotarod (Figure 6C).

Cliniquement, le diagnostic de la maladie de Parkinson intervient à partir du moment où une triade de symptômes moteurs apparaît : une akinésie (difficulté à initier certains mouvements), une rigidité des membres et des tremblements au repos. Néanmoins, il est fréquent que ces patients se plaignent également de divers symptômes non-moteurs comme des symptômes neuropsychiatriques (anxiété, dépression, trouble du sommeil), des troubles du système autonome (nausée, constipation, perte de poids) et des troubles du système sensoriel (douleur, paresthésie) et il est désormais reconnu que ces symptômes apparaissent parfois des années avant l'apparition des premiers symptômes moteurs (Chaudhuri et al., 2006; Park and Stacy, 2009). C'est dans ce contexte que nous avons entrepris d'évaluer la présence de certain de ces symptômes dans un modèle de maladie de Parkinson afin de pouvoir vérifier si l'ablation de la tVTA pouvait également permettre de les compenser. Devant le peu de connaissance sur les symptômes non-moteurs dans les modèles pré-clinique de la maladie de Parkinson, il nous a paru important de réaliser une étude de la littérature afin de voir si ces symptômes avaient déjà été observés par d'autres équipes et d'entreprendre l'écriture d'une revue sur ce sujet.

c2. The hidden side of Parkinson's disease: studying pain, anxiety and depression in pre-clinical models.

The hidden side of Parkinson's disease:
studying pain, anxiety and depression in animal models

Fanny Faivre [a], Anil Joshi [a], Erwan Bezard [b,c], Michel Barrot [a,*]

[a] Centre National de la Recherche Scientifique, Université de Strasbourg, Institut des Neurosciences Cellulaires et Intégratives, F-67000 Strasbourg, France

[b] Université de Bordeaux, Institut des Maladies Neurodégénératives, UMR 5293, F-33000 Bordeaux, France;

[c] Centre National de la Recherche Scientifique, Institut des Maladies Neurodégénératives, UMR 5293, F-33000 Bordeaux, France

* Corresponding author at: Institut des Neurosciences Cellulaires et Intégratives, 5 rue Blaise Pascal, F-67000 Strasbourg, France
E-mail address: mbarrot@inci-cnrs.unistra.fr

ABSTRACT

Parkinson's disease is a neurodegenerative disease leading to the loss of midbrain dopamine neurons. It is well known and characterized by motor symptoms that are secondary to the loss of dopamine innervation, but it is also accompanied by a range of various non-motor symptoms, including pain and psychiatric disorders such as anxiety and depression. These non-motor symptoms usually appear at early stages of the disease, sometimes even before the first motor symptoms, and have a dramatic impact on the quality of life of the patients. We review here the present state-of-the-art concerning pain, anxiety and depression-like parameters in animal models of Parkinson's disease.

Keywords: Parkinson's disease; non-motor symptoms; pain; anxiety; depression

Parkinson's disease is a neurodegenerative disorder classically known for the loss of dopamine neurons in the midbrain, and most often accompanied by the presence of cytoplasmic inclusions of α-synuclein proteins called Lewy bodies. However, although the disease is primarily related to the loss of the nigrostriatal pathway, several other brain areas are also degenerating (often to a lesser extent), including the locus coeruleus, the dorsal raphe nucleus, the nucleus basalis of Meynert, the pedunculopontine nucleus, with a cortical thinning occuring at later stage(Ehringer and Hornykiewicz, 1960; Halliday et al., 1990; Jellinger, 1991; Zarow et al., 2003). Synuclein pathology is not restricted either to the nigrostriatal pathway but displays extensive spread in the nervous system. Indeed, observations of post-mortem human brains (Braak et al., 2002, 2003, 2004) showed early Lewy bodies inclusions in the IX (glossopharyngeal) and X (vagal) nerves and in the olfactory bulbs, later spreading beyond these structures to include the lower raphe nuclei, the magnocellular portion of the reticular formation and the locus coeruleus, to then affect the substantia nigra pars compacta, and finally gradually invade the entire neocortex.

Clinically, Parkinson's disease is classically defined by a triad of motor symptoms: bradykinesia (*i.e.* a slowdown to initiate voluntary movements), muscle rigidity and resting tremors. Beside these classical symptoms, different non-motor symptoms can be present and sometimes even appear a long time before the first motor symptoms (Bezard and Fernagut, 2014; Blanchet and Brefel-Courbon, 2017; Pont-Sunyer et al., 2015), which may lead to a misdiagnosis or delayed diagnosis (O'Sullivan et al., 2008) and has a negative impact on the quality of life of the patients (Nègre-Pagès et al., 2008; Rieu et al., 2016). Three major phases have thus been proposed to describe the development of Parkinson's disease (Stern et al., 2012). The phase 1, the "preclinical Parkinson's disease", corresponds to the beginning of the α-synuclein accumulation in the central and/or the peripheral autonomic nervous system, in the absence of detectable clinical signs. The second phase, referred to either as "pre-motor" or "prodromal" phase, can exceed ten years before the clinical diagnosis of the disease and is usually associated to the apparition of non-motor symptoms due in part to extranigral alterations. It should also be noticed that early subtle motor symptoms can often be present in this prodromal phase of the disease (Mahlknecht et al., 2015). During this phase, Parkinson's disease patient can display higher anxiety as early as 16 years before the diagnosis of the disease; and depression becomes significantly prevalent among Parkinson's disease patients in the last 2-3 years preceding the diagnostic (Darweesh et al., 2017). The phase 3 is the "motor Parkinson's disease", which is the one that is clinically visible and more easily diagnosed.

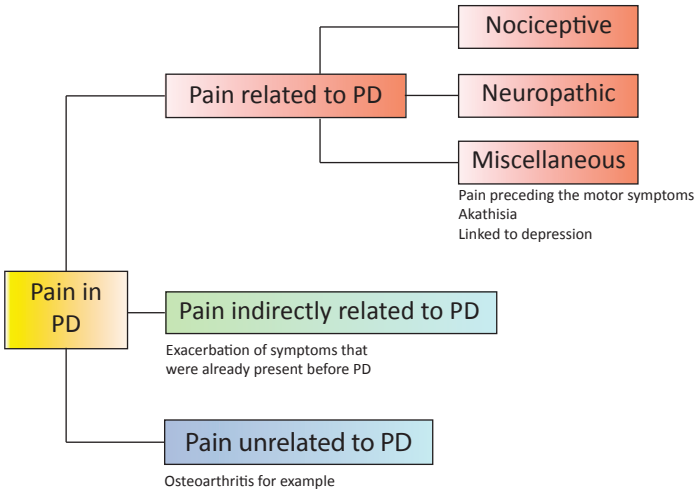

Figure 7. Classification of pain in Parkinson's disease (adapted from Wasner and Deuschl, 2012). Pain directly or partly related to PD can be either nociceptive pain, neuropathic pain or miscellaneous pain. Other types of pain include pain indirectly related to PD, pain that can be aggravated by the disease, and pain unrelated to PD. PD, Parkinson's disease.

The non-motor symptoms include notably (but not exclusively) sleep disorders, gastrointestinal and autonomic symptoms (nausea, constipation), sensory symptoms (olfactory disturbance), pain and neuropsychiatric symptoms (depression, anxiety) (Barone et al., 2009; Chaudhuri et al., 2006; O'Sullivan et al., 2008; Park and Stacy, 2009; Pont-Sunyer et al., 2015). The anxiety, depression and pain symptoms display significantly greater severity than in the general population (Rana et al., 2016), and an increased frequency of the non-motor symptoms is associated with Parkinson's disease duration and severity (Barone et al., 2009).

Understanding the pathophysiological mechanisms underlying non-motor symptoms in Parkinson's disease is important, but requires relevant pre-clinical models. Alterations concerning olfaction, sleep and the gastrointestinal tract are clinically well known (Reichmann, 2017) and addressed in models of the disease (Titova et al., 2017). On the other hand, pain, anxiety and depression still remain understudied. In this review, we provide an overview of the present state-of-the-art in the field by rapidly presenting pain and mood non-motor symptoms in Parkinson's disease patients, by evoking the different pre-clinical models used in research and by detailing the literature on measures of nociception, anxiety-like and depression-like symptoms in rodent and non-human primate models of Parkinson's disease.

1. The non-motor symptoms in Parkinson's disease patients

This section provides a rapid overview of some clinical data concerning pain, anxiety and depression in Parkinson's disease. For more details concerning these clinical aspects, please refer to the following references (Blanchet and Brefel-Courbon, 2017; Chaudhuri et al., 2006; Schapira et al., 2017).

1.1.Pain in Parkinson's disease (Figure 7)

Parkinson's disease patients exhibit sensory symptoms such as numbness, coldness, burning or pain (Koller, 1984). Pain is one of the often neglected non-motor symptoms for which there is no truly effective treatment (Wasner and Deuschl, 2012), even though it was already noted in the original description of the disorder by James Parkinson. Nevertheless, it is the non-motor symptoms which is the most frequent in Parkinson's disease patients (O'Sullivan et al., 2008), with a prevalence between 30% and 83% of the patients depending on the considered epidemiological study (Allen et al., 2016; Beiske et al., 2009; Nègre-Pagès et al., 2008; Wasner and Deuschl, 2012).

Clinical data showed that both pain thresholds and tolerance to pain are significantly lower in Parkinson's disease patients compared to the control population (Blanchet and Brefel-Courbon, 2017; Zambito Marsala et al., 2011), and that these patients can suffer from a variety of different pain (Beiske et al., 2009; Lee et al., 2006). Because of the variety of pain expressed by Parkinson's disease patients, a classification was proposed to identify different types by using criterions such as "topography, duration, frequency, aggravating factors, temporal and topographical relationship to Parkinson's disease, influence of motor complications, influence of antiparkinson medication, and patient's opinion about the relationship between pain and Parkinson's disease" (Wasner and Deuschl, 2012). Such classification led to separate pain directly/partly related to Parkinson's disease itself, indirectly related to it (*i.e.* aggravated by Parkinson's disease) and unrelated to the disease itself (Fig. 7) (Blanchet and Brefel-Courbon, 2017; Nègre-Pagès et al., 2008; Wasner and Deuschl, 2012).

Pain in Parkinson's disease can be a nociceptive pain, defined by the International Association for the Study of Pain as "pain that arises from actual or threatened damage to non-neural tissue and is due to the activation of nociceptors" (https://www.iasp-pain.org/). Those include for example pain that is associated with the motor disturbances and partly due to muscle rigidity. Indeed, rigidity, akinesia, postural abnormality or dystonia can lead to musculoskeletal nociceptive pain and back pain (Wasner and Deuschl, 2012). Patients can also display neuropathic pain, *i.e.* "pain caused by a lesion or disease of the somatosensory nervous system", which may be of peripheral origin, such as radicular pain, or of central one (Blanchet and Brefel-Courbon, 2017; Wasner and Deuschl, 2012). Miscellaneous pain, which cannot be classified in the above two categories, can also be observed. Those include for example akathisia (*i.e.* restless legs syndrome) and pain associated with depression, which is the one that appears mostly during the prodromal phase (Schapira et al., 2017; Wasner and Deuschl, 2012) (Fig. 7). The patients with pain more directly related to Parkinson's disease itself are often younger at non-motor and motor disease onsets and show higher parkinsonism severity than those without pain or with pain unrelated to the disease (Nègre-Pagès et al., 2008; Zambito Marsala et al., 2011). The gender has also an influence, with women more frequently reporting pain symptoms (Beiske et al., 2009; Zambito Marsala et al., 2011). The loss of dopamine in the basal ganglia may partly explain the changes in pain thresholds; however, the absence of a total recuperation of these symptoms with dopaminergic medication suggests also a role of non-dopaminergic mechanisms in the appearance or maintenance of pain symptoms (Brefel-Courbon et al., 2005; Schapira et al., 2017).

1.2.Anxiety and depression in Parkinson's disease

There is a notable comorbidity of mood disorders with Parkinson's disease (Dissanayaka et al., 2010). Moreover, the risk to be diagnosed with Parkinson's disease is significantly increased in patients that have already been diagnosed with affective disorders (Nilsson et al., 2001), which reflect the fact that these psychiatric pathologies are part of the early non-motor symptoms appearing during the prodromal phase of the disease (Jacob et al., 2010). Mood disorders can indeed appear 5 to 20 years before the motor symptoms (Shiba et al., 2000).

According to the Diagnostic and Statistical Manual of Mental Disorders, 5th edition (American Psychiatric Association, 2013), "anxiety disorders include disorders that share features of excessive fear and anxiety and related behavioral disturbances". 34 to 65% of Parkinson's disease patients experience anxiety, including panic disorders, generalized anxiety disorder or social phobia (Barone et al., 2009; Chaudhuri et al., 2006; Dissanayaka et al., 2010; Park and Stacy, 2009; Schapira et al., 2017; Szatmari et al., 2017). The risk to develop these disorders has been observed to be much higher (ninefold) in "younger" patients (<62 years old) than in older subjects (Dissanayaka et al., 2010). The pathophysiological basis for these symptoms is however not clearly identified yet. Beside alterations in dopaminergic system, including a correlation between striatal dopamine transporter availability and anxiety (Erro et al., 2012; Moriyama et al., 2011; Weintraub et al., 2005), a structural change in amygdala size has also been proposed to contribute to this symptom (Vriend et al., 2016). Moreover, a loss of noradrenaline neurons in the locus coeruleus (Bertrand et al., 1997; Delaville et al., 2011; German et al., 1992; Hughes et al., 1992) and of serotonin cells in the dorsal raphe (Kish, 2003) has been described in patients, which could also contribute to the presence of anxiety and depression (Marsh, 2013; Remy et al., 2005; Schapira et al., 2017).

Depressive disorders are common psychiatric disorders characterized by the presence of a sad, empty or irritable mood, accompanied by somatic and cognitive changes that impact everyday life function. According to the World Health Organization, they affect 300 million people worldwide (http://www.who.int/). Approximatively 40% of the patients with Parkinson's disease display depressive disorders (Burn, 2002; Chaudhuri et al., 2006; Cummings, 1992; Jacob et al., 2010). Anhedonia and apathy are frequent symptoms that can occur during the prodromal phase (Ishihara and Brayne, 2006; Pont-Sunyer et al., 2015), which leads to the fact that, at time of Parkinson's disease diagnosis, the proportion of patients who already consulted for depression is more than twice higher than in the control population (Leentjens et al., 2003). Classical antidepressant drugs as well as deep brain stimulation and L-

DOPA therapy can be useful to improve these symptoms (Czernecki et al., 2002; Schapira et al., 2017). Even if the detailed mechanism underlying depression is unknown, different hypotheses have been proposed. Indeed, alterations in the monoaminergic systems (Chaudhuri et al., 2006; Reichmann, 2017; Schapira et al., 2017), as well as in structural and metabolic alterations in brain regions known for their implication in affective disorders, such as the hippocampus and the amygdala (Huang et al., 2013; Surdhar et al., 2012; van Mierlo et al., 2015), may likely contribute to the depressive symptoms in Parkinson's disease.

2. Animal models to study Parkinson's disease

This section mostly focuses on animal models (rodents and monkeys) of Parkinson's disease for which data related to pain, anxiety or depression like behaviors are available. For a more exhaustive view of existing models, readers can consult following reviews (Bastías-Candia et al., 2018; Bové and Perier, 2012; Creed and Goldberg, 2018; Francardo, 2018; Grandi et al., 2018; Koprich et al., 2017; Volta and Melrose, 2017).

2.1.Toxin-induced Parkinson's disease models

The more widely used models of Parkinson's disease are based on 6-hydroxydopamine (6-OHDA), a drug that selectively acts on catecholamine containing terminals and cells bodies (Ungerstedt, 1968). Due to its homology with dopamine and noradrenaline, 6-OHDA is caught by plasma membrane dopamine and noradrenaline transporters to enter into cells. It accumulates into the cytosol, producing reactive oxygen species that are toxic to the cell and quinones that inactivate biological macromolecules important to neuronal integrity (Bové and Perier, 2012; Dauer and Przedborski, 2003; Sachs and Jonsson, 1975). 6-OHDA does not easily cross the brain-blood barrier, it is thus injected directly into the structure of interest, either in the area of dopamine cell bodies (substantia nigra *pars compacta*), in the dopamine passing fibers (medial forebrain bundle) or at terminal level (striatal complex) (Blum et al., 2001; Gubellini and Kachidian, 2015; McDowell and Chesselet, 2012). This 6-OHDA administration induces a degeneration of dopamine neurons, leading to motor impairments that partially mimic the motor-symptoms of Parkinson's disease (Bové and Perier, 2012; Ungerstedt, 1968). The injection can be unilateral, producing a hemiparkinsonism model with asymmetric circling behaviors that can be used to test treatments for motor symptoms (Bové and Perier, 2012; Dauer and Przedborski, 2003; Hefti et al., 1980; Ungerstedt and Arbuthnott, 1970). The bilateral injection in the mesencephalic region of dopamine cell bodies can however induce a notable

mortality of the animals, due to adverse effects such as aphagia, adipsia and seizures (Bezard and Przedborski, 2011; Bové and Perier, 2012; Ungerstedt, 1971), which limits in part this direct targeting of cell bodies. As 6-OHDA is toxic for all catecholamine neurons, a pretreatment with a blocker of noradrenaline re-uptake and/or catabolism (monoamine oxidase B inhibitor) may be used to protect noradrenaline neurons and have a more specific dopamine lesion. However, it has also been proposed that administration of 6-OHDA without such neuroprotection may lead to a richer phenotype that better mimics Parkinson's disease (Bezard et al., 2013).

The use of 1-methyl-4-phenyl-1,2,3,6-tetrahydropyridine (MPTP) to mimic the disease was discovered in the 1980's, after the observation that an accidental production of MPTP during the manufacture of a synthetic opioid drug could lead to symptoms similar to those observe in Parkinson's disease in users of this drug (Blum et al., 2001; Davis et al., 1979; Langston et al., 1983). In animal research, MPTP is mainly used in non-human primates and in mice, even though rodents are less sensitive to its toxicity (Schober, 2004), especially rats in which dopamine neurons are resistant to systemic delivery of MPTP (Betarbet et al., 2002; Bové and Perier, 2012; Boyce et al., 1984; Chiueh et al., 1984b; Sahgal et al., 1984). However, local intracerebral delivery of the active metabolite MPP+ can induce dopamine neuron loss in rats and in guinea-pigs (Chiueh et al., 1984a). The effects of MPTP depend on various parameters, such as the administration mode, species and age (Blum et al., 2001). Due to its facility to cross the brain-blood barrier, MPTP is classically administered through systemic injection (Bankiewicz et al., 2001). After such injection, MPTP enters the brain and is metabolized in 1-methyl-4-phenyl-2,3-dihydropyridinium ion (MPP+). The MPP+ binding site is located in the electron leak site, within the complex I of the electron transport chain of the mitochondria (Betarbet et al., 2002). MPP+ inhibits the complex I of the mitochondrial electron transport chain, leading to significant ATP depletion, production of reactive oxygen species and cell loss, particularly in the nigrostriatal pathway which is the brain region the most sensitive to the compound, but not the only one (Betarbet et al., 2002; Chan et al., 1991; Dauer and Przedborski, 2003; Engeln et al., 2015; Fabre et al., 1999).

The above two toxins are the most used to model Parkinson's disease, but other drugs can be found in the literature. Rotenone is a compound used as pesticide which easily crosses the brain-blood barrier, entering neuron mitochondria through the same mechanism as MPP+ and inhibiting mitochondrial complex I (Dauer and Przedborski, 2003; Heinz et al., 2017; Li et al., 2003). It produces α-synuclein accumulation and causes a degeneration of the nigrostriatal dopaminergic pathway following oxidative stress (Betarbet et al., 2000, 2002). In rodents,

rotenone can be administrated by systemic injections or by stereotaxic delivery directly into the brain. However, its use is strongly limited by the high mortality that follows its administration at high doses (Antkiewicz-Michaluk et al., 2003). Based on epidemiological toxicology, the herbicide paraquat (1,1'-dimethyl-4,4'-bypyridinium dichloride), the fungicide maneb (Mn-ethylene-1,2-bisdithiocarbamate) and the cycad flour (from *cycas micronesica*) are also used to model Parkinson's disease. Paraquat is in fact a structural analog of MPP+, the active metabolite of MPTP (Betarbet et al., 2002; Bové and Perier, 2012). Its systemic injections induce α-synuclein accumulation and causes degeneration of dopamine neurons of the substantia nigra *pars compacta* (Dauer and Przedborski, 2003; Manning-Bog et al., 2002; McCormack et al., 2002; McDowell and Chesselet, 2012). Maneb easily crosses the brain-blood barrier neuron and causes damage in the substantia nigra *pars compacta* and the striatum, leading to locomotor and coordination impairments. Combined exposure to maneb potentiates the effect of paraquat (Bastías-Candia et al., 2015; Thiruchelvam et al., 2003). Finally, mice fed with cycad flour exhibit α-synuclein accumulation in multiple brain regions and dopamine neuron loss in the substantia nigra *pars compacta*, which induces cognitive deficits and Parkinson's disease-like symptoms (McDowell and Chesselet, 2012; Wilson et al., 2002).

Moreover, it has been shown that an intranigral, intrastriatal or intra-pallidal injection of lipopolysaccharides induces an inflammation process associated with the activation of microglia. This inflammation favors a degeneration of the dopamine neurons of the nigrostriatal pathway and lead to locomotor impairments similar to the ones seen in other models of Parkinson's disease (Castaño et al., 1998; Liu and Bing, 2011; Zhang et al., 2005).

Lastly, injections of Lewy body extracts from post mortem Parkinson's disease patients in the substantia nigra *pars compacta* or the striatum in mice or monkey induce a progressive nigrostriatal degeneration. In mice, this degeneration is accompanied by an astrogliosis in the substantia nigra and impaired motor coordination and balance in the pole test (Recasens et al., 2014).

2.2.Genetic models of Parkinson's disease

While Parkinson's disease is often sporadic, familial forms have also been described which are due to autosomal dominant or recessive genetic mutations (Singleton et al., 2013), and corresponding animal models have been developed.

In 1997, a family form of Parkinson's disease caused by a mutation of the α-synuclein gene (*SNCA* gene) was discovered (Polymeropoulos et al., 1997). This mutation consists of a single

base pair change from a guanine to an adenosine at position 209, leading to an alanine to threonine substitution in the protein at position 53 (p.A53T) (Polymeropoulos et al., 1997). Other point mutations of the *SNCA* gene were also linked to familial forms of Parkinson's disease, such as the p.A30P mutation (Krüger et al., 1998) corresponding to an alanine to proline substitution in the position 30 of the protein and the p.E46K mutation (Zarranz et al., 2004) corresponding to a glutamic acid to lysine substitution in position 46. All of these mutations lead to an autosomal dominant form of the disease (Hernandez et al., 2016). Beside these point mutations, whole locus duplication or triplication of the *SNCA* gene has also been reported as a cause of family forms of the disease (Ibáñez et al., 2004; Singleton et al., 2003), the number of *SNCA* copies correlating with the early-onset and severity of the disease, suggesting a dose dependent effect (Ibáñez et al., 2004). The discovery of these different familial forms was the starting point for the development of transgenic models for the study of Parkinson's disease.

To explore the function of the α-synuclein protein and its implication in the disease, several lines of transgenic mice expressing either the wild-type or a mutated (p.A53T or p.A30P) human α-synuclein were produced (for review, see Fernagut and Chesselet, 2004). The first transgenic mouse overexpressing human α-synuclein used the wild-type form of the protein under the control of the plateled-derived growth factor β promoter (Fernagut and Chesselet, 2004; Masliah et al., 2000), leading to α-synuclein accumulation in synapses from the neocortex, the hippocampus, the substantia nigra and the olfactory regions (Masliah et al., 2000). However, the use of other promoters and/or forms of α-synuclein can lead to different patterns and levels of α-synuclein expression and of behavioral phenotypes (Fernagut and Chesselet, 2004). For example, α-synuclein expression driven by the Thy-1 promoter has been used to produce various transgenic lines that differ in terms of presence (Kahle et al., 2000; Rockenstein et al., 2002) or absence (Rabl et al., 2017) of α-synuclein accumulation in the striatum or in the presence (Fleming et al., 2004; Rabl et al., 2017) or absence (Kahle et al., 2000) of motor impairment. This variability is not only related to the chosen protein form (wild-type or mutated) but may also be related to the transgene insertion site (Chesselet, 2008).

An expression of the wild-type (Lim et al., 2010; Nuber et al., 2008) or the p.A30P mutated (Marxreiter et al., 2013) human α-synuclein driven by the calmodulin-dependent protein kinase IIα promoter induces a degeneration of neurons in the dentate gyrus, the olfactory bulb and in some midbrain and forebrain regions (Lim et al., 2010; Marxreiter et al., 2013; Nuber et al., 2008). This α-synuclein accumulation leads to cognitive and progressive motor impairments (Nuber et al., 2008). Interestingly, if the construct was repressed until weaning, no neuronal loss was observed in the hippocampal region, indicating that the dentate gyrus neurons are more

vulnerable during development than after maturation (Lim et al., 2010). Transgenic mice expressing either wild-type or A53T mutated α-synuclein under the mouse prion protein promoter display age-dependent intracytoplasmic neuronal α-synuclein inclusions (Giasson et al., 2002) and motor impairments that lead to paralysis and death a few days after the first motor symptoms due to motoneuron loss (Giasson et al., 2002; Giraldo et al., 2018). In this model, intracerebral injections of preformed α-synuclein fibrils in young asymptomatic mice accelerate the formation of intracellular inclusions and the development of neurological symptoms (Luk et al., 2012).

To more specifically target α-synuclein expression to dopamine neurons (which is a useful model of dopamine cell loss but does not reflect the more widespread expression observed in both central and peripheral nervous system in patients), lines of transgenic mice with a truncated wild-type (Tofaris et al., 2006) or mutated (p.A53T) (Wakamatsu et al., 2008) α-synuclein expression under the control of the tyrosine hydroxylase promoter were developed. These mice display pathological α-synuclein-positive inclusions in the substantia nigra and in the olfactory bulb, and a decrease in striatal dopamine levels associated with a progressive reduction of the spontaneous activity (Tofaris et al., 2006; Wakamatsu et al., 2008).

In addition to the classical transgenic models exposed above, the use of adeno-associated viral vectors to overexpress α-synuclein has also been developed. This overexpression in the midbrain induces a nigrostriatal degeneration and the formation of insoluble α-synuclein aggregates in mice, rats and non-human primates (Bourdenx et al., 2015; Ip et al., 2017; Ulusoy et al., 2010). This method reproduces many characteristics of the pathology and provides an interesting model in both rodents and primates (Ulusoy et al., 2010).

Mutations in the *PARK8* gene coding for the leucine-rich repeat kinase 2 (LRRK2) protein have also been described to be associated with familial autosomal-dominant and sporadic forms of Parkinson's disease (Funayama et al., 2002; Healy et al., 2008; Paisán-Ruiz et al., 2013). Mutations of this protein mostly target the GTPase and kinase domains of the protein (Dawson et al., 2010; Gubellini and Kachidian, 2015) and cause late-onset forms of the disease (Dawson et al., 2010; Healy et al., 2008). Transgenic mice with bacterial artificial chromosome (BAC) expressing LRRK2 R1441C/G (*i.e.* mutation in the GTPase domain) have been used to model Parkinson's disease, showing age-dependent and progressive motor symptoms but no nigrostriatal degeneration (Li et al., 2009). The development of LRRK2 knock-in mice also failed to produce the classical brain alterations of the disease, such as dopamine cell degeneration or α-synuclein accumulation (Bezard et al., 2013; Dawson et al., 2010; Volta and Melrose, 2017). More conclusively, a rat LRRK2 model has been developed, using adenoviral-

mediated expression of LRRK2 G2019S mutation (*i.e*. mutation in the kinase) to induce a progressive degeneration of nigral dopamine neurons (Dusonchet et al., 2011).

Mutations in the *PRKN* gene (or *PARK2*), which encodes for parkin, an E3 ubiquitin ligase, were identified as a genetic cause of autosomal-recessive and early-onset Parkinson's disease, as well as of some forms of sporadic cases (Gubellini and Kachidian, 2015; Dawson et al, 2010). These parkin mutations lead to a loss-of-function and are responsible for a loss of substantia nigra *pars compacta* dopamine neurons without formation of Lewy bodies (Dauer and Przedborski, 2003). However, mouse models produced by partial or full deletion of the parkin gene exhibit few or no dopamine loss (Itier et al., 2003; Perez and Palmiter, 2005; Von Coelln et al., 2004) and only limited behavioral deficits (Perez and Palmiter, 2005). On the other hand, the overexpression of the mutant human *parkin* using a BAC transgenic mouse model leads to a late-onset and progressive degeneration of dopamine neurons, associated with progressive motor deficits (Dawson et al., 2010; Gubellini and Kachidian, 2015; Lu et al., 2009).

Mutations in the *PINK-1* (PTEN-induced putative kinase 1) gene can cause autosomal recessive forms of the disease (Dawson et al., 2010; Gubellini and Kachidian, 2015; Valente et al., 2004). PINK-1 interacts with parkin to induce parkin-mediated autophagy of damaged mitochondria and thus protect cells from mitochondrial dysfunctions (Gubellini and Kachidian, 2015; Lazarou et al., 2013; Narendra et al., 2008). However, similar to *parkin* null mice, *PINK-1* knock-out mice do not display notable neurodegeneration of substantia nigra dopamine neurons, and show few or no Lewy body-like inclusions (Gispert et al., 2009; Kitada et al., 2007).

A missense mutation in the DJ-1 gene (PARK7) is responsible for an autosomal recessive and early-onset form of Parkinson's disease (Bonifati et al., 2003a, 2003b; Dawson et al., 2010; Lim and Ng, 2009). DJ-1 knock out mice have been developed, but failed to show nigrostriatal dopaminergic loss. However, a reduced striatal dopamine release and a decreased locomotor activity has been observed, making this model interesting as model of early stages of the disease (Chandran et al., 2008; Chen et al., 2005; Dawson et al., 2010; Goldberg et al., 2005; Lim and Ng, 2009; Yamaguchi and Shen, 2007).

Beside the above genetic models that are based on human gene mutations associated with the disease, other transgenic models have also been designed targeting the dopamine system. One of these models is based on the mutation or the deletion of the homeobox transcription factor *Pitx3* which is known to be selective to dopamine neurons, thus inducing a dopaminergic loss in the nigrostriatal pathway. The *Pitx3*-null mice exhibit different markers of the disease, including a decline in substantia nigra *pars compacta* cell number, a reduction in striatal

dopamine release, and motor symptoms such as motor coordination impairment, body tremors and decreased locomotion (Filali and Lalonde, 2016; Le et al., 2015). The *Pitx3*^{416insG} mutant mice, relying on a spontaneous mutation (an inserted G in position 416 of the *Pitx3* gene in the chromosome 19), induces microphtalmia or anophtalmia and a loss of dopamine neurons in the substantia nigra, which induces motor impairment and increased nociceptive response (Rosemann et al., 2010). Another interesting mouse model, MitoPark, has been obtained by selectively removing the mitochondrial transcription factor A (Tfam) from dopamine midbrain neurons. These transgenic mice model an adult-onset of the disease, with a progressive loss of dopamine cell bodies and terminals, associated with tremors, limb rigidity and a progressive decline of locomotion and rearing (Ekstrand et al., 2007; Galter et al., 2010).

3. Non-motor symptoms in animal models of Parkinson's disease

3.1.Nociception and pain in rodent Parkinson's disease models (Figure 8)

According to the definition from the International Association for the Study of Pain, pain is "an unpleasant sensory and emotional experience associated with actual or potential tissue damage or described in terms of such damage". This sensory/emotional duality is a critical element. It distinguishes pain from nociception, which encompasses "the neural process of encoding noxious stimuli" and do not necessarily imply the presence of pain. However, distinguishing pain from nociception remains challenging in animal-based research, and tests that are referred to as "pain tests" are usually based on reflex responses that may reflect nociceptive responses (Barrot, 2012). Moreover, because of the implication of reflex motor responses in most of the tests used to study nociception in rodents and the potential slow-down of motor reflexes in Parkinson's disease, it can also be challenging to correctly assess and interpret some nociceptive responses in rodent models of this disease.

Data reported below show that the nociceptive hypersensitivity observed in patients with Parkinson's disease (response to evoked pain) can be reproduced in some of the animal models. However, the presence of spontaneous pain, which may for example result from rigidity, akinesia, postural abnormality or dystonia, has not been studied yet in these models. While challenging, such question could now also be addressed in rodents. Indeed, procedures were developed in the past decade to test the aversive state induced by ongoing pain in rats and mice (Barthas et al., 2015; Johansen et al., 2001; King et al., 2009; Qu et al., 2011; Sellmeijer et al., 2018)

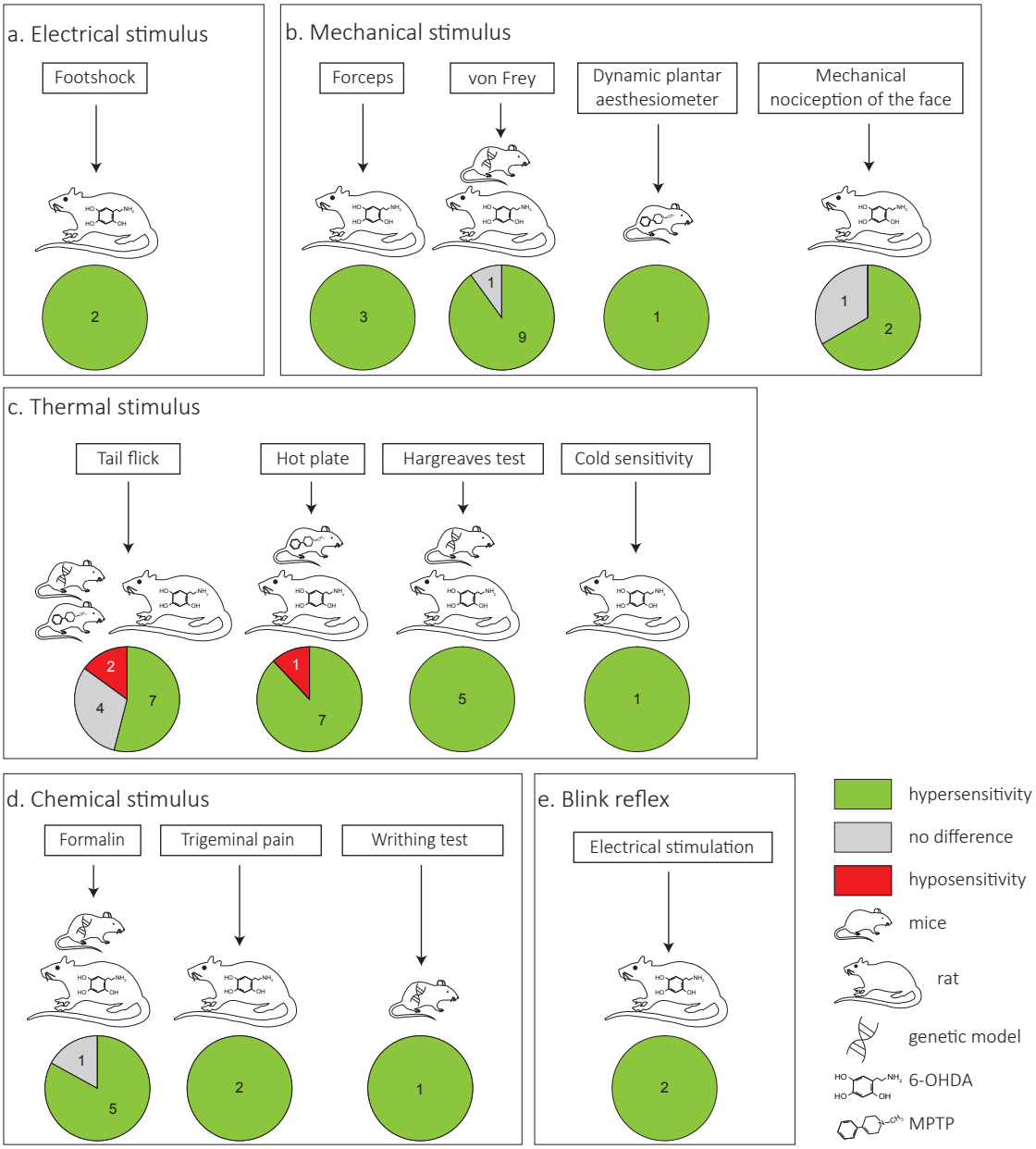

Figure 8. Nociceptive responses in animal models of Parkinson's disease. Various nociceptive modalities have been tested in models of the disease. For a majority of these modalities and animal models, the existing literature converges to highlight a nociceptive hypersensitivity. The heat modality, and in particular the tail-flick test, shows the highest heterogeneity in reported findings, which might be related to potential slow-down of some withdrawal reflexes. "n" displayed in the figure correspond to the number of publications relative to the test (see Table 1 for more details and references). 6-OHDA, 6-hydroxydopamine; MPTP, 1-methyl-4-phenyl-1,2,3,6-tetrahydropyridine.

Table 4 Nociception in Parkinson's disease models

Species	Model	Test	Results	Ref.
Rat	6-OHDA	Footshock	↗ contralat. jump thresholds and ↘ ipsilat. one	(Carey, 1986)
			↘ nociceptive thresholds	(Chen et al., 2013)
Rat	6-OHDA	Paw pressure	↘ latency for contralat. hindpaw	(Saadé et al., 1997)
			↘ latency at 1,2 and 12 weeks for ipsilat. hindpaw	(Takeda et al., 2005)
			↘ mechanical thresholds at 3 weeks	(Chudler and Lu, 2008)
Rat	6-OHDA	von Frey	↘ mechanical thresholds	(Zengin-Toktas et al., 2013)
			↘ mechanical thresholds for ipsilat. hindpaw	(Takeda et al., 2014)
			↘ mechanical thresholds for both hindpaws	(Gee et al., 2015)
			↘ mechanical thresholds after 4 weeks	(Cao et al., 2016)
			↘ mechanical thresholds after 4 weeks	(Wang et al., 2017)
			↘ mechanical thresholds for both hindpaws	(Gómez-Paz et al., 2017)
			↘ mechanical thresholds for both hindpaws	(Nascimento et al., 2018)
			↘ mechanical thresholds for controlat. hindpaw	(Charles et al., 2018)
			No ≠	(Ogata et al., 2015)
Mice	*Pitx3*^{416insG}	von Frey	↘ mechanical thresholds	(Rosemann et al., 2010)
Mice	MPTP	Dynamic plantar aesthesiometer	↘ mechanical thresholds	(Park et al., 2015)
Rat	6-OHDA	von Frey (vibrissae)	No ≠	(Chudler and Lu, 2008)
			↗ pain score	(Dieb et al., 2016)
		Air puff (face)	↗ pain score	(Dieb et al., 2014)
Rat	6-OHDA	Tail flick	↘ latency	(Saadé et al., 1997) (Dolatshahi et al., 2015) (Gómez-Paz et al., 2017) (Haddadi et al., 2018) (Nascimento et al., 2018)
			No ≠	(Morgan and Franklin, 1990)
			↗ latency	(Gee et al., 2015) (Ogata et al., 2015) (Grossmann et al., 1973) (Tassorelli et al., 2007)
Mice	MPTP	Tail flick	↘ latency	(Rosland et al., 1992) (Park et al., 2015)
Mice	*Pitx3*^{416insG}	Tail flick	No ≠	(Rosemann et al., 2010)
Rat	6-OHDA	Hot plate	↘ latency	(Lin et al., 1981) (Saadé et al., 1997) (Chen et al., 2013) (Dolatshahi et al., 2015) (Gee et al., 2015) (Nascimento et al., 2018)
Mice	MPTP	Hot plate	↗ latency	(Rosland et al., 1992)
			↘ latency	(Park et al., 2015)
Rat	6-OHDA	Hargreaves test	↘ latency on the contralat. side	(Chudler and Lu, 2008)
			↘ latency at 4 weeks	(Cao et al., 2016)
			↘ latency at 2 and 4 weeks	(Wang et al., 2017)
			↘ latency on the contralat. side	(Charles et al., 2018)
Mice	*Pitx3*^{416insG}	Hargreaves test	↘ latency in males and females	(Rosemann et al., 2010)
Rat	6-OHDA	Acetone	↗ behavioral responses	(Gómez-Paz et al., 2017)
Rat	6-OHDA	Formalin test	↘ effect of analgesics in the formalin test	(Morgan and Franklin, 1990)
			↗ responses in the second phase	(Ogata et al., 2015)
			↗ responses in both phases	(Cao et al., 2016)
			↗ responses (contralat.) in both phases	(Tassorelli et al., 2007)
			↗ responses (bilateral) in both phases	(Gómez-Paz et al., 2017)
Mice	LRRK2	Formalin test	No ≠ in both phases	(Bichler et al., 2013)
Rat	6-OHDA	Formalin test (orofacial)	↗ face grooming during the second phase	(Chudler and Lu, 2008)
			↗ face rubbing on the left lip in both phases	(Maegawa et al., 2015)
Mice	*Pitx3*^{416insG}	Writhing test	↗ number of responses	(Rosemann et al., 2010)
Rat	6-OHDA	Blink reflex	Hyperexcitability	(Basso et al., 1993)
			Hyperexcitability, impaired blink plasticity of the R2 but not the R1 component and lower spontaneous blink rate	(Kaminer et al., 2015)

6-OHDA, 6-hydroxydopamine; contralat., contralateral; ipsilat., ipsilateral; MPTP, 1-methyl-4-phenyl-1,2,3,6-tetrahydropyridine. Note that "6-OHDA" gathers various models, either unilateral or bilateral, and with different lesion sites, with or without neuroprotection of non-dopamine systems.

3.1.1. Electrical sensitivity

The threshold responses to electrical shocks can be used to assess pain sensitivity. In such test, electrical stimuli of increasing intensities are delivered through a grid floor and the threshold intensity eliciting the first response (*i.e.* flinch, vocalization, jumping or running) is measured (Barrot, 2012). Rats with a unilateral 6-OHDA lesion of the dopamine neurons show an hypersensitivity either in the ispsilateral (Chen et al., 2013) of the contralateral body side of the lesion (Carey, 1986) (Table 4).

3.1.2 Mechanical sensitivity

Although different tests are available to assess the response to mechanical stimuli in rodents (Barrot, 2012), particularly in rats (von Frey filaments, Randall-Selitto's paw pressure test…), most of the data from Parkinson's disease rodent models found in the literature are based on the von Frey filaments test. Mechanical nociceptive thresholds are usually lower in animal models of Parkinson's disease, regardless of the rodent species (mice or rat) or of the chosen model (6-OHDA, MPTP, *Pitx3*) (Cao et al., 2016; Charles et al., 2018; Chudler and Lu, 2008; Gee et al., 2015; Gómez-Paz et al., 2017; Nascimento et al., 2018; Park et al., 2015; Rosemann et al., 2010; Saadé et al., 1997; Takeda et al., 2005, 2014; Wang et al., 2017; Zengin-Toktas et al., 2013). While this mechanical hypersensitivity now appears as well established, there are some discrepancies among published reports using a unilateral lesion (Charles et al., 2018; Chudler and Lu, 2008; Gee et al., 2015; Gómez-Paz et al., 2017; Nascimento et al., 2018; Saadé et al., 1997; Takeda et al., 2005, 2014), with results that may differ regarding the time-course and/or the laterality of the hypersensivity. Changes in mechanical sensitivity have been correlated with decreased tyrosine hydroxylase expression in the substantia nigra *pars compacta* (Zengin-Toktas et al., 2013) and can be compensated by a neural transplantation of fetal ventral mesencephalon tissue in lesioned animals (Takeda et al., 2014) (Table 4).

Painful rigidity of the face, chin or jaw and trigeminal neuralgia-like pain can be present in the prodromal phase of Parkinson's disease (Waseem and Gwinn-Hardy, 2001). This trigeminal sensitivity can be tested in rodents with different approaches, using procedures assessing static or dynamic mechanical sensitivity. To test static (pressure) mechanical allodynia of the face, von Frey filaments can be applied to the vibrissae region. The bilateral lesion of the substantia nigra *pars compacta* leads to an increased nociceptive sensitivity of the two side of the face (Dieb et al., 2016), while a unilateral lesion in the caudate/putamen does not affect this response (Chudler and Lu, 2008). To test the dynamic mechanical allodynia, gentle air puff is applied on the animal face. Bilateral lesioned animals display a dynamic mechanical allodynia of the face,

which is inversely correlated with the number of tyrosine hydroxylase positive cells (Dieb et al., 2014) (Table 4).

3.1.3 Thermal sensitivity

The tail flick test measures the withdrawal latency following tail exposure to a heat stimulus, by using an infrared heat beam or a warm-controlled water bath (Barrot, 2012; Le Bars et al., 2001). The response in this test is a nociceptive spinal reflex that is, however, influenced by descending controls from the brain. Mice with intraperitoneal injections of MPTP have reduced tail flick latency (Park et al., 2015; Rosland et al., 1992), whereas *Pitx3*^{416insG} mutant mice showed no significant difference (Rosemann et al., 2010). On the other hand, the literature concerning the thermal sensitivity in 6-OHDA models of Parkinson's disease is controversial, with opposite results that can be reported: increased latency (Grossmann et al., 1973; Tassorelli et al., 2007), no difference (Gee et al., 2015; Morgan and Franklin, 1990; Ogata et al., 2015) or decreased latency (Dolatshahi et al., 2015; Gómez-Paz et al., 2017; Haddadi et al., 2018; Nascimento et al., 2018; Saadé et al., 1997). A possible explanation for these discrepancies could be the co-presence of thermal hypersensitivity and of reflex slow-down. Depending on the location and the extent of the lesion, and on the test procedure and temperature settings, one or the other aspect may be predominant, which highlights the potential difficulty to interpret tail-flick results in these models. (Table 4).

The hot plate test measures the response to nociceptive heat by placing the animal on a plate at fixed and controlled temperature, often set in the 52 to 55°C range with a 0.1°C precision. The latency before the apparition of a withdrawal behavior, such as paw licking, paw withdrawal or eventually jumping, is measured (Barrot, 2012; Le Bars et al., 2001). Usually, whatever the model (MPTP or 6-OHDA) and the species (mouse or rat) that is used, the articles report an increased pain sensitivity (Chen et al., 2013; Dolatshahi et al., 2015; Gee et al., 2015; Lin et al., 1981; Nascimento et al., 2018; Park et al., 2015; Rosland et al., 1992; Saadé et al., 1997). In the paw immersion test, consisting in placing the animal's paw in a water bath at a fixed and controlled temperature, rats with 6-OHDA lesion in the ventral tegmental area and the substantia nigra displayed a decreased withdrawal latency, *i.e.* a hypersensitivity, concerning the paw contralateral to the lesion (Saadé et al., 1997) (Table 4).

In the radiant heat paw-withdrawal test, often referred to as the Hargreaves's method (Hargreaves et al., 1988), a controlled heat beam system is directed toward the plantar surface of the animal's hind paws in order to measure the withdrawal latency (Barrot, 2012). In this test, *Pitx3*^{416insG} mutant mice (Rosemann et al., 2010), rats at 3 weeks following 6-OHDA lesion of the caudate/putamen nuclei (Chudler and Lu, 2008) rats with 6-OHDA lesion of the right

medial forebrain bundle (Charles et al., 2018), rats at 4 and 5 weeks following 6-OHDA bilateral lesion of the striatum (Cao et al., 2016) and rats with bilateral lesion of the substantia nigra *pars compacta* at 2 and 4 weeks post-surgery (Wang et al., 2017), displayed hyperalgesia as illustrated by decreased paw withdrawal latencies (Table 4).

Cold sensitivity is more rarely tested but can be assessed by for example applying a drop of acetone on the animal's paw. Rat with a unilateral lesion of the substantia nigra *pars compacta*, but not control animals, exhibit nocifensive responses such as paw withdrawal, licking, shaking or rubbing (Gómez-Paz et al., 2017), showing the presence of a cold allodynia.

3.1.4 Response to nociceptive chemical exposure

The intradermal injection of a formalin solution models short-term inflammatory pain. It results in paw withdrawal, licking, biting or shacking. In rodents, these responses are classically divided in 2 phases: an initial phase during the first 5 or 10 minutes after the injection, related to the stimulation of nociceptors; and a second phase, lasting between 20 to 40 min, corresponding to both inflammatory mechanisms and central sensitization within the dorsal horn (Barrot, 2012; Le Bars et al., 2001). It has been shown that rats with 6-OHDA lesion, either in the cell bodies or terminals, displayed enhanced behavioral responses in the formalin test (Cao et al., 2016; Chudler and Lu, 2008; Gómez-Paz et al., 2017; Ogata et al., 2015; Tassorelli et al., 2007), thus reflecting hyperalgesia. This hyperalgesia was however detected in the second phase only (Chudler and Lu, 2008; Ogata et al., 2015) or in both phases (Cao et al., 2016; Gómez-Paz et al., 2017; Tassorelli et al., 2007), depending on the study. When formalin was delivered in the face (trigeminal pain) of rats with an unilateral striatal 6-OHDA lesion, grooming was significantly enhanced during the second (Chudler and Lu, 2008) or both phases of the test (Maegawa et al., 2015), reflecting an increased inflammatory pain response. Changes in the formalin test following 6-OHDA lesion could also affect the sensitivity to pain relief, indeed midbrain 6-OHDA lesions suppressed D-amphetamine and morphine-induced analgesia in this test (Morgan and Franklin, 1990). On the other hand, in a transgenic LRRK2 model of Parkinson's disease, mutant mice did not show alteration of formalin test responses (Bichler et al., 2013), but this model displayed an overall limited range of symptoms. (Table 4)

In the writhing test, the irritant chemical are delivered intraperitoneally, which provokes abdominal contractions and twisting of dorso-abdominal muscles that can be quantified as an indicator of peritovisceral nociception (Le Bars et al., 2001). In *Pitx3*^{416insG} mutant mice, visceral pain following intraperitoneal acetic acid delivery was significantly enhanced (Rosemann et al., 2010) (Table 4).

3.2.Blink reflex abnormalities in Parkinson's disease models (Figure 8)

The blink reflex is related to the activity of the *orbicularis oculi* muscle and may be considered as a protective nociceptive response. The electrical stimulation of this muscle results in an electromyographic response composed of 2 different phases, the R1 and R2 components. The R1 component is the early component, which is only present on the stimulated side. The R2 component is present in both sides and appears later (Pearce, 2008). In Parkinson's disease, patients exhibit a hyperexcitability of the blink reflex, with shorter latency, increased amplitude and an increased habituation index (Esteban and Giménez-Roldàn, 1975). In 6-OHDA lesioned rats, as in patients, a hyperexcitability of the blink reflex has also been observed, together with an impaired blink plasticity and a lower spontaneous blink rate (Basso et al., 1993; Kaminer et al., 2015) (Table 4).

3.3.Anxiety-like and depression-like behaviors in rodent Parkinson's disease models

Animal studies concerning anxiety and depression in Parkinson's disease mainly focused on dopaminergic mechanism, which unlikely reflects the complexity underlying the occurrence of these symptoms in patients. There is still indeed a paucity of studies addressing, beyond dopamine, the role of the other alterations of the nervous system, in particular for early stages of the disease.

3.3.1. Anxiety-like behavior in Parkinson's disease models (Figure 9)

Tests for anxiety-like behaviors in rodents, such as the elevated plus maze, the open field test and the hole-board test, are mostly based on exploratory behaviors in a novel environment. They more specifically rely on the natural tendency of rodents to explore novel environments and their innate avoidance of open, illuminated and/or elevated environment, and their behavioral response to anxiolytic drugs leading them to behave against their nature.

In the elevated plus maze, anxiety-like behavior is expressed by an increased time spend in the closed arms (or decreased time in the open arms) of the test (Pellow et al., 1985). This classical test has been used in various studies of experimental parkinsonism, but the motor disturbances present in some models may affect the response to this test, making important to have a control measure of locomotor activity (such as the number of crossing). Depending on the model, the species or the lesioned side, different findings were reported. In 6-OHDA models, most of the literature converge to report an increased anxiety-like profile in lesioned animals, corresponding to decreased time spent in the open arms of the test (Bonito-Oliva et

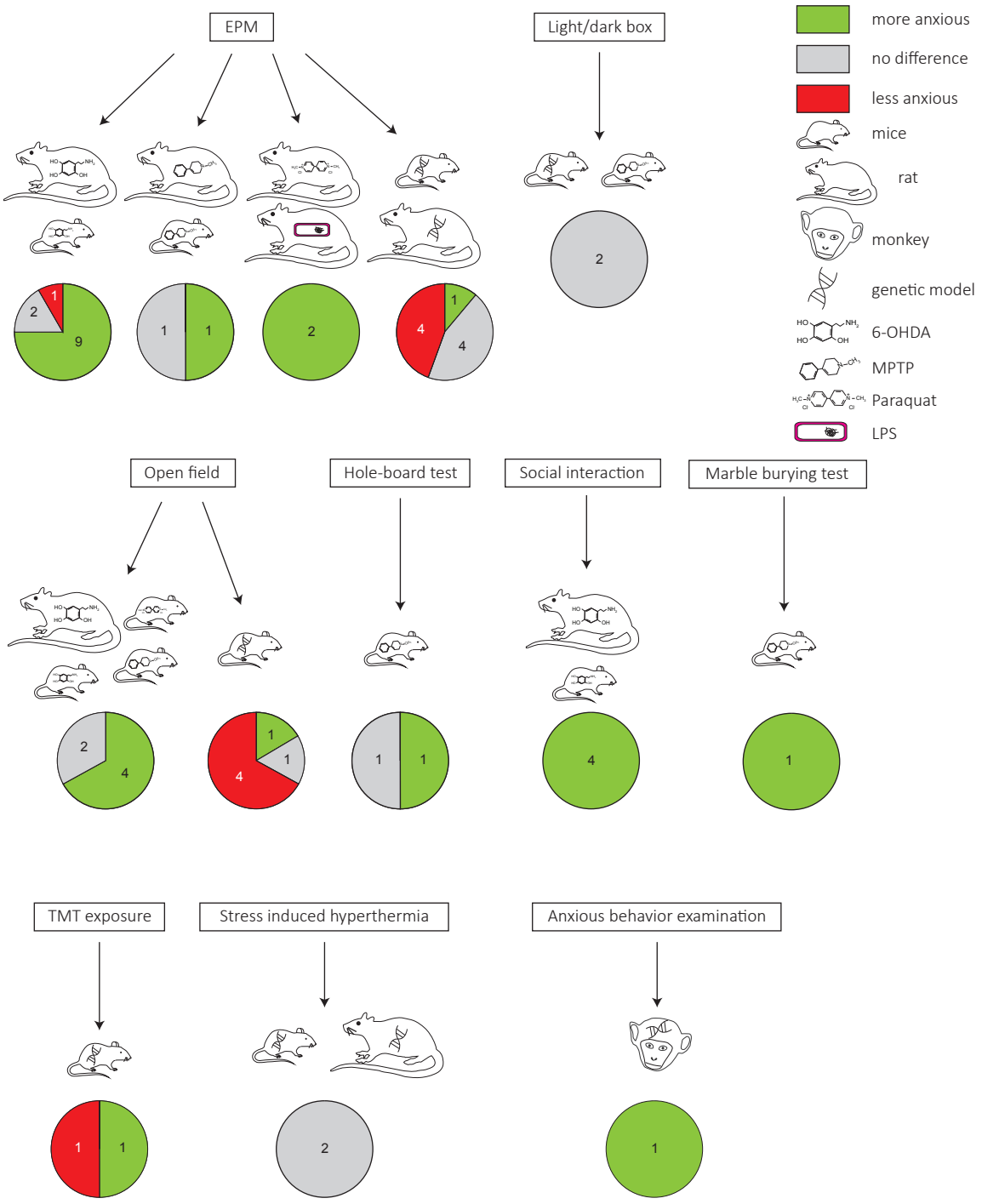

Figure 9. Anxiety-like behaviors in animal models of Parkinson's disease. While in neurotoxin-based models of the disease most studies reported increased anxiety-like behaviors, literature is more controversial concerning genetic-based models of the disease. "n" displayed in the figure correspond to the number of publications relative to the test (see Table 2 for more details and references). 6-OHDA, 6-hydroxydopamine; EPM, elevated plus maze; LPS, lipopolysaccharide; MPTP, 1-methyl-4-phenyl-1,2,3,6-tetrahydropyridine; TMT, 2,3,5-trimethyl-3-thiazoline (i.e. fox odor).

Table 5 Anxiety-like behaviors in Parkinson's disease models

Species	Model	Test	Results	Ref.
Rat	6-OHDA	EPM	↗ entries/time spent in the open arms	(Branchi et al., 2008)
			No ≠	(Carvalho et al., 2013) (Matheus et al., 2016)
			↘ entries/time spent in the open arms	(Tadaiesky et al., 2008) (Jungnickel et al., 2011) (Campos et al., 2013) (Hui et al., 2015) (Sun et al., 2015) (Silva et al., 2016) (Faggiani et al., 2018)
			↘ entries/time spent in the open arms if depleting at least 2 of the monoamines	(Delaville et al., 2012)
Mice	6-OHDA	EPM	↘ time spent in the open arms	(Bonito-Oliva et al., 2014)
Rat	MPTP	EPM	↘ time spent in the open arms	(Ho et al., 2011)
Mice	MPTP	EPM	No ≠	(Gorton et al., 2010)
Rat	Paraquat	EPM	↘ time spent in the open arms	(Campos et al., 2013)
Rat	LPS	EPM	↘ entries/time spent in the open arms	(Hritcu and Gorgan, 2014)
Rat	α-syn	EPM	No ≠	(Campos et al., 2013) (Caudal et al., 2015)
Mice	A53T	EPM	↗ entries/time spent in the open arms	(George et al., 2008) (Oaks et al., 2013) (Rothman et al., 2013)
Mice	VMAT2	EPM	↘ time spent in open arms in young mice	(Taylor et al., 2009)
Mice	α-syn	EPM	No ≠	(Peña-Oliver et al., 2010)
			↗ entries/time spent in open arms	(Yamakado et al., 2012)
Mice	*LRRK2*	EPM	No ≠	(Bichler et al., 2013)
Mice	MPTP α-syn	Light/Dark	No ≠	(Vuković et al., 2008) (Peña-Oliver et al., 2010)
Rat	6-OHDA	Open field	↘ center entries and center vertical movements	(Eskow Jaunarajs et al., 2010)
			↘ time spent in the center area	(Hui et al., 2015) (Sun et al., 2015)
Mice	6-OHDA	Open field	↘ time spent and distance covered in the center area	(Bonito-Oliva et al., 2014)
Mice	Paraquat	Open field	No ≠	(Litteljohn et al., 2008)
Mice	MPTP	Open field	No ≠	(Park et al., 2015)
Mice	α-syn	Open field	Tendency to a ↘ in entries and time spent in the center	(Peña-Oliver et al., 2010)
			↗ time spent in the central area	(Yamakado et al., 2012)
Mice	A53T	Open field	No ≠	(George et al., 2008)
			↗ time spent in the center area	(Oaks et al., 2013) (Paumier et al., 2013) (Rothman et al., 2013)
Mice	MPTP	Hole-board test	No ≠	(Vuković et al., 2008)
			↗ head dips	(Janakiraman et al., 2017)
Rat	6-OHDA	Social interactions	↘ offensive behavior but ↗ propensity to interact	(Branchi et al., 2008)
			↘ frequency to approach counterpart	(Eskow Jaunarajs et al., 2010)
			↘ social interaction	(Matheus et al., 2016)
Mice	6-OHDA	Social interactions	↘ time in contact	(Chiu et al., 2015)
Mice	MPTP	Marble burying	↗ buried marbles	(Gorton et al., 2010)
Mice	A30P	TMT exposure	↘ time spent freezing	(Nuber et al., 2011)
			↘ time spent in the odor area	(Marxreiter et al., 2013)
Rat	α-syn	Stress induced hyperthermia	No ≠	(Caudal et al., 2015)
Mice	A53T	Stress induced hyperthermia	No ≠	(Paumier et al., 2013)
Rhesus monkey	α-syn	Behavioral examination	↗ behavioral stereotypies	(Niu et al., 2015)

6-OHDA, 6-hydroxydopamine; α-syn, α-synuclein; EPM, elevated plus maze; LPS, lipopolyssacharide; MPTP, 1-methyl-4-phenyl-1,2,3,6-tetrahydropyridine; TMT, 2,3,5-trimethyl-3-thiazoline. Note that "6-OHDA" gathers various models, either unilateral or bilateral, with different lesion sites, and with or without neuroprotection of non-dopamine systems.

al., 2014; Campos et al., 2013; Delaville et al., 2012; Faggiani et al., 2018; Hui et al., 2015; Jungnickel et al., 2011; Silva et al., 2016; Sun et al., 2015; Tadaiesky et al., 2008); but some articles reported no difference (Carvalho et al., 2013; Matheus et al., 2016) or even less anxiety-like behavior (Branchi et al., 2008). In these 6-OHDA models, the present number of studies does not allow to conclude whether the presence/absence of anxiety could be related to the lesion side, to its unilateral/bilateral aspect or to the presence or no of a protection of noradrenergic fibers during the lesion procedure. However, a study showed that a co-lesion of either noradrenergic or serotonergic systems strongly potentiate anxiety-like behaviors after dopamine lesion (Delaville et al., 2012). Increased anxiety in the elevated plus maze has also been reported once in the paraquat (Campos et al., 2013) and lipopolysaccharide (Hritcu and Gorgan, 2014) models in rats, while the 2 studies in MPTP models reported either a lack (in mice) (Gorton et al., 2010) or a presence (in rats) (Ho et al., 2011) of increased anxiety. Results from neurotoxin-based models also mostly reported increased anxiety-like behaviors in other tests. This is the case for studies assessing social interactions (Branchi et al., 2008; Chiu et al., 2015; Eskow Jaunarajs et al., 2010; Matheus et al., 2016), for the marble burying test (Gorton et al., 2010), for two third of the literature concerning the open field test (Bonito-Oliva et al., 2014; Eskow Jaunarajs et al., 2010; Hui et al., 2015; Sun et al., 2015) and for one of the two publications using the hole-board test (Campos et al., 2013).

Conversely, genetic models mostly showed either a lack of change (Bichler et al., 2013; Campos et al., 2013; Caudal et al., 2015; Peña-Oliver et al., 2010) or a decrease (George et al., 2008; Oaks et al., 2013; Rothman et al., 2013; Yamakado et al., 2012) in anxiety-like behavior in the elevated plus maze test, thus differing from the above mentioned neurotoxin-based models (Table 5). While changes in behavior were observed in the presence of a predator odor (TMT) in a genetic model (Marxreiter et al., 2013; Nuber et al., 2008), a lack of increased anxiety-related responses has also been reported in the light-dark test (Peña-Oliver et al., 2010) and when looking at changes in body temperature under a stress condition (Caudal et al., 2015; Paumier et al., 2013). In the open-field test, genetic models were even mostly associated with an increased time spent in the center area (Oaks et al., 2013; Paumier et al., 2013; Rothman et al., 2013; Yamakado et al., 2012), which would normally reflect lower anxiety (Belzung, 1999) (Table 2). However, increased locomotor activity in the open-field, which may interfere with anxiety-related data in this test, has for example been noted in Thy-1 α-synuclein mice (Lam et al., 2011). Studies may thus still be needed to understand whether these discrepancies between neurotoxin-based and genetic models reflect biological differences between models, in

particular in their respective impact on aminergic and limbic systems, or reflect technical challenges in appropriately testing anxiety-like behaviors.

Lastly, only one article mentioned anxiety-like behaviors in a non-human primate model of Parkinson's disease (Niu et al., 2015). Authors analyzed potential ethological signs of anxiety (walking in circle, sucking on a finger or a toe, self-grasping) in 3 transgenic α-synuclein rhesus monkeys and observed increased stereotypic behaviors in one of them (Niu et al., 2015) (Table 2). However, such "case report" does not allow concluding between pathological consequence and individual characteristics as explanation. More interestingly, some studies are now proposing measures of "spontaneous" abnormal or atypical behaviors in order to identify depressive-like behaviors in non-human primates (Camus et al., 2013a, 2013b, 2014). Using rhesus monkeys or cynomologus macaques, it proposes to look at inactivity, feeding behaviors, social behaviors and body postures/orientations in these species. Applying this ethological approach to Parkinson's disease models still remains to be done.

3.3.2. Depression-like behavior in Parkinson's disease models (Figure 10)

The forced swim test consists of placing the animal in a water-filled cylinder with no possibility to escape. After an initial period of activity, *i.e.* swimming or attempts at climbing, the animal will stop to move and only make movements necessary to let its head above water. This immobility was qualified by Porsolt and colleagues as a characteristic of despair and resignation, and as a mean to screen antidepressant drugs because they reduce the duration of immobility in this test (Porsolt et al., 1977). Almost all studies with neurotoxin models of Parkinson's disease showed a decreased swimming time and/or increased immobility time (Berghauzen-Maciejewska et al., 2014; Bonito-Oliva et al., 2014; Branchi et al., 2008; Campos et al., 2013; Casas et al., 2011; Chiu et al., 2015; Delaville et al., 2012; Hritcu and Gorgan, 2014; Ilkiw et al., 2018; Liu et al., 2015; Matheus et al., 2016; Santiago et al., 2014, 2010, Tadaiesky et al., 2010, 2008; Tuon et al., 2014). However, this effect is not always seen within the same time-frame, even in similar models (Berghauzen-Maciejewska et al., 2014; Matheus et al., 2016). Moreover, due to the potential presence of motor deficits, caution should likely be present when interpreting forced swim test data in models of Parkinson's disease. With the use of transgenic models, data are less consistent, with reports of increased immobility (Caudal et al., 2015; Taylor et al., 2009), of no difference (Bichler et al., 2013; Campos et al., 2013) or of decreased immobility (Nuber et al., 2011; Oaks et al., 2013). One hypothesis to explain these discrepancies would be that the deficits observed in genetic models could be progressive and age-dependent (Taylor et al., 2009) (Table 6).

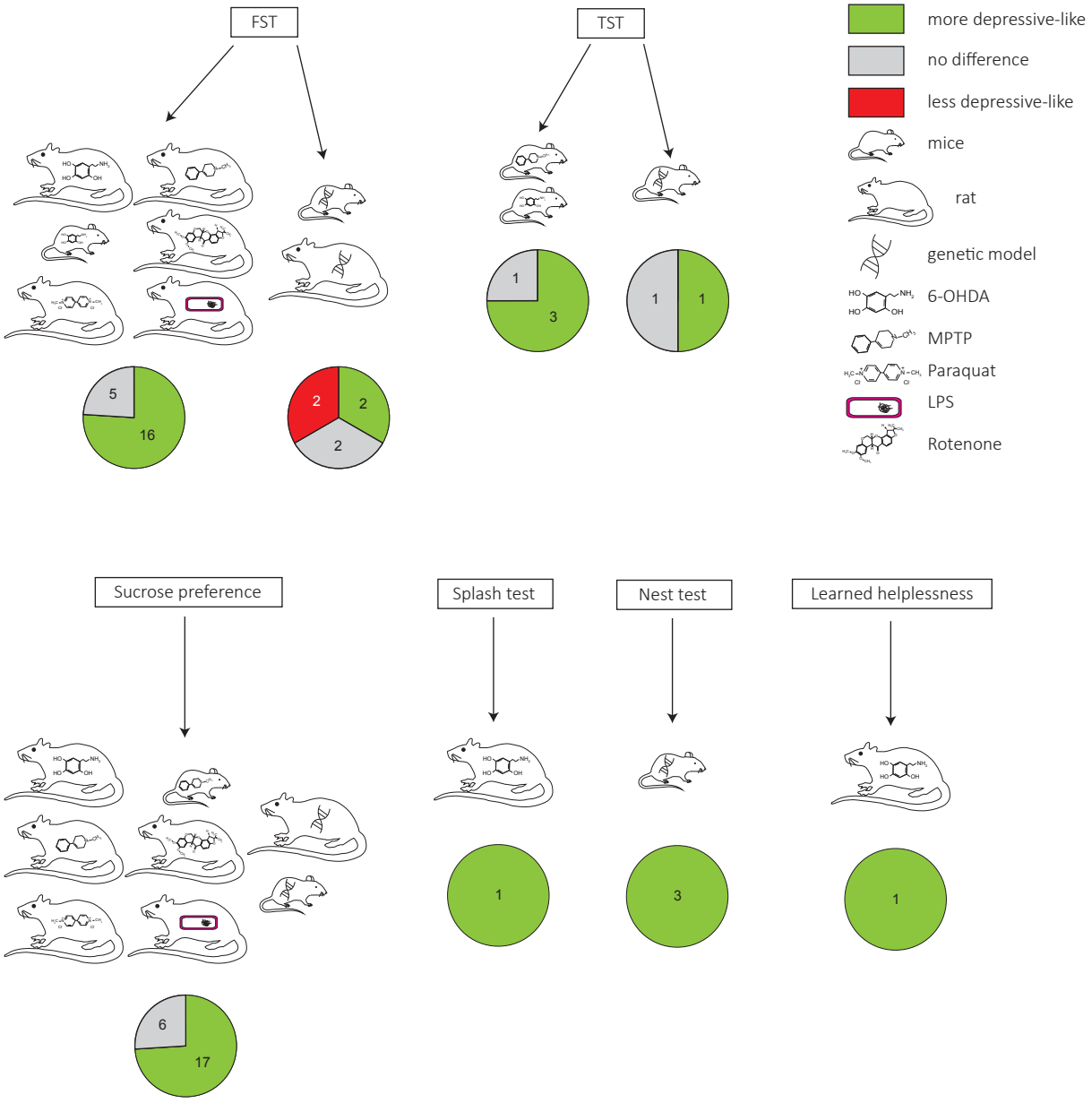

Figure 10. Depressive-like behaviors in animal models of Parkinson's disease. Studies mostly reported the presence of depressive-like behaviors in models of Parkinson's disease, even though FST data are more variable in genetic-based models. "n" displayed in the figure correspond to the number of publications relative to the test (see Table 3 for more details and references). 6-OHDA, 6-hydroxydopamine; FST, forced swim test; LPS, lipopolysaccharide; MPTP, 1-methyl-4-phenyl-1,2,3,6-tetrahydropyridine; TST, tail suspension test.

Table 6 Depressive-like behaviors in Parkinson's disease models

Species	Model	Test	Results	Ref.
Rat	6-OHDA	FST	↘ swimming time / ↗ immobility time	(Branchi et al., 2008) (Tadaiesky et al., 2008) (Santiago et al., 2010) (Tadaiesky et al., 2010) (Casas et al., 2011) (Berghauzen-Maciejewska et al., 2014) (Santiago et al., 2014) (Liu et al., 2015) (Matheus et al., 2016) (Ilkiw et al., 2018)
			↗ immobility time when the 3 monoamines are depleted	(Delaville et al., 2012)
			No ≠	(Eskow Jaunarajs et al., 2010) (Campos et al., 2013)
Mice	6-OHDA	FST	↗ immobility time	(Bonito-Oliva et al., 2014) (Tuon et al., 2014) (Chiu et al., 2015)
Rat	Rotenone	FST	No ≠	(Santiago et al., 2010)
	Paraquat		↗ immobility time	(Campos et al., 2013)
	MPTP		No ≠	(Santiago et al., 2010)
	LPS		No ≠	(Santiago et al., 2010)
			↗ immobility time	(Hritcu and Gorgan, 2014)
Rat	α-syn	FST	No ≠	(Campos et al., 2013)
			↘ climbing	(Caudal et al., 2015)
Mice	VMAT2	FST	↗ immobility in old mice	(Taylor et al., 2009)
Mice	A30P	FST	↘ immobility time	(Nuber et al., 2011)
Mice	LRRK2	FST	No ≠	(Bichler et al., 2013)
Mice	A53T	FST	↘ immobility time	(Oaks et al., 2013)
Mice	6-OHDA	TST	↗ immobility time	(Antunes et al., 2014) (Bonito-Oliva et al., 2014)
Mice	MPTP	TST	↗ immobility time	(Vucković et al., 2008)
			No ≠	(Gorton et al., 2010)
Mice	VMAT2	TST	↗ immobility time in old mice	(Taylor et al., 2009)
Mice	*LRRK2*	TST	No ≠	(Bichler et al., 2013)
Rat	6-OHDA	Sucrose pref.	↘ preference/consumption	(Tadaiesky et al., 2008) (Santiago et al., 2010) (Carvalho et al., 2013) (Santiago et al., 2010) (Liu et al., 2015) (Matheus et al., 2016) (Silva et al., 2016) (Kamińska et al., 2017) (Vecchia et al., 2018) (Ilkiw et al., 2018)
			↘ preference when the 3 monoamines are depleted	(Delaville et al., 2012)
			No ≠	(Branchi et al., 2008) (Campos et al., 2013)
Rat	Rotenone	Sucrose pref.	↘ preference	(Santiago et al., 2010)
Rat	LPS	Sucrose pref.	↘ preference	(Santiago et al., 2010)
Rat	Paraquat	Sucrose pref.	No ≠	(Campos et al., 2013)
Rat	MPTP	Sucrose pref.	↘ preference	(Krupina et al., 1995) (Santiago et al., 2010)
Mice	MPTP	Sucrose pref.	No ≠	(Vucković et al., 2008) (Gorton et al., 2010)
Rat	α-syn	Sucrose pref.	↘ consumption	(Caudal et al., 2015)
			No ≠	(Campos et al., 2013)
Mice	MitoPark	Sucrose pref.	↘ preference	(Chen et al., 2018)
Rat	6-OHDA	Splash test	↘ grooming time	(Matheus et al., 2016)
Mice	α-syn	Nest test	Deficit and delay to build nest	(Fleming et al., 2004)
Mice	A53T	Nest test	↘ in nest building score	(Paumier et al., 2013)
Mice	MitoPark	Nest test	↘ in nest building score	(Chen et al., 2018)
Rat	6-OHDA	LH	↗ escape latency and ↗ % of helpless rats	(Winter et al., 2007)

6-OHDA, 6-hydroxydopamine; α-syn, α-synuclein; FST, forced swim test; LH, learned helplessness ; LPS, lipopolyssacharide; MPTP, 1-methyl-4-phenyl-1,2,3,6-tetrahydropyridine; TST, tail suspension test. Note that "6-OHDA" gathers various models, either unilateral or bilateral, with different lesion sites, and with or without neuroprotection of non-dopamine systems.

Similar to the forced swim test, the tail suspension test is also based on an increased immobility response in a stress situation. In this test, used in mice only, the animal is suspended by its tail and the immobility time is measured. Acute antidepressant treatment given prior to the test is able to decrease this immobility (Duman, 2010). If some studies reported longer immobility time in mouse models of Parkinson's disease (Antunes et al., 2014; Bonito-Oliva et al., 2014; Taylor et al., 2009; Vuckovi ć et al., 2008), one third of the literature reported no difference with control animals (Bichler et al., 2013; Gorton et al., 2010). Again, this lack of phenotype has been proposed to be potentially related to the time-dependent development of the considered model (Taylor et al., 2009) (Table 6).

The sucrose preference test or sucrose consumption test is classically used as an indicator of anhedonia (lack of interest in rewarding stimuli), which is one of the symptoms that can be present in major depressive disorder. In pre-clinical models, the test usually consists in a two-bottle choice paradigm, with free access to a bottle with sucrose and one of water. A lack of preference (50% of preference) would be a sign of anhedonia, but the total amount of sucrose intake can also be considered as a relevant parameter. Some studies reported no difference between animal models of Parkinson's disease and their controls (Branchi et al., 2008; Campos et al., 2013; Gorton et al., 2010; Vuckovi ć et al., 2008), but most of published data showed a significant reduction in either sucrose consumption and/or sucrose preference(Carvalho et al., 2013; Caudal et al., 2015; Chen et al., 2018; Delaville et al., 2012; Ilkiw et al., 2018; Kamińska et al., 2017; Krupina et al., 1995; Liu et al., 2015; Matheus et al., 2016; Santiago et al., 2010; Silva et al., 2016; Tadaiesky et al., 2008; Vecchia et al., 2018). As mentioned above, this difference can be time-dependent in the considered models (Caudal et al., 2015; Matheus et al., 2016; Santiago et al., 2010, 2014), and it has been suggested for both the forced swim test and the sucrose preference that adding a co-lesion of noradrenergic and serotonergic systems to the dopamine lesion favors depression-like behaviors (Delaville et al., 2012).

A recent trend for addressing depression-like phenotypes in rodents is to consider alterations of naturally occurring behaviors of animals, such as grooming or nesting. The splash test consists in a pulverization of a sugar solution on the coat of the animal and the measure of the grooming time. A reduction in this grooming time may relate to apathy in human, which is one of the symptoms of major depressive disorder. A 6-OHDA lesion of the dorsal striatum decreases grooming time at one week (but no more at 3 weeks) post-lesion (Matheus et al., 2016). In A53T mutant mice, a deficit in overall grooming behavior is also present, particularly at 2 and 6 months of age (Paumier et al., 2013). On the other hand, the nesting test consists in evaluating the quality of a nest made by the animal, with for example a score ranging from 0 to

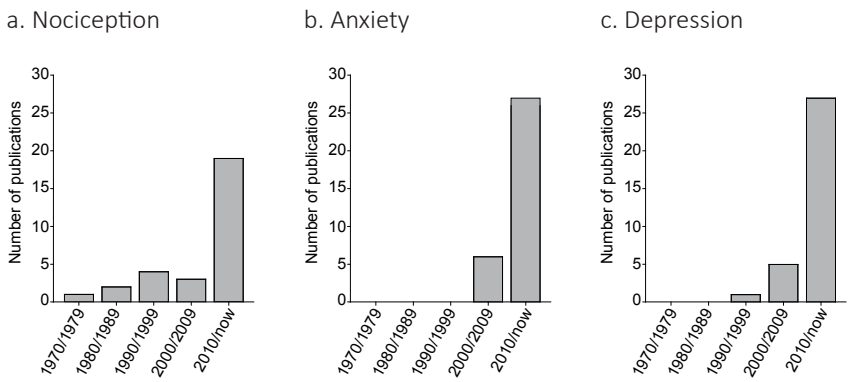

Figure 11. Number of publications reporting data on pain, anxiety and depression related parameters in animal models of Parkinson's disease.

4 or 5, 0 corresponding to an absence of nest and the highest score to a fully finished nest. This test is responsive to antidepressant drugs. A deficit and delay in cotton use for nest building has been observed in the Thy-1 α-synuclein mice (Fleming et al., 2004), which was proposed to be related to both deficits in fine motor skills and decreased motivation to build nest. In this test, both the A53T mutant mice (Paumier et al., 2013) and the MitoPark model (Chen et al., 2018) also display a significant deficit in nest building (Table 6).

The learned helplessness paradigm consists in the exposure to an inescapable stress (*i.e.* footshocks), followed by an active avoidance test. Pre-exposed animals that display a reduced ability to escape from the shocks (Duman, 2010) are qualified as "helpless". It is used as a model of either major depressive disorder or posttraumatic stress disorder, depending on the considered protocol. Both complete (98%) and partial (75% and 45%) 6-OHDA lesion increased the latency to escape shock presentation and the proportion of rats meeting "helpless" criteria (Winter et al., 2007) (Table 6). However, interpretation of those findings is not easy. Indeed, independently from shock pre-exposure, it has been reported 40 years ago that 6-OHDA injections into dopamine cell bodies or terminals induces a decrease in the number of avoidance responses in the active avoidance test (Delacour et al., 1977; Lin et al., 1978). While such deficit can be present even in the absence of significant alteration in locomotor activity (Delacour et al., 1977), it is unsure whether it is reflecting a deficit in learning the avoidance procedure or it is reflecting an actual "helpless" state.

4. Conclusion

Beyond dopamine cell loss and motor symptoms, Parkinson's disease is a complex disease that leads to a variety of non-motor symptoms, including pain, anxiety and depression in a notable proportion of patients. For decades, experimental research on Parkinson's disease has focused on the motor symptoms as well as on the dopamine system. Indeed, until recently, most data in animal models were limited to dopaminergic alterations, which could not explain Parkinson's disease semiology, particularly in the early stage of the disease. A given symptom, however, may not necessarily arise from changes in a single given system. It can also be hypothesized that alterations in different systems (including the dopamine one) may add-on to a symptom and cumulatively contribute to its severity.

While the search for disease-modifying strategies is intense, the acknowledgment of the non-motor symptoms' burden upon Parkinson's disease patient's quality of life has only recently come to experimental researchers' attention, as witnessed by the relatively sparse and recent literature (Fig. 11). Nevertheless, the present literature suggests that existing models of

Parkinson's disease allow modeling non-motor symptoms, thus making possible to address mechanistic aspects and/or take such symptoms into consideration for preclinical testing of new therapeutic approaches. Preclinical studies of non-motor symptoms will however still require more systematic characterization to establish their presence/absence and time-line in various models, in order to provide standardization with robust and reliable outputs for some of them. On the other hand, one might consider that individual variability in the presence/absence of these symptoms may be naturally present in experimental models as it is in patients, which may partly contribute to the heterogeneity in reporting these symptoms in experimental studies that are classically based on small cohorts. Progress would anyway require that these aspects of Parkinson's disease are more often tested and studied in rodent and non-human primate models.

5. Acknowledgments

This work was supported by the Centre National de la Recherche Scientifique [contracts UPR3212 and UMR5293], the University of Strasbourg, the University of Bordeaux, the Agence Nationale de la Recherche [ANR-15-CE37-0005-02; Euridol ANR-17-EURE-0022], the Fondation pour la Recherche Médicale [FDT20170437322], the NeuroTime Erasmus Mondus Joint Doctorate and by a NARSAD distinguish investigator grant from the Brain and Behavior Research Foundation [24220].

6. Conflict of interest statement

The authors declare no conflict of interest.

7. References

Allen, N.E., Wong, C.M., Canning, C.G., Moloney, N., 2016. The Association Between Parkinson's Disease Motor Impairments and Pain. Pain Med. 17, 456–462. https://doi.org/10.1111/pme.12898

Antkiewicz-Michaluk, L., Karolewicz, B., Romańska, I., Michaluk, J., Bojarski, A.J., Vetulani, J., 2003. 1-methyl-1,2,3,4-tetrahydroisoquinoline protects against rotenone-induced mortality and biochemical changes in rat brain. Eur. J. Pharmacol. 466, 263–269.

Antunes, M.S., Goes, A.T.R., Boeira, S.P., Prigol, M., Jesse, C.R., 2014. Protective effect of hesperidin in a model of Parkinson's disease induced by 6-hydroxydopamine in aged mice. Nutrition30, 1415–1422. https://doi.org/10.1016/j.nut.2014.03.024

Bankiewicz, K.S., Sanchez-Pernaute, R., Oiwa, Y., Kohutnicka, M., Cummins, A., Eberling, J., 2001. Preclinical Models of Parkinson's Disease. Curr. Protoc. Neurosci. https://doi.org/10.1002/0471142301.ns0904s09

Barone, P., Antonini, A., Colosimo, C., Marconi, R., Morgante, L., Avarello, T.P., Bottacchi, E., Cannas, A., Ceravolo, G., Ceravolo, R., Cicarelli, G., Gaglio, R.M., Giglia, R.M., Iemolo, F., Manfredi, M., Meco, G., Nicoletti, A., Pederzoli, M., Petrone, A., Pisani, A., Pontieri, F.E., Quatrale, R., Ramat, S., Scala, R., Volpe, G., Zappulla, S., Bentivoglio, A.R., Stocchi, F., Trianni, G., Dotto, P.D., PRIAMO study group, 2009. The PRIAMO study: A multicenter assessment of nonmotor

symptoms and their impact on quality of life in Parkinson's disease. Mov. Disord. 24, 1641–1649. https://doi.org/10.1002/mds.22643

Barrot, M., 2012. Tests and models of nociception and pain in rodents. Neuroscience 211, 39–50. https://doi.org/10.1016/j.neuroscience.2011.12.041

Barthas, F., Sellmeijer, J., Hugel, S., Waltisperger, E., Barrot, M., Yalcin, I., 2015. The anterior cingulate cortex is a critical hub for pain-induced depression. Biol. Psychiatry 77, 236–245. https://doi.org/10.1016/j.biopsych.2014.08.004

Basso, M.A., Strecker, R.E., Evinger, C., 1993. Midbrain 6-hydroxydopamine lesions modulate blink reflex excitability. Exp. Brain Res. 94, 88–96.

Bastías-Candia, S., Di Benedetto, M., D'Addario, C., Candeletti, S., Romualdi, P., 2015. Combined exposure to agriculture pesticides, paraquat and maneb, induces alterations in the N/OFQ-NOPr and PDYN/KOPr systems in rats: Relevance to sporadic Parkinson's disease. Environ. Toxicol. 30, 656–663. https://doi.org/10.1002/tox.21943

Bastías-Candia, S., Zolezzi, J.M., Inestrosa, N.C., 2018. Revisiting the Paraquat-Induced Sporadic Parkinson's Disease-Like Model. Mol. Neurobiol. https://doi.org/10.1007/s12035-018-1148-z

Beiske, A.G., Loge, J.H., Rønningen, A., Svensson, E., 2009. Pain in Parkinson's disease: Prevalence and characteristics. Pain 141, 173–177. https://doi.org/10.1016/j.pain.2008.12.004

Belzung, C., 1999. Chapter 4.11 Measuring rodent exploratory behavior, in: Crusio, W.E., Gerlai, R.T. (Eds.), Techniques in the Behavioral and Neural Sciences, Handbook of Molecular-Genetic Techniques for Brain and Behavior Research. Elsevier, pp. 738–749. https://doi.org/10.1016/S0921-0709(99)80057-1

Berghauzen-Maciejewska, K., Kuter, K., Kolasiewicz, W., Głowacka, U., Dziubina, A., Ossowska, K., Wardas, J., 2014. Pramipexole but not imipramine or fluoxetine reverses the "depressive-like" behaviour in a rat model of preclinical stages of Parkinson's disease. Behav. Brain Res. 271, 343–353. https://doi.org/10.1016/j.bbr.2014.06.029

Bertrand, E., Lechowicz, W., Szpak, G.M., Dymecki, J., 1997. Qualitative and quantitative analysis of locus coeruleus neurons in Parkinson's disease. Folia Neuropathol. 35, 80–86.

Betarbet, R., Sherer, T.B., Greenamyre, J.T., 2002. Animal models of Parkinson's disease. BioEssays 24, 308–318. https://doi.org/10.1002/bies.10067

Betarbet, R., Sherer, T.B., MacKenzie, G., Garcia-Osuna, M., Panov, A.V., Greenamyre, J.T., 2000. Chronic systemic pesticide exposure reproduces features of Parkinson's disease. Nat. Neurosci. 3, 1301–1306. https://doi.org/10.1038/81834

Bezard, E., Fernagut, P.-O., 2014. Premotor parkinsonism models. Parkinsonism Relat. Disord. 20 Suppl 1, S17-19. https://doi.org/10.1016/S1353-8020(13)70007-5

Bezard, E., Przedborski, S., 2011. A tale on animal models of Parkinson's disease. Mov. Disord. 26, 993–1002. https://doi.org/10.1002/mds.23696

Bezard, E., Yue, Z., Kirik, D., Spillantini, M.G., 2013. Animal models of Parkinson's disease: limits and relevance to neuroprotection studies. Mov. Disord. 28, 61–70. https://doi.org/10.1002/mds.25108

Bichler, Z., Lim, H.C., Zeng, L., Tan, E.K., 2013. Non-motor and motor features in LRRK2 transgenic mice. PloS One 8, e70249. https://doi.org/10.1371/journal.pone.0070249

Blanchet, P.J., Brefel-Courbon, C., 2017. Chronic pain and pain processing in Parkinson's disease. Prog. Neuropsychopharmacol. Biol. Psychiatry. In press. https://doi.org/10.1016/j.pnpbp.2017.10.010

Blum, D., Torch, S., Lambeng, N., Nissou, M., Benabid, A.L., Sadoul, R., Verna, J.M., 2001. Molecular pathways involved in the neurotoxicity of 6-OHDA, dopamine and MPTP: contribution to the apoptotic theory in Parkinson's disease. Prog. Neurobiol. 65, 135–172.

Bonifati, V., Rizzu, P., Baren, M.J. van, Schaap, O., Breedveld, G.J., Krieger, E., Dekker, M.C.J., Squitieri, F., Ibanez, P., Joosse, M., Dongen, J.W. van, Vanacore, N., Swieten, J.C. van, Brice, A., Meco, G., Duijn, C.M. van, Oostra, B.A., Heutink, P., 2003a. Mutations in the DJ-1 Gene Associated with Autosomal Recessive Early-Onset Parkinsonism. Science 299, 256–259. https://doi.org/10.1126/science.1077209

Bonifati, V., Rizzu, P., Squitieri, F., Krieger, E., Vanacore, N., van Swieten, J.C., Brice, A., van Duijn, C.M., Oostra, B., Meco, G., Heutink, P., 2003b. DJ-1(PARK7), a novel gene for autosomal recessive, early onset parkinsonism. Neurol. Sci. 24, 159–160. https://doi.org/10.1007/s10072-003-0108-0

Bonito-Oliva, A., Masini, D., Fisone, G., 2014. A mouse model of non-motor symptoms in Parkinson's disease: focus on pharmacological interventions targeting affective dysfunctions. Front. Behav. Neurosci. 8, 290. https://doi.org/10.3389/fnbeh.2014.00290

Bourdenx, M., Dovero, S., Engeln, M., Bido, S., Bastide, M.F., Dutheil, N., Vollenweider, I., Baud, L., Piron, C., Grouthier, V., Boraud, T., Porras, G., Li, Q., Baekelandt, V., Scheller, D., Michel, A., Fernagut, P.-O., Georges, F., Courtine, G., Bezard, E., Dehay, B., 2015. Lack of additive role of ageing in nigrostriatal neurodegeneration triggered by α-synuclein overexpression. Acta Neuropathol. Commun. 3, 46. https://doi.org/10.1186/s40478-015-0222-2

Bové, J., Perier, C., 2012. Neurotoxin-based models of Parkinson's disease. Neuroscience 211, 51–76. https://doi.org/10.1016/j.neuroscience.2011.10.057

Boyce, S., Kelly, E., Reavill, C., Jenner, P., Marsden, C.D., 1984. Repeated administration of N-methyl-4-phenyl 1,2,5,6-tetrahydropyridine to rats is not toxic to striatal dopamine neurones. Biochem. Pharmacol. 33, 1747–1752.

Braak, H., Del Tredici, K., Bratzke, H., Hamm-Clement, J., Sandmann-Keil, D., Rüb, U., 2002. Staging of the intracerebral inclusion body pathology associated with idiopathic Parkinson's disease (preclinical and clinical stages). J. Neurol. 249 Suppl 3, III/1-5.

Braak, H., Del Tredici, K., Rüb, U., de Vos, R.A.I., Jansen Steur, E.N.H., Braak, E., 2003. Staging of brain pathology related to sporadic Parkinson's disease. Neurobiol. Aging 24, 197–211.

Braak, H., Ghebremedhin, E., Rüb, U., Bratzke, H., Del Tredici, K., 2004. Stages in the development of Parkinson's disease-related pathology. Cell Tissue Res. 318, 121–134. https://doi.org/10.1007/s00441-004-0956-9

Branchi, I., D'Andrea, I., Armida, M., Cassano, T., Pèzzola, A., Potenza, R.L., Morgese, M.G., Popoli, P., Alleva, E., 2008. Nonmotor symptoms in Parkinson's disease: investigating early-phase onset of behavioral dysfunction in the 6-hydroxydopamine-lesioned rat model. J. Neurosci. Res. 86, 2050–2061. https://doi.org/10.1002/jnr.21642

Brefel-Courbon, C., Payoux, P., Thalamas, C., Ory, F., Quelven, I., Chollet, F., Montastruc, J.L., Rascol, O., 2005. Effect of levodopa on pain threshold in Parkinson's disease: a clinical and positron emission tomography study. Mov. Disord. 20, 1557–1563. https://doi.org/10.1002/mds.20629

Burn, D.J., 2002. Beyond the iron mask: towards better recognition and treatment of depression associated with Parkinson's disease. Mov. Disord. 17, 445–454. https://doi.org/10.1002/mds.10114

Campos, F.L., Carvalho, M.M., Cristovão, A.C., Je, G., Baltazar, G., Salgado, A.J., Kim, Y.-S., Sousa, N., 2013. Rodent models of Parkinson's disease: beyond the motor symptomatology. Front. Behav. Neurosci. 7, 175. https://doi.org/10.3389/fnbeh.2013.00175

Camus, S.M.J., Blois-Heulin, C., Li, Q., Hausberger, M., Bezard, E., 2013a. Behavioural profiles in captive-bred cynomolgus macaques: towards monkey models of mental disorders? PloS One 8, e62141. https://doi.org/10.1371/journal.pone.0062141

Camus, S.M.J., Rochais, C., Blois-Heulin, C., Li, Q., Hausberger, M., Bezard, E., 2014. Depressive-like behavioral profiles in captive-bred single- and socially-housed rhesus and cynomolgus macaques: a species comparison. Front. Behav. Neurosci. 8, 47. https://doi.org/10.3389/fnbeh.2014.00047

Camus, S.M.J., Rochais, C., Blois-Heulin, C., Li, Q., Hausberger, M., Bezard, E., 2013b. Birth origin differentially affects depressive-like behaviours: are captive-born cynomolgus monkeys more vulnerable to depression than their wild-born counterparts? PloS One 8, e67711. https://doi.org/10.1371/journal.pone.0067711

Cao, L.-F., Peng, X.-Y., Huang, Y., Wang, B., Zhou, F.-M., Cheng, R.-X., Chen, L.-H., Luo, W.-F., Liu, T., 2016. Restoring Spinal Noradrenergic Inhibitory Tone Attenuates Pain Hypersensitivity in a Rat Model of Parkinson's Disease. Neural Plast. 2016, 6383240. https://doi.org/10.1155/2016/6383240

Carey, R.J., 1986. Acute ipsilateral hyperalgesia and chronic contralateral hypoalgesia after unilateral 6-hydroxydopamine lesions of the substantia nigra. Exp. Neurol. 91, 277–284.

Carvalho, M.M., Campos, F.L., Coimbra, B., Pêgo, J.M., Rodrigues, C., Lima, R., Rodrigues, A.J., Sousa, N., Salgado, A.J., 2013. Behavioral characterization of the 6-hydroxidopamine model of Parkinson's disease and pharmacological rescuing of non-motor deficits. Mol. Neurodegener. 8, 14. https://doi.org/10.1186/1750-1326-8-14

Casas, S., García, S., Cabrera, R., Nanfaro, F., Escudero, C., Yunes, R., 2011. Progesterone prevents depression-like behavior in a model of Parkinson's disease induced by 6-hydroxydopamine in male

rats. Pharmacol. Biochem. Behav. 99, 614–618. https://doi.org/10.1016/j.pbb.2011.06.012
Castaño, A., Herrera, A.J., Cano, J., Machado, A., 1998. Lipopolysaccharide intranigral injection induces inflammatory reaction and damage in nigrostriatal dopaminergic system. J. Neurochem. 70, 1584–1592.
Caudal, D., Alvarsson, A., Björklund, A., Svenningsson, P., 2015. Depressive-like phenotype induced by AAV-mediated overexpression of human α-synuclein in midbrain dopaminergic neurons. Exp. Neurol. 273, 243–252. https://doi.org/10.1016/j.expneurol.2015.09.002
Chan, P., DeLanney, L.E., Irwin, I., Langston, J.W., Di Monte, D., 1991. Rapid ATP loss caused by 1-methyl-4-phenyl-1,2,3,6-tetrahydropyridine in mouse brain. J. Neurochem. 57, 348–351.
Chandran, J.S., Lin, X., Zapata, A., Höke, A., Shimoji, M., Moore, S.O., Galloway, M.P., Laird, F.M., Wong, P.C., Price, D.L., Bailey, K.R., Crawley, J.N., Shippenberg, T., Cai, H., 2008. Progressive behavioral deficits in DJ-1-deficient mice are associated with normal nigrostriatal function. Neurobiol. Dis. 29, 505–514. https://doi.org/10.1016/j.nbd.2007.11.011
Charles, K.-A., Naudet, F., Bouali-Benazzouz, R., Landry, M., De Deurwaerdère, P., Fossat, P., Benazzouz, A., 2018. Alteration of nociceptive integration in the spinal cord of a rat model of Parkinson's disease. Mov. Disord. https://doi.org/10.1002/mds.27377
Chaudhuri, K.R., Healy, D.G., Schapira, A.H.V., National Institute for Clinical Excellence, 2006. Non-motor symptoms of Parkinson's disease: diagnosis and management. Lancet Neurol. 5, 235–245. https://doi.org/10.1016/S1474-4422(06)70373-8
Chen, C., Li, X., Ge, G., Liu, J., Biju, K.C., Laing, S.D., Qian, Y., Ballard, C., He, Z., Masliah, E., Clark, R.A., O'Connor, J.C., Li, S., 2018. GDNF-expressing macrophages mitigate loss of dopamine neurons and improve Parkinsonian symptoms in MitoPark mice. Sci. Rep. 8, 5460. https://doi.org/10.1038/s41598-018-23795-4
Chen, C.-C.V., Shih, Y.-Y.I., Chang, C., 2013. Dopaminergic imaging of nonmotor manifestations in a rat model of Parkinson's disease by fMRI. Neurobiol. Dis. 49, 99–106. https://doi.org/10.1016/j.nbd.2012.07.020
Chen, L., Cagniard, B., Mathews, T., Jones, S., Koh, H.C., Ding, Y., Carvey, P.M., Ling, Z., Kang, U.J., Zhuang, X., 2005. Age-dependent motor deficits and dopaminergic dysfunction in DJ-1 null mice. J. Biol. Chem. 280, 21418–21426. https://doi.org/10.1074/jbc.M413955200
Chesselet, M.-F., 2008. In vivo alpha-synuclein overexpression in rodents: a useful model of Parkinson's disease? Exp. Neurol. 209, 22–27. https://doi.org/10.1016/j.expneurol.2007.08.006
Chiu, W.-H., Depboylu, C., Hermanns, G., Maurer, L., Windolph, A., Oertel, W.H., Ries, V., Höglinger, G.U., 2015. Long-term treatment with L-DOPA or pramipexole affects adult neurogenesis and corresponding non-motor behavior in a mouse model of Parkinson's disease. Neuropharmacology 95, 367–376. https://doi.org/10.1016/j.neuropharm.2015.03.020
Chiueh, C.C., Markey, S.P., Burns, R.S., Johannessen, J.N., Jacobowitz, D.M., Kopin, I.J., 1984a. Neurochemical and behavioral effects of 1-methyl-4-phenyl-1,2,3,6- tetrahydropyridine (MPTP) in rat, guinea pig, and monkey. Psychopharmacol. Bull. 20, 548–553.
Chiueh, C.C., Markey, S.P., Burns, R.S., Johannessen, J.N., Pert, A., Kopin, I.J., 1984b. Neurochemical and behavioral effects of systemic and intranigral administration of N-methyl-4-phenyl-1,2,3,6-tetrahydropyridine in the rat. Eur. J. Pharmacol. 100, 189–194.
Chudler, E.H., Lu, Y., 2008. Nociceptive behavioral responses to chemical, thermal and mechanical stimulation after unilateral, intrastriatal administration of 6-hydroxydopamine. Brain Res. 1213, 41–47. https://doi.org/10.1016/j.brainres.2008.03.053
Creed, R.B., Goldberg, M.S., 2018. New Developments in Genetic rat models of Parkinson's Disease. Mov. Disord. 33, 717–729. https://doi.org/10.1002/mds.27296
Cummings, J.L., 1992. Depression and Parkinson's disease: a review. Am. J. Psychiatry 149, 443–454. https://doi.org/10.1176/ajp.149.4.443
Czernecki, V., Pillon, B., Houeto, J.L., Pochon, J.B., Levy, R., Dubois, B., 2002. Motivation, reward, and Parkinson's disease: influence of dopatherapy. Neuropsychologia 40, 2257–2267. https://doi.org/10.1016/S0028-3932(02)00108-2
Darweesh, S.K.L., Verlinden, V.J.A., Stricker, B.H., Hofman, A., Koudstaal, P.J., Ikram, M.A., 2017. Trajectories of prediagnostic functioning in Parkinson's disease. Brain J. Neurol. 140, 429–441. https://doi.org/10.1093/brain/aww291
Dauer, W., Przedborski, S., 2003. Parkinson's disease: mechanisms and models. Neuron 39, 889–909.

Davis, G.C., Williams, A.C., Markey, S.P., Ebert, M.H., Caine, E.D., Reichert, C.M., Kopin, I.J., 1979. Chronic Parkinsonism secondary to intravenous injection of meperidine analogues. Psychiatry Res. 1, 249–254.

Dawson, T.M., Ko, H.S., Dawson, V.L., 2010. Genetic animal models of Parkinson's disease. Neuron 66, 646–661. https://doi.org/10.1016/j.neuron.2010.04.034

Delacour, J., Echavarria, M.T., Senault, B., Houcine, O., 1977. Specificity of avoidance deficits produced by 6-hydroxydopamine lesions of the nigrostriatal system of the rat. J. Comp. Physiol. Psychol. 91, 875–885.

Delaville, C., Chetrit, J., Abdallah, K., Morin, S., Cardoit, L., De Deurwaerdère, P., Benazzouz, A., 2012. Emerging dysfunctions consequent to combined monoaminergic depletions in Parkinsonism. Neurobiol. Dis. 45, 763–773. https://doi.org/10.1016/j.nbd.2011.10.023

Delaville, C., Deurwaerdère, P.D., Benazzouz, A., 2011. Noradrenaline and Parkinson's disease. Front. Syst. Neurosci. 5, 31. https://doi.org/10.3389/fnsys.2011.00031

Dieb, W., Ouachikh, O., Durif, F., Hafidi, A., 2016. Nigrostriatal dopaminergic depletion produces orofacial static mechanical allodynia. Eur. J. Pain 20, 196–205. https://doi.org/10.1002/ejp.707

Dieb, W., Ouachikh, O., Durif, F., Hafidi, A., 2014. Lesion of the dopaminergic nigrostriatal pathway induces trigeminal dynamic mechanical allodynia. Brain Behav. 4, 368–380. https://doi.org/10.1002/brb3.214

Dissanayaka, N.N.W., Sellbach, A., Matheson, S., O'Sullivan, J.D., Silburn, P.A., Byrne, G.J., Marsh, R., Mellick, G.D., 2010. Anxiety disorders in Parkinson's disease: prevalence and risk factors. Mov. Disord. 25, 838–845. https://doi.org/10.1002/mds.22833

Dolatshahi, M., Farbood, Y., Sarkaki, A., Mansouri, S.M.T., Khodadadi, A., 2015. Ellagic acid improves hyperalgesia and cognitive deficiency in 6-hydroxidopamine induced rat model of Parkinson's disease. Iran. J. Basic Med. Sci. 18, 38–46.

Duman, C.H., 2010. Models of depression. Vitam. Horm. 82, 1–21. https://doi.org/10.1016/S0083-6729(10)82001-1

Dusonchet, J., Kochubey, O., Stafa, K., Young, S.M., Zufferey, R., Moore, D.J., Schneider, B.L., Aebischer, P., 2011. A rat model of progressive nigral neurodegeneration induced by the Parkinson's disease-associated G2019S mutation in LRRK2. J. Neurosci. 31, 907–912. https://doi.org/10.1523/JNEUROSCI.5092-10.2011

Ehringer, H., Hornykiewicz, O., 1960. Distribution of noradrenaline and dopamine (3-hydroxytyramine) in the human brain and their behavior in diseases of the extrapyramidal system. Klin. Wochenschr. 38, 1236–1239.

Ekstrand, M.I., Terzioglu, M., Galter, D., Zhu, S., Hofstetter, C., Lindqvist, E., Thams, S., Bergstrand, A., Hansson, F.S., Trifunovic, A., Hoffer, B., Cullheim, S., Mohammed, A.H., Olson, L., Larsson, N.-G., 2007. Progressive parkinsonism in mice with respiratory-chain-deficient dopamine neurons. Proc. Natl. Acad. Sci. U. S. A. 104, 1325–1330. https://doi.org/10.1073/pnas.0605208103

Engeln, M., De Deurwaerdère, P., Li, Q., Bezard, E., Fernagut, P.-O., 2015. Widespread Monoaminergic Dysregulation of Both Motor and Non-Motor Circuits in Parkinsonism and Dyskinesia. Cereb. Cortex 1991 25, 2783–2792. https://doi.org/10.1093/cercor/bhu076

Erro, R., Pappatà, S., Amboni, M., Vicidomini, C., Longo, K., Santangelo, G., Picillo, M., Vitale, C., Moccia, M., Giordano, F., Brunetti, A., Pellecchia, M.T., Salvatore, M., Barone, P., 2012. Anxiety is associated with striatal dopamine transporter availability in newly diagnosed untreated Parkinson's disease patients. Parkinsonism Relat. Disord. 18, 1034–1038. https://doi.org/10.1016/j.parkreldis.2012.05.022

Eskow Jaunarajs, K.L., Dupre, K.B., Ostock, C.Y., Button, T., Deak, T., Bishop, C., 2010. Behavioral and neurochemical effects of chronic L-DOPA treatment on nonmotor sequelae in the hemiparkinsonian rat. Behav. Pharmacol. 21, 627–637. https://doi.org/10.1097/FBP.0b013e32833e7e80

Esteban, A., Giménez-Roldàn, S., 1975. Blink reflex in Huntingon's chorea and Parkinson's disease. Acta Neurol. Scand. 52, 145–157.

Fabre, E., Monserrat, J., Herrero, A., Barja, G., Leret, M.L., 1999. Effect of MPTP on brain mitochondrial H2O2 and ATP production and on dopamine and DOPAC in the striatum. J. Physiol. Biochem. 55, 325–331.

Faggiani, E., Naudet, F., Janssen, M.L.F., Temel, Y., Benazzouz, A., 2018. Serotonergic neurons

mediate the anxiolytic effect of l-DOPA: Neuronal correlates in the amygdala. Neurobiol. Dis. 110, 20–28. https://doi.org/10.1016/j.nbd.2017.11.001

Fernagut, P.-O., Chesselet, M.-F., 2004. Alpha-synuclein and transgenic mouse models. Neurobiol. Dis. 17, 123–130. https://doi.org/10.1016/j.nbd.2004.07.001

Filali, M., Lalonde, R., 2016. Neurobehavioral Anomalies in the Pitx3/ak Murine Model of Parkinson's Disease and MPTP. Behav. Genet. 46, 228–241. https://doi.org/10.1007/s10519-015-9753-3

Fleming, S.M., Salcedo, J., Fernagut, P.-O., Rockenstein, E., Masliah, E., Levine, M.S., Chesselet, M.-F., 2004. Early and progressive sensorimotor anomalies in mice overexpressing wild-type human alpha-synuclein. J. Neurosci. 24, 9434–9440. https://doi.org/10.1523/JNEUROSCI.3080-04.2004

Francardo, V., 2018. Modeling Parkinson's disease and treatment complications in rodents: Potentials and pitfalls of the current options. Behav. Brain Res. 352, 142–150. https://doi.org/10.1016/j.bbr.2017.12.014

Funayama, M., Hasegawa, K., Kowa, H., Saito, M., Tsuji, S., Obata, F., 2002. A new locus for Parkinson's disease (PARK8) maps to chromosome 12p11.2-q13.1. Ann. Neurol. 51, 296–301.

Galter, D., Pernold, K., Yoshitake, T., Lindqvist, E., Hoffer, B., Kehr, J., Larsson, N.-G., Olson, L., 2010. MitoPark mice mirror the slow progression of key symptoms and L-DOPA response in Parkinson's disease. Genes Brain Behav. 9, 173–181. https://doi.org/10.1111/j.1601-183X.2009.00542.x

Gee, L.E., Chen, N., Ramirez-Zamora, A., Shin, D.S., Pilitsis, J.G., 2015. The effects of subthalamic deep brain stimulation on mechanical and thermal thresholds in 6OHDA-lesioned rats. Eur. J. Neurosci. 42, 2061–2069. https://doi.org/10.1111/ejn.12992

George, S., van den Buuse, M., San Mok, S., Masters, C.L., Li, Q.-X., Culvenor, J.G., 2008. Alpha-synuclein transgenic mice exhibit reduced anxiety-like behaviour. Exp. Neurol. 210, 788–792. https://doi.org/10.1016/j.expneurol.2007.12.017

German, D.C., Manaye, K.F., White, C.L., Woodward, D.J., McIntire, D.D., Smith, W.K., Kalaria, R.N., Mann, D.M., 1992. Disease-specific patterns of locus coeruleus cell loss. Ann. Neurol. 32, 667–676. https://doi.org/10.1002/ana.410320510

Giasson, B.I., Duda, J.E., Quinn, S.M., Zhang, B., Trojanowski, J.Q., Lee, V.M.-Y., 2002. Neuronal alpha-synucleinopathy with severe movement disorder in mice expressing A53T human alpha-synuclein. Neuron 34, 521–533.

Giraldo, G., Brooks, M., Giasson, B.I., Janus, C., 2018. Locomotor differences in mice expressing wild-type human α-synuclein. Neurobiol. Aging 65, 140–148. https://doi.org/10.1016/j.neurobiolaging.2018.01.020

Gispert, S., Ricciardi, F., Kurz, A., Azizov, M., Hoepken, H.-H., Becker, D., Voos, W., Leuner, K., Müller, W.E., Kudin, A.P., Kunz, W.S., Zimmermann, A., Roeper, J., Wenzel, D., Jendrach, M., García-Arencíbia, M., Fernández-Ruiz, J., Huber, L., Rohrer, H., Barrera, M., Reichert, A.S., Rüb, U., Chen, A., Nussbaum, R.L., Auburger, G., 2009. Parkinson phenotype in aged PINK1-deficient mice is accompanied by progressive mitochondrial dysfunction in absence of neurodegeneration. PloS One 4, e5777. https://doi.org/10.1371/journal.pone.0005777

Goldberg, M.S., Pisani, A., Haburcak, M., Vortherms, T.A., Kitada, T., Costa, C., Tong, Y., Martella, G., Tscherter, A., Martins, A., Bernardi, G., Roth, B.L., Pothos, E.N., Calabresi, P., Shen, J., 2005. Nigrostriatal dopaminergic deficits and hypokinesia caused by inactivation of the familial Parkinsonism-linked gene DJ-1. Neuron 45, 489–496. https://doi.org/10.1016/j.neuron.2005.01.041

Gómez-Paz, A., Drucker-Colín, R., Milán-Aldaco, D., Palomero-Rivero, M., Ambriz-Tututi, M., 2017. Intrastriatal chromospheres' transplant reduces nociception in hemiparkinsonian rats. Neuroscience. https://doi.org/10.1016/j.neuroscience.2017.08.052

Gorton, L.M., Vuckovic, M.G., Vertelkina, N., Petzinger, G.M., Jakowec, M.W., Wood, R.I., 2010. Exercise effects on motor and affective behavior and catecholamine neurochemistry in the MPTP-lesioned mouse. Behav. Brain Res. 213, 253–262. https://doi.org/10.1016/j.bbr.2010.05.009

Grandi, L.C., Di Giovanni, G., Galati, S., 2018. Animal models of early-stage Parkinson's disease and acute dopamine deficiency to study compensatory neurodegenerative mechanisms. J. Neurosci. Methods 308, 205–218. https://doi.org/10.1016/j.jneumeth.2018.08.012

Grossmann, W., Jurna, I., Nell, T., Theres, C., 1973. The dependence of the anti-nociceptive effect of morphine and other analgesic agents on spinal motor activity after central monoamine depletion. Eur. J. Pharmacol. 24, 67–77.

Gubellini, P., Kachidian, P., 2015. Animal models of Parkinson's disease: An updated overview. Rev. Neurol. (Paris) 171, 750–761. https://doi.org/10.1016/j.neurol.2015.07.011

Haddadi, H., Rajaei, Z., Alaei, H., Shahidani, S., 2018. Chronic treatment with carvacrol improves passive avoidance memory in a rat model of Parkinson's disease. Arq. Neuropsiquiatr. 76, 71–77. https://doi.org/10.1590/0004-282X20170193

Halliday, G.M., Li, Y.W., Blumbergs, P.C., Joh, T.H., Cotton, R.G., Howe, P.R., Blessing, W.W., Geffen, L.B., 1990. Neuropathology of immunohistochemically identified brainstem neurons in Parkinson's disease. Ann. Neurol. 27, 373–385. https://doi.org/10.1002/ana.410270405

Hargreaves, K., Dubner, R., Brown, F., Flores, C., Joris, J., 1988. A new and sensitive method for measuring thermal nociception in cutaneous hyperalgesia. Pain 32, 77–88.

Healy, D.G., Falchi, M., O'Sullivan, S.S., Bonifati, V., Durr, A., Bressman, S., Brice, A., Aasly, J., Zabetian, C.P., Goldwurm, S., Ferreira, J.J., Tolosa, E., Kay, D.M., Klein, C., Williams, D.R., Marras, C., Lang, A.E., Wszolek, Z.K., Berciano, J., Schapira, A.H.V., Lynch, T., Bhatia, K.P., Gasser, T., Lees, A.J., Wood, N.W., International LRRK2 Consortium, 2008. Phenotype, genotype, and worldwide genetic penetrance of LRRK2-associated Parkinson's disease: a case-control study. Lancet Neurol. 7, 583–590. https://doi.org/10.1016/S1474-4422(08)70117-0

Hefti, F., Melamed, E., Sahakian, B.J., Wurtman, R.J., 1980. Circling behavior in rats with partial, unilateral nigro-striatal lesions: effect of amphetamine, apomorphine, and DOPA. Pharmacol. Biochem. Behav. 12, 185–188.

Heinz, S., Freyberger, A., Lawrenz, B., Schladt, L., Schmuck, G., Ellinger-Ziegelbauer, H., 2017. Mechanistic Investigations of the Mitochondrial Complex I Inhibitor Rotenone in the Context of Pharmacological and Safety Evaluation. Sci. Rep. 7, 45465. https://doi.org/10.1038/srep45465

Hernandez, D.G., Reed, X., Singleton, A.B., 2016. Genetics in Parkinson disease: Mendelian versus non-Mendelian inheritance. J. Neurochem. 139 Suppl 1, 59–74. https://doi.org/10.1111/jnc.13593

Ho, Y.-J., Ho, S.-C., Pawlak, C.R., Yeh, K.-Y., 2011. Effects of D-cycloserine on MPTP-induced behavioral and neurological changes: potential for treatment of Parkinson's disease dementia. Behav. Brain Res. 219, 280–290. https://doi.org/10.1016/j.bbr.2011.01.028

Hritcu, L., Gorgan, L.D., 2014. Intranigral lipopolysaccharide induced anxiety and depression by altered BDNF mRNA expression in rat hippocampus. Prog. Neuropsychopharmacol. Biol. Psychiatry 51, 126–132. https://doi.org/10.1016/j.pnpbp.2014.01.016

Huang, C., Ravdin, L.D., Nirenberg, M.J., Piboolnurak, P., Severt, L., Maniscalco, J.S., Solnes, L., Dorfman, B.J., Henchcliffe, C., 2013. Neuroimaging markers of motor and nonmotor features of Parkinson's disease: an 18f fluorodeoxyglucose positron emission computed tomography study. Dement. Geriatr. Cogn. Disord. 35, 183–196. https://doi.org/10.1159/000345987

Hughes, A.J., Daniel, S.E., Kilford, L., Lees, A.J., 1992. Accuracy of clinical diagnosis of idiopathic Parkinson's disease: a clinico-pathological study of 100 cases. J. Neurol. Neurosurg. Psychiatry 55, 181–184.

Hui, Y.P., Wang, T., Han, L.N., Li, L.B., Sun, Y.N., Liu, J., Qiao, H.F., Zhang, Q.J., 2015. Anxiolytic effects of prelimbic 5-HT(1A) receptor activation in the hemiparkinsonian rat. Behav. Brain Res. 277, 211–220. https://doi.org/10.1016/j.bbr.2014.04.053

Ibáñez, P., Bonnet, A.-M., Débarges, B., Lohmann, E., Tison, F., Pollak, P., Agid, Y., Dürr, A., Brice, A., 2004. Causal relation between alpha-synuclein gene duplication and familial Parkinson's disease. Lancet 364, 1169–1171. https://doi.org/10.1016/S0140-6736(04)17104-3

Ilkiw, J.L., Kmita, L.C., Targa, A.D.S., Noseda, A.C.D., Rodrigues, L.S., Dorieux, F.W.C., Fagotti, J., Dos Santos, P., Lima, M.M.S., 2018. Dopaminergic Lesion in the Olfactory Bulb Restores Olfaction and Induces Depressive-Like Behaviors in a 6-OHDA Model of Parkinson's Disease. Mol. Neurobiol. https://doi.org/10.1007/s12035-018-1134-5

Ip, C.W., Klaus, L.-C., Karikari, A.A., Visanji, N.P., Brotchie, J.M., Lang, A.E., Volkmann, J., Koprich, J.B., 2017. AAV1/2-induced overexpression of A53T-α-synuclein in the substantia nigra results in degeneration of the nigrostriatal system with Lewy-like pathology and motor impairment: a new mouse model for Parkinson's disease. Acta Neuropathol. Commun. 5, 11. https://doi.org/10.1186/s40478-017-0416-x

Ishihara, L., Brayne, C., 2006. A systematic review of depression and mental illness preceding Parkinson's disease. Acta Neurol. Scand. 113, 211–220. https://doi.org/10.1111/j.1600-0404.2006.00579.x

Itier, J.-M., Ibanez, P., Mena, M.A., Abbas, N., Cohen-Salmon, C., Bohme, G.A., Laville, M., Pratt, J., Corti, O., Pradier, L., Ret, G., Joubert, C., Periquet, M., Araujo, F., Negroni, J., Casarejos, M.J., Canals, S., Solano, R., Serrano, A., Gallego, E., Sanchez, M., Denefle, P., Benavides, J., Tremp, G., Rooney, T.A., Brice, A., Garcia de Yebenes, J., 2003. Parkin gene inactivation alters behaviour and dopamine neurotransmission in the mouse. Hum. Mol. Genet. 12, 2277–2291. https://doi.org/10.1093/hmg/ddg239

Jacob, E.L., Gatto, N.M., Thompson, A., Bordelon, Y., Ritz, B., 2010. Occurrence of depression and anxiety prior to Parkinson's disease. Parkinsonism Relat. Disord. 16, 576–581. https://doi.org/10.1016/j.parkreldis.2010.06.014

Jellinger, K.A., 1991. Pathology of Parkinson's disease. Changes other than the nigrostriatal pathway. Mol. Chem. Neuropathol. 14, 153–197.

Johansen, J.P., Fields, H.L., Manning, B.H., 2001. The affective component of pain in rodents: direct evidence for a contribution of the anterior cingulate cortex. Proc. Natl. Acad. Sci. U. S. A. 98, 8077–8082. https://doi.org/10.1073/pnas.141218998

Jungnickel, J., Kalve, I., Reimers, L., Nobre, A., Wesemann, M., Ratzka, A., Halfer, N., Lindemann, C., Schwabe, K., Töllner, K., Gernert, M., Grothe, C., 2011. Topology of intrastriatal dopaminergic grafts determines functional and emotional outcome in neurotoxin-lesioned rats. Behav. Brain Res. 216, 129–135. https://doi.org/10.1016/j.bbr.2010.07.023

Kahle, P.J., Neumann, M., Ozmen, L., Muller, V., Jacobsen, H., Schindzielorz, A., Okochi, M., Leimer, U., van Der Putten, H., Probst, A., Kremmer, E., Kretzschmar, H.A., Haass, C., 2000. Subcellular localization of wild-type and Parkinson's disease-associated mutant alpha -synuclein in human and transgenic mouse brain. J. Neurosci. 20, 6365–6373.

Kaminer, J., Thakur, P., Evinger, C., 2015. Effects of subthalamic deep brain stimulation on blink abnormalities of 6-OHDA lesioned rats. J. Neurophysiol. 113, 3038–3046. https://doi.org/10.1152/jn.01072.2014

Kamińska, K., Lenda, T., Konieczny, J., Czarnecka, A., Lorenc-Koci, E., 2017. Depressive-like neurochemical and behavioral markers of Parkinson's disease after 6-OHDA administered unilaterally to the rat medial forebrain bundle. Pharmacol. Rep. PR 69, 985–994. https://doi.org/10.1016/j.pharep.2017.05.016

King, T., Vera-Portocarrero, L., Gutierrez, T., Vanderah, T.W., Dussor, G., Lai, J., Fields, H.L., Porreca, F., 2009. Unmasking the tonic-aversive state in neuropathic pain. Nat. Neurosci. 12, 1364–1366. https://doi.org/10.1038/nn.2407

Kish, S.J., 2003. Biochemistry of Parkinson's disease: is a brain serotonergic deficiency a characteristic of idiopathic Parkinson's disease? Adv. Neurol. 91, 39–49.

Kitada, T., Pisani, A., Porter, D.R., Yamaguchi, H., Tscherter, A., Martella, G., Bonsi, P., Zhang, C., Pothos, E.N., Shen, J., 2007. Impaired dopamine release and synaptic plasticity in the striatum of PINK1-deficient mice. Proc. Natl. Acad. Sci. U. S. A. 104, 11441–11446. https://doi.org/10.1073/pnas.0702717104

Koller, W.C., 1984. Sensory symptoms in Parkinson's disease. Neurology 34, 957–959.

Koprich, J.B., Kalia, L.V., Brotchie, J.M., 2017. Animal models of α-synucleinopathy for Parkinson disease drug development. Nat. Rev. Neurosci. 18, 515–529. https://doi.org/10.1038/nrn.2017.75

Krüger, R., Kuhn, W., Müller, T., Woitalla, D., Graeber, M., Kösel, S., Przuntek, H., Epplen, J.T., Schöls, L., Riess, O., 1998. Ala30Pro mutation in the gene encoding alpha-synuclein in Parkinson's disease. Nat. Genet. 18, 106–108. https://doi.org/10.1038/ng0298-106

Krupina, N.A., Orlova, I.N., Kryzhanovskiĭ, G.N., 1995. [The effect of parlodel on development of depressive syndrome in rats, caused by administering 1-methyl-4-phenyl-1,2,3,6-tetrahydropyridine (MPTP)]. Biull. Eksp. Biol. Med. 120, 66–70.

Lam, H.A., Wu, N., Cely, I., Kelly, R.L., Hean, S., Richter, F., Magen, I., Cepeda, C., Ackerson, L.C., Walwyn, W., Masliah, E., Chesselet, M.-F., Levine, M.S., Maidment, N.T., 2011. Elevated tonic extracellular dopamine concentration and altered dopamine modulation of synaptic activity precede dopamine loss in the striatum of mice overexpressing human α-synuclein. J. Neurosci. Res. 89, 1091–1102. https://doi.org/10.1002/jnr.22611

Langston, J.W., Ballard, P., Tetrud, J.W., Irwin, I., 1983. Chronic Parkinsonism in humans due to a product of meperidine-analog synthesis. Science 219, 979–980.

Lazarou, M., Narendra, D.P., Jin, S.M., Tekle, E., Banerjee, S., Youle, R.J., 2013. PINK1 drives Parkin

self-association and HECT-like E3 activity upstream of mitochondrial binding. J. Cell Biol. 200, 163–172. https://doi.org/10.1083/jcb.201210111

Le Bars, D., Gozariu, M., Cadden, S.W., 2001. Animal models of nociception. Pharmacol. Rev. 53, 597–652.

Le, W., Zhang, L., Xie, W., Li, S., Dani, J.A., 2015. Pitx3 deficiency produces decreased dopamine signaling and induces motor deficits in Pitx3(-/-) mice. Neurobiol. Aging 36, 3314–3320. https://doi.org/10.1016/j.neurobiolaging.2015.08.012

Lee, M.A., Walker, R.W., Hildreth, T.J., Prentice, W.M., 2006. A Survey of Pain in Idiopathic Parkinson's Disease. J. Pain Symptom Manage. 32, 462–469. https://doi.org/10.1016/j.jpainsymman.2006.05.020

Leentjens, A.F.G., Van den Akker, M., Metsemakers, J.F.M., Lousberg, R., Verhey, F.R.J., 2003. Higher incidence of depression preceding the onset of Parkinson's disease: a register study. Mov. Disord. 18, 414–418. https://doi.org/10.1002/mds.10387

Li, N., Ragheb, K., Lawler, G., Sturgis, J., Rajwa, B., Melendez, J.A., Robinson, J.P., 2003. Mitochondrial complex I inhibitor rotenone induces apoptosis through enhancing mitochondrial reactive oxygen species production. J. Biol. Chem. 278, 8516–8525. https://doi.org/10.1074/jbc.M210432200

Li, Y., Liu, W., Oo, T.F., Wang, L., Tang, Y., Jackson-Lewis, V., Zhou, C., Geghman, K., Bogdanov, M., Przedborski, S., Beal, M.F., Burke, R.E., Li, C., 2009. Mutant LRRK2(R1441G) BAC transgenic mice recapitulate cardinal features of Parkinson's disease. Nat. Neurosci. 12, 826–828. https://doi.org/10.1038/nn.2349

Lim, K.-L., Ng, C.-H., 2009. Genetic models of Parkinson disease. Biochim. Biophys. Acta 1792, 604–615. https://doi.org/10.1016/j.bbadis.2008.10.005

Lim, Y., Kehm, V.M., Li, C., Trojanowski, J.Q., Lee, V.M.-Y., 2010. Forebrain overexpression of alpha-synuclein leads to early postnatal hippocampal neuron loss and synaptic disruption. Exp. Neurol. 221, 86–97. https://doi.org/10.1016/j.expneurol.2009.10.005

Lin, M.T., Chia, W.Y., Tsai, C.T., Yin, T.H., 1978. Effects of brain monoamine depletion on thermoregulation, active avoidance, and food and water intake in rats. Experientia 34, 756–757.

Lin, M.T., Wu, J.J., Chandra, A., Tsay, B.L., 1981. Activation of striatal dopamine receptors induces pain inhibition in rats. J. Neural Transm. 51, 213–222.

Liu, K.-C., Li, J.-Y., Tan, H.-H., Du, C.-X., Xie, W., Zhang, Y.-M., Ma, W.-L., Zhang, L., 2015. Serotonin$_6$ receptors in the dorsal hippocampus regulate depressive-like behaviors in unilateral 6-hydroxydopamine-lesioned Parkinson's rats. Neuropharmacology 95, 290–298. https://doi.org/10.1016/j.neuropharm.2015.03.031

Liu, M., Bing, G., 2011. Lipopolysaccharide Animal Models for Parkinson's Disease. Park. Dis. https://doi.org/10.4061/2011/327089

Luk, K.C., Kehm, V.M., Zhang, B., O'Brien, P., Trojanowski, J.Q., Lee, V.M.Y., 2012. Intracerebral inoculation of pathological α-synuclein initiates a rapidly progressive neurodegenerative α-synucleinopathy in mice. J. Exp. Med. 209, 975–986. https://doi.org/10.1084/jem.20112457

Maegawa, H., Morimoto, Y., Kudo, C., Hanamoto, H., Boku, A., Sugimura, M., Kato, T., Yoshida, A., Niwa, H., 2015. Neural mechanism underlying hyperalgesic response to orofacial pain in Parkinson's disease model rats. Neurosci. Res. 96, 59–68. https://doi.org/10.1016/j.neures.2015.01.006

Mahlknecht, P., Seppi, K., Poewe, W., 2015. The Concept of Prodromal Parkinson's Disease. J. Park. Dis. 5, 681–697. https://doi.org/10.3233/JPD-150685

Manning-Bog, A.B., McCormack, A.L., Li, J., Uversky, V.N., Fink, A.L., Di Monte, D.A., 2002. The herbicide paraquat causes up-regulation and aggregation of alpha-synuclein in mice: paraquat and alpha-synuclein. J. Biol. Chem. 277, 1641–1644. https://doi.org/10.1074/jbc.C100560200

Marsh, L., 2013. Depression and Parkinson's disease: current knowledge. Curr. Neurol. Neurosci. Rep. 13, 409. https://doi.org/10.1007/s11910-013-0409-5

Marxreiter, F., Ettle, B., May, V.E.L., Esmer, H., Patrick, C., Kragh, C.L., Klucken, J., Winner, B., Riess, O., Winkler, J., Masliah, E., Nuber, S., 2013. Glial A30P alpha-synuclein pathology segregates neurogenesis from anxiety-related behavior in conditional transgenic mice. Neurobiol. Dis. 59, 38–51. https://doi.org/10.1016/j.nbd.2013.07.004

Masliah, E., Rockenstein, E., Veinbergs, I., Mallory, M., Hashimoto, M., Takeda, A., Sagara, Y., Sisk,

A., Mucke, L., 2000. Dopaminergic loss and inclusion body formation in alpha-synuclein mice: implications for neurodegenerative disorders. Science 287, 1265–1269.

Matheus, F.C., Rial, D., Real, J.I., Lemos, C., Takahashi, R.N., Bertoglio, L.J., Cunha, R.A., Prediger, R.D., 2016. Temporal Dissociation of Striatum and Prefrontal Cortex Uncouples Anhedonia and Defense Behaviors Relevant to Depression in 6-OHDA-Lesioned Rats. Mol. Neurobiol. 53, 3891–3899. https://doi.org/10.1007/s12035-015-9330-z

McCormack, A.L., Thiruchelvam, M., Manning-Bog, A.B., Thiffault, C., Langston, J.W., Cory-Slechta, D.A., Di Monte, D.A., 2002. Environmental risk factors and Parkinson's disease: selective degeneration of nigral dopaminergic neurons caused by the herbicide paraquat. Neurobiol. Dis. 10, 119–127.

McDowell, K., Chesselet, M.-F., 2012. Animal models of the non-motor features of Parkinson's disease. Neurobiol. Dis. 46, 597–606. https://doi.org/10.1016/j.nbd.2011.12.040

Morgan, M.J., Franklin, K.B., 1990. 6-Hydroxydopamine lesions of the ventral tegmentum abolish D-amphetamine and morphine analgesia in the formalin test but not in the tail flick test. Brain Res. 519, 144–149.

Moriyama, T.S., Felicio, A.C., Chagas, M.H.N., Tardelli, V.S., Ferraz, H.B., Tumas, V., Amaro-Junior, E., Andrade, L.A.F., Crippa, J.A., Bressan, R.A., 2011. Increased dopamine transporter density in Parkinson's disease patients with Social Anxiety Disorder. J. Neurol. Sci. 310, 53–57. https://doi.org/10.1016/j.jns.2011.06.056

Narendra, D., Tanaka, A., Suen, D.-F., Youle, R.J., 2008. Parkin is recruited selectively to impaired mitochondria and promotes their autophagy. J. Cell Biol. 183, 795–803. https://doi.org/10.1083/jcb.200809125

Nascimento, G.C., Bariotto-Dos-Santos, K., Leite-Panissi, C.R.A., Del-Bel, E.A., Bortolanza, M., 2018. Nociceptive Response to L-DOPA-Induced Dyskinesia in Hemiparkinsonian Rats. Neurotox. Res. https://doi.org/10.1007/s12640-018-9896-0

Nègre-Pagès, L., Regragui, W., Bouhassira, D., Grandjean, H., Rascol, O., DoPaMiP Study Group, 2008. Chronic pain in Parkinson's disease: the cross-sectional French DoPaMiP survey. Mov. Disord. 23, 1361–1369. https://doi.org/10.1002/mds.22142

Nilsson, F.M., Kessing, L.V., Bolwig, T.G., 2001. Increased risk of developing Parkinson's disease for patients with major affective disorder: a register study. Acta Psychiatr. Scand. 104, 380–386.

Niu, Y., Guo, X., Chen, Y., Wang, C.-E., Gao, J., Yang, W., Kang, Y., Si, W., Wang, H., Yang, S.-H., Li, S., Ji, W., Li, X.-J., 2015. Early Parkinson's disease symptoms in α-synuclein transgenic monkeys. Hum. Mol. Genet. 24, 2308–2317. https://doi.org/10.1093/hmg/ddu748

Nuber, S., Petrasch-Parwez, E., Arias-Carrión, O., Koch, L., Kohl, Z., Schneider, J., Calaminus, C., Dermietzel, R., Samarina, A., Boy, J., Nguyen, H.P., Teismann, P., Velavan, T.P., Kahle, P.J., von Hörsten, S., Fendt, M., Krüger, R., Riess, O., 2011. Olfactory neuron-specific expression of A30P α-synuclein exacerbates dopamine deficiency and hyperactivity in a novel conditional model of early Parkinson's disease stages. Neurobiol. Dis. 44, 192–204. https://doi.org/10.1016/j.nbd.2011.06.017

Nuber, S., Petrasch-Parwez, E., Winner, B., Winkler, J., von Hörsten, S., Schmidt, T., Boy, J., Kuhn, M., Nguyen, H.P., Teismann, P., Schulz, J.B., Neumann, M., Pichler, B.J., Reischl, G., Holzmann, C., Schmitt, I., Bornemann, A., Kuhn, W., Zimmermann, F., Servadio, A., Riess, O., 2008. Neurodegeneration and motor dysfunction in a conditional model of Parkinson's disease. J. Neurosci. 28, 2471–2484. https://doi.org/10.1523/JNEUROSCI.3040-07.2008

Oaks, A.W., Frankfurt, M., Finkelstein, D.I., Sidhu, A., 2013. Age-dependent effects of A53T alpha-synuclein on behavior and dopaminergic function. PloS One 8, e60378. https://doi.org/10.1371/journal.pone.0060378

Ogata, M., Noda, K., Akita, H., Ishibashi, H., 2015. Characterization of nociceptive response to chemical, mechanical, and thermal stimuli in adolescent rats with neonatal dopamine depletion. Neuroscience 289, 43–55. https://doi.org/10.1016/j.neuroscience.2015.01.002

O'Sullivan, S.S., Williams, D.R., Gallagher, D.A., Massey, L.A., Silveira-Moriyama, L., Lees, A.J., 2008. Nonmotor symptoms as presenting complaints in Parkinson's disease: a clinicopathological study. Mov. Disord. 23, 101–106. https://doi.org/10.1002/mds.21813

Paisán-Ruiz, C., Lewis, P.A., Singleton, A.B., 2013. LRRK2: cause, risk, and mechanism. J. Park. Dis. 3, 85–103. https://doi.org/10.3233/JPD-130192

Park, A., Stacy, M., 2009. Non-motor symptoms in Parkinson's disease. J. Neurol. 256 Suppl 3, 293–298. https://doi.org/10.1007/s00415-009-5240-1

Park, J., Lim, C.-S., Seo, H., Park, C.-A., Zhuo, M., Kaang, B.-K., Lee, K., 2015. Pain perception in acute model mice of Parkinson's disease induced by 1-methyl-4-phenyl-1,2,3,6-tetrahydropyridine (MPTP). Mol. Pain 11, 28. https://doi.org/10.1186/s12990-015-0026-1

Paumier, K.L., Sukoff Rizzo, S.J., Berger, Z., Chen, Y., Gonzales, C., Kaftan, E., Li, L., Lotarski, S., Monaghan, M., Shen, W., Stolyar, P., Vasilyev, D., Zaleska, M., D Hirst, W., Dunlop, J., 2013. Behavioral characterization of A53T mice reveals early and late stage deficits related to Parkinson's disease. PloS One 8, e70274. https://doi.org/10.1371/journal.pone.0070274

Pearce, J.M.S., 2008. Observations on the blink reflex. Eur. Neurol. 59, 221–223. https://doi.org/10.1159/000114053

Pellow, S., Chopin, P., File, S.E., Briley, M., 1985. Validation of open:closed arm entries in an elevated plus-maze as a measure of anxiety in the rat. J. Neurosci. Methods 14, 149–167.

Peña-Oliver, Y., Buchman, V.L., Stephens, D.N., 2010. Lack of involvement of alpha-synuclein in unconditioned anxiety in mice. Behav. Brain Res. 209, 234–240. https://doi.org/10.1016/j.bbr.2010.01.049

Perez, F.A., Palmiter, R.D., 2005. Parkin-deficient mice are not a robust model of parkinsonism. Proc. Natl. Acad. Sci. U. S. A. 102, 2174–2179. https://doi.org/10.1073/pnas.0409598102

Polymeropoulos, M.H., Lavedan, C., Leroy, E., Ide, S.E., Dehejia, A., Dutra, A., Pike, B., Root, H., Rubenstein, J., Boyer, R., Stenroos, E.S., Chandrasekharappa, S., Athanassiadou, A., Papapetropoulos, T., Johnson, W.G., Lazzarini, A.M., Duvoisin, R.C., Di Iorio, G., Golbe, L.I., Nussbaum, R.L., 1997. Mutation in the alpha-synuclein gene identified in families with Parkinson's disease. Science 276, 2045–2047.

Pont-Sunyer, C., Hotter, A., Gaig, C., Seppi, K., Compta, Y., Katzenschlager, R., Mas, N., Hofeneder, D., Brücke, T., Bayés, A., Wenzel, K., Infante, J., Zach, H., Pirker, W., Posada, I.J., Álvarez, R., Ispierto, L., De Fàbregues, O., Callén, A., Palasí, A., Aguilar, M., Martí, M.J., Valldeoriola, F., Salamero, M., Poewe, W., Tolosa, E., 2015. The onset of nonmotor symptoms in Parkinson's disease (the ONSET PD study). Mov. Disord. 30, 229–237. https://doi.org/10.1002/mds.26077

Porsolt, R.D., Le Pichon, M., Jalfre, M., 1977. Depression: a new animal model sensitive to antidepressant treatments. Nature 266, 730–732.

Qu, C., King, T., Okun, A., Lai, J., Fields, H.L., Porreca, F., 2011. Lesion of the rostral anterior cingulate cortex eliminates the aversiveness of spontaneous neuropathic pain following partial or complete axotomy. Pain 152, 1641–1648. https://doi.org/10.1016/j.pain.2011.03.002

Rabl, R., Breitschaedel, C., Flunkert, S., Duller, S., Amschl, D., Neddens, J., Niederkofler, V., Rockenstein, E., Masliah, E., Roemer, H., Hutter-Paier, B., 2017. Early start of progressive motor deficits in Line 61 α-synuclein transgenic mice. BMC Neurosci. 18, 22. https://doi.org/10.1186/s12868-017-0341-8

Rana, A.Q., Qureshi, A.R.M., Rahman, L., Jesudasan, A., Hafez, K.K., Rana, M.A., 2016. Association of restless legs syndrome, pain, and mood disorders in Parkinson's disease. Int. J. Neurosci. 126, 116–120. https://doi.org/10.3109/00207454.2014.994208

Recasens, A., Dehay, B., Bové, J., Carballo-Carbajal, I., Dovero, S., Pérez-Villalba, A., Fernagut, P.-O., Blesa, J., Parent, A., Perier, C., Fariñas, I., Obeso, J.A., Bezard, E., Vila, M., 2014. Lewy body extracts from Parkinson disease brains trigger α-synuclein pathology and neurodegeneration in mice and monkeys. Ann. Neurol. 75, 351–362. https://doi.org/10.1002/ana.24066

Reichmann, H., 2017. Premotor Diagnosis of Parkinson's Disease. Neurosci. Bull. 33, 526–534. https://doi.org/10.1007/s12264-017-0159-5

Remy, P., Doder, M., Lees, A., Turjanski, N., Brooks, D., 2005. Depression in Parkinson's disease: loss of dopamine and noradrenaline innervation in the limbic system. Brain J. Neurol. 128, 1314–1322. https://doi.org/10.1093/brain/awh445

Rieu, I., Houeto, J.L., Pereira, B., De Chazeron, I., Bichon, A., Chéreau, I., Ulla, M., Brefel-Courbon, C., Ory-Magne, F., Dujardin, K., Tison, F., Krack, P., Durif, F., 2016. Impact of Mood and Behavioral Disorders on Quality of Life in Parkinson's disease. J. Park. Dis. 6, 267–277. https://doi.org/10.3233/JPD-150747

Rockenstein, E., Mallory, M., Hashimoto, M., Song, D., Shults, C.W., Lang, I., Masliah, E., 2002. Differential neuropathological alterations in transgenic mice expressing alpha-synuclein from the

platelet-derived growth factor and Thy-1 promoters. J. Neurosci. Res. 68, 568–578. https://doi.org/10.1002/jnr.10231

Rosemann, M., Ivashkevich, A., Favor, J., Dalke, C., Hölter, S.M., Becker, L., Rácz, I., Bolle, I., Klempt, M., Rathkolb, B., Kalaydjiev, S., Adler, T., Aguilar, A., Hans, W., Horsch, M., Rozman, J., Calzada-Wack, J., Kunder, S., Naton, B., Gailus-Durner, V., Fuchs, H., Schulz, H., Beckers, J., Busch, D.H., Burbach, J.P.H., Smidt, M.P., Quintanilla-Martinez, L., Esposito, I., Klopstock, T., Klingenspor, M., Ollert, M., Wolf, E., Wurst, W., Zimmer, A., de Angelis, M.H., Atkinson, M., Heinzmann, U., Graw, J., 2010. Microphthalmia, parkinsonism, and enhanced nociception in Pitx3 (416insG) mice. Mamm. Genome 21, 13–27. https://doi.org/10.1007/s00335-009-9235-0

Rosland, J.H., Hunskaar, S., Broch, O.J., Hole, K., 1992. Acute and long term effects of 1-methyl-4-phenyl-1,2,3,6-tetrahydropyridine (MPTP) in tests of nociception in mice. Pharmacol. Toxicol. 70, 31–37.

Rothman, S.M., Griffioen, K.J., Vranis, N., Ladenheim, B., Cong, W., Cadet, J.-L., Haran, J., Martin, B., Mattson, M.P., 2013. Neuronal expression of familial Parkinson's disease A53T α-synuclein causes early motor impairment, reduced anxiety and potential sleep disturbances in mice. J. Park. Dis. 3, 215–229. https://doi.org/10.3233/JPD-120130

Saadé, N.E., Atweh, S.F., Bahuth, N.B., Jabbur, S.J., 1997. Augmentation of nociceptive reflexes and chronic deafferentation pain by chemical lesions of either dopaminergic terminals or midbrain dopaminergic neurons. Brain Res. 751, 1–12.

Sachs, C., Jonsson, G., 1975. Mechanisms of action of 6-hydroxydopamine. Biochem. Pharmacol. 24, 1–8.

Sahgal, A., Andrews, J.S., Biggins, J.A., Candy, J.M., Edwardson, J.A., Keith, A.B., Turner, J.D., Wright, C., 1984. N-methyl-4-phenyl-1,2,3,6-tetrahydropyridine (MPTP) affects locomotor activity without producing a nigrostriatal lesion in the rat. Neurosci. Lett. 48, 179–184.

Santiago, R.M., Barbieiro, J., Lima, M.M.S., Dombrowski, P.A., Andreatini, R., Vital, M.A.B.F., 2010. Depressive-like behaviors alterations induced by intranigral MPTP, 6-OHDA, LPS and rotenone models of Parkinson's disease are predominantly associated with serotonin and dopamine. Prog. Neuropsychopharmacol. Biol. Psychiatry 34, 1104–1114. https://doi.org/10.1016/j.pnpbp.2010.06.004

Santiago, R.M., Barbiero, J., Gradowski, R.W., Bochen, S., Lima, M.M.S., Da Cunha, C., Andreatini, R., Vital, M.A.B.F., 2014. Induction of depressive-like behavior by intranigral 6-OHDA is directly correlated with deficits in striatal dopamine and hippocampal serotonin. Behav. Brain Res. 259, 70–77. https://doi.org/10.1016/j.bbr.2013.10.035

Schapira, A.H.V., Chaudhuri, K.R., Jenner, P., 2017. Non-motor features of Parkinson disease. Nat. Rev. Neurosci. 18, 509. https://doi.org/10.1038/nrn.2017.91

Schober, A., 2004. Classic toxin-induced animal models of Parkinson's disease: 6-OHDA and MPTP. Cell Tissue Res. 318, 215–224. https://doi.org/10.1007/s00441-004-0938-y

Sellmeijer, J., Mathis, V., Hugel, S., Li, X.-H., Song, Q., Chen, Q.-Y., Barthas, F., Lutz, P.-E., Karatas, M., Luthi, A., Veinante, P., Aertsen, A., Barrot, M., Zhuo, M., Yalcin, I., 2018. Hyperactivity of Anterior Cingulate Cortex Areas 24a/24b Drives Chronic Pain-Induced Anxiodepressive-like Consequences. J. Neurosci. 38, 3102–3115. https://doi.org/10.1523/JNEUROSCI.3195-17.2018

Shiba, M., Bower, J.H., Maraganore, D.M., McDonnell, S.K., Peterson, B.J., Ahlskog, J.E., Schaid, D.J., Rocca, W.A., 2000. Anxiety disorders and depressive disorders preceding Parkinson's disease: a case-control study. Mov. Disord. 15, 669–677.

Silva, T.P. da, Poli, A., Hara, D.B., Takahashi, R.N., 2016. Time course study of microglial and behavioral alterations induced by 6-hydroxydopamine in rats. Neurosci. Lett. 622, 83–87. https://doi.org/10.1016/j.neulet.2016.04.049

Singleton, A.B., Farrer, M., Johnson, J., Singleton, A., Hague, S., Kachergus, J., Hulihan, M., Peuralinna, T., Dutra, A., Nussbaum, R., Lincoln, S., Crawley, A., Hanson, M., Maraganore, D., Adler, C., Cookson, M.R., Muenter, M., Baptista, M., Miller, D., Blancato, J., Hardy, J., Gwinn-Hardy, K., 2003. alpha-Synuclein locus triplication causes Parkinson's disease. Science 302, 841. https://doi.org/10.1126/science.1090278

Singleton, A.B., Farrer, M.J., Bonifati, V., 2013. The genetics of Parkinson's disease: progress and therapeutic implications. Mov. Disord. 28, 14–23. https://doi.org/10.1002/mds.25249

Stern, M.B., Lang, A., Poewe, W., 2012. Toward a redefinition of Parkinson's disease. Mov. Disord.

27, 54–60. https://doi.org/10.1002/mds.24051

Sun, Y.-N., Wang, T., Wang, Y., Han, L.-N., Li, L.-B., Zhang, Y.-M., Liu, J., 2015. Activation of 5-HT_1A receptors in the medial subdivision of the central nucleus of the amygdala produces anxiolytic effects in a rat model of Parkinson's disease. Neuropharmacology 95, 181–191. https://doi.org/10.1016/j.neuropharm.2015.03.007

Surdhar, I., Gee, M., Bouchard, T., Coupland, N., Malykhin, N., Camicioli, R., 2012. Intact limbic-prefrontal connections and reduced amygdala volumes in Parkinson's disease with mild depressive symptoms. Parkinsonism Relat. Disord. 18, 809–813. https://doi.org/10.1016/j.parkreldis.2012.03.008

Szatmari, S., Illigens, B.M.-W., Siepmann, T., Pinter, A., Takats, A., Bereczki, D., 2017. Neuropsychiatric symptoms in untreated Parkinson's disease. Neuropsychiatr. Dis. Treat. 13, 815–826. https://doi.org/10.2147/NDT.S130997

Tadaiesky, M.T., Dombrowski, P.A., Da Cunha, C., Takahashi, R.N., 2010. Effects of SR141716A on Cognitive and Depression-Related Behavior in an Animal Model of Premotor Parkinson's Disease. Park. Dis. 2010, 238491. https://doi.org/10.4061/2010/238491

Tadaiesky, M.T., Dombrowski, P.A., Figueiredo, C.P., Cargnin-Ferreira, E., Da Cunha, C., Takahashi, R.N., 2008. Emotional, cognitive and neurochemical alterations in a premotor stage model of Parkinson's disease. Neuroscience 156, 830–840. https://doi.org/10.1016/j.neuroscience.2008.08.035

Takeda, R., Ikeda, T., Tsuda, F., Abe, H., Hashiguchi, H., Ishida, Y., Nishimori, T., 2005. Unilateral lesions of mesostriatal dopaminergic pathway alters the withdrawal response of the rat hindpaw to mechanical stimulation. Neurosci. Res. 52, 31–36. https://doi.org/10.1016/j.neures.2005.01.005

Takeda, R., Ishida, Y., Ebihara, K., Abe, H., Matsuo, H., Ikeda, T., Koganemaru, G., Kuramashi, A., Funahashi, H., Magata, Y., Kawai, K., Nishimori, T., 2014. Intrastriatal grafts of fetal ventral mesencephalon improve allodynia-like withdrawal response to mechanical stimulation in a rat model of Parkinson's disease. Neurosci. Lett. 573, 19–23. https://doi.org/10.1016/j.neulet.2014.05.007

Tassorelli, C., Armentero, M.-T., Greco, R., Fancellu, R., Sandrini, G., Nappi, G., Blandini, F., 2007. Behavioral responses and Fos activation following painful stimuli in a rodent model of Parkinson's disease. Brain Res. 1176, 53–61. https://doi.org/10.1016/j.brainres.2007.08.012

Taylor, T.N., Caudle, W.M., Shepherd, K.R., Noorian, A., Jackson, C.R., Iuvone, P.M., Weinshenker, D., Greene, J.G., Miller, G.W., 2009. Nonmotor symptoms of Parkinson's disease revealed in an animal model with reduced monoamine storage capacity. J. Neurosci. 29, 8103–8113. https://doi.org/10.1523/JNEUROSCI.1495-09.2009

Thiruchelvam, M., McCormack, A., Richfield, E.K., Baggs, R.B., Tank, A.W., Di Monte, D.A., Cory-Slechta, D.A., 2003. Age-related irreversible progressive nigrostriatal dopaminergic neurotoxicity in the paraquat and maneb model of the Parkinson's disease phenotype. Eur. J. Neurosci. 18, 589–600.

Titova, N., Schapira, A.H.V., Chaudhuri, K.R., Qamar, M.A., Katunina, E., Jenner, P., 2017. Nonmotor Symptoms in Experimental Models of Parkinson's Disease. Int. Rev. Neurobiol. 133, 63–89. https://doi.org/10.1016/bs.irn.2017.05.018

Tofaris, G.K., Garcia Reitböck, P., Humby, T., Lambourne, S.L., O'Connell, M., Ghetti, B., Gossage, H., Emson, P.C., Wilkinson, L.S., Goedert, M., Spillantini, M.G., 2006. Pathological changes in dopaminergic nerve cells of the substantia nigra and olfactory bulb in mice transgenic for truncated human alpha-synuclein(1-120): implications for Lewy body disorders. J. Neurosci. 26, 3942–3950. https://doi.org/10.1523/JNEUROSCI.4965-05.2006

Tuon, T., Valvassori, S.S., Dal Pont, G.C., Paganini, C.S., Pozzi, B.G., Luciano, T.F., Souza, P.S., Quevedo, J., Souza, C.T., Pinho, R.A., 2014. Physical training prevents depressive symptoms and a decrease in brain-derived neurotrophic factor in Parkinson's disease. Brain Res. Bull. 108, 106–112. https://doi.org/10.1016/j.brainresbull.2014.09.006

Ulusoy, A., Decressac, M., Kirik, D., Björklund, A., 2010. Viral vector-mediated overexpression of α-synuclein as a progressive model of Parkinson's disease. Prog. Brain Res. 184, 89–111. https://doi.org/10.1016/S0079-6123(10)84005-1

Ungerstedt, U., 1971. Adipsia and aphagia after 6-hydroxydopamine induced degeneration of the nigro-striatal dopamine system. Acta Physiol. Scand. Suppl. 367, 95–122.

Ungerstedt, U., 1968. 6-Hydroxy-dopamine induced degeneration of central monoamine neurons. Eur. J. Pharmacol. 5, 107–110.

Ungerstedt, U., Arbuthnott, G.W., 1970. Quantitative recording of rotational behavior in rats after 6-hydroxy-dopamine lesions of the nigrostriatal dopamine system. Brain Res. 24, 485–493.

Valente, E.M., Salvi, S., Ialongo, T., Marongiu, R., Elia, A.E., Caputo, V., Romito, L., Albanese, A., Dallapiccola, B., Bentivoglio, A.R., 2004. PINK1 mutations are associated with sporadic early-onset parkinsonism. Ann. Neurol. 56, 336–341. https://doi.org/10.1002/ana.20256

van Mierlo, T.J., Chung, C., Foncke, E.M., Berendse, H.W., van den Heuvel, O.A., 2015. Depressive symptoms in Parkinson's disease are related to decreased hippocampus and amygdala volume. Mov. Disord. 30, 245–252. https://doi.org/10.1002/mds.26112

Vecchia, D.D., Kanazawa, L.K.S., Wendler, E., de Almeida Soares Hocayen, P., Bruginski, E., Campos, F.R., Stern, C.A.J., Vital, M.A.B.F., Miyoshi, E., Wöhr, M., Schwarting, R.K.W., Andreatini, R., 2018. Effects of ketamine on vocal impairment, gait changes, and anhedonia induced by bilateral 6-OHDA infusion into the substantia nigra pars compacta in rats: Therapeutic implications for Parkinson's disease. Behav. Brain Res. 342, 1–10. https://doi.org/10.1016/j.bbr.2017.12.041

Volta, M., Melrose, H., 2017. LRRK2 mouse models: dissecting the behavior, striatal neurochemistry and neurophysiology of PD pathogenesis. Biochem. Soc. Trans. 45, 113–122. https://doi.org/10.1042/BST20160238

Von Coelln, R., Thomas, B., Savitt, J.M., Lim, K.L., Sasaki, M., Hess, E.J., Dawson, V.L., Dawson, T.M., 2004. Loss of locus coeruleus neurons and reduced startle in parkin null mice. Proc. Natl. Acad. Sci. U. S. A. 101, 10744–10749. https://doi.org/10.1073/pnas.0401297101

Vriend, C., Boedhoe, P.S.W., Rutten, S., Berendse, H.W., van der Werf, Y.D., van den Heuvel, O.A., 2016. A smaller amygdala is associated with anxiety in Parkinson's disease: a combined FreeSurfer-VBM study. J. Neurol. Neurosurg. Psychiatry 87, 493–500. https://doi.org/10.1136/jnnp-2015-310383

Vuković, M.G., Wood, R.I., Holschneider, D.P., Abernathy, A., Togasaki, D.M., Smith, A., Petzinger, G.M., Jakowec, M.W., 2008. Memory, mood, dopamine, and serotonin in the 1-methyl-4-phenyl-1,2,3,6-tetrahydropyridine-lesioned mouse model of basal ganglia injury. Neurobiol. Dis. 32, 319–327. https://doi.org/10.1016/j.nbd.2008.07.015

Wakamatsu, M., Ishii, A., Iwata, S., Sakagami, J., Ukai, Y., Ono, M., Kanbe, D., Muramatsu, S., Kobayashi, K., Iwatsubo, T., Yoshimoto, M., 2008. Selective loss of nigral dopamine neurons induced by overexpression of truncated human alpha-synuclein in mice. Neurobiol. Aging 29, 574–585. https://doi.org/10.1016/j.neurobiolaging.2006.11.017

Wang, C.-T., Mao, C.-J., Zhang, X.-Q., Zhang, C.-Y., Lv, D.-J., Yang, Y.-P., Xia, K.-L., Liu, J.-Y., Wang, F., Hu, L.-F., Xu, G.-Y., Liu, C.-F., 2017. Attenuation of hyperalgesia responses via the modulation of 5-hydroxytryptamine signalings in the rostral ventromedial medulla and spinal cord in a 6-hydroxydopamine-induced rat model of Parkinson's disease. Mol. Pain 13, 1744806917691525. https://doi.org/10.1177/1744806917691525

Waseem, S., Gwinn-Hardy, K., 2001. Pain in Parkinson's disease. Common yet seldom recognized symptom is treatable. Postgrad. Med. 110, 33–34, 39–40, 46.

Wasner, G., Deuschl, G., 2012. Pains in Parkinson disease--many syndromes under one umbrella. Nat. Rev. Neurol. 8, 284–294. https://doi.org/10.1038/nrneurol.2012.54

Weintraub, D., Newberg, A.B., Cary, M.S., Siderowf, A.D., Moberg, P.J., Kleiner-Fisman, G., Duda, J.E., Stern, M.B., Mozley, D., Katz, I.R., 2005. Striatal dopamine transporter imaging correlates with anxiety and depression symptoms in Parkinson's disease. J. Nucl. Med. 46, 227–232.

Wilson, J.M.B., Khabazian, I., Wong, M.C., Seyedalikhani, A., Bains, J.S., Pasqualotto, B.A., Williams, D.E., Andersen, R.J., Simpson, R.J., Smith, R., Craig, U.-K., Kurland, L.T., Shaw, C.A., 2002. Behavioral and neurological correlates of ALS-parkinsonism dementia complex in adult mice fed washed cycad flour. Neuromolecular Med. 1, 207–221. https://doi.org/10.1385/NMM:1:3:207

Winter, C., von Rumohr, A., Mundt, A., Petrus, D., Klein, J., Lee, T., Morgenstern, R., Kupsch, A., Juckel, G., 2007. Lesions of dopaminergic neurons in the substantia nigra pars compacta and in the ventral tegmental area enhance depressive-like behavior in rats. Behav. Brain Res. 184, 133–141. https://doi.org/10.1016/j.bbr.2007.07.002

Yamaguchi, H., Shen, J., 2007. Absence of dopaminergic neuronal degeneration and oxidative damage in aged DJ-1-deficient mice. Mol. Neurodegener. 2, 10. https://doi.org/10.1186/1750-1326-2-10

Yamakado, H., Moriwaki, Y., Yamasaki, N., Miyakawa, T., Kurisu, J., Uemura, K., Inoue, H., Takahashi, M., Takahashi, R., 2012. α-Synuclein BAC transgenic mice as a model for Parkinson's disease manifested decreased anxiety-like behavior and hyperlocomotion. Neurosci. Res. 73, 173–177. https://doi.org/10.1016/j.neures.2012.03.010

Zambito Marsala, S., Tinazzi, M., Vitaliani, R., Recchia, S., Fabris, F., Marchini, C., Fiaschi, A., Moretto, G., Giometto, B., Macerollo, A., Defazio, G., 2011. Spontaneous pain, pain threshold, and pain tolerance in Parkinson's disease. J. Neurol. 258, 627–633. https://doi.org/10.1007/s00415-010-5812-0

Zarow, C., Lyness, S.A., Mortimer, J.A., Chui, H.C., 2003. Neuronal loss is greater in the locus coeruleus than nucleus basalis and substantia nigra in Alzheimer and Parkinson diseases. Arch. Neurol. 60, 337–341.

Zarranz, J.J., Alegre, J., Gómez-Esteban, J.C., Lezcano, E., Ros, R., Ampuero, I., Vidal, L., Hoenicka, J., Rodriguez, O., Atarés, B., Llorens, V., Gomez Tortosa, E., del Ser, T., Muñoz, D.G., de Yebenes, J.G., 2004. The new mutation, E46K, of alpha-synuclein causes Parkinson and Lewy body dementia. Ann. Neurol. 55, 164–173. https://doi.org/10.1002/ana.10795

Zengin-Toktas, Y., Ferrier, J., Durif, F., Llorca, P.-M., Authier, N., 2013. Bilateral lesions of the nigrostriatal pathways are associated with chronic mechanical pain hypersensitivity in rats. Neurosci. Res. 76, 261–264. https://doi.org/10.1016/j.neures.2013.05.003

Zhang, J., Stanton, D.M., Nguyen, X.V., Liu, M., Zhang, Z., Gash, D., Bing, G., 2005. Intrapallidal lipopolysaccharide injection increases iron and ferritin levels in glia of the rat substantia nigra and induces locomotor deficits. Neuroscience 135, 829–838. https://doi.org/10.1016/j.neuroscience.2005.06.049

D- Objectifs de la thèse.

La multiplication des articles concernant la tVTA nous a fait nous questionner sur sa définition et sur ses rôles potentiels. Nous avons donc entrepris différentes études afin de produire une définition plus complète et universelle de la tVTA et d'approfondir les connaissances concernant ses rôles fonctionnels. Mon projet de thèse comporte donc 3 parties :

- La première partie a consisté à reconsidérer les définitions utilisées par les équipes travaillant sur cette structure, tant neurochimique, qu'anatomique et hodologique, afin d'aboutir à une reconstruction en trois dimensions de celle-ci. Nous avons également réalisé une analyse génomique de cette structure par *RNA sequencing* afin de fournir pour la première fois une liste de gènes enrichis dans la tVTA. Les résultats de ces expériences ont donné lieu à un article en préparation dont le manuscrit est présenté dans le chapitre 1 de la partie résultats.
- La deuxième partie de mon projet a permis de compléter les données concernant l'implication de la tVTA dans la réponse à des stimuli aversifs. Les données de ces expériences ont donné lieu à un article publié en 2017 dans le journal *Neuropsychopharmacology* (Sánchez-Catalán et al., 2017) et sont présentés dans le chapitre 2 de la partie résultats.
- La dernière partie de mon projet de thèse a consisté à montrer l'impact d'une lésion de la tVTA sur les symptômes moteurs et non-moteurs dans un modèle de maladie de Parkinson. Pour cela nous avons d'abord vérifié la présence de ces symptômes non-moteurs dans notre modèle par une batterie de tests comportementaux évaluant les seuils nociceptifs mécaniques et thermiques ainsi que les symptômes de type anxio-dépressifs. Nous avons ensuite regardé l'impact d'une co-lésion de la tVTA sur les réponses à certains de ces tests. Ces résultats ont donné lieu à un article en préparation dont le manuscrit est présenté dans le chapitre 3 de la partie résultats.

RESULTATS

Chapitre 1 : ANATOMO-MOLECULAR DEFINITION OF THE TAIL OF THE VENTRAL TEGMENTAL AREA.

Chapitre 2 : RESPONSE OF THE TAIL OF THE VENTRAL TEGMENTAL AREA TO AVERSIVE STIMULI.

Chapitre 3 : INFLUENCE OF A LESION OF THE TAIL OF THE VENTRAL TEGMENTAL AREA IN A RAT MODEL OF PARKINSON'S DISEASE.

Chapitre 1

ANATOMO-MOLECULAR DEFINITION OF THE TAIL OF THE VENTRAL TEGMENTAL AREA IN THE RAT.

Fanny Faivre, Clémentine Fillinger, Jennifer Kaufling, Cristina Sandu, Dorothée Daniel, Elodie Deschatrettes, Damien Plassard D, Christelle Thibault-Carpentier, Jean Zwiller, Pascal Romieu, Pierre Veinante, Pierre-Eric Lutz, Michel Barrot.

Historiquement, la tVTA a été mise en évidence par une approche immunohistochimique utilisant les facteurs de transcription de la famille Fos. Une exposition aiguë à une drogue entraîne en effet l'expression transitoire de c-Fos et FosB dans la tVTA, mais une exposition chronique à de telles substances entraîne aussi celle d'une forme tronquée de FosB : ΔFosB. C'est par cette expression de protéines FosB/ΔFosB que la tVTA a pu être décrite pour la première fois et que ses contours neuroanatomiques ont été définis chez le rat (Perrotti et al., 2005 ; Kaufling et al., 2009). La tVTA exprime différents marqueurs qui la distinguent des régions l'entourant. Cette structure présente en effet une immunoréactivité pour l'enzyme GAD67 (glutamate décarboxylase) permettant la synthèse du GABA (Barrot et al, 2012). Ainsi, 75% des neurones de la tVTA expriment la GAD67 (Jhou et al., 2009a). Mais d'autres marqueurs peuvent aussi servir à l'identification de la tVTA, comme son enrichissement en récepteurs μ des opioïdes (MOPR) (Jhou et al., 2009b ; Jalabert et al., 2011 ; Jhou et al., 2012).

D'un autre côté, l'existence du RMTg, autre nom de la tVTA, a d'abord été mise en évidence à la suite de l'observation de l'influence d'un petit groupe de neurones GABAergiques, situés latéralement au noyau du raphé médian, qui régule les comportements d'immobilité dans un test de peur conditionnée (Jhou, 2005). L'analyse de la connectivité de ces neurones par l'injection de traceurs a montré que le RMTg reçoit de nombreuses afférences issues de différentes régions cérébrales (Jhou et al., 2009b ; Kaufling et al., 2009), comme par exemple le cortex cingulaire, l'hypothalamus latéral, le collicule supérieur ou le noyau du raphé dorsal mais son afférence principale est issue de l'habénula latérale (LHb), c'est pourquoi elle est souvent utilisée pour définir la tVTA (Lecca et al., 2011, 2012 ; Stamatakis and Stuber, 2012). Du côté des efférences, le RMTg projette dans l'hypothalamus latéral, le noyau du raphé dorsal et le noyau pédonculopontin, mais son efférence principale se situe au niveau des neurones dopaminergiques mésencéphaliques (Barrot et al., 2012). Les neurones GABAergiques de la tVTA contactent en effet les neurones dopaminergiques de la SNc et de la VTA (Kaufling et al., 2010a ; Barrot et al., 2012).

Bien que cette structure ai déjà été étudiée chez la souris et le singe en se basant sur sa connectivité et chez le rongeur (rat, souris) en se basant sur sa nature neurochimique, il n'est pas encore certain que toutes les données présentes dans la littérature désignent une seule et même structure. L'enjeu de notre étude a donc été de vérifier si différentes approches définissant la tVTA en offrent une définition unitaire chez le rat.

Dans un premier temps, différents marqueurs utilisés dans la littérature pour définir les contours de la tVTA ont été comparés par immunohistochimie, ceci afin d'aboutir à une reconstruction en 3D de la tVTA. Nos résultats ont montré que les divers marqueurs neurochimiques de la tVTA définissent une structure bilatérale de forme et de localisation identique dans la région mésencéphalo-pontique.

Dans un deuxième temps, les expériences historiques ont été réitérées afin de comparer le recrutement des différents facteurs de transcription dans deux formes d'administration de cocaïne. Ainsi, nous avons pu voir que la tVTA contient environ 2400 neurones par côté et qu'environ la moitié sont recrutés par l'administration aigue ou chronique de cocaïne.

Des études de traçage rétrograde et antérograde nous ont permis de vérifier l'existence des connexions LHb/tVTA/VTA mais ont également mis en évidence une différence entre la définition neurochimique et la définition hodologique de la tVTA.

Enfin et pour la première fois, nous avons obtenu une définition génomique de la tVTA par RNA sequencing et hybridation *in situ*.

En conclusion, ces diverses données appellent à une meilleure définition anatomique de cette structure cérébrale, définition nécessaire au développement des études fonctionnelles sur les rôles de la tVTA. De plus, la découverte d'une définition génomique de la tVTA ouvre les portes à une meilleure connaissance de cette structure à travers les espèces et jusqu'à l'Homme.

Ma contribution à ce travail, qui sera signé en premier auteur, a été de réaliser les diverses études immunohistochimiques, la reconstruction 3D ainsi que les études de traçage. J'ai également écrit et réalisé les figures du manuscrit. Le manuscrit présenté dans cette partie sera complété par des données d'autres collègues avant soumission, notamment pour réaliser les cartographies RNAscope et entre espèces sur la base des données génomiques.

ANATOMO-MOLECULAR DEFINITION OF THE TAIL OF THE VENTRAL TEGMENTAL AREA IN THE RAT.

Fanny Faivre[a], Clémentine Fillinger[a], Jennifer Kaufling[a], Cristina Sandu[a], Dorothée Daniel[a], Elodie Deschatrettes[b], Plassard D[c], Christelle Thibault-Carpentier[de], Jean Zwiller[b], Pascal Romieu[b], Pierre Veinante[a], Pierre-Eric Lutz[a], Michel Barrot[a*].

[a] Centre National de la Recherche Scientifique, Université de Strasbourg, Institut des Neurosciences Cellulaires et Intégratives, F-67000 Strasbourg, France

[b] Centre National de la Recherche Scientifique, Université de Strasbourg, Laboratoire de Neurosciences Cognitives et Adaptatives, F-67000 Strasbourg, France

[c] Plateforme GenomEast, Institut de Génétique et de Biologie Moléculaire et Cellulaire, F-67400 Illkrich, France

[d] Centre National de la Recherche Scientifique, Institut National de la Santé et de la Recherche Médicale, Université de Strasbourg, Institut de Génétique et de Biologie Moléculaire et Cellulaire, F-67400 Illkirch, France

[e] Equipe labélisée de la ligue contre le cancer, Paris, France

* Corresponding author at: Institut des Neurosciences Cellulaires et Intégratives, 5 rue Blaise Pascal, F-67000 Strasbourg, France

E-mail address: mbarrot@inci-cnrs.unistra.fr

Abbreviated title: Definition of the tail of the ventral tegmental area

Number of pages: 23

Number of figures: 5

Number of tables: 2

Number of words: abstract 239, introduction 676, discussion 1331

Conflict of interest statement

The authors declare no conflict of interest.

Acknowledgments

This work was supported by the Centre National de la Recherche Scientifique [contracts UPR3212 and UMR5293], the University of Strasbourg, the University of Bordeaux, the Agence Nationale de la Recherche [ANR-15-CE37-0005-02; Euridol ANR-17-EURE-0022],

the Fondation pour la Recherche Médicale [FDT20170437322], and by a NARSAD distinguish investigator grant from the Brain and Behavior Research Foundation [24220]. We want to thank the Chronobiotron UMS3415 for animal care.

Abstract

The tail of the ventral tegmental area (tVTA) also known as the rostromedial tegmental nucleus (RMTg) is a mesencephalon structure that was described in the rat brain based on anatomical and functional experiments. It is a GABAergic structure described following the observation of a local FosB/ΔFosB induction after psychostimulant administration. It also expresses μ-opioid receptors. Considering its connectivity, the tVTA receives strong inputs from the lateral habenula (LHb) and sends projections to the midbrain dopamine neurons of the ventral tegmental area (VTA) and the substantia nigra *pars compacta*. Ten years after the first description of its connectivity, the tVTA is still not present in atlases. The aim of this work was to study whether all parameters used to define the tVTA indeed refer to a unique structure. To do that, we used immunohistochemistry, track-tracing and RNA sequencing to complete the definition of this structure. Our results show that: 1) all the classical markers used to define the tVTA describe a structure with the same shape and localization in the mesencephalopontine area, 2) the tVTA is constituted of around 2400 neurons per side and half of them respond to cocaine administration, 3) the connectivity-based and the neurochemical-based definition do not completely overlap, 4) the RNA sequencing analysis allows identifying specific markers of the tVTA. Together, these data provides a re-definition of the tVTA/RMTg in order to permit to extend its description to other species from the mice to the man.

Keywords: tail of the ventral tegmental area, rostromedial tegmental nucleus, lateral habenula, ventral tegmental area, c-Fos, μ-opioid receptor, RNA sequencing.

Significant statement

The tail of the ventral tegmental area also known as the rostromedial tegmental nucleus is a structure that was described in the rat brain, based on its connectivity and its Fos response to cocaine administration. However, ten years after its first description, no definitive definition was provided and it is not present in atlases yet. Our study provides a complete description of this structure based on its neurochemistry and its connectivity. Moreover, a genomic analysis highlights specific enriched genes that could be used to make a phylogenic study of the tVTA in mammals.

Introduction

The tail of the ventral tegmental area (tVTA) (Perrotti et al., 2005; Kaufling et al., 2009) also known as rostromedial tegmental nucleus (RMTg) (Jhou et al., 2009a, 2009b) is a key structure that exert a major inhibitory brake over dopamine neurons (Matsui et al., 2014; Sanchez-Catalan et al., 2014), that are known to be involved in motivated behavior, reward circuitry and in processing salient signals (Bromberg-Martin et al., 2010).

Exposure to cocaine led to the first characterization of the tVTA in the rat brain (Perrotti et al., 2005; Kaufling et al., 2009). Indeed, cocaine exposure induced the production of transcription factors such as cFos and FosB that delimited in the midbrain a structure easily visualized and delineated (Perrotti et al., 2005; Jhou et al., 2009b; Kaufling et al., 2009, 2010a, 2010b). The tVTA neurons strongly express the glutamate decarboxylase GAD67 (Jhou et al., 2009b; Kaufling et al., 2010) and a higher density of μ opioid receptor (MOPR), expressed by GABA neurons, than the nearby ventral tegmental area (VTA) (Jhou et al., 2009b; Jalabert et al., 2011; Jhou et al., 2012; Sánchez-Catalán et al., 2017).

Connectivity has also been frequently used to define the tVTA in functional studies. Thus, the tVTA has been defined as a structure targeted by the lateral habenula (LHb) (Jhou et al., 2009b; Kaufling et al., 2009; Balcita-Pedicino et al., 2011; Lecca et al., 2011, 2012; Stamatakis and Stuber, 2012) and projecting to the VTA and substantia nigra *pars compacta* dopamine neurons (Jhou et al., 2009b; Kaufling et al., 2010a; Balcita-Pedicino et al., 2011; Jalabert et al., 2011; Lecca et al., 2011, 2012).

Functionally, the tVTA is notably involved in behavioral avoidance and in response to aversive stimuli. Indeed, both footshocks (Jhou et al., 2009a; Sánchez-Catalán et al., 2017) and shock-predictive cues (Jhou et al., 2009a) increase Fos expression in the tVTA and footshocks also increase the LHb to tVTA glutamate release probability (Stamatakis and Stuber, 2012). In mice, optogenic stimulation of the LHb/tVTA pathway results in active, passive and conditioned behavioral avoidance and can interrupt the positive reinforcement induced by a sucrose solution (Stamatakis and Stuber, 2012). The tVTA is also implicated in reward prediction error, as shown in monkeys (Hong et al., 2011). This structure also contribute to the response to opiates. Indeed, the *ex vivo* application of morphine, $[Met]^5$ enkephalin or DAMGO hyperpolarizes tVTA neurons (Lecca et al., 2011; Matsui and Williams, 2011; Matsui et al., 2014) and morphine administration decreases the *in vivo* spontaneous firing rate of tVTA neurons (Jalabert et al., 2011; Lecca et al., 2011; Kaufling and Aston-Jones, 2015) and is responsible for opioid-mediated disinhibition of dopamine neurons. In rats, intra-tVTA delivery of the MOPR agonist endomorphin-1 can support self-administration and induce conditioned

place preference (Jhou et al., 2012). Similarly, in mice, the optogenetic stimulation of tVTA neurons expressing MOPR induces real time place preference (Siuda et al., 2015).

More recently, developmental studies have shown that the tVTA GABA neurons came from specific precursor, different from the ones conducting to VTA GABA neurons (Lahti et al., 2016), and that may be identified in mice by the expression of Sox2, Sox14 and FoxP1 (Lahti et al., 2016; Polter et al., 2018).

In view of the characterization of the tVTA/RMTg done in 2009, pictures and mentions of a corresponding structure have been found in earlier studies. Those studies used different denominations, such as “retro-VTA” (Scammell et al., 2000), “Area 2” (Olson and Nestler, 2007), “ventral tegmental tail” (Ikemoto, 2007), “rostromedial pontine tegmentum” (Geisler et al., 2008) or even “caudal pole of the VTA” (Ferreira et al., 2008) to refer to a structure that may be the tVTA. Ultimately, several morphological (connectivity, neurochemistry, *etc*…) or functional aspects (Fos induction, self-administration) has been used to define the tVTA. All these considerations added to the difficulty to clearly define the tVTA since it has not yet been verify whether all these definitions converge. The aim of this study is then to compare neurochemical and connectivity-based definition and provide a genomic analysis of the tVTA, to obtain a reliable definition of this structure.

Material and methods

Animals

Results were obtained from 97 male Sprague-Dawley rats (280-350g, Janvier, Le Genet-St-Isle, France); 71 were used for tracer injection procedures; 12 for tVTA RNA sequencing, 14 for tVTA for neurochemical analysis and cell counting (one of them for tVTA 3D cell reconstruction). Animals were housed under standard conditions (22°C, 12/12-hour light/dark cycle, lights on at 7 am), with food and water available *ad libitum*. The procedures were performed in accordance with the European Council Directive and approved by the local ethical committee (CREMEAS, Strasbourg, France).

Surgery

Stereotaxic surgery for tracer injection were performed under ketamine (80 mg/kg) / xylazine (4 mg/kg) and acepromazine (1 mg/kg) intraperitoneally (i.p.). Animals were placed in a stereotaxic frame, and holes were drilled above the LHb or VTA. Stereotaxic coordinates relative to bregma (Paxinos and Watson, 2014) were: LHb, anteroposterior (AP) -3.6 mm, lateral (L) +0.7 mm, vertical (V) -4.6 mm; VTA, AP -5.2mm, L +0.7 mm, V -6.7/7.5 mm. Verticality was taken from the dura. For anatomical study, the retrograde tracer fluorogold® (hydroxystilbamidine methanesulfonate 2% in 0.9% NaCl, Molecular Probes), cholera toxin subunit β (CTb) (0.25% in 0.1M Tris and 0.1% NaCl, Sigma-Aldrich) and anterograde tracer *Phaseolus vulgaris* leucoagglutinin (2.5% in 0.01M phosphate, pH 8.0, biovalley) were iontophoretically delivered (+3 µA, 7-sec on/off cycles for 10-15 min) with glass micropipettes (tip diameter: 10-40 µm). All the injections were unilateral in the right hemisphere. Fluorogold® was used in case of single anterograde tracer injection in the VTA. In case of double injection, *Phaseolus vulgaris* leucoagglutinin was used as anterograde tracer for the LHb in combination with the retrograde tracer β subunit of the choleric toxin for VTA injection. One week following tracer injection and 3 hours following acute cocaine injection (30 mg/kg, i.p.), rats underwent intra-cardiac perfusion.

For the tVTA RNA sequencing experiment, an undiluted suspension of fluorescent microspheres (0.15µL, Red RetroBeads^{TM} IX, #FP-DX2100, Interchim, Mont Luçon, France) was used as a retrograde tracer, injected by pressure bilaterally into the VTA. One week after microbeads injection, rats were killed with pentobarbital overdose (800mg/kg, Dolethal, Vetoquinol S.A., Lure, France), brains were dissected, immediately frozen in isopentane and stored at -80 °C.

Intravenous catheterization surgery for cocaine self-administration was performed under anesthesia with ketamine (80 mg/kg) / xylazine (4 mg/kg) and acepromazine (1 mg/kg) (i.p.). Chronic indwelling jugular catheters (Silastic, 0.3mm inner diameter, 0.63mm outer diameter) were implanted as described previously (Deschatrettes et al., 2013). During postoperative recovery, catheters were flushed daily with 0.2 ml ampicillin (0.1 g/ml; Coophavet) in heparinized saline (300 IU heparin per ml 0.9% NaCl) for 6 days. Catheter patency was verified with an infusion of the short-acting barbiturate hypnomidate (2 mg/ml, Janssen-Cilag), when necessary.

Drugs

Acute treatment with cocaine, D-amphetamine or chronic cocaine operant self-administration were used to locate the tVTA by cFos or FosB-like immunohistochemistry (Perrotti et al., 2005, Kaufling et al., 2010b). Acute cocaine (30 mg/kg in 0.9% NaCl; 1 mL/kg injection, Cooper, Melun, France) or D-amphetamine (1 mg/kg in 0.9% NaCl; 1 mL/kg, Sigma-Aldrich, St Quentin Fallavier, France) were injected i.p., 3 hours before animal perfusion. Cocaine (0.33 mg/kg/injection) was used for intravenous (i.v.) self-administration and the animals were perfused 2h after the last session.

Cocaine self-administration

Intravenous cocaine self administration was done as previously described (Deschatrettes et al., 2013). The apparatus is constituted of operant chambers (30 x 30 x 30 cm) located in a dark and sound attenuated room. A computer-driven syringe pump (Imetronic, France) activated a 10 mL syringe and pushed fluid into silastic tubing. The two chambers were equipped with two 3 cm diameter holes on the same wall, located 4 cm above the floor; one was chosen as the active hole to deliver cocaine and the other was the inactive hole. Disruption of an infrared photobeam in each hole was detected by a digital input card (DIO-24; National Instrument, USA) and homemade LabView software (National Instrument).

Fixed-ratio schedule of reinforcement was used in this study. The animals underwent 2h session by day during 10 days. During each session, each nose poke into the active hole led to an injection of cocaine (0.33 mg/kg/injection). A cue light, located 20 cm above the active hole was paired contingently with the delivery of cocaine. Ambient lighting was turned on at the end of each injection and persisted during a 40 s time-out period.

Tissue preparation

For immunohistochemistry procedures, rats were anesthetized with sodium pentobarbital (Dolethal®, 800mg/kg, Vetoquinol S.A., Lure, France) and intracardially perfused with 100 mL phosphate buffer (PB, 0.1M, pH 7.4) followed by 500 mL of a paraformaldehyde solution (PFA, 4% in PB 0.1M). Brains were removed, post-fixed overnight in the same fixative at 4°C and then kept at 4°C in phosphate buffer saline (PBS) diluted in a sodium chloride solution (PBS, 0.1M, 0.9% NaCl, pH 7.4) until cutting. Coronal sections (40 µm) were obtained with a Vibratome (VT 1000S, Leica, Deerfield, IL) and were serially collected in PBS.

For *egr*-1 (early growth response protein 1) *in situ* hybridization, animals (4 per groups) were rapidly anesthetized with an overdose of sodium pentobarbital (Dolethal®, 800mg/kg, Vetoquinol S.A., Lure, France), brains immediately removed, frozen in dry ice and stored at -80°C. For each animal, coronal sections (14 µm) of the tVTA were obtained using a cryostat (HM650, Microm). Each slice contained 4 consecutive sections and the hybridization was done on 4 slices per animal, the first and the last one containing sections before and after the tVTA.

Immunohistochemistry

Sections were washed in PBS (3 x 10 minutes), incubated for 20 minutes in a 1% H_2O_2/ 50% ethanol solution if used for a peroxidase reaction, washed in PBS (3 x 10 minutes), and incubated in PBS containing Triton X-100 and 5% donkey serum for 45 minutes. Sections were then incubated overnight at room temperature in PBS with Triton X-100, 1% donkey serum, and primary antibody (see table 1 for references and dilutions). The optimal antibody concentration was individually determined for each antibody. Control experiments omitting primary antibodies confirmed the absence of immunostaining in these conditions. The next day, sections were washed in PBS (3 x 10 minutes), incubated with the corresponding biotinylated secondary antibody (in PBS, 0.5% Triton X-100, 1% donkey serum; see table 2 for references and dilution) for 1 hour and 30 minutes, washed in PBS (3 x 10 minutes), and incubated with PBS containing the avidin-biotin-peroxidase complex (ABC Elite,0.2% A and 0.2% B; Vector) for 90 minutes. After washing in Tris-HCl buffer (0.05 M, pH 7.5; 3 x 10 minutes, TB), bound peroxidase was detected by incubation in 0.025% 3.3'-diaminobenzidine tetrahydrochloride (DAB, Sigma) and 0.0006% H_2O_2 (Sigma) in TB for approximately 5 min. The reaction was stopped by 2 x 10 min of TB and 2 x 10 min of PBS washing. Sections were then serially mounted on gelatin-coated slides, air-dried, dehydrated in graded alcohol baths (1x 70%, 1x 95% and 2x 100%), cleared in Roti-Histol (Carl Roth, Karlsruhe, Germany), and coverslipped with Eukitt.

3D reconstruction of the tVTA

An optical microscope (Nikon Eclipse 80i) associated with the NeuroLucida system (MBF Biosciences) and the CX9000 camera was used. 54 continuous frontal sections covering the posterior VTA and all tVTA extend were used. Three markers (FosB/ΔFosB, GAD67 and MOPR) were detected alternatively in a serial way (1 section every 3 for each marker). Boundaries on each section and brain structures were determined and drew by using the markers, anatomical landmarks and differences in background staining. The NeuroLucida 3D module associated the sections to generate a 3D reconstruction of the structure.

tVTA counting

The evaluation of the number of Fos+ nuclei induced by psychostimulant drugs in the tVTA was performed using the optical fractionator technique with optical dissectors (30 µm height, 5 µm guard zone), under the Stereoinvestigator software (MBF Biosciences). Fos immunostaining allowed delimiting the tVTA at × 10 objective, and counting was performed at ×40 on 10 randomly positioned counting frames per section (7–12 sections analyzed per animal, 4 to 6 animals per conditions).

In situ hybridization

Preparation

Sections were defatted with acetone (3 to 5 minutes bath) and then dried. Sections were fixed with a paraformaldehyde solution (4% in phosphate buffer, 15 min, 4°C) and rinsed with phosphate buffer. They were then incubated in a triethanolamine solution (0.1M, pH 8, 0.25% acetic acid), rinsed in a saline sodium citrate buffer (SSC 2X: NaCl 0.3 M, sodium citrate 0.03 M; 2 x 2 min), pre-hybridized in a formamide solution (formamide 50% - SSC 2X; 10 min, 60°C), dehydrated with increased concentration ethanol baths (50, 75 and 100%) and then dried. 30 µL of probes were placed on the slides, diluted in the hybridization buffer (formamide 50%; SSC 4X, dextran sulfate 10%; dithiothréitol 10 mM) during one night at 52°C. There were rinsed with a formamide solution (50% formamide, SSC 1X; 2x 1h, 55°C), and with a SSC 2X solution (2 x 5 min, 55°C). Non hybridized RNA were hydrolyzed with RNAase A (6 x 10^{-3} U/mL; 30 min, 37°C) in TPE buffer (NaCl 100 mM; Tris-HCl pH 8, 10 mM; EDTA 1 mM). Sections were rinsed again (formamide 50%-SSC 2X, 2 x 1h, 55°C; then SSC 2X, 15 min), dehydrated in increased concentration ethanol baths (50, 75, 100%) and dried. Slides were

exposed for autoradiography (Kodak BIOMAX-MR) during 6 and 11 days in room temperature.

Autoradiography

Detection was done using an automatic processor (Hyperprocessor, Amersham Pharmacia Biotech). The digitized images of the autoradiograms were then acquired with an optical bench with a CCD camera (XC-ST50, Canon). Grey level was measured using the Image J software. The grey level calibration was made by the measure of a section area with low background staining (fiber track area). The reported signal was obtained by subtracting this background signal.

tVTA RNA sequencing

tVTA laser microdissection

tVTA sections (100 µm coronal sections) were defrosted at room temperature and placed in a cresyl violet solution (0.1% w/v in 70% ethanol) for 2 minutes. They were dehydrated in a series of ethanol baths (twice for 2 minutes in 75%, twice for 2 minutes in 95% and twice for 2 minutes in 100%) followed by air-drying and finally were dried in a desiccant containing vacuum chamber for 60 minutes. Immediately after dehydration, laser microdissection was performed using Arcturus Veritas microdissection system. With the help of retrograde labeling and fluorescence microscope, tVTA was selected for dissection at x2 magnification and dissection was carried out at x10. The procedure of capture and cut was followed to dissect the slices. Therefore initial IR laser power of 70-100 mW, 2500-5000 µsec of pulse and 1-3 hits was used to melt the film of microdissection caps (Arcturus®Capsure®Macro LCM caps; cat:LCM0211) with Polyethylene naphthalate (PEN) membrane (Arcturus®PEN membrane Frame slides; ref: LCM0521); followed by UV laser power of 22.13 mW and 0.5 µm of spot size for cutting the captured slice. Microdissected samples were collected in 1.5 mL reaction tubes and stored at -80°C until RNA extraction.

Whole brain samples

Three rats were used to obtain whole brain samples for RNA extraction. Whole brains were disrupted using a POLYTRON. The tissue obtain was separated in 3 samples for RNA extraction due to the huge quantity of materials and RNA extracted samples were pulled together at the end of the extraction.

RNA extraction and library preparation

Total RNA was extracted using the Qiagen RNeasy Micro Kit (QIAGEN Company, Hilden, Germany, #74004), according to manufacturer's instructions. The library preparation was

performed at the GenomEast genomic platform (IGBMC, Illkirch, France), as described before (Henriques et al., 2017; El Nagar et al., 2018). Full length cDNA were generated from 5 ng of total RNA using the SMART-Seq v4 Ultra Low Input RNA kit for Sequencing (Clontech, Part number 634890) according to manufacturer's instructions with 9 cycles of PCR for cDNA amplification by Seq-Amp polymerase (Clontech). Six hundreds ng of pre-amplified cDNA were then used as input for Tn5 transposon tagmentation by the Nextera XT kit (Illumina, Part number FC-131-1096) followed by 12 cycles of library amplification. Following purification using Agencourt AMPure XP beads (Beckman Coulter, Part number A63882), the size and concentration of library DNA were assessed on an Agilent 2100 Bioanalyzer.

Bioinformatics analyses

The bioinformatic processing of RNA-Seq data was performed by the IGBMC GenomEast core facilities, a member of France Genomics. Hundred bp paired-end reads were mapped onto the rn6 assembly of the Rattus norvegicus genome using Tophat 2.0.14 (Trapnell et al., 2009; Kim et al., 2013) and bowtie version 2-2.1.0 (Langmead et al., 2009). Quantification of gene expression was performed using HTSeq-0.6.1 (http://www-huber.embl.de/users/anders/HTSeq/doc/overview.html), with annotations coming from Ensembl 86. Read counts were then normalized across libraries with the median-of-ratios method proposed by Anders and Huber (Anders and Huber, 2010). The results were then combined to form a count matrix, providing expression level for each gene in each biological sample. Comparisons between tVTA and whole brain samples was performed using DESeq2, the statistical method proposed by Anders and Huber (Love et al., 2014). The Wald test was used to estimate the p-values and they were adjusted for multiple testing with the Benjamini and Hochberg method (Benjamini and Hochberg, 1995).

Gene functional classification

For functional analyses, we used the DAVID website (DAVID Bioinformatics Resources 6.7, National Institute of Allergy and Infectious Diseases NIAID, NIH; https://david.ncifcrf.gov). The DAVID Bioinformatics Resources (DAVID) was one of the earliest bioinformatics tools for functional analyses of large gene lists, which are usually obtained from genome-wide studies (Huang da et al., 2009). It relies on the focus on specific sets of genes, *i.e.* groups of genes that are known to share common biological function. Such analysis is based on the list of genes displaying significant expression changes, which is dependent upon the significance threshold chosen for differential expression (here: $p < 0.01$).

Illustrative picture acquisition

For brightfield microscopy, sections were examined with a Nikon Eclipse 80i microscope associated with a digital camera (CX 9000, MBF biosciences). Large views of sections were made with a combination of multiple pictures superposed with Photoshop CS3 software (Adobe). For more detailed pictures, higher magnification was used (x10, x20 and x40).

Statistical analysis

Statistical analyses were performed with the Statistica 13 software (Statsoft) and graphs were made with the Sigma-plot software (Systat Software, Inc). Graphs display mean ± SEM. For Fos comparisons, results were analyzed with a Kruskal-Wallis ANOVA to compare different independent groups. For the *egr-1* mRNA expression, a Mann-Whitney test for the comparison of 2 independent groups was performed.

Results

Comparison of NeuN, FosB/ΔFosB, MOPR and GAD67 immunostainings

The tVTA is localized between -6 and -7 mm posterior to the bregma (Figure 1 ***A***). Immunostaining for the neuronal marker Neuronal Nuclear antigen NeuN (Figure 1 *A* & Figure 1 ***B***) and for the early gene FosB/ΔFosB induced by cocaine administration (Figure 1 ***C***) allow defining the limits of the tVTA. For these two markers, we observed a group of nuclei well delimited, all along the anteroposterior extend of the tVTA. For NeuN staining (Figure 1 ***B***), a group of densely packed neurons is slightly separated from the surrounding structures by a line with fewer or no labeled neurons. For FosB/ΔFosB staining (Figure 1 ***C***), a group of cells was easily visible due to the expression of these markers in the tVTA and their absence in the structures at the vicinity. In addition, immunostaining for MOPR (Figure 1 ***D***) and for the GABA neuron marker GAD67 (Figure 1 ***E***) were also used to highlight the tVTA shape and limits. Contrary to NeuN and FosB/ΔFosB nuclear staining, MOPR and GAD67 staining labeled both neuronal cell bodies and fibers. While those staining are more diffuse and do not provide a sharp detection of the tVTA boundaries, they permit to visualize a similar shape of the tVTA than the one highlighted by the nuclear staining.

Recruitment of immediate early genes in the tVTA by cocaine

Acute cocaine administration is known to induce the expression of FosB and cFos proteins in the rat tVTA (Perrotti et al., 2005; Jhou et al., 2009b; Kaufling et al., 2009), whereas repeated cocaine exposure lead to the expression of the truncated form of FosB, ΔFosB (Perrotti et al., 2005). We thus compared FosB/ΔFosB and cFos staining after cocaine acute injection or 10-day self-administration. A similar staining distribution was observed in the tVTA for both proteins and both ways of administrion (Figure 2 ***A***).

Quantitatively, the number of NeuN positive nuclei obtained by the stereological counting of 8 animals was about 2400 per side (Figure 2 ***B***). The mean number of FosB/ΔFosB positive nuclei after an i.p cocaine injection was about 1200 per side. This result was comparable to what we obtained after chronic self-administration or after a cFos staining ($H(2,15) = 0.97$, $p = 0.614$). In serial sections of the same animal, we performed NeuN and Fos staining in consecutives sections in order to obtain an approximate ratio of tVTA cells recruited by cocaine. After cocaine administration and whatever the administration protocol, almost half of the tVTA neurons are recruited ($p = 0.46$).

egr-1 is also a transcription factor recruited in different brain regions, such as the nucleus accumbens, after acute psychostimulant treatment (Moratalla et al., 1992; Thiriet et al., 2000;

Jouvert et al., 2002) but was not studied in the tVTA. The quantification of the autoradiographic signal revealed significant *egr-1* mRNA induction 40 min after an acute cocaine injection (Figure 2 ***C***) ($Z = 2.17$, $p = 0.029$), highly localized in the tVTA.

3D reconstruction of the tVTA

In order to facilitate the global visualization of the tVTA within the encephalon, we performed three-dimensional reconstruction (3D) of the brain area containing the tVTA. The three immunostainings (FosB/ΔFosB, GAD67 and MOPR, Figure 3 ***A***) used to reconstruct the tVTA were stackable, highlighting similar shape and limits of the structure (Figure 3 ***B***).

On the anteroposterior axis, in each hemisphere, the tVTA thus reconstituted shows a 1.1 mm long tubular shape starting, in the mesencephalon, within the VTA as defined in present atlases at -6 mm from the bregma and finishing in the pons at -7.1 mm from the bregma (Figure 3 ***A***). In its mesencephalic part the tVTA circumference is relatively small, starting around 96 µm in its most anterior part within the atlas-based VTA region, and increasing progressively along the anteroposterior axis to reach a diameter of 680 µm at its largest extend (Figure 3 ***B***). The tVTA is thus inserted for over a third of its length inside the VTA. Along the anteroposterior plan (Figure 3 ***C***), the tVTA position moves dorsally to end under the periaqueducal gray (PAG). In a sagittal view (Figure 3 ***C***, left), the tVTA has a horn-like shape inserted in the VTA.

Connectivity-based definition of the tVTA

We injected the anterograde tracer *Phaseolus vulgaris* leucoagglutinin inside the LHb (Figure 4 ***A***) and used the cFos expression to delimit the tVTA. In the mesecenphalopontine area, labelled fibers are present in the same area as the cFos positive nuclei. In the anterior tVTA, these fibers are localized in the posterior part of the paranigral nucleus of the VTA, just above the interpeduncular nucleus. Posteriorly, labelled fibers are embedded inside the fibers of the superior cerebellar peduncle. Fibers from the LHb are mostly connected to the ipsilateral tVTA even though some fibers are present contralaterally. However, the overlap of the labelled fiber zone did not fully overlap with cFos positive nuclei. The LHb projections inside the tVTA seemed to be organized in different zones: one enriched in fibers (red dotted lines in Figure 4 ***A***) and one with fewer fibers (blue dotted lines in Figure 4 ***A***), the c-Fos area superposing over these two areas.

After injection of the retrograde tracer Fluorogold® inside the VTA (Figure 4 ***B***) and comparison with cFos expression, we observed retrogradely labelled cells in the same area as

the cFos area. At higher magnification, some of the retrograde cells are also cFos positive (close-up in Figure 4 ***B***).

To compare retrograde and anterograde tracing, double tracing was used, with *Phaseolus vulgaris* leucoagglutinin as anterograde tracer and β subunit of the choleric toxin as retrograde tracer (Figure 4 ***C***). cFos staining allowed to define the shape of the tVTA. At different anteroposterior levels, fibers from the LHb and cells projecting to the VTA were localized in the same area. More closely, these two stainings were not completely stackable. As described above, two areas could be defined by LHb fibers. Conversely, the retrogradely labeled cells were regularly found within the tVTA, with appositions from the LHb fibers on the retrogradely labeled cells.

Genomic analysis of the tVTA

Results from the RNA sequencing of tVTA microdissected samples (Figure 5 ***A***) highly differed from to the whole brain gene population, as shown by the clustering that exists between samples (dark blue squares) (Figure 5 ***B1***). Indeed, few or no homologies was present between tVTA and whole brain RNA populations (light green, Figure 5 ***B1***). Further analyses demonstrated differences in the RNA expression between the two populations (red dots correspond to $p < 0.05$) (Figure 5 ***B2/B3***). There are 9631 genes enriched in the tVTA compared to whole brain (data not shown). Among these genes, we found genes already proposed to be either expressed or enriched in the tVTA. It is the case for example for the prepronociceptin (Log_2 fold change = 4.11, p = 9.4E-293), Sox2 (Log_2(FC) = 0.84, p = 4.25E-24), Gata2 (Log_2(FC) = 2.08, p = 8.2E-41), Gad1 (Log_2(FC) = 0.93, p = 8.24E-35), Gad2 (Log_2(FC) = 0.83, P = 2.38E-24) and Oprm1 (Log_2(FC) = 0.86, p = 0.01). Some other genes and proteins that were reported to be expressed or even enriched in the tVTA were found to display fewer mRNAs in the tVTA than in the whole brain as it is the case for Tal2 (Log_2(FC) = -0.03, p = 0.96), somatostatine (Log_2(FC) = -0.6, p = 3.95E-5), CB1 receptor (Log_2(FC) = -2.28, p = 4.54), GPR151 (Log_2(FC) = -1.5, p = 0.01), and different α subunit of the GABA-A receptor α2 (Log_2(FC) = -1.3, p = 5.55E-28), α4 (Log_2(FC) = -2.3, p = 8.13E-31), α5 (Log_2(FC) = -1.36, p = 2.8) and α6 (Log_2(FC) = -6.47, p = 6.2E-49). Finally, we found some genes that are not classically used to define the tVTA, such as the somatostatin receptor Ssr5 (Log_2(FC) = 2.49, p = 0.0001) and the cannabinoid receptor CB2 (Log_2(FC) = 1.04, p = 0.0003).

Among these enriched genes, we chose 50 genes that present the higher fold change to go further in the genetic identification of the tVTA (Figure 5 ***C***). However, preliminary analysis needs to be made to separate genes enriched in the tVTA from contaminations from the VTA

dopamine neurons or serotonin raphe neurons. Indeed, in red, we found genes that may results from such sample contaminations: Slc6a4, serotonin transporter; Slc6a3, dopamine transporter; Ddc, dopa-decarboxylase; Pitx3, dopamine neurons precursor; and Tph2, tryptophan hydroxylase 2 a gene involved in the serotonin biosynthesis. Finally, we performed a DAVID gene functional classification on the 400 RNA that present the higher fold change and that are find to be enriched in the tVTA. This analysis allows finding pathways in which the tVTA may be involved (Figure 5 ***D***).

Discussion

In this study, we show that proposed molecular markers of the tVTA, FosB/ΔFosB, GAD67 and MOPR, define in the mesopontine area of the rat a structure with the same localization and boundaries, which can also be defined using NeuN. We estimated the proportion of tVTA neurons responding to cocaine treatment, either with acute or chronic injections, to correspond to half of the neurons composing the tVTA. The connectivity-based definition of the tVTA using tract-tracing was also compared to the neurochemical one. Results showed that, the LHb-tVTA-VTA pathway does not perfectly overlap with the neurochemical definition. Finally, we provide a whole-genome analysis of gene expression enriched in the tVTA compared to the whole brain.

The tVTA may be characterized by different neurochemical markers, but their concordance was not controlled yet. We tested markers used in the literature to define either the tVTA or its functions, such as FosB/ΔFosB or cFos in response to a psychostimulant (Perrotti et al., 2005; Kaufling et al., 2009, 2010a; Rotllant et al., 2010; Zahm et al., 2010; Lecca et al., 2011; Cornish et al., 2012; Quina et al., 2015; Yetnikoff et al., 2015; Brown and Shepard, 2016; Sánchez-Catalán et al., 2017), GAD67 (Perrotti et al., 2005; Olson and Nestler, 2007; Jhou et al., 2009a; Kaufling et al., 2009, 2010a) and MOPR (Jhou et al., 2009b; Jalabert et al., 2011; Jhou et al., 2012; Kaufling and Aston-Jones, 2015; Yetnikoff et al., 2015; Wasserman et al., 2016). We also considered NeuN in order to obtain the number of neurons that compose the tVTA. We show here that all markers permit to define the boundaries of the tVTA and to highlight its localization along the antero-posterior axis. Indeed, the tVTA, in the most posterior part, is localized dorsolaterally to the IP whereas, in at more posterior levels, it is embedded among the fiber tracks of the superior cerebellar peduncle, as previously reported (Jhou et al., 2009b; Kaufling et al., 2009).

Following cocaine injection, FosB/ΔFosB accumulates in the tVTA, which initially allowed defining the tVTA (Perrotti et al., 2005; Kaufling et al., 2009). Dose-response studies previously showed that the dose of 30 mg/kg acute cocaine leads to the maximal possible cell recruitment in the tVTA (Kaufling et al., 2010b), and we show here that it corresponds to half of the total population of tVTA neurons. Interestingly, similarly large recruitment was also seen with cocaine self-administration. The lack of qualitative and quantitative difference between i.p. injection of cocaine (30 mg/kg) and a self-administration protocol (0.33 mg/kg/injection; 30mg/kg per day) is supportive of a ceiling effect in cellular recruitment. We also extended tVTA recruitment to another immediate early gene coding a transcription factor, *egr*-1. Fos transcription factors are thus not the only ones to be expressed in the tVTA after

psychostimulant drug administration, and these results are supportive of a major molecular alteration of the tVTA following exposure to a psychostimulant.

For several research groups, the tVTA is defined as the structure that receives inputs from the LHb and sends projections to midbrain dopamine neurons (Jhou et al., 2009b; Balcita-Pedicino et al., 2011; Lecca et al., 2011; Li et al., 2011; Maroteaux and Mameli, 2012; Stamatakis and Stuber, 2012). Here, we provided evidence that some differences are present between the neurochemical definition provided by FosB/ΔFosB and the connectivity-based definition. Indeed, the FosB/ΔFosB nuclei area after cocaine is straddling between an area with dense LHb fibers and an area which was weakly innervated. This fiber density difference may be partly related to the size and placement of the injections as was previously described (Jhou et al., 2009b; Balcita-Pedicino et al., 2011), indeed injections in different areas of the tVTA induced retrograde labelling in different subnuclei of the LHb (Gonçalves et al., 2012). However, as the VTA itself (Geisler and Zahm, 2005), the tVTA is considered as part of the reticular formation (Jhou et al., 2009a, 2009b). The reticular formation is characterized by a lack of clear-cut cytoarchitectural structures (Horn, 2006), and the afferents do not always correspond to identifiable cellular groups which may be also the case for the LHb-tVTA terminals. Concerning the tVTA/VTA connections, the concordance between the neurochemical and the connectivity-based definitions appears more appropriate as suggested by the literature (Geisler et al., 2008). Finally, the presence of the LHb-tVTA-VTA pathway was controlled using tracer co-injections. Together, data confirmed the importance of the tVTA as a relay between LHb and midbrain dopamine neurons. However, in conclusion, the neurochemical definition appears more relevant than the connectivity-based definition to describe the tVTA and identify tVTA neurons.

The comparison between rat tVTA and whole brain allowed establishing a list of genes whose expression is enriched in this structure. The first highlighted gene is *Sox14*. In the mouse, this gene has been shown to permit specific developmental GABA differentiation of tVTA neurons (Lahti et al., 2016). As VTA GABA neurons did not express this marker in the mouse, it could be a possible candidate for a phylogenic definition of this structure in mammals. This RNA sequencing analysis also converges with previous reports on specific molecular markers reported to be expressed in the tVTA. It is the case for example for the prepronociceptin (Jhou et al., 2009b, 2012), that is two times enriched in the tVTA compared to the whole brain, Sox2 (Lahti et al., 2016), Gata2 (Achim et al., 2013; Lahti et al., 2016) and Oprm1 (*i.e.* the μ-opioid receptor gene) (Jhou et al., 2009b; Jalabert et al., 2011; Jhou et al., 2012; Kaufling and Aston-Jones, 2015; Yetnikoff et al., 2015; Wasserman et al., 2016) and the glutamate decarboxylase

Gad1 and Gad2 which is consistent with the literature as the tVTA is constituted mostly by GABA neurons (Gao et al., 2002; Olson et al., 2005; Perrotti et al., 2005; Jhou et al., 2009a, 2009b; Brinschwitz et al., 2010; Kaufling et al., 2010a, 2010b; Rotllant et al., 2010; Wasserman et al., 2013; Kaufling and Aston-Jones, 2015; Wasserman et al., 2016). More surprising, somatostatin, found to be enriched in the tVTA (Jhou et al., 2009b), was found to be depleted at gene level whereas the gene of its receptor, Ssr5 is enriched. The same results was obtained for the CB1 receptor (Lecca et al., 2012; Melis et al., 2014), found to be depleted in the tVTA compared to the whole brain whereas CB2 is enriched. The most likely explanation would be that some of these proteins previously reported in the tVTA mostly originated from afferent terminals in the tVTA rather than local expression. On the other hand, as we did a comparison between the tVTA and the whole brain, in enrichment of some other brain structures in a given protein may also hide results related to the tVTA composition, as for the gene coding GABA-A receptor for example. A comparison between zones that are closer to the tVTA, could be a good alternative to better separate locally enriched neuronal populations.

Our results suggest that some of the genes expressed in the tVTA could contribute to specific functional pathways, such as the response to drugs of abuse including cocaine (Jhou et al., 2013 ; Kaufling et al., 2009, 2010a, 2010b) or morphine, which is in agreement with functional findings of the past decade concerning this brain region (Barrot et al., 2016). It also further support the GABA aspect of the tVTA, as the GABA synapse pathway was also highlighted by the genomic analysis.

This study permits to verify that definitions used in the literature by different team highlighted the same structure in the rat brain. Thus, the rat tVTA can be considered, based on its neurochemistry, as a structure that express Fos after cocaine administration and that express also a notable density of MOPR and GAD67. Based on its connection, this structure can be define as a structure that receives projection from the LHb and sends outputs to the VTA. Finally, the tVTA can be detected by transcription factors such as Sox14. This study completes the definition of the tVTA, and should help guiding future anatomical and functional studies.

References

Achim K, Peltopuro P, Lahti L, Tsai H-H, Zachariah A, Astrand M, Salminen M, Rowitch D, Partanen J (2013) The role of Tal2 and Tal1 in the differentiation of midbrain GABAergic neuron precursors. Biol Open 2:990–997.

Anders S, Huber W (2010) Differential expression analysis for sequence count data. Genome Biol 11:R106.

Araki M, McGeer PL, Kimura H (1988) The efferent projections of the rat lateral habenular nucleus revealed by the PHA-L anterograde tracing method. Brain Res 441:319–330.

Balcita-Pedicino JJ, Omelchenko N, Bell R, Sesack SR (2011) The inhibitory influence of the lateral habenula on midbrain dopamine cells: ultrastructural evidence for indirect mediation via the rostromedial mesopontine tegmental nucleus. J Comp Neurol 519:1143–1164.

Barrot M, Georges F, Veinante P (2016) Chapter25. The Tail of the Ventral Tegmental Area/ Rostromedial Tegmental Nucleus: A Modulator of Midbrain Dopamine Systems. In: Handbook of Basal Ganglia Structure and Function, pp 495–511. Academic Press.

Benjamini Y, Hochberg Y (1995) Controlling the False Discovery Rate: A Practical and Powerful Approach to Multiple Testing. J R Stat Soc Ser B Methodol 57:289–300.

Brinschwitz K, Dittgen A, Madai VI, Lommel R, Geisler S, Veh RW (2010) Glutamatergic axons from the lateral habenula mainly terminate on GABAergic neurons of the ventral midbrain. Neuroscience 168:463–476.

Bromberg-Martin ES, Matsumoto M, Hikosaka O (2010) Dopamine in motivational control: rewarding, aversive, and alerting. Neuron 68:815–834.

Brown PL, Palacorolla H, Brady D, Riegger K, Elmer GI, Shepard PD (2017) Habenula-Induced Inhibition of Midbrain Dopamine Neurons Is Diminished by Lesions of the Rostromedial Tegmental Nucleus. J Neurosci 37:217–225.

Brown PL, Shepard PD (2016) Functional evidence for a direct excitatory projection from the lateral habenula to the ventral tegmental area in the rat. J Neurophysiol 116:1161–1174.

Cornish JL, Hunt GE, Robins L, McGregor IS (2012) Regional c-Fos and FosB/ΔFosB expression associated with chronic methamphetamine self-administration and methamphetamine-seeking behavior in rats. Neuroscience 206:100–114.

Deschatrettes E, Romieu P, Zwiller J (2013) Cocaine self-administration by rats is inhibited by cyclic GMP-elevating agents: involvement of epigenetic markers. Int J Neuropsychopharmacology 16:1587–1597.

El Nagar S, Zindy F, Moens C, Martin L, Plassard D, Roussel MF, Lamonerie T, Billon N (2018) A new genetically engineered mouse model of choroid plexus carcinoma. Biochem Biophys Res Commun 496:568–574.

Ferreira JGP, Del-Fava F, Hasue RH, Shammah-Lagnado SJ (2008) Organization of ventral tegmental area projections to the ventral tegmental area-nigral complex in the rat. Neuroscience 153:196–213.

Gao H-M, Jiang J, Wilson B, Zhang W, Hong J-S, Liu B (2002) Microglial activation-mediated delayed and progressive degeneration of rat nigral dopaminergic neurons: relevance to Parkinson's disease. J Neurochem 81:1285–1297.

Geisler S, Marinelli M, Degarmo B, Becker ML, Freiman AJ, Beales M, Meredith GE, Zahm DS (2008) Prominent activation of brainstem and pallidal afferents of the ventral tegmental area by cocaine. Neuropsychopharmacology 33:2688–2700.

Geisler S, Zahm DS (2005) Afferents of the ventral tegmental area in the rat-anatomical substratum for integrative functions. J Comp Neurol 490:270–294.

Gonçalves L, Sego C, Metzger M (2012) Differential projections from the lateral habenula to the rostromedial tegmental nucleus and ventral tegmental area in the rat. J Comp Neurol 520:1278–1300.

Henriques A, Huebecker M, Blasco H, Keime C, Andres CR, Corcia P, Priestman DA, Platt FM, Spedding M, Loeffler J-P (2017) Inhibition of β-Glucocerebrosidase Activity Preserves Motor Unit Integrity in a Mouse Model of Amyotrophic Lateral Sclerosis. Sci Rep 7:5235.

Hong S, Jhou TC, Smith M, Saleem KS, Hikosaka O (2011) Negative reward signals from the lateral habenula to dopamine neurons are mediated by rostromedial tegmental nucleus in primates. J Neurosci 31:11457–11471.

Horn AKE (2006) The reticular formation. In: Progress in Brain Research (Büttner-Ennever JA, ed), pp 127–155. Elsevier.

Ikemoto S (2007) Dopamine reward circuitry: two projection systems from the ventral midbrain to the nucleus accumbens-olfactory tubercle complex. Brain Res Rev 56:27–78.

Jalabert M, Bourdy R, Courtin J, Veinante P, Manzoni OJ, Barrot M, Georges F (2011) Neuronal circuits underlying acute morphine action on dopamine neurons. Proc Natl Acad Sci U S A 108:16446–16450.

Jhou TC, Fields HL, Baxter MG, Saper CB, Holland PC (2009a) The rostromedial tegmental nucleus (RMTg), a GABAergic afferent to midbrain dopamine neurons, encodes aversive stimuli and inhibits motor responses. Neuron 61:786–800.

Jhou TC, Geisler S, Marinelli M, Degarmo BA, Zahm DS (2009b) The mesopontine rostromedial tegmental nucleus: A structure targeted by the lateral habenula that projects to the ventral tegmental area of Tsai and substantia nigra compacta. J Comp Neurol 513:566–596.

Jhou TC, Xu S-P, Lee MR, Gallen CL, Ikemoto S (2012) Mapping of reinforcing and analgesic effects of the mu opioid agonist endomorphin-1 in the ventral midbrain of the rat. Psychopharmacology 224:303–312.

Jouvert P, Dietrich JB, Aunis D, Zwiller J (2002) Differential rat brain expression of EGR proteins and of the transcriptional corepressor NAB in response to acute or chronic cocaine administration. Neuromolecular Med 1:137–151.

Kaufling J, Aston-Jones G (2015) Persistent Adaptations in Afferents to Ventral Tegmental Dopamine Neurons after Opiate Withdrawal. J Neurosci 35:10290–10303.

Kaufling J, Veinante P, Pawlowski SA, Freund-Mercier M-J, Barrot M (2009) Afferents to the GABAergic tail of the ventral tegmental area in the rat. J Comp Neurol 513:597–621.

Kaufling J, Veinante P, Pawlowski SA, Freund-Mercier M-J, Barrot M (2010a) gamma-Aminobutyric acid cells with cocaine-induced DeltaFosB in the ventral tegmental area innervate mesolimbic neurons. Biol Psychiatry 67:88–92.

Kaufling J, Waltisperger E, Bourdy R, Valera A, Veinante P, Freund-Mercier M-J, Barrot M (2010b) Pharmacological recruitment of the GABAergic tail of the ventral tegmental area by acute drug exposure. Br J Pharmacol 161:1677–1691.

Kim D, Pertea G, Trapnell C, Pimentel H, Kelley R, Salzberg SL (2013) TopHat2: accurate alignment of transcriptomes in the presence of insertions, deletions and gene fusions. Genome Biol 14:R36.

Kim U (2009) Topographic commissural and descending projections of the habenula in the rat. J Comp Neurol 513:173–187.

Lahti L, Haugas M, Tikker L, Airavaara M, Voutilainen MH, Anttila J, Kumar S, Inkinen C, Salminen M, Partanen J (2016) Differentiation and molecular heterogeneity of inhibitory and excitatory neurons associated with midbrain dopaminergic nuclei. Dev Camb Engl 143:516–529.

Langmead B, Trapnell C, Pop M, Salzberg SL (2009) Ultrafast and memory-efficient alignment of short DNA sequences to the human genome. Genome Biol 10:R25.

Lecca S, Melis M, Luchicchi A, Ennas MG, Castelli MP, Muntoni AL, Pistis M (2011) Effects of drugs of abuse on putative rostromedial tegmental neurons, inhibitory afferents to midbrain dopamine cells. Neuropsychopharmacology 36:589–602.

Lecca S, Melis M, Luchicchi A, Muntoni AL, Pistis M (2012) Inhibitory inputs from rostromedial tegmental neurons regulate spontaneous activity of midbrain dopamine cells and their responses to drugs of abuse. Neuropsychopharmacology 37:1164–1176.

Li B, Piriz J, Mirrione M, Chung C, Proulx CD, Schulz D, Henn F, Malinow R (2011) Synaptic potentiation onto habenula neurons in the learned helplessness model of depression. Nature 470:535–539.

Love MI, Huber W, Anders S (2014) Moderated estimation of fold change and dispersion for RNA-seq data with DESeq2. Genome Biol 15:550.

Maroteaux M, Mameli M (2012) Cocaine evokes projection-specific synaptic plasticity of lateral habenula neurons. J Neurosci 32:12641–12646.

Matsui A, Jarvie BC, Robinson BG, Hentges ST, Williams JT (2014) Separate GABA afferents to dopamine neurons mediate acute action of opioids, development of tolerance, and expression of withdrawal. Neuron 82:1346–1356.

Matsui A, Williams JT (2011) Opioid-sensitive GABA inputs from rostromedial tegmental nucleus synapse onto midbrain dopamine neurons. J Neurosci 31:17729–17735.

Melis M, Sagheddu C, De Felice M, Casti A, Madeddu C, Spiga S, Muntoni AL, Mackie K, Marsicano G, Colombo G, Castelli MP, Pistis M (2014) Enhanced endocannabinoid-mediated modulation of rostromedial tegmental nucleus drive onto dopamine neurons in Sardinian alcohol-preferring rats. J Neurosci 34:12716–12724.

Moratalla R, Robertson HA, Graybiel AM (1992) Dynamic regulation of NGFI-A (zif268, egr1) gene expression in the striatum. J Neurosci 12:2609–2622.

Olson VG, Nestler EJ (2007) Topographical organization of GABAergic neurons within the ventral tegmental area of the rat. Synapse 61:87–95.

Olson VG, Zabetian CP, Bolanos CA, Edwards S, Barrot M, Eisch AJ, Hughes T, Self DW, Neve RL, Nestler EJ (2005) Regulation of drug reward by cAMP response element-binding protein: evidence for two functionally distinct subregions of the ventral tegmental area. J Neurosci 25:5553–5562.

Paxinos G, Watson C (2014) The Rat Brain in Stereotaxic Coordinates. Academic Press.

Perrotti LI, Bolaños CA, Choi K-H, Russo SJ, Edwards S, Ulery PG, Wallace DL, Self DW, Nestler EJ, Barrot M (2005) DeltaFosB accumulates in a GABAergic cell population in the posterior tail of the ventral tegmental area after psychostimulant treatment. Eur J Neurosci 21:2817–2824.

Polter AM, Barcomb K, Tsuda AC, Kauer JA (2018) Synaptic function and plasticity in identified inhibitory inputs onto VTA dopamine neurons. Eur J Neurosci [in press].

Quina LA, Tempest L, Ng L, Harris JA, Ferguson S, Jhou TC, Turner EE (2015) Efferent pathways of the mouse lateral habenula. J Comp Neurol 523:32–60.

Rotllant D, Márquez C, Nadal R, Armario A (2010) The brain pattern of c-fos induction by two doses of amphetamine suggests different brain processing pathways and minor contribution of behavioural traits. Neuroscience 168:691–705.

Sánchez-Catalán M-J, Faivre F, Yalcin I, Muller M-A, Massotte D, Majchrzak M, Barrot M (2017) Response of the Tail of the Ventral Tegmental Area to Aversive Stimuli. Neuropsychopharmacology 42:638–648.

Sanchez-Catalan MJ, Kaufling J, Georges F, Veinante P, Barrot M (2014) The antero-posterior heterogeneity of the ventral tegmental area. Neuroscience 282:198–216.

Scammell TE, Estabrooke IV, McCarthy MT, Chemelli RM, Yanagisawa M, Miller MS, Saper CB (2000) Hypothalamic arousal regions are activated during modafinil-induced wakefulness. J Neurosci 20:8620–8628.

Siuda ER, Copits BA, Schmidt MJ, Baird MA, Al-Hasani R, Planer WJ, Funderburk SC, McCall JG, Gereau RW, Bruchas MR (2015) Spatiotemporal control of opioid signaling and behavior. Neuron 86:923–935.

Stamatakis AM, Stuber GD (2012) Activation of lateral habenula inputs to the ventral midbrain promotes behavioral avoidance. Nat Neurosci 15:1105–1107.

Thiriet N, Aunis D, Zwiller J (2000) C-fos and egr-1 immediate-early gene induction by cocaine and cocaethylene in rat brain: a comparative study. Ann N Y Acad Sci 914:46–57.

Trapnell C, Pachter L, Salzberg SL (2009) TopHat: discovering splice junctions with RNA-Seq. Bioinformatics 25:1105–1111.

Wasserman DI, Tan JMJ, Kim JC, Yeomans JS (2016) Muscarinic control of rostromedial tegmental nucleus GABA neurons and morphine-induced locomotion. Eur J Neurosci 44:1761–1770.

Wasserman DI, Wang HG, Rashid AJ, Josselyn SA, Yeomans JS (2013) Cholinergic control of morphine-induced locomotion in rostromedial tegmental nucleus versus ventral tegmental area sites. Eur J Neurosci 38:2774–2785.

Yetnikoff L, Cheng AY, Lavezzi HN, Parsley KP, Zahm DS (2015) Sources of input to the rostromedial tegmental nucleus, ventral tegmental area, and lateral habenula compared: A study in rat. J Comp Neurol 523:2426–2456.

Zahm DS, Becker ML, Freiman AJ, Strauch S, Degarmo B, Geisler S, Meredith GE, Marinelli M (2010) Fos after single and repeated self-administration of cocaine and saline in the rat: emphasis on the Basal forebrain and recalibration of expression. Neuropsychopharmacology 35:445–463.

Abbreviations

DAB: 3.3'-diaminobenzidine tetrahydrochloride; *egr*-1: *early growth response protein* 1; GAD67: glutamate decarboxylase 67 KDa; L: lateral; LHb: lateral habenula; MOPR: μ-opioid receptor; NaCl: sodium chloride; NeuN: neuronal nuclear antigen; PB: phosphate buffer; PBS: phosphate buffer saline; PFA: paraformaldehyde; RMTg: rostromedial tegmental nucleus; SEM: standard error of the mean; SSC: saline sodium citrate buffer; TB: Tris-HCl buffer; TH: tyrosine hydroxylase; TPE: Tris-HCl EDTA buffer; tVTA: tail of the ventral tegmental area; V: ventral; VTA: ventral tegmental area.

Figure legends

Figure 1. Neurochemical markers of the tVTA. ***A*** The tVTA extend along the antero-posterior axis. Details of the boxed area are presented in ***B***. Shape of the tVTA as highlighted using NeuN ***B***, FosB/ΔFosB ***C*** MOPR ***D*** and GAD67 ***E*** staining. Abbreviations: GAD67, glutamate decarboxylase 67 kDa isoform; IPC, interpedoncular nucleus, caudal subnucleus; IPL, interpedoncular nucleus, lateral; IPR, interpedoncular nucleus, rostral; MOPR, mu opioid receptor; ml, medial lemniscus; NeuN, neuronal nuclear antigen; tth, trigeminothalamic tract; xscp, decussation of the superior cerebellar peduncle. Scale bars: 1mm for ***A*** and 200μm for ***B*** to ***E***. (n = 4 per group).

Figure 2. Recruitment of immediate early genes in the tVTA induced by cocaine. ***A*** Cocaine-induced Fos expression in the tVTA for two markers (FosB/ΔFosB and cFos) and two cocaine ways of administration (acute injection and self-administration). ***B*** Stereological analysis of NeuN, FosB/ΔFosB and cFos immunohistochemistries. ***C*** *egr-1 in situ* hybridization in the tVTA after saline or cocaine injection (*, significantly different from control, p = 0.029). Abbreviations: IPC, interpedoncular nucleus, caudal subnucleus; IPL,interpedoncular nucleus, lateral; IPR, interpedoncular nucleus, rostral; ml, medial lemniscus; mRNA, messenger RNA; NeuN, neuronal nuclear antigen; tth, trigeminothalamic tract; xscp, decussation of the superior cerebellar peduncle. Results are presented as mean ± SEM. Scale bars: 1mm for entire coronal sections in ***A***, 200 µm for close-up sections in ***A***, 1 mm for entire coronal sections in ***C*** and 500 µm close-up sections in ***C***.

Figure 3. 3D reconstruction of the tVTA ***A*** 3D reconstruction of the tVTA obtained from 3 different stainings, FosB/ΔFosB, GAD67 and MOPR. ***B*** Anterior and posterior sections of the tVTA illustrating the overlay of 3 serial sections for each view (tyrosine hydroxylase area is highlighted in light green and PAG in grey). ***C*** 3D reconstruction and anatomical localization of the tVTA. Left: frontal view; right: sagittal view. Abbreviations: Aq, cerebral acqueduct; GAD67, glutamate decarboxylase 67 kDa isoform; IP, interpedoncular nucleus; ml, medial lemniscus; MOPR, mu opioid receptor; PAG, periaqueductal gray; SNc, substantia nigra *pars compacta*; tVTA, tail of the ventral tegmental area; VTA, ventral tegmental area. Scale bars: 2 mm for ***A*** and ***C***, 1 mm for ***B***.

Figure 4. Connectivity-based definition of the tVTA. ***A*** Anterograde tracer PhaL injected inside the LHb induces fiber staining in the tVTA. cFos staining permits to compare the neurochemical (black dotted line) and the connectivity-based definitions (red and blue dotted lines) of the boundaries of the tVTA. ***B*** Retrograde tracer CTb injected inside the VTA induced a retrograde cell staining in the tVTA. cFos staining permits to compare the neurochemical and the connectivity-based definitions of the boundaries of the tVTA. ***C*** Double tracing with anterograde and retrograde tracers allows assessing the LHb/tVTA/VTA pathway. The cFos immunochemistry was used to detect the boundaries of the tVTA. Abbreviations: CTb, cholera toxin subunit β; IP, interpedoncular nucleus; LHb, lateral habenula; MHb: medial habenula; ml, medial lemniscus; PhaL, *Phaseolus vulgaris* leucoagglutinin; tth, trigeminothalamic tract; tVTA, tail of the ventral tegmental area; VTA, ventral tegmental area; xscp, decussation of superior cerebellar peduncle.. Scale bars: 500 µm for left and middle pictures in ***A*** and ***B*** and

first and last lines in ***C***, 100 µm for right pictures in ***A*** and ***B*** and for the middle line in ***C***, 20 µm for the close-ups in ***C***, 1 mm for the entire sections in ***C***.

Figure 5. Results of the RNA sequencing comparison between tVTA and whole brain samples. ***A*** The tVTA was microdissected at different anteroposterior levels. Samples were then compared to whole brain for RNA sequencing analysis. ***B*** (b1) Sample clustering for the tVTA and whole brain comparison. A common variance function was estimated for all samples and used to apply a variance-stabilizing transformation. Dark blue color corresponds to zero distance between clusters; light green corresponds to large distance between clusters. The 3 tVTA samples on one side and the 3 whole brain samples on the other side shows high similarities. Conversely, tVTA and whole brain samples exhibits strong differences. (b2) Scatter plot for the tVTA versus whole brain counts. The red color marks genes detected as significantly different ($p < 0.05$) when Benjamini-Hochber multiple testing was used. Dots at the upper or lower place indicate genes with a large fold change. (b3) Volcano-plot of the results of the RNA sequencing of tVTA versus whole brain samples. Red dots correspond to genes significantly different from the mean ($p < 0.05$). Upper points correspond to genes that displays both large magnitude fold change and high statistical significance. ***C*** List of the 50 more enriched genes in the tVTA. Bars in red correspond to genes that may be from dopamine or serotonin contamination. ***D*** DAVID gene functional classification showed the involvement of tVTA enriched genes in different functional pathways. Scale bars: 1 mm for top pictures in ***A***, 500 µm for bottom pictures in ***A***.

Figure 1

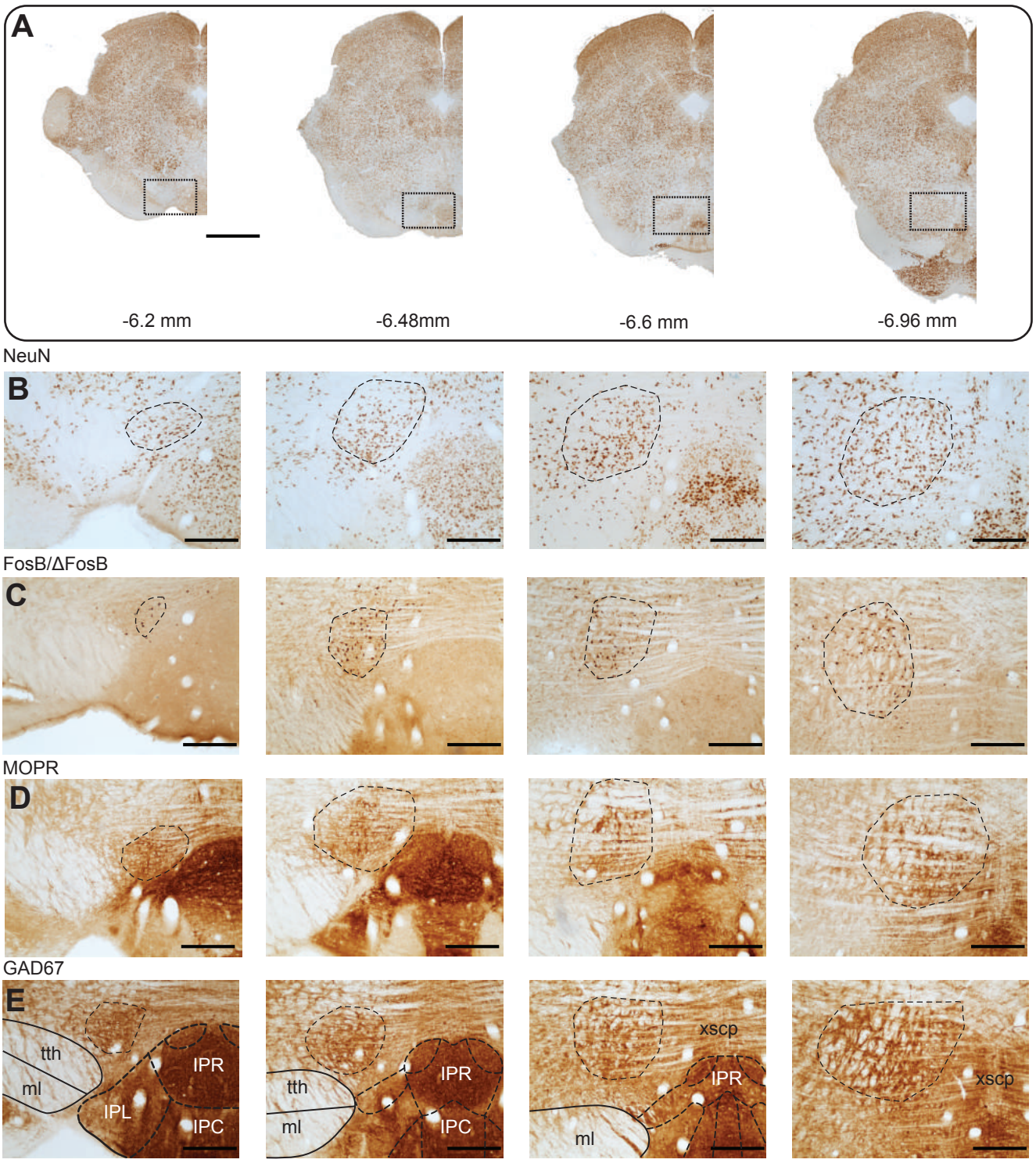
A
-6.2 mm
-6.48mm
-6.6 mm
-6.96 mm
NeuN
B
FosB/ΔFosB
C
MOPR
D
GAD67
E
tth
ml
IPR
IPL
IPC
tth
ml
IPR
IPC
xscp
IPR
ml
xscp

Figure 2

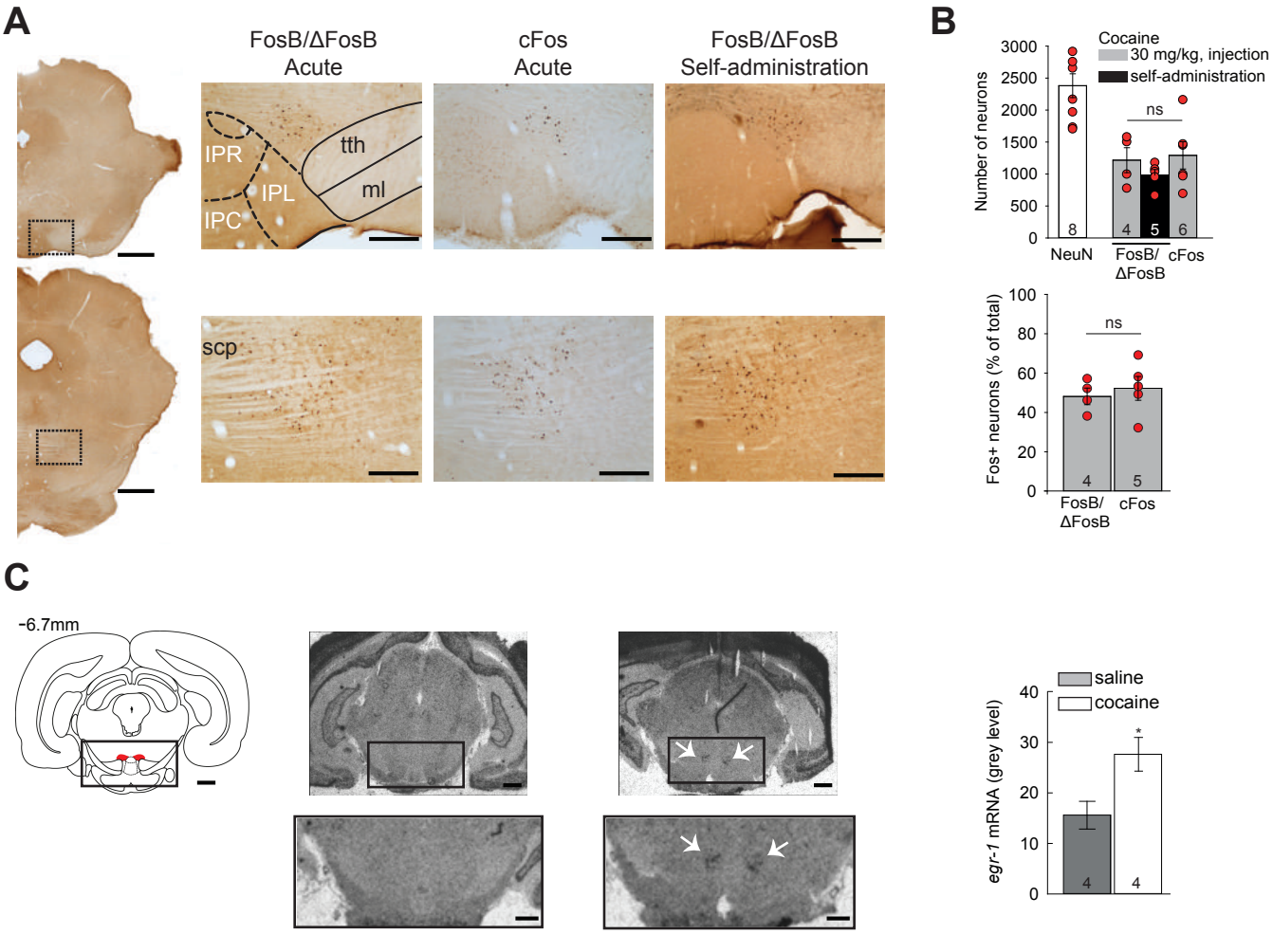
A
FosB/ΔFosB
Acute
cFos
Acute
FosB/ΔFosB
Self-administration
IPR
IPL
IPC
tth
ml
scp
B
Cocaine
30 mg/kg, injection
self-administration
Number of neurons
3000
2500
2000
1500
1000
500
0
ns
8
4
5
6
NeuN
FosB/
ΔFosB
cFos
Fos+ neurons (% of total)
100
80
60
40
20
0
ns
4
5
FosB/
ΔFosB
cFos
C
-6.7mm
saline
cocaine
egr-1 mRNA (grey level)
40
30
20
10
0
*
4
4

Figure 3

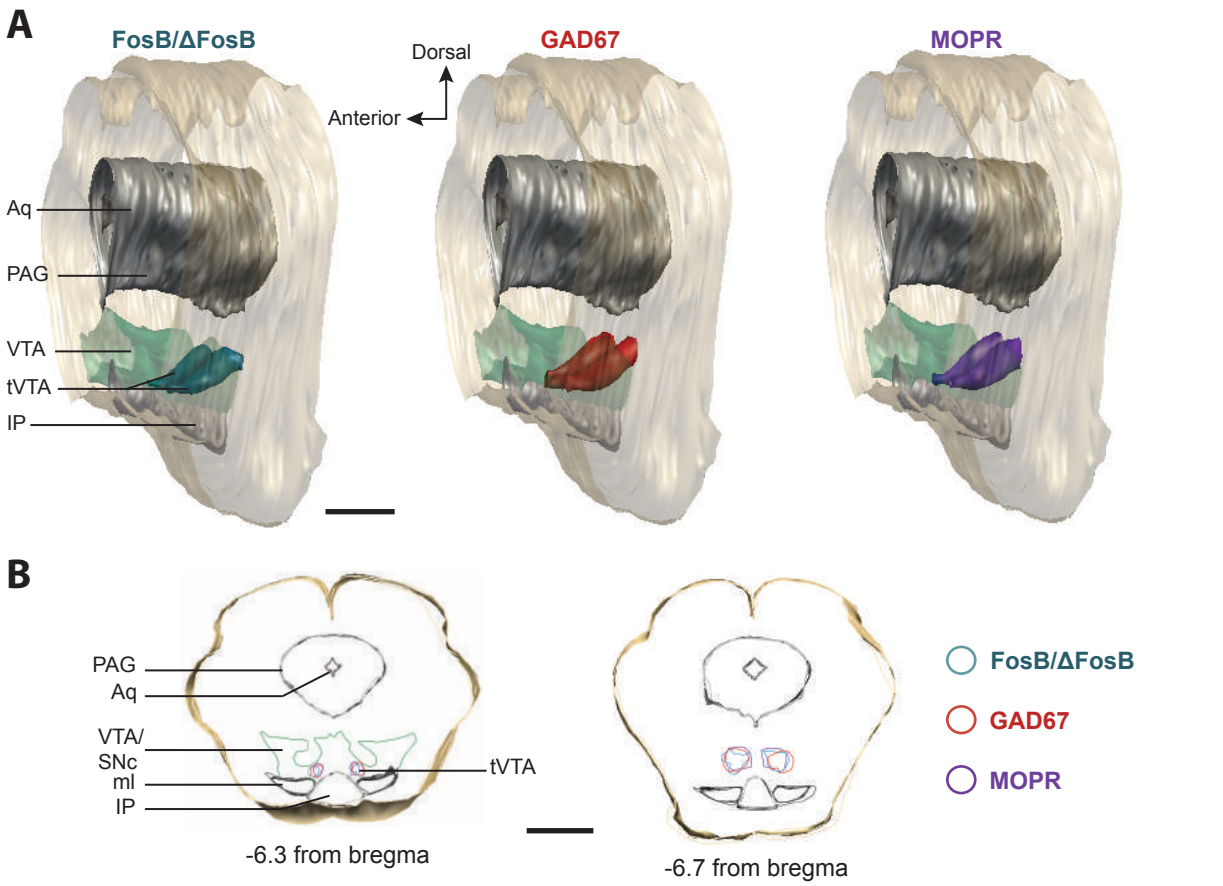
A
FosB/ΔFosB
GAD67
MOPR
Dorsal
Anterior
Aq
PAG
VTA
tVTA
IP
B
PAG
Aq
VTA/
SNc
ml
IP
tVTA
-6.3 from bregma
-6.7 from bregma
FosB/ΔFosB
GAD67
MOPR
C
PAG
tVTA
Dorsal
Anterior
PAG
Aq
ml
tVTA
IP
SNc
VTA
Dorsal
Lateral

Figure 4

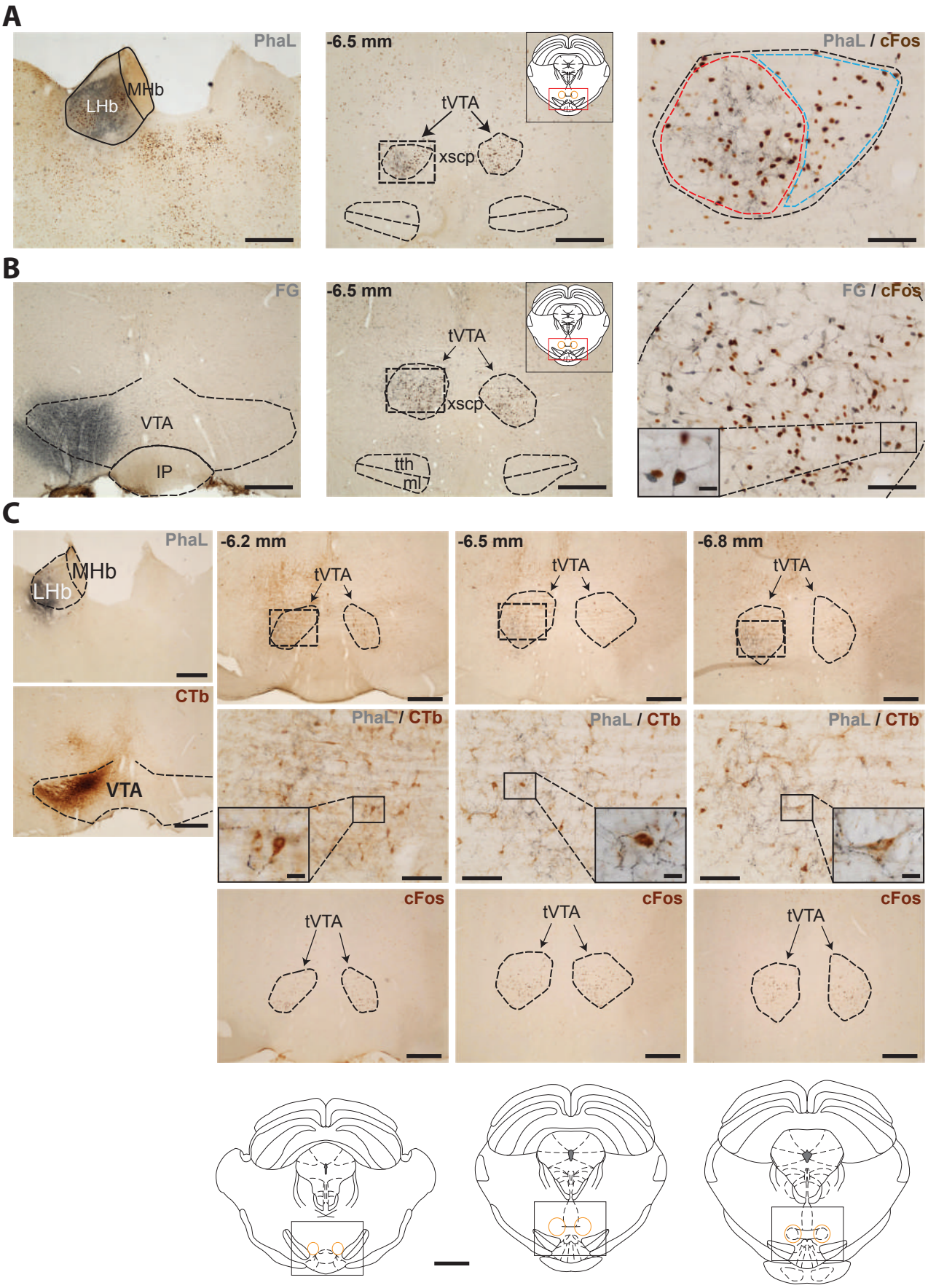
A
PhaL
MHb
LHb
-6.5 mm
tVTA
xscp
PhaL / cFos
B
FG
VTA
IP
-6.5 mm
tVTA
xscp
tth
ml
FG / cFos
C
PhaL
MHb
LHb
CTb
VTA
-6.2 mm
tVTA
-6.5 mm
tVTA
-6.8 mm
tVTA
PhaL / CTb
PhaL / CTb
PhaL / CTb
cFos
tVTA
cFos
tVTA
cFos
tVTA

Figure 5

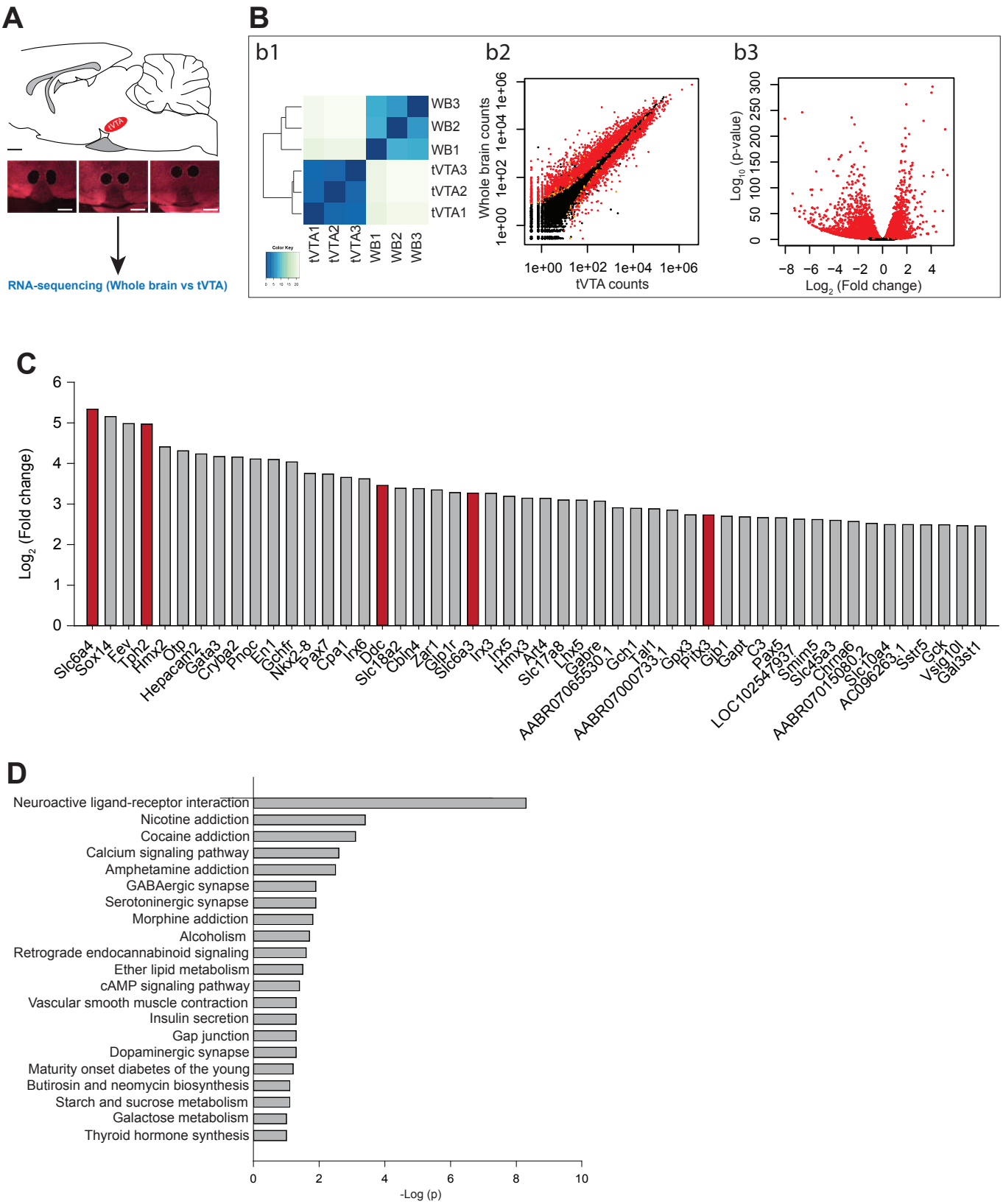
A
tVTA
RNA-sequencing (Whole brain vs tVTA)
B
b1
WB3
WB2
WB1
tVTA3
tVTA2
tVTA1
Color Key
b2
Whole brain counts
1e+00 1e+02 1e+04 1e+06
tVTA counts
b3
Log10 (p-value)
0 50 100 150 200 250 300
−8 −6 −4 −2 0 2 4
Log2 (Fold change)
C
Log2 (Fold change)
0 1 2 3 4 5 6
Slc6a4 Sox14 Fev Tph2 Hmx2 Otp Hepacam2 Gata3 Cryba2 Pnoc En1 Gchfr Nkx2-8 Pax7 Cpa1 Irx6 Ddc Slc18a2 Cdh4 Zar1 Glp1r Slc6a3 Irx3 Irx5 Hmx3 Art4 Slc17a8 Lhx5 Gabre AABR07065530.1 Gch1 Taf1 AABR07000733.1 Gpx3 Ptx3 Glb1 Gapt C3 Pax5 LOC102547937 Smim5 Slc45a3 Chrna6 AABR07015080.2 Slc10a4 AC096263.1 Sstr5 Gck Vsig10l Gal3st1
D
Neuroactive ligand-receptor interaction
Nicotine addiction
Cocaine addiction
Calcium signaling pathway
Amphetamine addiction
GABAergic synapse
Serotoninergic synapse
Morphine addiction
Alcoholism
Retrograde endocannabinoid signaling
Ether lipid metabolism
cAMP signaling pathway
Vascular smooth muscle contraction
Insulin secretion
Gap junction
Dopaminergic synapse
Maturity onset diabetes of the young
Butirosin and neomycin biosynthesis
Starch and sucrose metabolism
Galactose metabolism
Thyroid hormone synthesis
0 2 4 6 8 10
-Log (p)

Table1. Primary antibodies

Antigen	Manufacturer, species, type, catalogue number	Dilution
μ-opioid receptor	Millipore, guinea pig, polyclonal, #AB1774	1/20000
cFos	Santa Cruz, rabbit, polyclonal, #sc-52	1/10000
FosB/ΔFosB	Santa Cruz, rabbit, polyclonal, #sc-48	1/1500
GAD67	Millipore, mouse, monoclonal, #MAB5406	1/10000
TH	Millipore, mouse, monoclonal, #MAB318	1/10000
NeuN	Millipore, mouse, monoclonal, #MAB377	1/10000
FluoroGold®	Millipore, rabbit, polyclonal, #AB153	1/20000
PhaL	Vector Laboratories, goat, polyclonal, #AS-2244	1/50000
β Subunit of choleric toxin	Sigma, rabbit, polyclonal, #C3062	1/20000
β Subunit of choleric toxin	List biological, goat, polyclonal, #703	1/10000

Table 2. Secondary antibodies

Antigen	Manufacturer, species, catalogue number	Dilution
Anti mouse immunoglobulin	Vector, rat, #BA2001	1/400
Anti guinea pig immunoglobulin	Vector, goat, #BA7000	1/400
Anti rabbit immunoglobulin	Amersham, donkey, #RPN1004V	1/400
Anti goat immunoglobulin	Vector, hrose, #BA9500	1/400

Chapitre 2

RESPONSE OF THE TAIL OF THE VENTRAL TEGMENTAL AREA TO AVERSIVE STIMULI.

Sánchez-Catalán MJ*, **Faivre F***, Yalcin I, Muller MA, Massotte D, Majchrzak M, Barrot M. ***Neuropsychopharmacology***, 2017, 42 :638-48. (* co-first author).

Historiquement, la tVTA a été décrite comme une structure présentant une forte densité de neurones Fos positifs en réponse aux drogues psychostimulantes telles que les amphétamines ou la cocaïne (Perrotti et al., 2005; Kaufling et al., 2009, 2010). Les premières données fonctionnelles concernant la tVTA ont montré une implication de cette structure dans la réponse à des stimuli aversifs et à des comportements d'évitement. En effet, un test de peur conditionnée recrute la tVTA comme le montre la présence d'un marquage c-Fos local et la lésion excitotoxique de cette structure supprime les comportements d'immobilité des rats dans un test de peur conditionnée ou face à une odeur de prédateur et supprime les comportements de type anxio-dépressif dans un test de labyrinthe en croix surélevée (Jhou et al., 2009a). Enfin, chez la souris, la stimulation optogénique de la voie LHb-tVTA entraîne une aversion de place spontanée, une aversion de place conditionnée et une suppression du renforcement positif induit par le saccharose (Stamatakis and Stuber, 2012). Ces résultats suggèrent donc un rôle de la tVTA dans le circuit permettant la mise en place des comportements d'évitement.

Dans ce contexte, il paraissait important d'effectuer une analyse plus complète de la réponse de la tVTA à des stimuli aversifs de différentes natures, tant chimiques que physiques, ainsi que d'évaluer si l'absence de la tVTA affecte des comportements liés à de tels stimuli.

Dans un premier temps, nous avons étudié la réponse c-Fos de la tVTA à différents types de conditions aversives : réponse à des composés chimiques (chlorure de lithium (LiCl), β-carboline, naloxone, lipopolyssacharide (LPS)), réponse à la douleur (neuropathique et inflammatoire), réponse à des chocs électriques à la patte, à un stress de contention, à la nage forcée, à une odeur de prédateur et à un sevrage aux opiacés précipité par la naloxone. Afin d'avoir un contrôle positif lors de ces expériences, nous avons utilisé la réponse Fos à la D-amphétamine. Nos résultats montrent que seules quelques-unes des situations aversives étudiées entrainent la production de c-Fos dans la tVTA. Les chocs électriques ne produisent une réponse Fos localement que lorsque ceux-ci sont répétés. Dans le cadre du sevrage aux opiacés, le marquage Fos observé concerne essentiellement des cellules n'exprimant pas le récepteur μ des opioïdes (85%).

Dans un second temps, afin d'évaluer l'implication de la tVTA dans les comportements aversifs, nous avons étudié l'effet d'une lésion de la tVTA dans un test d'aversion conditionnée au goût par le LiCl et le LPS et dans le sevrage précipité par la naloxone. Une telle lésion n'affecte ni l'aversion au goût ni les symptômes physiques du sevrage aux opiacés. Nous n'avons néanmoins pas testé la composante aversive du sevrage par conditionnement de place.

En conclusion, bien que la stimulation de la tVTA favorise les comportements d'évitement, nos résultats suggèrent que le traitement des informations aversives n'est pas une caractéristique de la tVTA et que cette structure n'est pas nécessaire pour la réponse à tous les stimuli aversifs.

Pour ce travail, j'ai tout d'abord réalisé l'étude comportementale et immunohistochimique du sevrage aux opiacés précipité par la naloxone avec ou sans lésion de la tVTA (Figure 4 de l'article). En second lieu, j'ai réalisé les expériences et les analyses des chocs électriques uniques (Figure 3 de l'article). Enfin, j'ai complété les groupes d'animaux pour l'analyse de la réponse Fos au LiCl, à la β-carboline (Figure 1 de l'article) et au stress de contention (Figure 2 de l'article). Les autres expériences d'immunohistochimie et l'étude de l'aversion conditionnée au goût ont été réalisées par Maria-José Sanchez-Catalan, post-doctorante au laboratoire, le docteur Ipek Yalcin a réalisé les chirurgies pour la mise en place du modèle de douleur neuropathique, les docteurs Marc-Antoine Muller et Monique Majchrzak du laboratoire de Neurosciences Cognitives et Adaptatives ont réalisé les séries de chocs électriques dans le cadre d'expériences de peur conditionnée et le docteur Dominique Massotte a apporté son expertise dans l'analyse des co-marquages μ et Fos ainsi que pour le comptage stéréologique.

Neuropsychopharmacology (2017) 42, 638–648

www.neuropsychopharmacology.org

Response of the Tail of the Ventral Tegmental Area to Aversive Stimuli

María-José Sánchez-Catalán*[,1,2,5], Fanny Faivre[1,3,5], Ipek Yalcin[1], Marc-Antoine Muller[3,4], Dominique Massotte[1], Monique Majchrzak[3,4] and Michel Barrot[1]

[1]Institut des Neurosciences Cellulaires et Intégratives, Centre National de la Recherche Scientifique, Strasbourg, France; [2]Unitat Predepartamental de Medicina, Universitat Jaume I, Castelló de la Plana, Spain; [3]Université de Strasbourg, Strasbourg, France; [4]Laboratoire de Neurosciences Cognitives et Adaptatives, Faculté de Psychologie, Centre National de la Recherche Scientifique, Strasbourg, France

The GABAergic tail of the ventral tegmental area (tVTA), also named rostromedial tegmental nucleus (RMTg), exerts an inhibitory control on dopamine neurons of the VTA and substantia nigra. The tVTA has been implicated in avoidance behaviors, response to drugs of abuse, reward prediction error, and motor functions. Stimulation of the lateral habenula (LHb) inputs to the tVTA, or of the tVTA itself, induces avoidance behaviors, which suggests a role of the tVTA in processing aversive information. Our aim was to test the impact of aversive stimuli on the molecular recruitment of the tVTA, and the behavioral consequences of tVTA lesions. In rats, we assessed Fos response to lithium chloride (LiCl), β-carboline, naloxone, lipopolysaccharide (LPS), inflammatory pain, neuropathic pain, foot-shock, restraint stress, forced swimming, predator odor, and opiate withdrawal. We also determined the effect of tVTA bilateral ablation on physical signs of opiate withdrawal, and on LPS- and LiCl-induced conditioned taste aversion (CTA). Naloxone-precipitated opiate withdrawal induced Fos in μ-opioid receptor-positive (15%) and -negative (85%) tVTA cells, suggesting the presence of both direct and indirect mechanisms in tVTA recruitment during withdrawal. However, tVTA lesion did not impact physical signs of opiate withdrawal. Fos induction was also present with repeated, but not single, foot-shock delivery. However, such induction was mostly absent with other aversive stimuli. Moreover, tVTA ablation had no impact on CTA. Although stimulation of the tVTA favors avoidance behaviors, present findings suggest that this structure may be important to the response to some, but not all, aversive stimuli.
Neuropsychopharmacology (2017) **42,** 638–648; doi:10.1038/npp.2016.139; published online 31 August 2016

INTRODUCTION

Midbrain dopamine neurons have a crucial role in motor functions, motivated behaviors, reward-related learning, and in processing salient signals (Bromberg-Martin *et al*, 2010; Wise, 2004), as well as in associated pathologies. The GABAergic tail of the ventral tegmental area (tVTA) (Kaufling *et al*, 2009, 2010a; Perroti *et al*, 2005), or rostromedial tegmental nucleus (RMTg) (Jhou *et al*, 2009a, 2009b), is a mesopontine structure, which exerts a major inhibitory control over dopamine cells of the VTA and substantia nigra *pars compacta* (SNc) (Bourdy and Barrot, 2012; Matsui *et al*, 2014; Sánchez-Catalán *et al*, 2014). The tVTA has been implicated in motor functions (Bourdy *et al*, 2014; Lavezzi *et al*, 2015), responses to drugs of abuse (Jalabert *et al*, 2011; Jhou *et al*, 2012, 2013; Kaufling *et al*, 2010b; Lavezzi *et al*, 2012; Lecca *et al*, 2011, 2012; Matsui and Williams, 2011; Matsui *et al*, 2014; Melis *et al*, 2014; Rotllant *et al*, 2010), and reward prediction error (Hong *et al*, 2011). In addition, stimulation of the habenulo–tVTA pathway favors avoidance behaviors (Stamatakis and Stuber, 2012).

The tVTA receives inputs from the lateral habenula (LHb) (Balcita-Pedicino *et al*, 2011; Jhou *et al*, 2009a; Kaufling *et al*, 2009), a glutamatergic diencephalic structure involved in processing aversive information and reward prediction error (Matsumoto and Hikosaka, 2009). Thus, the tVTA has been proposed as an intermediate between the LHb and the VTA dopamine neurons, and to be important in promoting behavioral avoidance. Indeed, optogenetic stimulation of LHb terminals in the tVTA induces active, passive, and conditioned behavioral avoidance (Lammel *et al*, 2012; Stamatakis and Stuber, 2012). Moreover, pharmacological stimulation of the tVTA induces conditioned place aversion (Jhou *et al*, 2013). Otherwise, ablation of the tVTA inhibits fear-conditioned freezing, passive response to a predator odor, and anxiety-like behavior in an elevated plus maze (Jhou *et al*, 2009b). It also suppresses cocaine-induced avoidance behavior in a runway operant paradigm (Jhou *et al*, 2013), and cocaine excitation of LHb-tVTA neurons contributes to cocaine-induced depressive-like behaviors (Meye *et al*, 2015).

Various psychostimulants recruit the tVTA, as indicated by Fos induction in rats, suggesting that the tVTA is a

*Correspondence: Dr M-J Sánchez-Catalán, Unitat Predepartamental de Medicina, Universitat Jaume I, Avenue Vicent Sos Baynat, s/n, 13071 Castelló de la Plana, Spain, Tel: +34 964 38 74 40, Fax: +34 964 72 90 16, E-mail: macatala@uji.es
[5]The first two authors contributed equally to this work.
Received 22 March 2016; revised 19 July 2016; accepted 22 July 2016; accepted article preview online 29 July 2016

common target for those drugs (Kaufling *et al*, 2010b). Similarly, the tVTA displays Fos induction following exposure to series of foot shock (Brown and Shepard, 2013; Jhou *et al*, 2009b). However, to what extent other aversive stimuli similarly recruit the tVTA remains to be determined. As the tVTA might be part of the brain circuitry implicated in avoidance behaviors, it is important to further explore its response to aversive stimuli of different nature, and more particularly to determine whether the response observed with foot shocks may be generalized and constitutes a hallmark of the structure. Here, we assessed c-Fos expression in the rat tVTA in response to lithium chloride (LiCl), β-carboline, naloxone, lipopolysaccharide (LPS), inflammatory pain, neuropathic pain, foot-shock, loud tone, restraint stress, forced swimming, fox and cat odors, and opiate withdrawal. Moreover, we also assessed the effect of tVTA ablation on physical signs of opiate withdrawal and on LiCl and LPS-induced conditioned taste aversion (CTA).

MATERIALS AND METHODS

Animals

Experiments were performed in adult male Sprague–Dawley rats (Janvier, France) housed under standard conditions (22 ± 1 °C, 12-h light–dark cycle). Rats were habituated to the facilities for at least 1 week and daily handled the week preceding experimentation. They were 7–9 weeks old at testing or surgery time. Experiments were approved by the regional ethical committee (CREMEAS).

Drugs

Drugs (Sigma-Aldrich, France; unless otherwise stated) were prepared in 0.9% NaCl (unless otherwise stated) and injected (1 ml/kg, except for λ-carrageenan) at the following doses: D-amphetamine sulfate, 0.25, 0.5, and 1 mg/kg intraperitoneally; LiCl, 60 mg/kg intraperitoneally; β-carboline (FG7142), 15 mg/kg intraperitoneally in 45% cyclodextrin in water; naloxone hydrochloride, 10 mg/kg intraperitoneally or 1 mg/kg subcutaneously; LPS from *Escherichia coli* 0127-B8, 250 µg/kg intraperitoneally; λ-carrageenan type IV (lot. No. 80K133h), 150 µl of 3% solution, intraplantar; morphine hydrochloride, 10, 15, 20, 30, 40, 60, and 80 mg/kg intraperitoneally (Cooper, France). 2,4,5-trimethylthiazoline (TMT) (PheroTech, Delta, BC, Canada) was dissolved in diethylphtalate.

Aversive Procedures

Drugs producing aversive state were injected in animals: LiCl, β-carboline, naloxone, and LPS. Amphetamine was used as positive control for tVTA Fos induction. Rats were perfused 2 h postinjection, except for LPS (time course: 2, 4, and 8 h).

Inflammatory pain was induced by injection of λ-carrageenan in the right hind paw (Luis-Delgado *et al*, 2006a), with perfusion being carried out 2, 8, and 24 h later. To induce neuropathic pain, rats were anesthetized (ketamine, 87 mg/kg; xylazine, 13 mg/kg), and a 2 mm cuff of PE-90 polyethylene tubing was placed around the main branch of the right sciatic nerve (Yalcin *et al*, 2014; Benbouzid *et al*, 2008). The sham group underwent the same surgery without cuff implantation. The presence of mechanical hypersensitivity was tested using calibrated forceps (Bioseb, France) (Luis-Delgado *et al*, 2006b). On day 18 after surgery, rats were perfused 2 h after the last measure of mechanical thresholds.

For exposure to predator odors, rats were first habituated to the exposure cages ($25 \times 16 \times 22$ cm) for 15 min. On the following day, rats were exposed to the odor for 20 min, starting 3 min after beginning the session. One group was exposed to TMT, a component of red fox feces, by introducing a gauze pad with 20 µl of 10% TMT into the cage (Jhou *et al*, 2009b). Controls were exposed to the vehicle. Another group was exposed to a 25 mm piece of cat collar previously worn by a domestic cat for 2 weeks (McGregor *et al*, 2004). Controls were exposed to an unworn collar. Perfusion was carried out 2 h after starting the session.

One hour restraint stress was carried out in transparent cylinders (21×6 cm). Forced swimming was carried out by placing rats for 15 min in cylinders (50×30 cm diameter) filled to 30 cm with 25 °C water, rats were then removed, dried with towels, and placed in a warmed cage (Pliakas *et al*, 2001). Perfusion was carried out 2 h after the onset of stress procedure.

As repeated foot shocks have been shown to recruit the tVTA (Brown and Shepard, 2013; Jhou *et al*, 2009b), we tested them under different procedures. Rats were habituated for 30 min to behavioral chambers ($25 \times 27 \times 18$ cm; Med Associates, Saint Albans, Vermont) with a loudspeaker, camera, and grid floor. The following day, rats were exposed to these chambers in a 38 min session. The tone and tone/shock groups received, respectively, five pseudorandom tones (4000 Hz, 15 s) or five pseudorandom tones followed by foot shock (0.5 mA, 0.8 s). The foot-shock group received five pseudorandom shocks with no tone. Freezing behavior was assessed as aversive reaction (Marchand *et al*, 2003). Rats were perfused 2 h after starting the session. In an independent experiment, we tested exposure to a single foot shock or single tone. Rats were habituated to the chamber (soundproof, $51 \times 25 \times 24$ cm) for 2 min, and tested the following day in a 2-min session. One minute after beginning the session, rats were exposed to a single foot shock (0.5 mA, 0.8 s or 4 s; or 0.8 mA, 0.8 s) or a loud tone (3000 Hz, 1 s), placed in their home cages and perfused 1h30 after starting the test.

Morphine dependence was induced by escalating doses of morphine (2 ml/kg), two times a day for 7 days: 10, 15, 20, 30, 40, 60, and 80 mg/kg. On day 8, 1 h after the morning morphine injection (80 mg/kg), rats received naloxone (1 mg/kg, s.c.) or saline. Opiate withdrawal was assessed in transparent cages ($37 \times 25 \times 30$ cm), scoring behavioral and physiological variables over 30 min. Rats were perfused 2 h after naloxone or saline administration.

Lesion

Rats were anesthetized (sodium pentobarbital, 50 mg/kg, intraperitoneally) for stereotaxic surgery. Ibotenic acid (1% in phosphate-buffered saline (PBS) 0.1 M, 0.2 µl) was injected bilaterally into the tVTA (0.2 µl) (Bourdy *et al*, 2014). Stereotaxic coordinates relative to bregma were (in mm): anteroposteriority $-6.7/6.9$, laterality $\pm 1.4/1.5$, verticality (from dura) $-7.7/7.8$, $\pm 6°$ lateral angle (Paxinos and

Watson, 2007). Sham animals underwent the same procedure without lesion. Experiments started 1 to 2 weeks after surgery. After the experiments, rats were anesthetized and perfused to control for tVTA lesion.

Conditioned Taste Aversion

LiCl- or LPS-induced CTA (Slouzkey *et al*, 2013) was carried out using 30 min daily sessions over 7 days. Following 24 h of water deprivation, rats were trained in their home cage to drink water from two bottles for 30 min during 3 days. On the conditioning day, the two bottles were then filled with 0.1% saccharin solution. Ten minutes following the end of this session, rats received LiCl (Tenk *et al*, 2006), LPS (Konsman *et al*, 2008), or saline. The following 2 days, rats were exposed to two bottles of water during the session (baseline consumption). On test day, rats were allowed to drink from one bottle with water and one bottle with 0.1% saccharin, with randomized position. The aversion index was defined as (ml water/(ml water+ml saccharin) × 100) consumed during the test session.

Immunohistochemistry

Rats were anesthetized with pentobarbital overdose and perfused with 100 ml phosphate buffer (0.1 M, pH 7.4), followed by 500 ml of 4% paraformaldehyde in phosphate buffer. Brains were postfixed overnight, cryoprotected in 20% glycerol in PBS, and coronal sections (40 μm) were cut using a cryotome. Immunohistochemistry was performed as described previously (Bourdy *et al*, 2014; Kaufling *et al*, 2010b). Primary antibodies targeted: c-Fos (Santa-Cruz; sc-52, lot 1008, 1/10000 for DAB staining, 1/1000 for immunofluorescence), μ-opioid receptor (MOR) (Millipore; AB1724, 1/400 for immunofluorescence), tyrosine hydroxylase (TH) (Millipore-Chemicon; MAB318, 1/2500), or NeuN (Millipore; MAB377, 1/5000). Visualization was performed with biotinylated secondary antibodies and peroxidase/DAB reaction after avidin-biotin-peroxidase amplification (ABC Elite; Vector Laboratories, USA), except for multiple staining performed using Alexa488- and Cy3-conjugated secondary antibodies (1/400; Jackson ImmunoResearch) and DAPI for nuclei detection.

Coronal slices from −5.80 to −7.30 mm from bregma were used to count c-Fos-positive nuclei bilaterally in the tVTA. The tVTA is present between −6 mm and −7 mm from bregma, as identified by amphetamine-induced Fos expression. Rostrally, it starts within the VTA paranigral nucleus, and dorsolaterally to the interpeduncular nucleus. It then extends caudally and dorsally, laterally to the median raphe nuclei, and is partially embedded within the superior cerebellar peduncle fibers (Kaufling *et al*, 2010a; Sánchez-Catalán *et al*, 2014). We analyzed a section every 160 μm along the entire tVTA extent; after correction for missing sections, data were expressed per whole unilateral tVTA (Kaufling *et al*, 2010b). Images were acquired using a microscope (Eclipse E600; Nikon Instruments) with the Neurolucida software.

Analysis of c-Fos/MOR nuclei was performed using the optical fractionator technique with optical dissectors (30 μm height, 5 μm guard zone), under the Stereoinvestigator software (MBF Biosciences). MOR immunostaining allowed delimiting the tVTA (eg, Figure 4e) at × 10 objective, and counting was performed at × 40 on 10 randomly positioned counting frames per section (7–12 sections analyzed per animal). Microphotographs were acquired on a Leica SP5 II confocal microscope.

Analyses

Data are expressed as mean ± SEM. A power analysis was performed by using G*Power3 (version 3.1.9). Other statistical analyses were performed using STATISTICA 7.1 (Statsoft, Tulsa, OK, USA), with Student's *t*-test for two-group comparison and ANOVA for multiple comparisons. *Post hoc* analyses were carried out using either Dunnett or Bonferroni tests. For CTA experiments, a factorial two-way ANOVA was followed by a Duncan test. We performed a test of comparison between the mean and a standard value (50%) to compare aversion indices. Level of significance was $p<0.05$.

RESULTS

Aversive Drugs

As psychostimulants induce Fos proteins in the rat tVTA (Kaufling *et al*, 2010b; Perrotti *et al*, 2005), we used amphetamine as an internal positive control and showed that the amphetamine c-Fos induction is dose-dependent ($F_{3,16}=86.7$, $p<0.001$) (Figures 1a and g). Concerning aversive drugs ($F_{3,19}=21.9$, $p<0.001$), tVTA Fos induction was observed only with the anxiogenic drug β-carboline (File and Baldwin, 1987) ($p<0.001$) (Figures 1e and g). This induction was significant, but quantitatively small compared with psychostimulants. No significant induction was present with LiCl ($p=0.35$), a drug provoking visceral illness (Ossenkopp and Eckel, 1995), with naloxone at high dose ($p=1$), and with LPS ($F_{3,13}=1.3$, $p=0.31$), a bacterial endotoxin inducing sickness behavior (Figure 1) (Castanon *et al*, 2001; Konsman *et al*, 2008). Power analysis using the saline and β-carboline groups as a reference to calculate the effect size index (considering parametric *t*-test for two independent groups with $\alpha=0.05$ and power = 0.80) gave an estimated sample size of three animals per group, indicating that *n* in our groups was sufficient to detect relevant differences.

Painful Stimuli

Inhibition of the tVTA impacts nocifensive responses (Jhou *et al*, 2012). However, painful stimuli did not induce c-Fos locally. With λ-carrageenan-induced inflammatory pain (Luis-Delgado *et al*, 2006a, b), no c-Fos induction was present in the tVTA (Figures 2a–c and m). Similarly, no c-Fos was observed in the tVTA with neuropathic pain ($p=0.6$) (Figures 2d, e and m), whereas ipsilateral paw withdrawal thresholds were chronically lowered (group, $F_{1,12}=219.2$, $p<0.001$; paw, $F_{1,12}=297.1$, $p<0.001$; time × group × paw, $F_{6,72}=18.5$, $p<0.001$) (Figure 2f).

Stressful Stimuli

Predator odors induce unconditioned fear responses in rats, and tVTA lesion changes these responses (Jhou *et al*, 2009b). However, exposure to fox or cat odors did not induce c-Fos

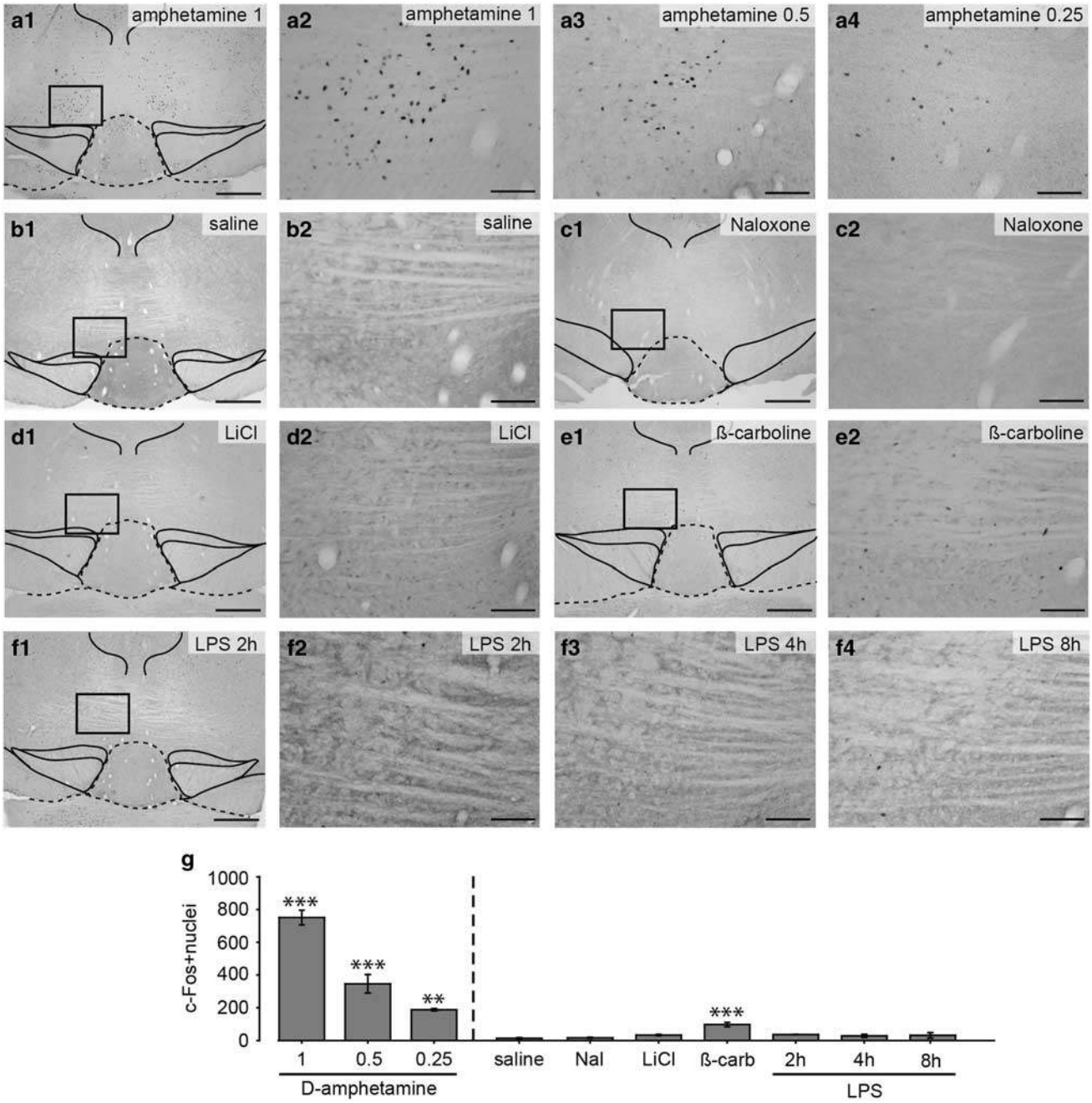

Figure 1 Aversive drugs barely induce c-Fos expression in the GABAergic tail of the ventral tegmental area (tVTA). (a) Amphetamine dose–response (0.25, 0.5, and 1 mg/kg intraperitoneally, $n=3$–4 per group) was used as a positive control for c-Fos expression in the tVTA. (b) Acute injection of saline ($n=5$) has no effect on c-Fos in the tVTA. (c–f) Illustrations for c-Fos in the tVTA after acute injection of naloxone 10 mg/kg ($n=4$) (c), lithium chloride (LiCl) 60 mg/kg ($n=5$) (d), β-carboline 15 mg/kg ($n=6$) (e), and lipopolysaccharide (LPS) 250 μg/kg (f). (g) Quantification of c-Fos-positive nuclei in the tVTA. Rats were perfused 2 h after injection, except for LPS (time course: 2, 4, and 8 h, $n=3$ per time point). The squares in a_1–f_1 indicate the regions shown at higher magnification in a_2–f_2. Scale bars, 500 μm (a_1–f_1) and 100 μm (a_2–f_2, a_3–a_4, and f_3–f_4). ***$p<0.001$, **$p<0.01$, and *$p<0.05$ (relative to the saline group).

Figure 2 Painful or stressful stimuli do not induce c-Fos expression in the GABAergic tail of the ventral tegmental area (tVTA). (a–c) Intraplantar injection of λ-carrageenan (Carr) does not induce c-Fos expression in the tVTA ($n=3$ per time point). (d and e) Neuropathic pain (NP) does not induce c-Fos expression in the tVTA. Sham animals underwent the same surgical procedure without cuff implantation ($n=4$ per group). (f) Cuff implantation results in a chronic ipsilateral allodynia (day 0: surgery, ***$p<0.001$ relative to the other groups). (g and h) Fox odor exposure (2,4,5-trimethylthiazoline (TMT); control group: TMTc) do not induce c-Fos expression in the tVTA ($n=3$ per group). (i and j) Cat odor exposure (CAT; control group: CATc) do not induce c-Fos expression in the tVTA ($n=3$ per group). (k and l) Acute restraint stress ($n=5$) and forced swimming test (FST, $n=5$) do not induce c-Fos expression in the tVTA. (m) Quantification of c-Fos-positive nuclei in the tVTA. An amphetamine group (amph, 1 mg/kg) ($n=3$) was included as a positive control group. Rats were perfused 2 h after starting the behavioral test or after the last measure of mechanical thresholds for neuropathic pain. The squares in (a_1–e_1 and g_1–l_1) indicate the regions shown at higher magnification in (a_2–l_2 and g_2–l_2). Scale bars, 500 μm (a_1–e_1 and g_1–l_1) and 100 μm (a_2–l_2 and g_2–l_2).

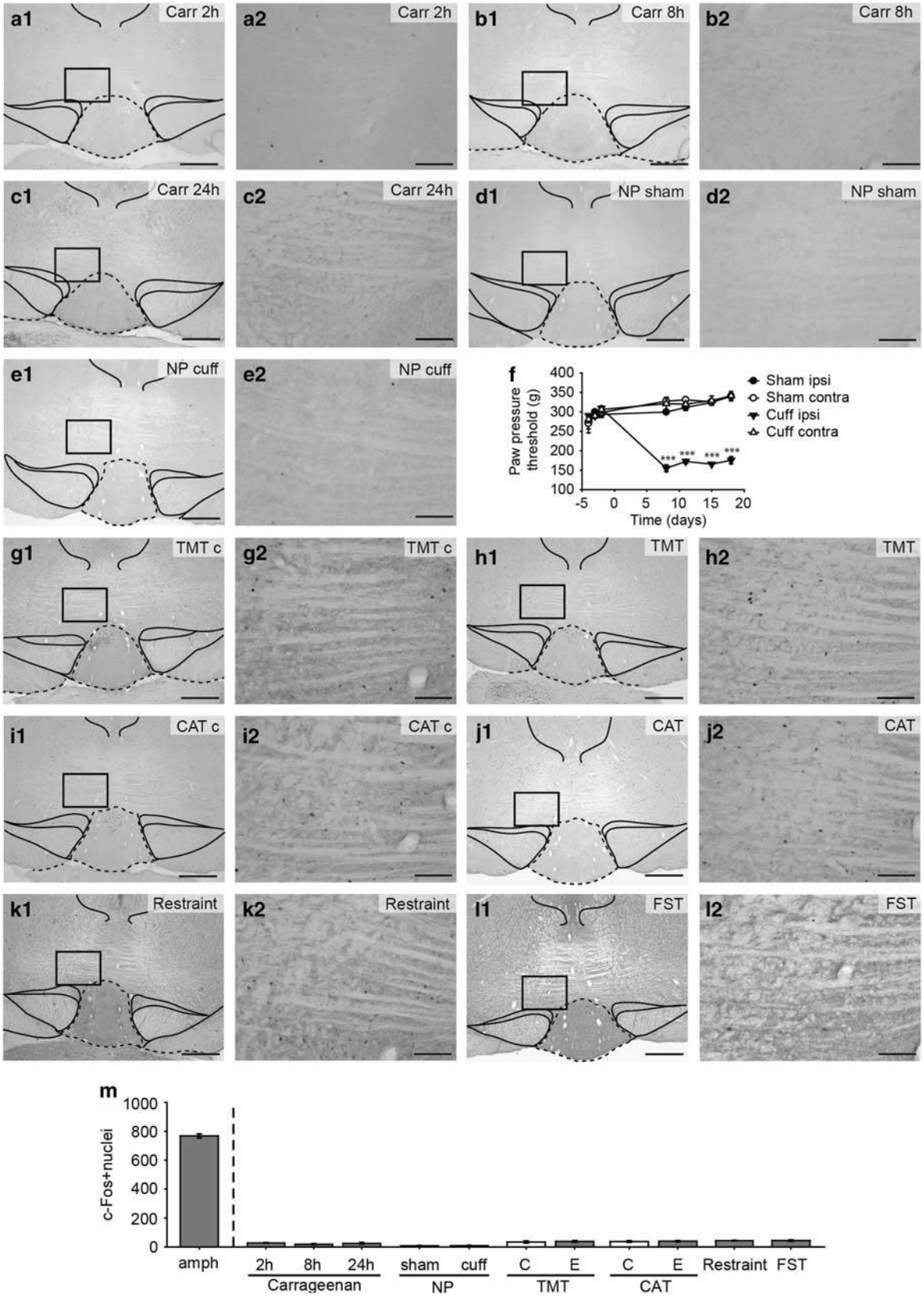

Figure 2 See for caption on page 641.

in the tVTA (TMT, $p = 0.69$; cat odor, $p = 0.79$) (Figures 2g–j and m). Similarly, restraint stress, or forced swimming as classically used in depression research, also failed to recruit the tVTA (Figures 2k–m).

The only stress procedure that led to significant c-Fos induction in the tVTA was the repeated exposure to mild foot shocks ($F_{3,22} = 23.4$, $p < 0.001$) delivered in a protocol usually used to elicit fear conditioning. Freezing behavior during the

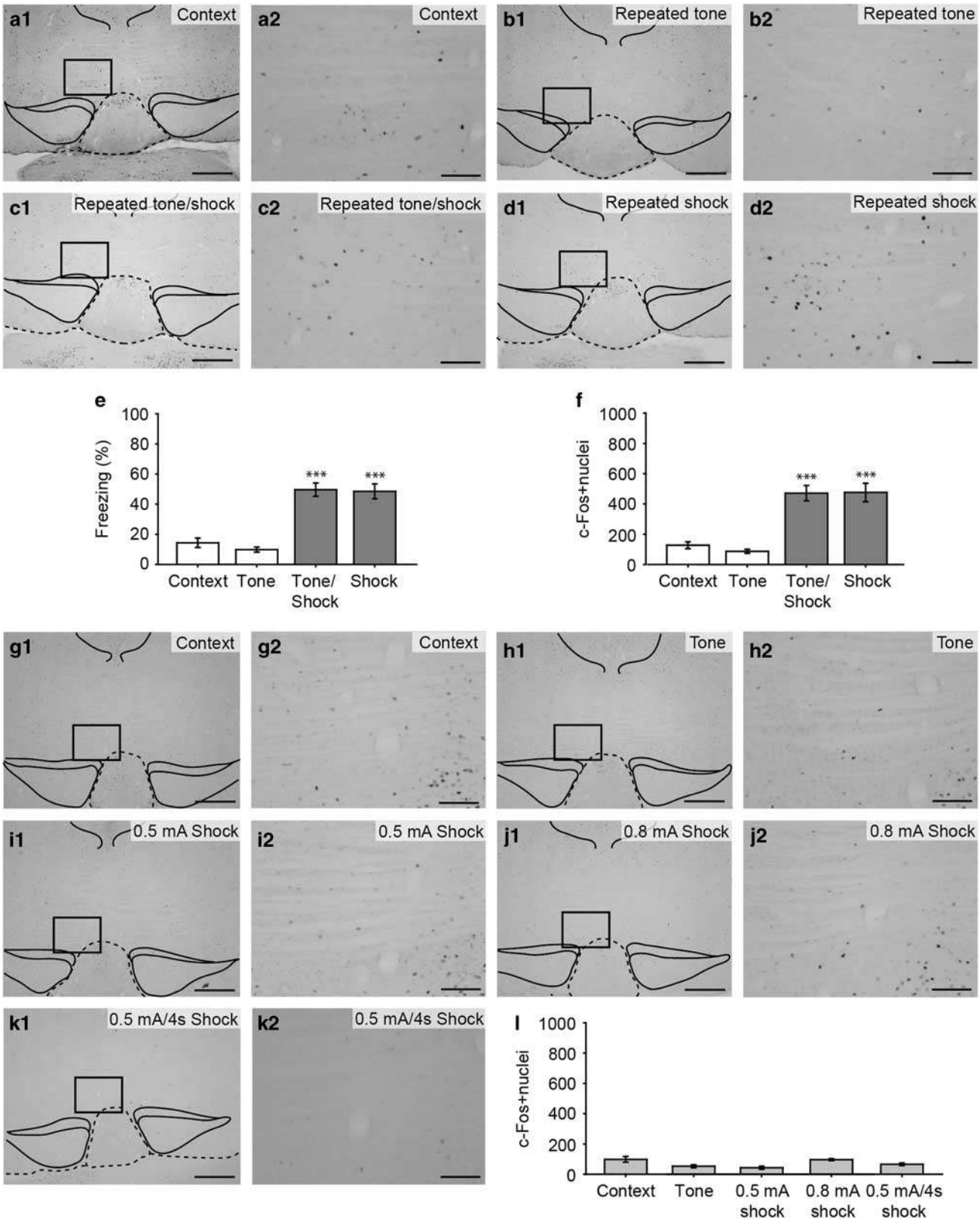

Figure 3 See for caption on page 644.

shock session was observed in foot-shock-exposed animals ($F_{3,21} = 28.7$, $p < 0.001$) (Figure 3e). This c-Fos induction was observed whether a predictive tone was present or not before each shock exposure (Figures 3a–d and f). However, a single foot shock did not evoke c-Fos in the tVTA. Indeed, no induction was observed with a single shock of intensity as used in fear conditioning (0.5 mA/0.8 s), with a single shock of intensity as used in fear conditioning but of a duration equivalent to the sum of five shocks (0.5 mA/4 s), or with a single shock of higher intensity (0.8 mA/0.8 s) (Figures 3g–l). Moreover, single salient information (arousing but non-nociceptive), such as a loud auditory stimulus, also failed to recruit the tVTA (Figure 3h). These findings support the idea that repetition of the stimulus was critical for inducing c-Fos in the tVTA as a consequence of foot shocks.

Opioid Withdrawal

The tVTA is a direct target of opiates (Jalabert *et al*, 2011), even though morphine itself does not induce Fos locally (Perrotti *et al*, 2005; Kaufling *et al*, 2010b). Here we show that precipitated opiate withdrawal (Supplementary Table S1) induces c-Fos in the tVTA ($F_{3,16} = 406.9$, $p < 0.001$) (Figures 4a and b). Morphine treatment *per se* did not affect the total number of MOR-positive neurons in the tVTA (data not shown). Withdrawal-induced c-Fos was present (15%) in MOR-expressing neurons, but mostly (85%) in neurons not expressing this receptor (Figures 4c–e). In a separate experiment, we also show that a bilateral lesion of the tVTA did not significantly change the individual physical signs of withdrawal or the global withdrawal score (Figure 4f and Supplementary Table S2, $p = 0.91$).

Conditioned Taste Aversion

The lack of tVTA c-Fos induction in response to most of the tested aversive stimuli raised the question of tVTA requirement for avoidance behaviors. We assessed the effect of tVTA ablation on the LiCl- and LPS-induced CTA, aversive-like behaviors not yet tested in tVTA studies. CTA being a robust conditioning, single conditioning procedures were used (Slouzkey *et al*, 2013). Only rats with lesions encompassing the tVTA were included in the results, TH immunostaining was used to control for the absence of VTA dopaminergic lesion (Figures 5a and b). Sham control rats (Sal-sham) displayed a preference for saccharin in the two-bottle choice test (Figure 5c). tVTA ablation did not abolish saccharin preference or affect the LiCl- or LPS-induced CTA (treatment, $F_{2,32} = 21.3$, $p < 0.001$; surgery, $F_{1,32} = 2.5$, $p = 0.12$; treatment × surgery, $F_{2,32} = 0.9$, $p = 0.41$). Indeed, rats showed decreased preference for the saccharin solution previously paired to LiCl or LPS injection in both sham ($p < 0.001$ and $p < 0.01$, respectively) and lesion groups ($p < 0.001$). Moreover, the aversive index differed from chance level (50%) in LPS-lesion, LiCl-lesion and LiCl-sham groups, even though it failed to differ from chance level in the LPS-sham group, because of high variability (Figure 5c).

DISCUSSION

By exploring the impact of aversive stimuli, we found that most of them failed to significantly induce c-Fos in the tVTA. Induction was only observed with repeated foot shocks and precipitated morphine withdrawal, and mildly with β-carboline at a high dose. Opiate withdrawal Fos response in the tVTA concerned MOR-expressing and -non-expressing cells. Last, we show that bilateral ablation of the tVTA did not affect physical signs of opiate withdrawal, or LPS- and LiCl-induced CTA.

Implication of the tVTA, which receives afferents from the LHb (Balcita-Pedicino *et al*, 2011; Jhou *et al*, 2009a; Kaufling *et al*, 2009) and controls dopamine cell activity (Bourdy *et al*, 2014; Jalabert *et al*, 2011; Jhou *et al*, 2009b; Matsui and Williams, 2011), has been described in active, passive, and conditioned avoidance behaviors and in the processing of aversive information (Jhou *et al*, 2009b, 2013; Lammel *et al*, 2012; Meye *et al*, 2015; Stamatakis and Stuber, 2012). To date, however, the most striking Fos responses in this structure were observed with psychostimulants (Cornish *et al*, 2012; Jhou *et al*, 2009a, 2013; Geisler *et al*, 2008; Kaufling *et al*, 2010b; Lecca *et al*, 2011; Perrotti *et al*, 2005; Zahm *et al*, 2010) (see Supplementary Table S3 and Supplementary Data). Our first aim was thus to test whether aversive stimuli would display a common molecular impact on the tVTA, as revealed by induction of c-Fos proteins. Surprisingly, the exposure to aversive drugs such as LiCl, naloxone at high dose, or LPS did not induce c-Fos expression in the tVTA. The anxiogenic agent β-carboline, used at a high dose to model panic attacks (Thiébot *et al*, 1988), resulted in a significant induction, although quantitatively mild compared with the response observed with amphetamine. More sustained aversive experiences, such as inflammatory pain and neuropathic pain, also failed to change c-Fos expression locally, even though inhibition of the tVTA by local microinjection of endomorphin or muscimol has an analgesic action in the formalin test (Jhou *et al*, 2012). Lesion of the tVTA prevents the freezing response to TMT odor, while increasing other defensive behaviors (Jhou *et al*, 2009b), which suggests that the tVTA is important to passive defensive behavior. However, we did not evidence c-Fos induction when testing unconditioned fear through predator odor exposure, or after stress elicited by immobilization or forced swimming. Importantly, a lack of

Figure 3 Repeated foot-shock exposure induces c-Fos expression in the GABAergic tail of the ventral tegmental area (tVTA). The context (a) and the tone (b) exposure hardly induces c-Fos expression in the tVTA, whereas (c and d) repeated foot shocks (0.5 mA, 5 × 0.8 s) induce c-Fos expression in the tVTA, under the presence of the tone or not ($n = 5$–6 per group). (e) Freezing behavior in the test session following repeated foot-shock exposures. (f) Quantification of c-Fos-positive nuclei in the tVTA following repeated foot-shock exposures. ***$p < 0.001$ (relative to the control group). (g–k) Single foot-shock exposure fails to induce c-Fos in the tVTA. Compared with controls (context, (g)), no c-Fos expression was present with 0.5 mA/0.8 s (i), 0.8 mA/0.8 s (j), or 0.5 mA/4 s (k) ($n = 4$ per group). The exposure to a salient loud auditory stimulus also failed to recruit the tVTA (h) ($n = 4$). (l) Quantification of c-Fos-positive nuclei in the tVTA following single foot-shock exposure or a loud auditory stimulus. Rats were perfused 2 h after the beginning of the session for repeated foot-shock experiments, or after 1h30 for single foot-shock experiments. The squares in (a_1–d_1 and g_1–k_1) indicate the regions shown at higher magnification in (a_2–d_2 and g_2–k_2). Scale bars, 500 μm (a_1–d_1, g_1–k_1) and 100 μm (a_2–d_2, g_2–k_2).

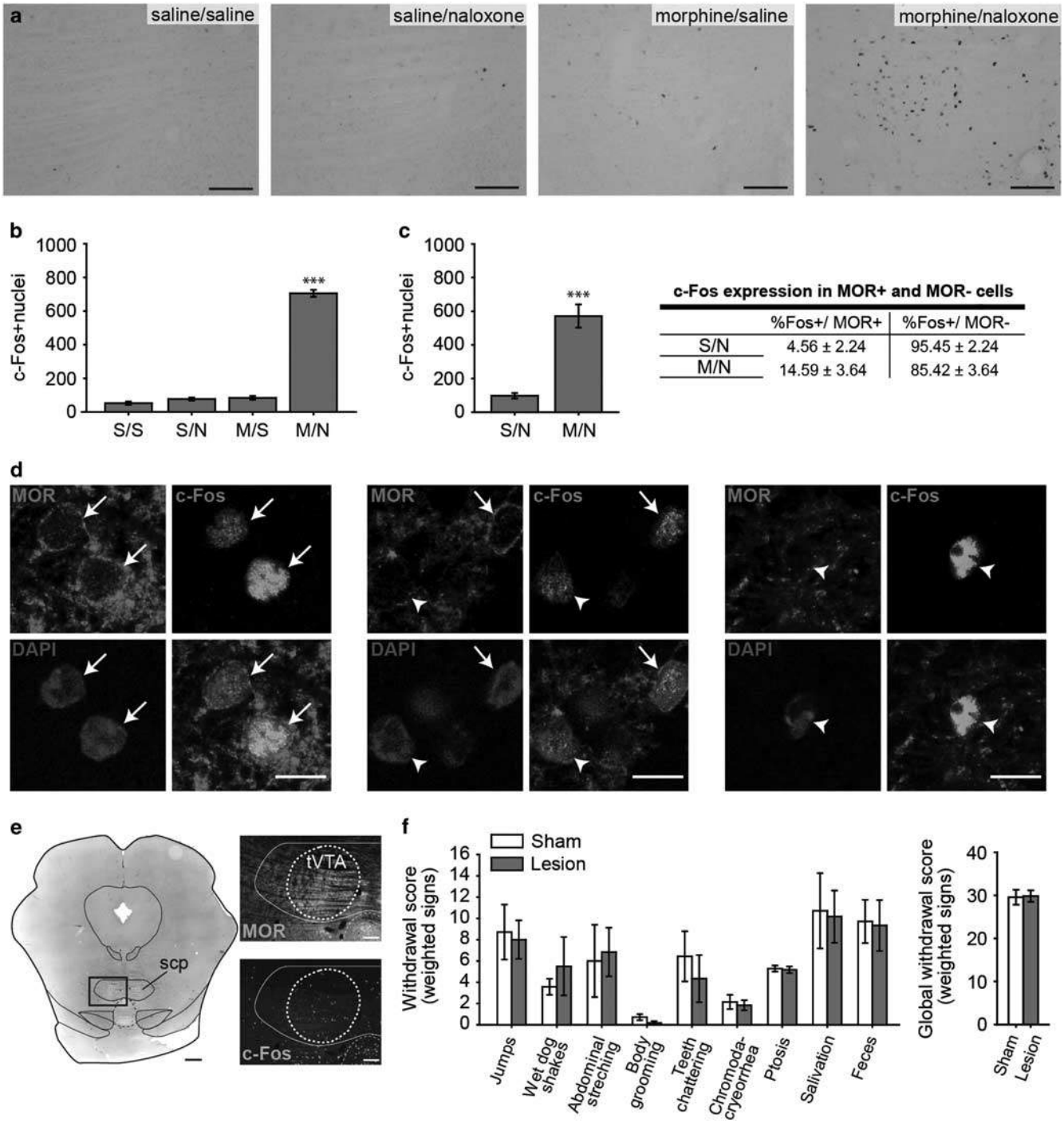

Figure 4 Opiate withdrawal induces c-Fos expression in the GABAergic tail of the ventral tegmental area (tVTA). (a) Animals receiving repeated saline injections and a saline (S/S) or naloxone (1 mg/kg) (S/N) challenge, or repeated morphine injections and a saline challenge (M/S), do not display c-Fos induction in the tVTA, whereas animals receiving repeated morphine injections and a naloxone challenge (M/N) exhibited opioid withdrawal symptoms (Supplementary Table S1) and high levels of c-Fos-positive nuclei in the tVTA. (b) Quantification of c-Fos-positive nuclei in the tVTA ($n = 4$–6 per group). (c) Quantification of c-Fos-positive nuclei in MOR-positive and -negative cells of the tVTA ($n = 5$ per group). $^{***}p < 0.001$ (relative to the control group). (d) After opiate withdrawal, c-Fos induction (in green) in the rat tVTA was present in MOR-expressing neurons (in red) (as indicated by the arrows), and in neurons not expressing them (as indicated by the arrow heads). Cell nuclei are labeled with DAPI (4',6-diamidino-2-phenylindole) (in blue). Rats were perfused 2 h after the naloxone or saline administration. Scale bars, 100 μm (a) and 10 μm (d). (e) Illustration of one of the sections used for stereological analysis (data in c). The square in left picture indicates the region shown at higher magnification in right pictures (top: MOR in orange; bottom: c-Fos in green). The dotted area in right pictures indicates the tVTA limits used for stereological analysis; at this anteroposterior level, the tVTA is embedded within fibers of the superior cerebellar peduncle. Scale bars, 500 μm (left picture) and 100 μm (right pictures). (f) The lesion of the tVTA did not significantly alter the physical signs or the global score (Gellert and Holtzman, 1978) of naloxone-precipitated opiate withdrawal (sham $n = 7$; lesion $n = 6$). A full color version of this figure is available at the *Neuropsychopharmacology* journal online.

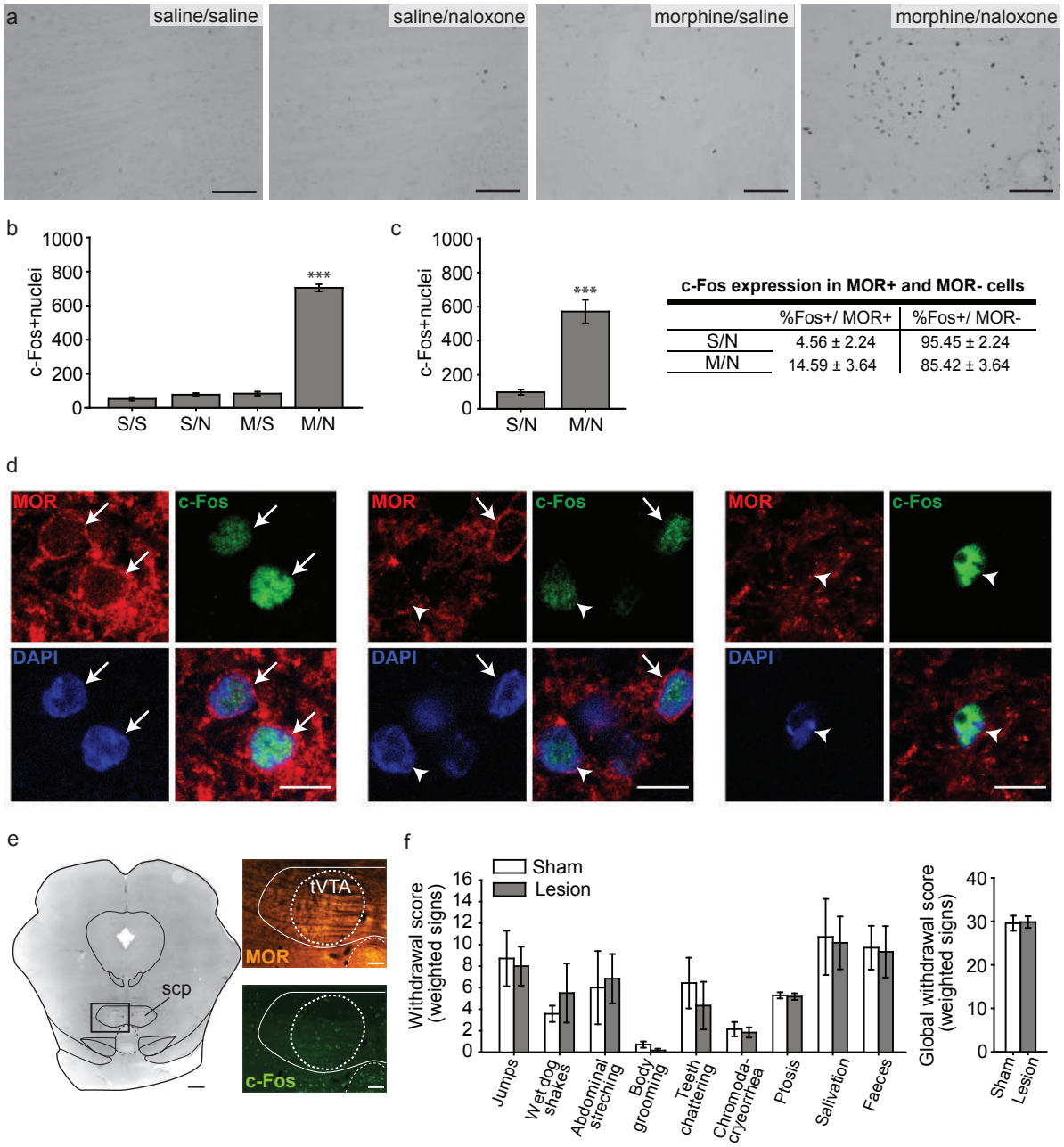

Figure 4 Opiate withdrawal induces c-Fos expression in the GABAergic tail of the ventral tegmental area (tVTA). (a) Animals receiving repeated saline injections and a saline (S/S) or naloxone (1 mg/kg) (S/N) challenge, or repeated morphine injections and a saline challenge (M/S), do not display c-Fos induction in the tVTA, whereas animals receiving repeated morphine injections and a naloxone challenge (M/N) exhibited opioid withdrawal symptoms (Supplementary Table S1) and high levels of c-Fos-positive nuclei in the tVTA. (b) Quantification of c-Fos-positive nuclei in the tVTA (n=4–6 per group). (c) Quantification of c-Fos-positive nuclei in MOR-positive and -negative cells of the tVTA (n=5 per group). ***p<0.001 (relative to the control group). (d) After opiate withdrawal, c-Fos induction (in green) in the rat tVTA was present in MOR-expressing neurons (in red) (as indicated by the arrows), and in neurons not expressing them (as indicated by the arrow heads). Cell nuclei are labeled with DAPI (4',6-diamidino-2-phenylindole) (in blue). Rats were perfused 2 h after the naloxone or saline administration. Scale bars, 100 µm (a) and 10 µm (d). (e) Illustration of one of the sections used for stereological analysis (data in c). The square in left picture indicates the region shown at higher magnification in right pictures (top: MOR in orange; bottom: c-Fos in green). The dotted area in right pictures indicates the tVTA limits used for stereological analysis; at this antero-posterior level, the tVTA is embedded within fibers of the superior cerebellar peduncle. Scale bars, 500 µm (left picture) and 100 µm (right pictures). (f) The lesion of the tVTA did not significantly alter the physical signs or the global score (Gellert and Holtzman, 1978) of naloxone-precipitated opiate withdrawal (sham n=7; lesion n=6).

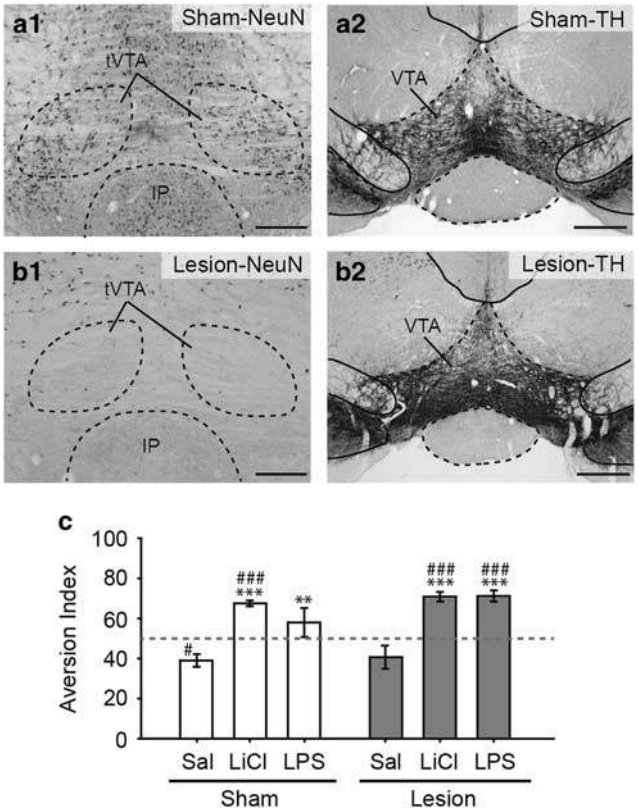

Figure 5 GABAergic tail of the ventral tegmental area (tVTA) ablation does not affect the lithium chloride (LiCl)- and lipopolysaccharide (LPS)-induced conditioned taste aversion (CTA). (a) Histological evidence for the tVTA sham group with NeuN (a_1) and tyrosine hydroxylase (TH) (a_2) immunostaining. (b) Histological evidence for the tVTA lesion group with NeuN (b_1) and TH (b_2) immunostaining. (c) Aversion index for the LiCl and LPS-induced CTA in sham controls and lesion animals ($n = 5$–8 per group). Scale bars, 200 μm (a_1 and b_1) and 500 μm (a_2 and b_2). $^{**}p < 0.01$, $^{***}p < 0.001$ (relative to their respective saline group). $^{\#}p < 0.05$ and $^{\#\#\#}p < 0.001$ (referred to 50%).

c-Fos expression does not imply a lack of functional recruitment of tVTA cells. For example, there is evidence for an electrophysiological impact on tVTA activity in the absence of Fos induction with drugs that inhibit the tVTA, such as opiates and cannabinoids (Kaufling *et al*, 2010b; Lecca *et al*, 2011). However, avoidance behaviors are supposedly associated with activation, and not inhibition, of the tVTA.

Contrary to most stressful stimuli described above, c-Fos expression in the tVTA was present following exposure to repeated mild foot shocks, similarly to previous reports (Brown and Shepard, 2013; Jhou *et al*, 2009b). The mechanism underlying this expression depends on LHb inputs. Indeed, a lesion of the fasciculus retroflexus impairs this response to mild foot shocks (Brown and Shepard, 2013), and acute unpredictable foot shocks potentiate glutamate release from the LHb to the tVTA (Stamatakis and Stuber, 2012). However, these procedures relied on a series of foot shocks, that is, the repetition of identical discrete aversive events. On the contrary, exposure to a single foot shock does not induce c-Fos in the tVTA, even though the duration of the single shock is extended to 4 s (mimicking the cumulated duration of the shock series), or if the intensity is increased to reach levels usually used for learned helplessness procedures (0.8 mA). These findings suggest that the effect of a series of foot shocks on the tVTA is unlikely related to their aversive impact *per se*, nor to the salient, arousing, or attentional properties of the shocks. These conclusions are also supported by the lack of c-Fos response following exposure to a single loud auditory tone. The present data more likely support the participation of the tVTA in learning and prediction processing associated with the repetition of discrete events. In this context, the tVTA has been shown, in monkeys, to process reward prediction error, which is mirroring the implication of the LHb in the same processing (Hong *et al*, 2011). It might be hypothesized that the response observed with a series of foot shocks may reflect attempts to predict, and/or failures in predicting, repeated occurrences of the shocks.

Present and previous data show that opiates do not induce Fos in the tVTA (Kaufling *et al*, 2010b; Perrotti *et al*, 2005). However, acute morphine withdrawal strongly induces c-Fos in this brain region. Behavioral studies support a role for the tVTA in opioid responses, as rats self-administer and develop conditioned place preference when endomorphin-1 is delivered into the tVTA (Jhou *et al*, 2012). In fact, part of the GABAergic tVTA neurons in rats express MOR (Jalabert *et al*, 2011; Jhou *et al*, 2009a, 2012; Kaufling and Aston-Jones, 2015). As a consequence, opioid administration decreases the electrophysiological activity of tVTA neurons (Jalabert *et al*, 2011; Kaufling and Aston-Jones, 2015; Lecca *et al*, 2011; Matsui and Williams, 2011), which enhances the activity of VTA dopaminergic neurons (Jalabert *et al*, 2011; Matsui and Williams, 2011). Under chronic morphine, partial tolerance develops (Matsui *et al*, 2014), and animals display altered activity of tVTA and VTA neurons, which is reversed by acute precipitated withdrawal (Kaufling and Aston-Jones, 2015). Following chronic morphine exposure, adaptive molecular changes that participate to opponent processes and were described in other brain regions (Nestler, 2015) might also be present in the tVTA and explain the c-Fos expression observed in MOR-expressing cells. This induction could thus be linked to a rebound induced by naloxone in the activity of MOR-expressing cells. On the contrary, the expression observed in MOR-non-expressing cells is more likely to be indirect, through tVTA inputs and even polysynaptic circuits. In this regard, the LHb has, for example, been shown to participate to tVTA Fos induction in response to other stimuli (Brown and Shepard, 2013; Cui *et al*, 2014). Notably, tVTA lesion had no impact on the physical signs of opiate withdrawal. However, it does not preclude its involvement in the aversiveness of opiate withdrawal.

Despite observations of c-Fos induction with a series of foot shocks or with precipitated opiate withdrawal, the lack of response to most tested conditions raises the question of the exact role of the tVTA in avoidance responses (see Supplementary Table S3 in Supplementary Data). The optogenetic stimulation of the mouse LHb recruits tVTA GABAergic neurons and induces conditioned place avoidance (Lammel *et al*, 2012). Moreover, the stimulation of terminals from the LHb in the tVTA induces passive and conditioned place avoidance, and can also decrease the reinforcing property of sucrose (Stamatakis and Stuber, 2012). Similarly, a direct S-AMPA stimulation of the tVTA induces conditioned place avoidance (Jhou *et al*, 2013). These findings from various groups converge to evidence

that stimulation of the tVTA promotes avoidance behavior. However, this does not imply that the tVTA is necessary for the physiological processing of all information leading to avoidance behavior. Indeed, we observed that the absence of the tVTA does not prevent LiCl- and LPS-induced CTAs. It shows that some forms of conditioned aversion can develop and be expressed in the absence of information processing through the tVTA.

The tVTA discovery was seminal, fostering research from various research groups. With evidence pointing to the tVTA as a major inhibitory control of dopamine systems, these studies converge to highlight the influence of the tVTA on dopamine-related functions, from responses to drug of abuse, to reward-related behaviors, reward prediction error, and control of motor responses. Generalization in trying to attribute simple functions to this brain region, while attractive for the sake of clarity, may however become a pitfall and mislead future research. The complexity of tVTA roles probably mirrors the complexity of dopamine systems themselves, which is not yet fully elucidated. This work participates to present efforts in understanding those functions of the tVTA. Foot-shock data suggest that the tVTA may be sensitive to the repetition of discrete emotional events, which could be related to previous evidence of reward prediction error processing by this brain region. The avoidance-inducing consequence of stimulating the tVTA reflects one of the functions of this brain region. Present data, however, suggest that all aversive situations may not be necessarily processed through the tVTA, and that some avoidance behavior can develop in the absence of the tVTA.

FUNDING AND DISCLOSURE

This research was supported by the Centre National de la Recherche Scientifique, Université de Strasbourg and its Neuropôle, and Agence Nationale de la Recherche (ANR-11-sv4-002). The authors declare no conflict of interest.

ACKNOWLEDGMENTS

We thank the UMS3415 Chronobiotron for animal housing, and the Neuropôle 'Plateforme imagerie *in vitro*' for confocal facilities.

REFERENCES

Balcita-Pedicino JJ, Omelchenko N, Bell R, Sesack SR (2011). The inhibitory influence of the lateral habenula on midbrain dopamine cells: ultrastructural evidence for indirect mediation via the rostromedial mesopontine tegmental nucleus. *J Comp Neurol* **519**: 1143–1164.

Benbouzid M, Pallage V, Rajalu M, Waltisperger E, Doridot S, Poisbeau P *et al* (2008). Sciatic nerve cuffing in mice: a model of sustained neuropathic pain. *Eur J Pain* **12**: 591–599.

Bourdy R, Barrot M (2012). A new control center for dopaminergic systems: pulling the VTA by the tail. *Trends Neurosci* **35**: 681–690.

Bourdy R, Sánchez-Catalán MJ, Kaufling J, Balcita-Pedicino JJ, Freund-Mercier MJ, Veinante P *et al* (2014). Control of the nigrostriatal dopamine neuron activity and motor function by the tail of the ventral tegmental area. *Neuropsychopharmacology* **39**: 2788–2798.

Bromberg-Martin ES, Matsumoto M, Hikosaka O (2010). Dopamine in motivational control: rewarding, aversive, and alerting. *Neuron* **68**: 815–834.

Brown PL, Shepard PD (2013). Lesions of the fasciculus retroflexus alter foot-shock-induced cFos expression in the mesopontine rostromedial tegmental area of rats. *PLoS One* **8**: e60678.

Castanon N, Bluthé RM, Dantzer R (2001). Chronic treatment with the atypical antidepressant tianeptine attenuates sickness behavior induced by peripheral but not central lipopolysaccharide and interleukin-1beta in the rat. *Psychopharmacology* **154**: 50–60.

Cornish JL, Hunt GE, Robins L, McGregor IS (2012). Regional c-Fos and FosB/ΔFosB expression associated with chronic methamphetamine self-administration and metamphetamine-seeking behavior in rats. *Neuroscience* **206**: 100–114.

Cui W, Mizukami H, Yanagisawa M, Aida T, Nomura M, Isomura Y *et al* (2014). Glial dysfunction in the mouse habenula causes depressive-like behaviors and sleep disturbance. *J Neurosci* **34**: 16273–16285.

File SE, Baldwin HA (1987). Effects of beta-carbolines in animal models of anxiety. *Brain Res Bull* **19**: 293–299.

Geisler S, Marinelli M, Degarmo B, Becker ML, Freiman AJ, Beales M *et al* (2008). Prominent activation of brainstem and pallidal afferents of the ventral tegmental area by cocaine. *Neuropsychopharmacology* **33**: 2688–2700.

Gellert VF, Holtzman SG (1978). Development and maintenance of morphine tolerance and dependence in the rat by scheduled access to morphine drinking solutions. *J Pharmacol Exp Ther* **205**: 536–546.

Hong S, Jhou TC, Smith M, Saleem KS, Hikosaka O (2011). Negative reward signals from the lateral habenula to dopamine neurons are mediated by rostromedial tegmental nucleus in primates. *J Neurosci* **31**: 11457–11471.

Jalabert M, Bourdy R, Courtin J, Veinante P, Manzoni OJ, Barrot M *et al* (2011). Neuronal circuits underlying acute morphine action on dopamine neurons. *Proc Natl Acad Sci USA* **108**: 16446–16450.

Jhou TC, Fields HL, Baxter MG, Saper CB, Holland PC (2009b). The rostromedial tegmental nucleus (RMTg), a GABAergic afferent to midbrain dopamine neurons, encodes aversive stimuli and inhibits motor responses. *Neuron* **61**: 786–800.

Jhou TC, Geisler S, Marinelli M, Degarmo BA, Zahm DS (2009a). The mesopontine rostromedial tegmental nucleus: a structure targeted by the lateral habenula that projects to the ventral tegmental area of Tsai and substantia nigra compacta. *J Comp Neurol* **513**: 566–596.

Jhou TC, Xu SP, Lee MR, Gallen CL, Ikemoto S (2012). Mapping of reinforcing and analgesic effects of the mu opioid agonist endomorphin-1 in the ventral midbrain of the rat. *Psychopharmacology* **224**: 303–312.

Jhou TC, Good CH, Rowley CS, Xu SP, Wang H, Burnham NW *et al* (2013). Cocaine drives aversive conditioning via delayed activation of dopamine-responsive habenular and midbrain pathways. *J Neurosci* **33**: 7501–7512.

Kaufling J, Veinante P, Pawlowski SA, Freund-Mercier MJ, Barrot M (2009). Afferents to the GABAergic tail of the ventral tegmental area in the rat. *J Comp Neurol* **513**: 597–621.

Kaufling J, Veinante P, Pawlowski SA, Freund-Mercier MJ, Barrot M (2010a). Gamma-aminobutyric acid cells with cocaine-induced DeltaFosB in the ventral tegmental area innervate mesolimbic neurons. *Biol Psychiatry* **67**: 88–92.

Kaufling J, Waltisperger E, Bourdy R, Valera A, Veinante P, Freund-Mercier MJ *et al* (2010b). Pharmacological recruitment of the GABAergic tail of the ventral tegmental area by acute drug exposure. *Br J Pharmacol* **161**: 1677–1691.

Kaufling J, Aston-Jones G (2015). Persistent adaptations in afferents to ventral tegmental dopamine neurons after opiate withdrawal. *J Neurosci* **35**: 10290–10303.

Konsman JP, Veeneman J, Combe C, Poole S, Luheshi GN, Dantzer R (2008). Central nervous action of interleukin-1 mediates activation of limbic structures and behavioural depression in response to peripheral administration of bacterial lipopolysaccharide. *Eur J Neurosci* **28**: 2499–2510.

Lammel S, Lim BK, Ran C, Huang KW, Betley MJ, Tye KM *et al* (2012). Input-specific control of reward and aversion in the ventral tegmental area. *Nature* **491**: 212–217.

Lavezzi HN, Parsley KP, Zahm DS (2012). Mesopontine rostromedial tegmental nucleus neurons projecting to the dorsal raphe and pedunculopontine tegmental nucleus: psychostimulant-elicited Fos expression and collateralization. *Brain Struct Funct* **217**: 719–734.

Lavezzi HN, Parsley KP, Zahm DS (2015). Modulation of locomotor activation by the rostromedial tegmental nucleus. *Neuropsychopharmacology* **40**: 676–687.

Lecca S, Melis M, Luchicchi A, Ennas MG, Castelli MP, Muntoni AL *et al* (2011). Effects of drugs of abuse on putative rostromedial tegmental neurons, inhibitory afferents to midbrain dopamine cells. *Neuropsychopharmacology* **36**: 589–602.

Lecca S, Melis M, Luchicchi A, Muntoni AL, Pistis M (2012). Inhibitory inputs from rostromedial tegmental neurons regulate spontaneous activity of midbrain dopamine cells and their responses to drugs of abuse. *Neuropsychopharmacology* **37**: 1164–1176.

Luis-Delgado OE, Barrot M, Rodeau JL, Ulery PG, Freund-Mercier MJ, Lasbennes F (2006a). The transcription factor DeltaFosB is recruited by inflammatory pain. *J Neurochem* **98**: 1423–1431.

Luis-Delgado OE, Barrot M, Rodeau JL, Schott G, Benbouzid M, Poisbeau P *et al* (2006b). Calibrated forceps: a sensitive and reliable tool for pain and analgesia studies. *J Pain* **7**: 32–39.

Marchand AR, Luck D, DiScala G (2003). Evaluation of an improved automated analysis of freezing behaviour in rats and its use in trace fear conditioning. *J Neurosci Methods* **126**: 145–153.

Matsui A, Williams JT (2011). Opioid-sensitive GABA inputs from rostromedial tegmental nucleus synapse onto midbrain dopamine neurons. *J Neurosci* **31**: 17729–17735.

Matsui A, Jarvie BC, Robinson BG, Hentges ST, Williams JT (2014). Separate GABA afferents to dopamine neurons mediate acute action of opioids, development of tolerance, and expression of withdrawal. *Neuron* **82**: 1346–1356.

Matsumoto M, Hikosaka O (2009). Representation of negative motivational value in the primate lateral habenula. *Nat Neurosci* **12**: 77–84.

Melis M, Sagheddu C, De Felice M, Casti A, Madeddu C, Spiga S *et al* (2014). Enhanced endocannabinoid-mediated modulation of rostromedial tegmental nucleus drive onto dopamine neurons in Sardinian alcohol-preferring rats. *J Neurosci* **34**: 12716–12724.

McGregor IS, Hargreaves GA, Apfelbach R, Hunt GE (2004). Neural correlates of cat odor-induced anxiety in rats: region-specific effects of the benzodiazepine midazolam. *J Neurosci* **24**: 4134–4144.

Meye FJ, Valentinova K, Lecca S, Marion-Poll L, Maroteaux MJ, Musardo S *et al* (2015). Cocaine-evoked negative symptoms require AMPA receptor trafficking in the lateral habenula. *Nat Neurosci* **18**: 376–378.

Nestler EJ (2015). Reflections on: 'A general role for adaptations in G-proteins and the cyclic AMP system in mediating the chronic actions of morphine and cocaine on neuronal function'. *Brain Res* **1645**: 71–74.

Ossenkopp KP, Eckel LA (1995). Toxin-induced conditioned changes in taste reactivity and the role of the chemosensitive area postrema. *Neurosci Biobehav Rev* **19**: 99–108.

Paxinos G, Watson C (2007). *The Rat Brain in Stereotaxic Coordinates*4th edn.Academic Press: San Diego, CA.

Perrotti LI, Bolaños CA, Choi KH, Russo SJ, Edwards S, Ulery PG *et al* (2005). ΔFosB accumulates in a GABAergic cell population in the posterior tail of the ventral tegmental area after psychostimulant treatment. *Eur J Neurosci* **21**: 2817–2824.

Pliakas AM, Carlson RR, Neve RL, Konradi C, Nestler EJ, Carlezon WA Jr (2001). Altered responsiveness to cocaine and increased immobility in the forced swim test associated with elevated cAMP response element-binding protein expression in nucleus accumbens. *J Neurosci* **21**: 7397–7403.

Rotllant D, Marquez C, Nadal R, Armario A (2010). The brain pattern of c-fos induction by two doses of amphetamine suggests different brain processing pathways and minor contribution of behavioural traits. *Neuroscience* **168**: 691–705.

Sánchez-Catalán MJ, Kaufling J, Georges F, Veinante P, Barrot M (2014). The antero-posterior heterogeneity of the ventral tegmental area. *Neuroscience* **282C**: 198–216.

Slouzkey I, Rosenblum K, Maroun M (2013). Memory of conditioned taste aversion is erased by inhibition of PI3K in the insular cortex. *Neuropsychopharmacology* **38**: 1143–1153.

Stamatakis AM, Stuber GD (2012). Activation of lateral habenula inputs to the ventral midbrain promotes behavioral avoidance. *Nat Neurosci* **15**: 1105–1107.

Tenk CM, Kavaliers M, Ossenkopp KP (2006). The effects of acute corticosterone on lithium chloride-induced conditioned place aversion and locomotor activity in rats. *Life Sci* **79**: 1069–1080.

Thiébot MH, Soubrié P, Sanger D (1988). Anxiogenic properties of beta-CCE and FG 7142: a review of promises and pitfalls. *Psychopharmacology* **9**: 452–463.

Wise RA (2004). Dopamine, learning and motivation. *Nat Rev Neurosci* **5**: 483–494.

Yalcin I, Megat S, Barthas F, Waltisperger E, Kremer M, Salvat E *et al* (2014). The sciatic nerve cuffing model of neuropathic pain in mice. *J Vis Exp* **89**.

Zahm DS, Becker ML, Freiman AJ, Strauch S, Degarmo B, Geisler S *et al* (2010). Fos after single and repeated self-administration of cocaine and saline in the rat: emphasis on the Basal forebrain and recalibration of expression. *Neuropsychopharmacology* **35**: 445–463.

Supplementary Information accompanies the paper on the Neuropsychopharmacology website (http://www.nature.com/npp)

Table S1

Behavioral assessment of opiate withdrawal. These data correspond to the animals used for the analysis of c-Fos in the tVTA, reported in Figure 4a,b. Morphine or saline were given twice a day for 7 days at escalading doses; on day8, naloxone (1 mg/kg) or saline were delivered one hour after a last injection of either saline or morphine. The behavioral and physiological variables were scored for 30 minutes following the naloxone or saline administration. n=4-6/group. S/S: saline/saline, S/N: saline/naloxone, M/S: morphine/saline, M/N: morphine/naloxone.

Behavioral assessment of opiate withdrawal

	S/S	S/N	M/S	M/N
Jumps	0	0	0	4.17 ± 1.6
Wet dog shakes	0	0	0	5.83 ±1.2
Abdominal stretching	0	0	0	19.33 ± 5.8
Weight loss (%)	1.42 ±0.38	0.74 ± 0.28	0.68 ± 0.27	4.47 ± 0.2
Diarrhea	0	0	0	3 ± 0.89
Micturition	0.25 ± 0.25	0.25 ± 0.25	0	2.67 ± 0.71
Chromodacryeorrhea	0	0	0	4.17 ± 1.08
Ptosis	0	1 ± 0.58	0	3.17 ± 0.91

Table S2

Behavioral assessment of opiate withdrawal signs in morphine-treated rats following saline administration. All rats (sham and tVTA lesion) were chronically treated with morphine. On day 7 of treatment, they received a saline injection one hour following the morning morphine injection, and the behavioral and physiological variables were scored over 30 minutes. These data are control for the evaluation of the naloxone-precipitated withdrawal that was done on the same animals on day 8, and presented in Figure 4e.

Behavioral assessment of opiate withdrawal signs following saline administration

	Sham	Lesion
Jumps	0	0
Wet dog shakes	0	0
Abdominal stretching	0	0
Body grooming	6.43 ± 1.81	6.67 ± 3.08
Teeth chattering	0	0
Chromodacryeorrhea	0	0
Ptosis	0.86 ± 0.59	1.33 ± 1.33
Salivation	0	0
Faeces	0	0

Table S3

Fos protein expression in the tVTA. Data presented in the table concern present and published information on Fos protein induction in the tVTA in response to aversive and other stimuli, to the exception of psychostimulants. Indeed, the large literature showing, in rats, that psychostimulant drugs share the property to induce Fos proteins in the tVTA is not reported here but has been previously summarized (for review: Sánchez-Catalán et al, 2014). Remark: a lack of c-Fos expression does not imply a lack of functional recruitment of tVTA cells.

Stimuli	Marker	Induction	Reference
Dissociative drugs			
Acute ketamine, phencyclidine	FosB/ ΔFosB	No	Kaufling *et al,* 2010b
Anticonvulsant drugs			
Acute valproate, gabapentin	FosB/ ΔFosB	No	Kaufling *et al,* 2010b
Antidepressant drugs			
Acute nortriptyline, reboxetine, fluoxetine, venlafaxine	FosB/ ΔFosB	No	Kaufling *et al,* 2010b
Repeated nortriptyline, fluoxetine			Perrotti *et al*, 2005
Other drugs			
Acute γ-hydroxybutyric acid Acute dexfenfluramine	FosB/ ΔFosB	No	Kaufling *et al,* 2010b
Ethanol, cannabinoid & opioid targeting			
Acute ethanol	FosB/ ΔFosB	No	Kaufling *et al*, 2010b
Δ9-tetrahydrocannabinol	FosB/ ΔFosB	No	Kaufling *et al*, 2010b
Acute morphine	FosB/ ΔFosB	No	Kaufling *et al*, 2010b
Morphine pellets (chronic)	FosB/ ΔFosB		Perrotti *et al*, 2005
Repeated morphine injections	FosB/ ΔFosB c-Fos		Perrotti *et al*, 2005 Present data
Acute naloxone	c-Fos	No	Present data
Precipitated opiate withdrawal	c-Fos	Yes	Present data
Painful stimuli			
λ-carrageenan (inflammatory, sustained)	c-Fos	No	Present data
Neuropathic pain (chronic)			
Single footshock exposure	c-Fos	No	Present data
Repeated footshock exposure (repeated discrete aversive events)	c-Fos	Yes	Jhou *et al*, 2009b Brown and Shepard, 2011 Present data
Conditioned stimulus			
Footshock-predictive cues	c-Fos	Yes	Jhou *et al*, 2009b
Sensory salient information			
Loud auditory stimulus	c-Fos	No	Present data
Predator odor (cat, TMT)			
Sickness behavior			
Acute LiCl	c-Fos	No	Present data
Lipopolysaccharide (immune response)	c-Fos	No	Present data
Anxiety-related manipulation			
Acute diazepam (anxiolytic)	FosB/ ΔFosB	No	Kaufling *et al,* 2010b
Acute β-carboline (anxiogenic)	c-Fos	Yes	Present data
Stressful stimuli			
Acute restraint stress	c-Fos	No	Present data
Repeated restraint stress	FosB/ ΔFosB	No	Perrotti *et al*, 2005
Forced swimming	c-Fos	No	Present data

References

Brown PL, Shepard PD (2013). Lesions of the fasciculus retroflexus alter foot-shock-induced cFos expression in the mesopontine rostromedial tegmental area of rats. *PLoS One* **8**: e60678.

Jhou TC, Fields HL, Baxter MG, Saper CB, Holland PC (2009b). The rostromedial tegmental nucleus (RMTg), a GABAergic afferent to midbrain dopamine neurons, encodes aversive stimuli and inhibits motor responses. *Neuron* **61**: 786–800.

Kaufling J, Waltisperger E, Bourdy R, Valera A, Veinante P, Freund-Mercier MJ *et al* (2010b). Pharmacological recruitment of the GABAergic tail of the ventral tegmental area by acute drug exposure. *Br J Pharmacol* **161**: 1677–1691.

Perrotti LI, Bolaños CA, Choi KH, Russo SJ, Edwards S, Ulery PG *et al* (2005). ΔFosB accumulates in a GABAergic cell population in the posterior tail of the ventral tegmental area after psychostimulant treatment. *Eur J Neurosci* **21**: 2817-2824.

Chapitre 3

INFLUENCE OF A LESION OF THE TAIL OF THE VENTRAL TEGMENTAL AREA IN A RAT MODEL OF PARKINSON'S DISEASE.

,**Fanny Faivre***, María-José Sánchez-Catalán*, Sandra Dovero, Simone Bido, Anil Joshi, Erwan Bezard and Michel Barrot (* co-first author).

La tVTA est une structure riche en neurones GABAergiques exerçant un important contrôle inhibiteur sur les neurones dopaminergiques du mésencéphale. En effet, *in vivo*, la stimulation de la tVTA entraîne l'inhibition phasique des neurones de la VTA (Lecca et al., 2011, 2012; Kaufling and Aston-Jones, 2015). Bien que l'essentiel des études fonctionnelles soient pour l'instant centrées sur l'impact de la projection de la tVTA sur la VTA, des expériences d'anatomie et d'électrophysiologie ont montré le contrôle inhibiteur qu'exerce la tVTA sur les neurones de la SNc, neurones projetant sur le striatum dorsal (Bourdy et al., 2014). Il a en effet été montré que 90% des neurones enregistrés dans la SNc étaient inhibés par une stimulation de la tVTA. Fonctionnellement, une lésion de la tVTA compense le biais de rotation induit par une injection d'amphétamines chez des animaux ayant une lésion unilatérale partielle de la SNc. De manière intéressante, une lésion de la tVTA entraîne également une amélioration des performances motrices et de l'apprentissage moteur.

C'est dans ce contexte que Marià-José Sanchez-Catalan, post-doctorante dans l'équipe, a évalué l'impact d'une co-lésion bilatérale de la tVTA sur les déficits moteurs induits par une lésion bilatérale de la SNc. Cette première expérience a montré que cette co-lésion permettait une récupération des performances motrices des animaux lésés dans le test du rotarod.

Ce résultat prometteur nous a fait nous questionner sur l'impact d'une telle co-lésion sur les symptômes non-moteurs couramment rencontrés par les patients atteints de la maladie. Pour cela, nous avons d'abord voulu évaluer la présence de ces symptômes dans notre modèle. Nous avons donc analysé la réponse des animaux à différents tests évaluant le seuil nociceptif thermique et mécanique mais également les réponses thermiques réflexes et l'apparition de symptômes de type dépressifs. Dans le test de la pince calibrée, les animaux lésés montrent une diminution de leur seuil nociceptif mécanique qui perdure jusqu'à 12 semaines après la chirurgie. Le seuil nociceptif thermique est également abaissé chez ces animaux, ce qui est notamment visible dans le test de la plaque chaude incrémentée, les animaux lésés apparaissant comme allodyniques. Etonnament, le seuil nociceptif réflexe est, à l'inverse, augmenté dans le

test de retrait de la queue. Enfin, le test de préférence au sucre montre l'apparition d'une anhédonie chez les animaux lésés ainsi que d'une diminution du volume de sucre ingéré.

Les tests les plus robustes et reproductibles (test de la pince calibrée et test de la préférence au sucre) ont été réitérés afin d'évaluer l'impact de la co-lésion SNc/tVTA. Cette co-lésion permet en effet de rétablir le seuil nociceptif à un niveau équivalent à celui des animaux contrôles et permet de supprimer l'anhédonie à 7 semaines post-chirurgie.

En conclusion, la co-lésion de la tVTA semble permettre la mise en place de phénomènes de compensation, entrainant un rétablissement des performances motrices et des seuils nociceptifs ainsi qu'une diminution des symptômes de type dépressifs dans un modèle murin de maladie de Parkinson.

Ma contribution à ce travail, signé en co-premier auteur, a été de réaliser les expériences d'évaluation des symptômes non-moteurs au cours du temps ainsi que l'évaluation de ces symptômes dans les expériences de co-lésion. J'ai également écrit le manuscrit de l'article et conçu les figures. Maria-José Sanchez-Catalan a réalisé les expériences concernant l'aspect moteur (Figure 1 de l'article) et a aidé dans l'écriture et la relecture du manuscrit. Les analyses de l'étendu des lésions ont été réalisées par Sandra Dovero et Simone Bido à Bordeaux.

PROPOSED JOURNAL SECTION: Research Report

Title: Influence of a lesion of the tail of the ventral tegmental area in a rat model of Parkinson's disease

Authors: Fanny Faivre*[1], María-José Sánchez-Catalán*[1,2], Sandra Dovero[3], Simone Bido[3], Anil Joshi[1], Erwan Bezard[3], Michel Barrot[1+]

*The first two authors contributed equally to this work

Authors' Address:

[1] Centre National de la Recherche Scientifique, Université de Strasbourg, Institut des Neurosciences Cellulaires et Intégratives, F-67000 Strasbourg, France

[2] Unitat Predepartemental de Medicina, Universitat Jaume In Castelló de la Plana, Spain

[3] Centre National de la Recherche Scientifique, Université de Bordeaux, Institut des Maladies Neurodégénératives, F-33000 Bordeaux, France

[+] **Corresponding author:** Institut des Neurosciences Cellulaires et Intégratives, 5 rue Blaise Pascal, F-67000 Strasbourg, France.

E-mail address: mbarrot@inci-cnrs.unistra.fr

Running title: Influence of the tVTA on Parkinson's disease symptoms

26 pages, 3 figures, 5591 words, abstract 226 words

Keywords: Rostromedial tegmental nucleus; 6-OHDA; non-motor symptoms; motor symptoms

Abstract

Parkinson's disease is a neurodegenerative disorder partly caused by the destruction of the dopamine neurons of the nigrostriatal pathway. It is accompanied by motor and non-motor symptoms, such as pain and depression. The tail of the ventral tegmental area (tVTA) or rostromedial tegmental nucleus (RMTg) is a GABAergic mesopontine structure that act as a major inhibitory brake for the substantia nigra *pars compacta* (SNc) dopamine cells, thus controlling their neuronal activity and related motor functions. The present study tested the influence of the tVTA on motor and non-motor symptoms in a rat model of Parkinson's disease. Using behavioural approaches, we showed that male Sprague-Dawley rats with a partial 6-hydroxydopamine (6-OHDA) SNc bilateral lesion displayed motor impairments in the rotarod test that can be compensated by a co-lesion of the tVTA. Using a set of behavioural tests, we also showed that such SNc lesion led to non-motor symptoms, including lower body weight, lower mechanical nociceptive thresholds in the forceps test and lower thermal nociceptive thresholds in the incremented hot-plate test, and a decreased sucrose preference in a 2-bottle choice paradigm. Finally, the excitotoxic co-lesion of the tVTA led to compensation of body weight, mechanical nociceptive thresholds and anhedonia-like behaviour. These findings illustrate the major influence that the tVTA exerts on the dopamine system, modulating the motor and non-motor symptoms related to a partial loss of dopamine cells.

INTRODUCTION

Parkinson's disease is a common and progressive neurodegenerative disorder, mainly characterized by the loss of dopaminergic neurons of the substantia nigra *pars compacta* (SNc) in the midbrain and the presence of cytoplasmic protein aggregates of α-synuclein (Lewy bodies) in the affected brain areas. The neurodegeneration in Parkinson's disease leads to a triad of motor symptoms such as bradykinesia, muscle rigidity and resting tremors. Likewise, a variety of non-motor symptoms have also been related to the progression of the disease, including sleep disorders, gastrointestinal and autonomic symptoms (nausea, constipation), sensory symptoms (olfactory impairment), pain and neuropsychiatric symptoms (depression, anxiety) (Chaudhuri *et al.*, 2006; Park & Stacy, 2009). The clinical diagnosis is mainly based on the motor symptoms which are noticeable when the disease is already advanced, whereas pain and emotional disturbances can be among prodromal symptoms whose early identification might facilitate early diagnosis and treatment (Antonini *et al.*, 2018; Marsili *et al.*, 2018).

A multitude of Parkinson's disease animal models have been established, attempting to reproduce parkinsonian-like symptoms. A combination of genetic and environmental factors contributes to this neurodegenerative pathology, which partially prevents to recapitulate full symptomatology in an animal model. Thus, an ideal model should include motor and non-motor symptoms (Vingill *et al.*, 2017). The 6-hydroxydopamine (6-OHDA) models have been classically used in Parkinson's disease studies, as the direct brain administration of this toxin allows a destruction of dopamine neurons terminals and soma (Ungerstedt, 1968), hence leading to motor symptoms comparable to those appearing in humans (Ungerstedt, 1968; Gubellini & Kachidian, 2015) as well as to non-motor symptoms (Bonito-Oliva *et al.*, 2014). Moreover, partial lesions with 6-OHDA might also provide a model of early stages of the disease (Gubellini & Kachidian, 2015).

The tail of the ventral tegmental area (tVTA) (Perrotti *et al.*, 2005; Kaufling *et al.*, 2009) also named rostromedial tegmental nucleus (RMTg) (Jhou *et al.*, 2009a, 2009b) is a GABAergic mesopontine structure that exerts an important inhibitory control on the midbrain dopamine neurons of the ventral tegmental area (VTA) and the SNc (Bourdy & Barrot, 2012; Sanchez-Catalan *et al.*, 2014). The tVTA functions have been explored in the response to drugs of abuse (Kaufling *et al.*, 2010a, 2010b; Jalabert *et al.*, 2011; Lecca *et al.*, 2011, 2012; Matsui & Williams, 2011; Jhou *et al.*, 2012, 2013; Kaufling & Aston-Jones, 2015), in avoidance behaviours (Jhou *et al.*, 2009a, 2009b; Stamatakis & Stuber, 2012; Sánchez-Catalán *et al.*, 2017), in reward prediction error (Hong *et al.*, 2011) and in the control of motor function (Bourdy *et al.*, 2014). Regarding the tVTA role in motor function, a tVTA-nigrostriatal pathway

has been described, as well as the inhibitory electrophysiological influence of the tVTA on SNc dopamine neurons. At behavioural level, the tVTA ablation can compensate the amphetamine-induced rotation bias after partial ipsilateral lesion of the SNc (Bourdy *et al.*, 2014). Moreover, animals with a bilateral ablation of the tVTA display increased motor performances and better motor skill learning compared to sham animals in a rotarod task (Bourdy *et al.*, 2014). Thus, the experimental evidence supports an influence of the tVTA on basal ganglia circuitry.

In the present study, we explored whether a bilateral tVTA ablation could compensate the motor impairment observed in a rat model of Parkinson's disease, which entailed a bilateral partial loss of SNc dopamine neurons. We performed a behavioural analysis of the model to include some motor and non-motor symptomatology. Regarding non-motor traits, we explored pain sensitivity by assessing mechanical nociception and thermal sensitivity, as well as depressive-like behaviour by using a sucrose preference test. Finally, we tested the impact of a co-ablation of the tVTA on chosen non-motor symptoms in the model.

MATERIAL AND METHODS

Ethical approval

All procedures involving animals were performed in accordance with the Centre National de la Recherche Scientifique (CNRS) and the European community's council directives, with animal facilities and procedures approved by the local ethical committee (CREMEAS, Strasbourg, France).

Subjects

Experiments were performed in adult male Sprague-Dawley rats (Janvier, France). The rats were habituated to the facilities for at least one week before starting the procedures, and were 7-9 weeks old (*i.e* 250-350g) at surgery time. They were housed under standard conditions (22°C, 12-hour light/dark cycle) and were provided with food and water *ad libitum*.

Drugs

Ibotenic acid (1% in phosphate-buffered saline (PBS) 0.1M; 0.3µL per side) was injected bilaterally into the tVTA using Hamilton syringes with 33-gauge needles. The 6-hydroxydopamine hydrochloride (6-OHDA; 0.25% in 0.9% NaCl with 0.01% ascorbic acid) was injected bilaterally into the SNc (1.75 µL per side for partial lesion). When no lesion was performed (Sham groups), the needle was placed in the target brain area but nothing was injected.

Surgical procedures

Experiment 1. After post-mortem control for the lesion extend, data from 36 rats (spread over 3 experimental waves) are reported concerning tVTA impact on motor coordination. Rats were randomly distributed in 4 groups: control (no lesion either of the tVTA or the SNc), SNc lesion (6-OHDA into the SNc and no lesion in the tVTA), tVTA lesion (ibotenic acid into the tVTA and no lesion in the SNc), and double lesion (both tVTA and SNc lesion). Animals were anaesthetized under sodium pentobarbital (50mg/kg, intraperitoneal (i.p.); Ceva Santé Animale, Libourne, France). The depth of anaesthesia was verified during surgery by checking pedal reflex and a third of the initial dose was reinjected if necessary. Before placing the animal in a stereotaxic frame (David Kopf, Tujunga, CA), a local anaesthetic (bupivacaine, 25mg/kg; Mylan, Saint Priest, France) and an anti-inflammatory drug (Metacam®, 1mL/kg; Boehringer Ingelheim/Rhein, Germany) were injected subcutaneously. A hydrating gel (Ocry-gel, TVM Laboratories, Lempdes, France) was regularly applied on animal's eyes to avoid dehydration. Stereotaxic coordinates relative to bregma were adjusted to the animal weight, coordinates (in mm) were as follows (Paxinos & Watson, 2014): tVTA, anteroposterior (AP) = - 6.6, lateral (L) = ±1.3, ventral (V) = - 7.6, ± 6° lateral angle and SNc, AP = - 5.2, L = ± 2.2, V = -7.7. Verticality was taken from the dura. After injection, the needle was left in place for 5 minutes before removal. Following surgery, animals were kept under a warming lamp for anaesthesia recovery and later returned back to the home cage. An oral anti-inflammatory treatment (Metacam®, 1 mL for 100 mL of water solution; Boehringer, Ingelheim/Rhein, Germany) and a special palatable food (gel-diet mixed with baby food) were available for 3 days post-surgery.

Experiment 2. After post-mortem control for the 6-OHDA lesion extend, data from 21 rats are reported concerning behavioural impact of the lesion. Rats were randomly distributed in 2 groups: control (no lesion) and SNc lesion (6-OHDA into the SNc). The surgical procedure was as described above for *experiment 1*.

Experiment 3. After post-mortem control for the lesion extend, data from 25 rats are reported concerning the impact of tVTA lesion on non-motor symptoms in a model of Parkinson's disease. Rats were randomly distributed in 4 groups: control (no lesion either of the tVTA or the SNc), SNc lesion (6-OHDA into the SNc and no lesion in the tVTA), tVTA lesion (ibotenic acid into the tVTA and no lesion in the SNc), and double lesion (both tVTA and SNc lesion). The surgical procedure was as described above for *experiment 1*.

Behavioural tests

Rotarod. To evaluate the effect of lesions on motor skill learning (*experiment 1*), animals were tested on the rotarod (Roto-Rod Series 8, IITC Life Science). Before surgery, they underwent training sessions, with one habituation session to the rotarod (5 min, 5 r.p.m.) and three

consecutive sessions over three consecutive days under an accelerating speed ramp (0-45 r.p.m., 180 s). After at least a week post-surgery, rotarod performance was evaluated with three sessions over three consecutive days under accelerated speed as described above. For each of the test days, results are expressed as the mean latency to fall for trials on this day.

To control for motor deficits in 6-OHDA animals (*experiment 2*), rotarod (Roto-Rod Series 8, IITC Life Science) performance was evaluated on week 12 after surgery, testing animals with different fixed speed (5, 10, 15 and 20 r.p.m.) and measuring the latency to fall.

Forceps. The mechanical sensitivity (*experiments 2 & 3*) was evaluated using digital calibrated forceps also referred to as rodent pincher-analgesiameter (Société Bioseb, Chaville, France) as previously described (Luis-Delgado *et al.*, 2006). Shortly, animals were loosely maintained on the bench surface by using a towel in order to mask the eyes and limit influences from environmental stimulations. The tips of the forceps were placed in the middle of the hind paw and the experimenter applied incremented force by hand until paw withdrawal. Measures were repeated 3 times for each hind paw during each testing session, and results were expressed as the mean (in g) of the 3 measures. For *experiment 3*, a baseline was done before surgery. Weekly values after surgery correspond to the average of the values for both paws.

Tail Flick. The tail flick reflex (*experiments 2 & 3*) was evaluated with a tail flick analgesia meter (52-495, Harvard apparatus, Massachusetts, United States). Animals were loosely maintained on the apparatus by using a towel in order to mask the eyes and limit influences from environmental stimulations. Light from the halogen lamp of the apparatus was focused on the tail of the animal, and the tail flick reflex was automatically detected and expressed as latency (seconds). For *experiment 3*, a baseline was done before surgery.

Hot plate. The response latency to a nociceptive heat stimulus (*experiment 2 & 3*) was evaluated using a hot plate (Series 8, IITC Life Science, Woodland Hill, California). The apparatus temperature was set at 52°C ± 0.1°C. The latency to the first hind paw licking or withdrawal was considered as nociceptive response. The cut off time was set at 15 seconds to avoid paw damage. For *experiment 3*, a baseline was done before surgery.

Dynamic hot plate. Thermal sensitivity in the dynamic hot plate (DHP) (*experiment 2*) was assessed as previously described (Yalcin *et al.*, 2009). Animals were placed on a hot plate (BIO-CHP, Société Bioseb, Chaville, France) set at 30° ± 0.1°C, and the plate temperature increased up to 40°C with 1°C.min^{-1} computer-controlled speed. During each degree interval, the number of hind paw lickings, paw withdrawals and rearing was scored. Results are expressed as number of responses for each degree interval, and as cumulative responses between 33 and 36°C at the 5 and 14 weeks post-surgery time-points.

Sucrose consumption test. Before surgery, animals were habituated for 48 hours to have two water bottles on their home cages, followed by 48 hours to sugar taste with two bottles of 1% sucrose (Euromedex, France). On the test day, animals underwent water deprivation at 12 A.M and were allowed to choose between sugar and water during the testing time period (from 6 to 7 P.M). Bottles were randomly positioned and were weighted before and after the test to evaluate sucrose consumption and preference. Solution consumption over 50% of total intake was considered as preference for the corresponding bottle. At the end of the experiments, the amount of water consumption (2 bottles of water) was also evaluated during 1 hour as control (*experiments 2 & 3*). For *experiment 3,* a baseline was done before surgery.

Tissue preparation

Experiments 1 and 3. At the end of the experiments, rats were anaesthetized under sodium pentobarbital overdose (Dolethal®, 800 mg/kg, Vetoquinol S.A., Lure, France). The depth of anaesthesia was controlled for by checking pedal reflex and animals were reinjected if necessary. Brains were collected and placed in a paraformaldehyde/glycerol solution (4% PFA, 20% glycerol in phosphate buffer) overnight at 4°C and then kept at 4°C in phosphate buffer saline solution (PBS, 0.1M, pH 7.4). After further cryopreservation (20% glycerol in PBS 0.1M, pH 7.4), coronal brain sections (40 µm) were obtained using a microtome with frozen station (SM 2000 R, Leica) and were serially collected in PBS (0.1M, pH 7.4).

Experiment 2. At the end of the experiment, rats were anaesthetized under sodium pentobarbital overdose (Dolethal®, 800 mg/kg, Vetoquinol S.A., Lure, France). The depth of anaesthesia was controlled for by checking pedal reflex and animals were reinjected if necessary. Using a peristaltic pump, rats were transcardially perfused with 100 mL of phosphate buffer (0.1M, pH 7.4) followed by 500 mL of paraformaldehyde/glutaraldehyde solution (2% paraformaldehyde, 0.2% glutaraldehyde in 0.2 M phosphate buffer). Brains were collected, postfixed overnight with PFA 2% and then cryoprotected in PBS containing 20% sucrose, frozen by immersion in a -45°C isopentane bath before being stored at -80°C until cutting. 40 µm thickness sections of both striatal and SNc levels were made by a Leica CM3050S cryostat (LEICA microsystems, Wetzler, Germany) at -20°C.

Immunohistochemistry

Experiments 1 and 3. Immunohistochemistry was performed as previously described (Bourdy *et al.*, 2014). Sections were washed in PBS (3x10 minutes), incubated for 20 minutes in a 1% H_2O_2/50% ethanol solution for peroxidase extinction, washed in PBS (3x10 minutes), and incubated with a solution of PBS-Triton X100 (0.3%) with donkey serum (5%) during 45 minutes. Then, sections were incubated overnight with a solution of PBS-Triton X100 (0.3%)

with donkey serum (1%) and the primary antibody (NeuN, #MAB377, Millipore, 1/2500; or tyrosine hydroxylase (TH), #MAB318, Millipore-Chemicon, 1/2000). All steps were performed under agitation at room temperature. After 3x10 minutes washing in PBS, sections were incubated with a biotinylated donkey anti-mouse secondary antibody (1/400, #BA2001, Vector Laboratories) and 1% donkey serum for 90 minutes. After PBS rinsing (3x10 minutes), the biotin system was amplified with the avidin-biotin-peroxidase complex (ABC; ABC Elite, 0.2% A and 0.2% B; Vector Laboratories) in PBS during 90 minutes. Sections were rinsed with 0.05 M Tris-HCl buffer (TB; pH 7.5; 3x10 minutes) and the bound peroxidase was revealed by incubation in 0.025% 3.3'-diaminobenzidine tetrahydrochloride (DAB, Sigma), 0.0006% H_2O_2 (Sigma) in TB for approximately 5 to 10 minutes. The reaction was stopped by 2x10 minutes of TB and 2x10 minutes of PBS washing. Sections were then serially mounted on Superfrost® slides (VWR), air-dried, dehydrated in graded alcohols baths (1x 70%, 1x 95% and 2x 100%), cleared in Roti-Histol (Carl Roth, Karlsruhe, Germany) and coverslipped with Eukitt. Evaluation of the lesion was performed using a Nikon Eclipse 80i and pictures were taken with a digital camera (CX 9000, MBF biosciences).

Experiment 2. Midbrain and striatal serial sections (40 µm) were processed for tyrosine hydroxylase immunohistochemistry. Serial Free-floating sections were incubated in mouse monoclonal TH antibody (Millipore, #MAB318, 1/5000) for one night at room temperature and revealed by an anti-mouse peroxidase EnVision^{TM} system followed by DAB staining. SNc and VTA sections were mounted on gelatinized slides, counterstain with a 0.1% cresyl violet solution, dehydrated and coversliped, while striatal sections were mounted on gelatinized slides and coversliped only.

Evaluation of the lesion

For animals of *experiment 2*, TH level in the striatum was quantified by densitometry. Sections were scanned in an Epson expression 10000XL high-resolution scanner. Images were then analysed in Image J software (Bethesda, MD, USA) to measure mean grey level in the delineated striatum, as previously described (Bourdenx *et al.*, 2015). TH-positive SNc or VTA cells were counted by stereology, blind with regard to the experimental condition, using a Leica DM6000B motorized microscope coupled with the Mercator Pro software (ExploraNova, La Rochelle, France), as previously described (Bourdenx *et al.*, 2015). The SNc or VTA were delineated for each section and probes for stereological counting were applied to the map obtained (sampling 1-6, dissector window 80x60 µm, spacing 240x180 µm). Each TH-positive cell with its nucleus included in the probe or intersecting any of the acceptance lines was counted. The optical fractionator method was finally used to estimate the total number of TH-

positive cells in the SNc of each animal. After this analysis, one animal of the SNc lesion group was removed because of the lack of lesion.

Data analysis

Results are expressed as mean ± standard error (SEM). Statistical tests were performed using STATISTICA 13 software (Statsoft, Tulsa, OK, USA). For all the experiments, we used multifactor analysis of variance (ANOVA) with, depending on the experiment, time, speed (r.p.m.) or temperature considered as within factors (*i.e.* repeated measure) and surgery groups as between factors (*i.e.* independent groups), followed by Duncan *post hoc* when applicable. The significance level was set at $P < 0.05$.

RESULTS

Experiment 1. We previously reported (Bourdy *et al.*, 2014) that the tVTA can modulate motor performance in a rotarod task, and that a tVTA lesion prevents the amphetamine-induced ipsilateral rotation bias observed after partial unilateral SNc lesion. Based on these findings, we tested here the impact of a bilateral lesion of the tVTA on motor impairments observed in a model of Parkinson's disease. To this end, we injected bilaterally 6-OHDA into the SNc and/or ibotenic acid into the tVTA. This resulted in a partial loss of dopaminergic cells in the SNc and a neuronal death into the tVTA, as illustrated by TH and NeuN immunostaining respectively (Fig. 1A). Bilateral SNc lesion induced a motor deficit in the rotarod task at days 2 and 3 compared to sham animals ($F_{6,60}$ = 23.40, P = 0.000119; *post hoc* results for day 2: P = 0.027, day 3: P = 0.0086). Conversely, a bilateral tVTA lesion induced an increase in motor performance over days compare to control animals (day 2: P = 0.0041, day 3: P = 0.000038). Concomitant lesions of the SNc and the tVTA resulted in a compensating effect on motor impairment, thus leading to performances that are similar to the ones observed in the control group (SNc/tVTA lesion vs sham: day 1: P = 0.9, day 2: P = 0.83, day 3: P = 0.19; SNc/tVTA lesion vs SNc lesion: day 1: P = 0.08, day 2: P = 0.02, day 3: P = 0.001; SNc/tVTA lesion vs tVTA lesion: day 1: P = 0.09, day2: P = 0.004, day 3: P = 0.000096) (Fig. 1B, 1C).

Experiment 2. In Parkinson's disease, patients suffer not only from motor deficits but also from non-motor symptoms, such as pain and depression. Before testing whether tVTA lesion may also affect these symptoms in the lesion model of Parkinson's disease, we first needed to characterize some of these non-motor symptoms in the model. The evaluation of the lesion conducted at the end of the experiment showed that 6-OHDA animals displayed a partial SNc bilateral lesion (left SNc 81.5±5.3% and right SNc 78.2±7.8% of lesion compared to sham animals), associated with the expected partial bilateral loss of TH fibres in the striatum (left striatum 62±8.6% and right striatum 68.3±4.9%) as previously described (Gómez-Paz *et al.*, 2017) and, to a much lesser extent, of the VTA dopamine cells (left VTA 21.3±7.8% and right VTA 17.4±6.5%) and the nucleus accumbens (NAc) TH fibres (left NAc 11.3±2.8% and right NAc 10.8±4.5%) (Fig. 2A). The motor deficit in SNc lesion animals, previously observed, was noticeable at the higher speed used in the rotatod task (Fig. 2B.). As previously described (Sakai & Gash, 1994), bilateral 6-OHDA lesion induced a decrease in body weight which persisted over time (Fig. 2C) ($F_{1,19}$ = 12.35, P = 0.0023, *post hoc*: P = 0.0038 on week 1, P = 0.0018 on week 2, P = 0.0034 on week 3, P = 0.004 on week 4, P = 0.004 on week 5 and P = 0.00018 on week 12). To test pain sensitivity, we first evaluated mechanical thresholds of paw withdrawal

using the forceps test (Luis-Delgado *et al.*, 2006). The SNc lesion group had lower mechanical paw withdrawal thresholds all over the sessions compared to the control group ($F_{1,19}$ = 39.53, P = 0.000005; *post hoc*: P = 0.0013 on week 2, P = 0.0024 on week 3, P = 0.00028 on week 4, P = 0.001 on week 5 and P = 0.000054 on week 12) (Fig. 2D). As the animal weight or age may influence results in this test (Luis-Delgado *et al.*, 2006b), we tested whether a relation was present between animals' weight and paw withdrawal thresholds at each time-point. No significant correlation was observed between the weight of animals and their mechanical threshold for paw withdrawal (R^2 comprised between 0.085 and 0.385). In order to evaluate the thermal sensitivity of the animals, we performed three different tests: the tail flick test, the hot plate test and the dynamic hot plate test. The tail flick is a spinal reflex that may be influenced by supraspinal descending controls (Barrot, 2012). In this test, SNc lesion animals showed a decreased tail-flick latency on week 13 after surgery ($F_{1,19}$ = 12.85, P = 0.0020; *post hoc*: P = 0.00013 on week 13) (Fig. 2E). In the hot plate test (Fig. 2F) which provides a more integrated supraspinal response, we observed a global group difference ($F_{1,18}$ = 5.27, P = 0.03) when including all time points together, suggesting heat hypersensitivity in animals with SNc lesion. However, *post hoc* analysis was significant at none of the individual time points (week 2: P = 0.13, week 3: P = 0.15, week 4: P = 0.06, week 5: P = 0.2, week 12: P = 0.21, week 13: P = 0.11), which, together with tail flick data, suggested a potential conflict between alterations in reflex and nociceptive responses. Thus, we considered using the dynamic hot plate test to have a more precise estimate of heat sensitivity. Indeed, the slow increase in temperature allowed minimizing the influence of reflex speed on the overall behavioural responses. In the dynamic hot plate test, SNc lesioned animals showed a thermal allodynia, *i.e.* nociceptive responses at normally non-nociceptive temperatures ($F_{1,19}$ = 14.29, P = 0.0013; *post hoc*: P = 0.05 at 35°C and P = 0.016 at 36°C at week 14) (Fig. 2G). This thermal allodynia was further highlighted by considering the cumulative behavioural responses between 33 and 36°C ($F_{1,19}$ = 21.83, P = 0.00017; *post hoc*: P = 0.013 on week 5 and P = 0.00037 on week 14) (Fig. 2G). Finally, we performed a sucrose preference test to assess anhedonia as symptom of depressive-like behaviour. Four weeks after surgery, SNc lesion animals showed a decreased sucrose preference and even a lack of preference 13 weeks after surgery ($F_{1,19}$ = 14.59, P = 0.0011; *post hoc*: P = 0.01 at 4 weeks and P = 0.0022 at 13 weeks). Moreover, when the total sucrose consumption was considered, it showed that SNc lesioned animals had a decreased sucrose consumption ($F_{1,19}$ = 8.41, P = 0.009) at 3 (*post hoc*: P = 0.034), 5 (P = 0.004) and 13 weeks after surgery (P = 0.0076), whereas no difference in water consumption was observed (Fig. 2G).

Experiment 3. Based on these results, we chose the most robust test for assessing pain-related responses (*i.e.* mechanical thresholds), and the sucrose preference test for assessing anhedonia-like behaviour, in order to evaluate the impact of a bilateral tVTA lesion on non-motor symptoms in the model of Parkinson's disease. As observed in *experiment 2* animals with a bilateral SNc lesion had a lower body weight than sham animals ($F_{3,21}$ = 6.51, P = 0.0028; *post hoc results* P = 0.047 at week 1 post surgery, P = 0.034 at week 2, P = 0.0067 at week 3, P = 0.0097 at week 4, P = 0.0076 at week 5, P = 0.0044 at week 6, P = 0.0028 at week 7), but also than tVTA lesion animals at 3, 5, 6 and 7 weeks post-surgery (week 1: P = 0.31, week 2: P = 0.065, week 3: P =0.017, week 4: P = 0.056, week 5: P = 0.019, week 6: P = 0.029, week 7: P = 0.009) and than animals with double lesion since week 4 (week 1: P = 0.44, week 2: P = 0.07, week 3: P = 0.058, week 4: P = 0.004, week 5: P = 0.004, week 6: P = 0.0005, week 7: P = 0.00016) (Fig. 3A), which showed that the double lesion allowed to compensate for body weight deficits related to SNc cell loss.

Likewise, SNc lesion animals showed a lower mechanical threshold in the forceps test compared to sham animals and to SNc/tVTA animals at the second week post-surgery and after ($F_{3,21}$ = 14.99, P = 0.000019; *post hoc* SNc lesion *vs* sham, P = 0.013 at week 2 post surgery, P = 0.007 at week 3, P = 0.007 at week 4 and P = 0.00012 at week 5; post hoc SNc lesion *vs* SNc/tVTA lesion, P = 0.004 at week 2 post-surgery, P = 0.00043 at week 3, P = 0.0033 at week 4 and P = 0.0062 at week 5) and to tVTA lesion animals after 3 weeks post-surgery (P = 0.11 at week 2, P = 0.005 at week3, P = 0.009 at week 4 and P = 0.00027 at week 5) (Fig. 3B). As for body weight, while tVTA lesion did not influence *per se* the nociceptive response, it allowed suppressing the impact of SNc cell loss. As observed in *experiment 2*, no significant correlation was present between the body weight of the animals and their mechanical threshold (R^2 comprised between 0.00002 and 0.27) (data not shown).

Regarding the sucrose preference test, SNc lesion animals showed a decreased preference for sucrose solution which became significant at the end of the experiment ($F_{3,21}$ = 3.50, P = 0.03; *post hoc*: P = 0.032 at week 5). No difference was observed in the volume of water consumed ($F_{3,21}$ = 0.64, P = 0.60). Otherwise, the tVTA lesion and the co-lesioned animals showed no differences when compared to control animals, showing that double lesion compensated for SNc lesion impact (Fig. 3C).

DISCUSSION

In the present study, we observed that a partial bilateral lesion of the SNc leads to both motor and non-motor symptoms, such as lower body weight, mechanical and thermal hypersensitivity, a potential slow-down of the tail reflex motor response and a depressive-like symptom in a sucrose preference test. By exploring the impact of the tVTA on those parkinsonian-like symptoms, we showed that the co-lesion of the tVTA can improve both motor and non-motor symptoms.

6-OHDA models have been widely used to study Parkinson's disease. This neurotoxin causes a depletion of the transmitter content of dopaminergic nerve terminals and cell bodies (Ungerstedt, 1968), and it has mostly been injected unilaterally into the SNc of the medial forebrain bundle to elicit the loss of dopamine neurons in animals. Indeed, a bilateral lesion often causes aphagia and adipsia, leading to a loss of body weight and even the death of the animals (Dauer & Przedborski, 2003; Bové *et al.*, 2005; Bezard & Przedborski, 2011). Conversely, partial bilateral lesion better mimic the neuropathy of Parkinson's disease in human in which there is usually an incomplete bilateral destruction of dopamine neurons in the SNc (German *et al.*, 1989). The partial bilateral SNc lesion combined with careful postsurgical care, including rehydration with saline solution and special palatable food inside the cage, helped preventing animal loss. Otherwise, it has been observed in human patients that the destruction of dopaminergic neurons is not exclusively limited to SNc but is also observed to a lower extent in the VTA (A10 area) and retrorubral field (A8 area). Moreover, the destruction of the SNc neurons leads to destruction of the nerve terminals in the caudate/putamen nucleus (Gómez-Paz *et al.*, 2017). Accordingly, we also observed a slight lesion in the VTA and NAc, whereas a noticeable lesion of the striatum was present, due to the partial bilateral lesion of the SNc dopamine neurons.

Regarding the motor symptoms, the bilateral lesion of the SNc induced motor impairment in the rotarod task. In the other hand, the bilateral lesion of the tVTA improved motor performance in animals with bilateral partial lesions of the SNc. Indeed, rats with co-lesion of the tVTA and the SNc displayed a similar level of motor performance as sham animals in the rotarod task. The tVTA control over SNc dopamine neurons has been previously demonstrated by using neuroanatomical (Ferreira *et al.*, 2008; Jhou *et al.*, 2009a, 2009b; Kaufling *et al.*, 2010a; Bourdy *et al.*, 2014) and *in vivo* electrophysiological approaches (Bourdy *et al.*, 2014), thus highlighting a tVTA-nigrostriatal pathway and the inhibitory influence of the tVTA on the activity of SNc dopamine neurons. Indeed, the electrical/chemical stimulation and chemical inhibition of the tVTA decreased and increased, respectively, the activity of the SNc dopamine

neurons (Bourdy *et al.*, 2014). Dopamine cells being under the control of excitatory and inhibitory inputs that regulate their activity (Morikawa & Paladini, 2011; Gantz *et al.*, 2018), suppressing the inhibitory influence of the tVTA on dopamine cells may facilitate excitatory impact and promote activity of these cells. Such control is also supported by previous findings showing that an unilateral lesion of the tVTA elicited an amphetamine-induced contralateral rotation bias and compensated for the ipsilateral bias in animal with unilateral SNc lesion, and that the bilateral ablation of the tVTA improved motor coordination and motor skill learning (Bourdy *et al.*, 2014). It shows a major influence of the tVTA over basal ganglia, which is a critical brain circuit in learning process that leads to habit formation and to the acquisition of skilled behaviour (White, 1997; White & McDonald, 2002). After SNc lesion, the compensatory action of tVTA lesion could be related to the loss of this inhibitory brake on the surviving dopamine neurons, and to the strong overlap of the terminal field of individual dopamine neurons within the striatal complex. Indeed, a single SNc neuron can, by its profuse arborisation (Gauthier *et al.*, 1999; Prensa & Parent, 2001; Matsuda *et al.*, 2009), cover up to 5.7% of the total volume of the striatum (Matsuda *et al.*, 2009).

Beside motor influence, we also explored tVTA impact on non-motor symptoms of Parkinson's disease. Such symptoms are indeed present in the 6-OHDA models (Faivre *et al.*, 2018). The animals displayed lower mechanical nociceptive thresholds as assessed using digital forceps, which is similar to previous reports with other models and tests (Zengin-Toktas *et al.*, 2013; Gee *et al.*, 2015), although some authors described that this effect may be time-dependant (Cao *et al.*, 2016; Wang *et al.*, 2017) or even side-dependent in case of unilateral lesion (Takeda *et al.*, 2014). We also assessed thermal hyperalgesia but obtained some contradictory results, with an apparent hyposensitivity in the tail flick test, a tendency to hypersensitivity in the hot plate test and a thermal allodynia in the dynamic hot plate. Interestingly, such discrepancies also exist in the literature, particularly concerning the tail flick test for which results vary depending on the model and the species (Grossmann *et al.*, 1973; Gee *et al.*, 2015; Ogata *et al.*, 2015; Park *et al.*, 2015; Gómez-Paz *et al.*, 2017; Nascimento *et al.*, 2018). Concerning the hot plate test, it has been documented that the thermal threshold is decreased in 6-OHDA models of Parkinson's disease (Lin *et al.*, 1981; Saadé *et al.*, 1997; Chen *et al.*, 2013; Dolatshahi *et al.*, 2015; Gee *et al.*, 2015; Nascimento *et al.*, 2018). An explanation for these differences between tests may be related to the spinal reflex component of the tail flick, which is predominant in this test and influenced by descending supraspinal controls. Indeed, patients with Parkinson's disease exhibit for example longer latency of the trigemino-cervical and trigemino-spinal reflexes (Perrotta *et al.*, 2005). The motor slow-down accompanying Parkinson's disease (Low

et al., 2002; Mazzoni *et al.*, 2012) and its models (Lindner *et al.*, 1999; Santana *et al.*, 2015) may thus mask in some protocols the nociceptive hypersensitivity. This technical limitation can however be overcome by using a slow ramp of temperature increment and by looking at the number of nociceptive responses instead of latencies. Finally, we assessed depressive-like behaviour in animals with partial bilateral lesion of the SNc, by using a sucrose preference test, and we observed a decreased preference as it has already been reported in the literature (Tadaiesky *et al.*, 2008; Santiago *et al.*, 2010, 2014; Carvalho *et al.*, 2013; Liu *et al.*, 2015; Matheus *et al.*, 2016; Silva *et al.*, 2016; Kamińska *et al.*, 2017; Ilkiw *et al.*, 2018; Vecchia *et al.*, 2018). Likewise, as we observed in our study, the evaluation of anhedonia in the sucrose preference test was time dependent (Caudal *et al.*, 2015).

To assess tVTA influence on non-motor symptoms, we chose tests with robust results: the body weight evaluation, the digital forceps test for nociceptive responses and the sucrose preference test for the depressive-like behaviour. The lesion of the tVTA had, *per se*, no impact on these parameters in animals with intact dopamine systems, suggesting that tVTA may not be essential to maintain or process these functions and behaviours. However, tVTA lesion compensated weight loss, mechanical hypersensitivity and sucrose anhedonia in animals with bilateral SNc lesion, showing that tVTA can notably influence non-motor symptoms associated with partial loss of dopamine cells.

Overall, behavioural evidence of the present study support a main influence of the tVTA in the control of the nigrostriatal pathway and in the expression of motor and non-motor symptoms related to the loss of dopamine cells. Likewise, those findings raise the question of the tVTA control over basal ganglia circuitry. While tVTA manipulation may not influence the evolution of the disease, it may alleviate symptoms. The tVTA lesion is clearly not an option to consider in patients, and tVTA deep brain stimulation may not relevant either due to the caudal and deep anatomical position of this structure and to its partial inclusion among passing fibres of the superior cerebellar peduncle. However, a better knowledge of the molecular profile of the tVTA might provide potential pharmacological targets for drugs that would allow manipulation of this brain region.

ACKNOWLEDGMENTS

This work was supported by the Centre National de la Recherche Scientifique [contracts UPR3212 and UMR5293], the University of Strasbourg, the University of Bordeaux, the Agence Nationale de la Recherche [ANR-15-CE37-0005-02; Euridol ANR-17-EURE-0022], the Fondation pour la Recherche Médicale [FDT20170437322], the NeuroTime Erasmus

Mundus Joint Doctorate, and by a NARSAD distinguish investigator grant from the Brain and Behavior Research Foundation [24220]. We want to thank Nathalie Biendon for her technical support, and the Chronobiotron UMS3415 for animal care.

CONFLICT OF INTEREST STATEMENT

The authors declare no conflict of interest.

AUTHOR CONTRIBUTIONS

F.F and M.J.S.C. designed and performed experiments, analysed data and drafted the manuscript; S.D. and S.B. performed experiments and analysed data for quantification of 6-OHDA lesion; A.J. performed experiments; E.B. supervised 6-OHDA lesion analysis and drafted the manuscript; M.B. designed the study and drafted the manuscript.

DATA ACCESSIBILITY

All data presented in the current manuscript can be obtained from the corresponding author.

ABBREVIATIONS:

6-OHDA: 6-hydroxydopamine; AP: anteroposterior; DAB: 3.3'-diaminobenzidine tetrahydrochloride; DHP: dynamic hot plate; L: lateral; NaCl: sodium chloride; PBS: phosphate buffer saline; RMTg: rostromedial tegmental nucleus; r.p.m.: rotations per minute; SEM: standard error of the mean; SNc: substantia nigra *pars compacta*; TH: tyrosine hydroxylase; tVTA: tail of the ventral tegmental area; V: ventral; VTA: ventral tegmental area.

REFERENCES

Antonini, A., Tinazzi, M., Abbruzzese, G., Berardelli, A., Chaudhuri, K.R., Defazio, G., Ferreira, J., Martinez-Martin, P., Trenkwalder, C., & Rascol, O. (2018) Pain in Parkinson's disease: facts and uncertainties. *Eur. J. Neurol.*, **25**, 697–969.

Barrot, M. (2012) Tests and models of nociception and pain in rodents. *Neuroscience*, **211**, 39–50.

Bezard, E. & Przedborski, S. (2011) A tale on animal models of Parkinson's disease. *Mov. Disord.*, **26**, 993–1002.

Bonito-Oliva, A., Masini, D., & Fisone, G. (2014) A mouse model of non-motor symptoms in Parkinson's disease: focus on pharmacological interventions targeting affective dysfunctions. *Front. Behav. Neurosci.*, **8**, 290.

Bourdenx, M., Dovero, S., Engeln, M., Bido, S., Bastide, M.F., Dutheil, N., Vollenweider, I., Baud, L., Piron, C., Grouthier, V., Boraud, T., Porras, G., Li, Q., Baekelandt, V., Scheller, D., Michel, A., Fernagut, P.-O., Georges, F., Courtine, G., Bezard, E., & Dehay, B. (2015) Lack of additive role of ageing in nigrostriatal neurodegeneration triggered by α-synuclein overexpression. *Acta Neuropathol. Commun.*, **3**, 46.

Bourdy, R. & Barrot, M. (2012) A new control center for dopaminergic systems: pulling the VTA by the tail. *Trends Neurosci.*, **35**, 681–690.

Bourdy, R., Sánchez-Catalán, M.-J., Kaufling, J., Balcita-Pedicino, J.J., Freund-Mercier, M.-J., Veinante, P., Sesack, S.R., Georges, F., & Barrot, M. (2014) Control of the nigrostriatal dopamine neuron activity and motor function by the tail of the ventral tegmental area. *Neuropsychopharmacology*, **39**, 2788–2798.

Bové, J., Prou, D., Perier, C., & Przedborski, S. (2005) Toxin-induced models of Parkinson's disease. *NeuroRx.*, **2**, 484–494.

Cao, L.-F., Peng, X.-Y., Huang, Y., Wang, B., Zhou, F.-M., Cheng, R.-X., Chen, L.-H., Luo, W.-F., & Liu, T. (2016) Restoring Spinal Noradrenergic Inhibitory Tone Attenuates Pain Hypersensitivity in a Rat Model of Parkinson's Disease. *Neural Plast.*, **2016**, 6383240.

Carvalho, M.M., Campos, F.L., Coimbra, B., Pêgo, J.M., Rodrigues, C., Lima, R., Rodrigues, A.J., Sousa, N., & Salgado, A.J. (2013) Behavioral characterization of the 6-hydroxidopamine model of Parkinson's disease and pharmacological rescuing of non-motor deficits. *Mol. Neurodegener.*, **8**, 14.

Caudal, D., Alvarsson, A., Björklund, A., & Svenningsson, P. (2015) Depressive-like phenotype induced by AAV-mediated overexpression of human α-synuclein in midbrain dopaminergic neurons. *Exp. Neurol.*, **273**, 243–252.

Chaudhuri, K.R., Healy, D.G., Schapira, A.H.V., & National Institute for Clinical Excellence (2006) Non-motor symptoms of Parkinson's disease: diagnosis and management. *Lancet Neurol.*, **5**, 235–245.

Chen, C.-C.V., Shih, Y.-Y.I., & Chang, C. (2013) Dopaminergic imaging of nonmotor manifestations in a rat model of Parkinson's disease by fMRI. *Neurobiol. Dis.*, **49**, 99–106.

Dauer, W. & Przedborski, S. (2003) Parkinson's disease: mechanisms and models. *Neuron*, **39**, 889–909.

Dolatshahi, M., Farbood, Y., Sarkaki, A., Mansouri, S.M.T., & Khodadadi, A. (2015) Ellagic acid improves hyperalgesia and cognitive deficiency in 6-hydroxidopamine induced rat model of Parkinson's disease. *Iran. J. Basic Med. Sci.*, **18**, 38–46.

Faivre, F., Joshi, A., Bezard, E., & Barrot, M. (2018) The hidden side of Parkinson's disease: studying pain, anxiety and depression in pre-clinical models. *Neurosci Biobehav Rev*,.

Ferreira, J.G.P., Del-Fava, F., Hasue, R.H., & Shammah-Lagnado, S.J. (2008) Organization of ventral tegmental area projections to the ventral tegmental area-nigral complex in the rat. *Neuroscience*, **153**, 196–213.

Gantz, S.C., Ford, C.P., Morikawa, H., & Williams, J.T. (2018) The Evolving Understanding of Dopamine Neurons in the Substantia Nigra and Ventral Tegmental Area. *Annu. Rev. Physiol.*, **80**, 219–241.

Gauthier, J., Parent, M., Lévesque, M., & Parent, A. (1999) The axonal arborization of single nigrostriatal neurons in rats. *Brain Res.*, **834**, 228–232.

Gee, L.E., Chen, N., Ramirez-Zamora, A., Shin, D.S., & Pilitsis, J.G. (2015) The effects of subthalamic deep brain stimulation on mechanical and thermal thresholds in 6OHDA-lesioned rats. *Eur. J. Neurosci.*, **42**, 2061–2069.

German, D.C., Manaye, K., Smith, W.K., Woodward, D.J., & Saper, C.B. (1989) Midbrain dopaminergic cell loss in Parkinson's disease: computer visualization. *Ann. Neurol.*, **26**, 507–514.

Gómez-Paz, A., Drucker-Colín, R., Milán-Aldaco, D., Palomero-Rivero, M., & Ambriz-Tututi, M. (2017) Intrastriatal chromospheres' transplant reduces nociception in hemiparkinsonian rats. *Neuroscience*, **In press**.

Grossmann, W., Jurna, I., Nell, T., & Theres, C. (1973) The dependence of the anti-nociceptive effect of morphine and other analgesic agents on spinal motor activity after central monoamine depletion. *Eur. J. Pharmacol.*, **24**, 67–77.

Gubellini, P. & Kachidian, P. (2015) Animal models of Parkinson's disease: An updated overview. *Rev. Neurol.*, **171**, 750–761.

Hong, S., Jhou, T.C., Smith, M., Saleem, K.S., & Hikosaka, O. (2011) Negative reward signals from the lateral habenula to dopamine neurons are mediated by rostromedial tegmental nucleus in primates. *J. Neurosci.*, **31**, 11457–11471.

Ilkiw, J.L., Kmita, L.C., Targa, A.D.S., Noseda, A.C.D., Rodrigues, L.S., Dorieux, F.W.C., Fagotti, J., Dos Santos, P., & Lima, M.M.S. (2018) Dopaminergic Lesion in the Olfactory Bulb Restores Olfaction and Induces Depressive-Like Behaviors in a 6-OHDA Model of Parkinson's Disease. *Mol. Neurobiol.*, **In press.**

Jalabert, M., Bourdy, R., Courtin, J., Veinante, P., Manzoni, O.J., Barrot, M., & Georges, F. (2011) Neuronal circuits underlying acute morphine action on dopamine neurons. *Proc. Natl. Acad. Sci. U. S. A.*, **108**, 16446–16450.

Jhou, T.C., Fields, H.L., Baxter, M.G., Saper, C.B., & Holland, P.C. (2009a) The rostromedial tegmental nucleus (RMTg), a GABAergic afferent to midbrain dopamine neurons, encodes aversive stimuli and inhibits motor responses. *Neuron*, **61**, 786–800.

Jhou, T.C., Geisler, S., Marinelli, M., Degarmo, B.A., & Zahm, D.S. (2009b) The mesopontine rostromedial tegmental nucleus: A structure targeted by the lateral habenula that projects to the ventral tegmental area of Tsai and substantia nigra compacta. *J. Comp. Neurol.*, **513**, 566–596.

Jhou, T.C., Good, C.H., Rowley, C.S., Xu, S.-P., Wang, H., Burnham, N.W., Hoffman, A.F., Lupica, C.R., & Ikemoto, S. (2013) Cocaine drives aversive conditioning via delayed activation of dopamine-responsive habenular and midbrain pathways. *J. Neurosci.*, **33**, 7501–7512.

Jhou, T.C., Xu, S.-P., Lee, M.R., Gallen, C.L., & Ikemoto, S. (2012) Mapping of reinforcing and analgesic effects of the mu opioid agonist endomorphin-1 in the ventral midbrain of the rat. *Psychopharmacology (Berl.)*, **224**, 303–312.

Kamińska, K., Lenda, T., Konieczny, J., Czarnecka, A., & Lorenc-Koci, E. (2017) Depressive-like neurochemical and behavioral markers of Parkinson's disease after 6-OHDA administered unilaterally to the rat medial forebrain bundle. *Pharmacol. Rep. PR*, **69**, 985–994.

Kaufling, J. & Aston-Jones, G. (2015) Persistent Adaptations in Afferents to Ventral Tegmental Dopamine Neurons after Opiate Withdrawal. *J. Neurosci.*, **35**, 10290–10303.

Kaufling, J., Veinante, P., Pawlowski, S.A., Freund-Mercier, M.-J., & Barrot, M. (2009) Afferents to the GABAergic tail of the ventral tegmental area in the rat. *J. Comp. Neurol.*, **513**, 597–621.

Kaufling, J., Veinante, P., Pawlowski, S.A., Freund-Mercier, M.-J., & Barrot, M. (2010a) gamma-Aminobutyric acid cells with cocaine-induced DeltaFosB in the ventral tegmental area innervate mesolimbic neurons. *Biol. Psychiatry*, **67**, 88–92.

Kaufling, J., Waltisperger, E., Bourdy, R., Valera, A., Veinante, P., Freund-Mercier, M.-J., & Barrot, M. (2010b) Pharmacological recruitment of the GABAergic tail of the ventral tegmental area by acute drug exposure. *Br. J. Pharmacol.*, **161**, 1677–1691.

Lecca, S., Melis, M., Luchicchi, A., Ennas, M.G., Castelli, M.P., Muntoni, A.L., & Pistis, M. (2011) Effects of drugs of abuse on putative rostromedial tegmental neurons, inhibitory afferents to midbrain dopamine cells. *Neuropsychopharmacology*, **36**, 589–602.

Lecca, S., Melis, M., Luchicchi, A., Muntoni, A.L., & Pistis, M. (2012) Inhibitory inputs from rostromedial tegmental neurons regulate spontaneous activity of midbrain dopamine cells and their responses to drugs of abuse. *Neuropsychopharmacology*, **37**, 1164–1176.

Lin, M.T., Wu, J.J., Chandra, A., & Tsay, B.L. (1981) Activation of striatal dopamine receptors induces pain inhibition in rats. *J. Neural Transm.*, **51**, 213–222.

Lindner, M.D., Cain, C.K., Plone, M.A., Frydel, B.R., Blaney, T.J., Emerich, D.F., & Hoane, M.R. (1999) Incomplete nigrostriatal dopaminergic cell loss and partial reductions in striatal dopamine produce akinesia, rigidity, tremor and cognitive deficits in middle-aged rats. *Behav. Brain Res.*, **102**, 1–16.

Liu, K.-C., Li, J.-Y., Tan, H.-H., Du, C.-X., Xie, W., Zhang, Y.-M., Ma, W.-L., & Zhang, L. (2015) Serotonin$_6$ receptors in the dorsal hippocampus regulate depressive-like behaviors in unilateral 6-hydroxydopamine-lesioned Parkinson's rats. *Neuropharmacology*, **95**, 290–298.

Low, K.A., Miller, J., & Vierck, E. (2002) Response slowing in Parkinson's disease: a psychophysiological analysis of premotor and motor processes. *Brain J. Neurol.*, **125**, 1980–1994.

Luis-Delgado, O.E., Barrot, M., Rodeau, J.-L., Schott, G., Benbouzid, M., Poisbeau, P., Freund-Mercier, M.-J., & Lasbennes, F. (2006a) Calibrated forceps: a sensitive and reliable tool for pain and analgesia studies. *J. Pain*, **7**, 32–39.

Luis-Delgado, O.E., Barrot, M., Rodeau, J.-L., Schott, G., Benbouzid, M., Poisbeau, P., Freund-Mercier, M.-J., & Lasbennes, F. (2006b) Calibrated Forceps: A Sensitive and Reliable Tool for Pain and Analgesia Studies. *J. Pain*, **7**, 32–39.

Marsili, L., Rizzo, G., & Colosimo, C. (2018) Diagnostic Criteria for Parkinson's Disease: From James Parkinson to the Concept of Prodromal Disease. *Front. Neurol.*, **9**, 156.

Matheus, F.C., Rial, D., Real, J.I., Lemos, C., Takahashi, R.N., Bertoglio, L.J., Cunha, R.A., & Prediger, R.D. (2016) Temporal Dissociation of Striatum and Prefrontal Cortex Uncouples Anhedonia and Defense Behaviors Relevant to Depression in 6-OHDA-Lesioned Rats. *Mol. Neurobiol.*, **53**, 3891–3899.

Matsuda, W., Furuta, T., Nakamura, K.C., Hioki, H., Fujiyama, F., Arai, R., & Kaneko, T. (2009) Single nigrostriatal dopaminergic neurons form widely spread and highly dense axonal arborizations in the neostriatum. *J. Neurosci.*, **29**, 444–453.

Matsui, A. & Williams, J.T. (2011) Opioid-sensitive GABA inputs from rostromedial tegmental nucleus synapse onto midbrain dopamine neurons. *J. Neurosci.*, **31**, 17729–17735.

Mazzoni, P., Shabbott, B., & Cortés, J.C. (2012) Motor control abnormalities in Parkinson's disease. *Cold Spring Harb. Perspect. Med.*, **2**, a009282.

Morikawa, H. & Paladini, C.A. (2011) Dynamic regulation of midbrain dopamine neuron activity: intrinsic, synaptic, and plasticity mechanisms. *Neuroscience*, **198**, 95–111.

Nascimento, G.C., Bariotto-Dos-Santos, K., Leite-Panissi, C.R.A., Del-Bel, E.A., & Bortolanza, M. (2018) Nociceptive Response to L-DOPA-Induced Dyskinesia in Hemiparkinsonian Rats. *Neurotox. Res.*, **In press.**

Ogata, M., Noda, K., Akita, H., & Ishibashi, H. (2015) Characterization of nociceptive response to chemical, mechanical, and thermal stimuli in adolescent rats with neonatal dopamine depletion. *Neuroscience*, **289**, 43–55.

Park, A. & Stacy, M. (2009) Non-motor symptoms in Parkinson's disease. *J. Neurol.*, **256 Suppl 3**, 293–298.

Park, J., Lim, C.-S., Seo, H., Park, C.-A., Zhuo, M., Kaang, B.-K., & Lee, K. (2015) Pain perception in acute model mice of Parkinson's disease induced by 1-methyl-4-phenyl-1,2,3,6-tetrahydropyridine (MPTP). *Mol. Pain*, **11**, 28.

Paxinos, G. & Watson, C. (2014) *The Rat Brain in Stereotaxic Coordinates*. Academic Press.

Perrotta, A., Serrao, M., Bartolo, M., Valletta, L., Locuratolo, N., Pujia, F., Fattapposta, F., Bramanti, P., Amabile, G.A., Pierelli, F., & Parisi, L. (2005) Abnormal head nociceptive withdrawal reaction to facial nociceptive stimuli in Parkinson's disease. *Clin. Neurophysiol.*, **116**, 2091–2098.

Perrotti, L.I., Bolaños, C.A., Choi, K.-H., Russo, S.J., Edwards, S., Ulery, P.G., Wallace, D.L., Self, D.W., Nestler, E.J., & Barrot, M. (2005) DeltaFosB accumulates in a GABAergic cell population in the posterior tail of the ventral tegmental area after psychostimulant treatment. *Eur. J. Neurosci.*, **21**, 2817–2824.

Prensa, L. & Parent, A. (2001) The nigrostriatal pathway in the rat: A single-axon study of the relationship between dorsal and ventral tier nigral neurons and the striosome/matrix striatal compartments. *J. Neurosci.*, **21**, 7247–7260.

Saadé, N.E., Atweh, S.F., Bahuth, N.B., & Jabbur, S.J. (1997) Augmentation of nociceptive reflexes and chronic deafferentation pain by chemical lesions of either dopaminergic terminals or midbrain dopaminergic neurons. *Brain Res.*, **751**, 1–12.

Sakai, K. & Gash, D.M. (1994) Effect of bilateral 6-OHDA lesions of the substantia nigra on locomotor activity in the rat. *Brain Res.*, **633**, 144–150.

Sánchez-Catalán, M.-J., Faivre, F., Yalcin, I., Muller, M.-A., Massotte, D., Majchrzak, M., & Barrot, M. (2017) Response of the Tail of the Ventral Tegmental Area to Aversive Stimuli. *Neuropsychopharmacology*, 638–648.

Sanchez-Catalan, M.J., Kaufling, J., Georges, F., Veinante, P., & Barrot, M. (2014) The antero-posterior heterogeneity of the ventral tegmental area. *Neuroscience*, **282**, 198–216.

Santana, M., Palmér, T., Simplício, H., Fuentes, R., & Petersson, P. (2015) Characterization of long-term motor deficits in the 6-OHDA model of Parkinson's disease in the common marmoset. *Behav. Brain Res.*, **290**, 90–101.

Santiago, R.M., Barbieiro, J., Lima, M.M.S., Dombrowski, P.A., Andreatini, R., & Vital, M.A.B.F. (2010) Depressive-like behaviors alterations induced by intranigral MPTP, 6-OHDA, LPS and rotenone models of Parkinson's disease are predominantly associated with serotonin and dopamine. *Prog. Neuropsychopharmacol. Biol. Psychiatry*, **34**, 1104–1114.

Santiago, R.M., Barbiero, J., Gradowski, R.W., Bochen, S., Lima, M.M.S., Da Cunha, C., Andreatini, R., & Vital, M.A.B.F. (2014) Induction of depressive-like behavior by intranigral 6-OHDA is directly correlated with deficits in striatal dopamine and hippocampal serotonin. *Behav. Brain Res.*, **259**, 70–77.

Silva, T.P. da, Poli, A., Hara, D.B., & Takahashi, R.N. (2016) Time course study of microglial and behavioral alterations induced by 6-hydroxydopamine in rats. *Neurosci. Lett.*, **622**, 83–87.

Stamatakis, A.M. & Stuber, G.D. (2012) Activation of lateral habenula inputs to the ventral midbrain promotes behavioral avoidance. *Nat. Neurosci.*, **15**, 1105–1107.

Tadaiesky, M.T., Dombrowski, P.A., Figueiredo, C.P., Cargnin-Ferreira, E., Da Cunha, C., & Takahashi, R.N. (2008) Emotional, cognitive and neurochemical alterations in a premotor stage model of Parkinson's disease. *Neuroscience*, **156**, 830–840.

Takeda, R., Ishida, Y., Ebihara, K., Abe, H., Matsuo, H., Ikeda, T., Koganemaru, G., Kuramashi, A., Funahashi, H., Magata, Y., Kawai, K., & Nishimori, T. (2014) Intrastriatal grafts of fetal ventral mesencephalon improve allodynia-like withdrawal response to mechanical stimulation in a rat model of Parkinson's disease. *Neurosci. Lett.*, **573**, 19–23.

Ungerstedt, U. (1968) 6-Hydroxy-dopamine induced degeneration of central monoamine neurons. *Eur. J. Pharmacol.*, **5**, 107–110.

Vecchia, D.D., Kanazawa, L.K.S., Wendler, E., de Almeida Soares Hocayen, P., Bruginski, E., Campos, F.R., Stern, C.A.J., Vital, M.A.B.F., Miyoshi, E., Wöhr, M., Schwarting, R.K.W., & Andreatini, R. (2018) Effects of ketamine on vocal impairment, gait changes, and anhedonia induced by bilateral 6-OHDA infusion into the substantia nigra pars compacta in rats: Therapeutic implications for Parkinson's disease. *Behav. Brain Res.*, **342**, 1–10.

Vingill, S., Connor-Robson, N., & Wade-Martins, R. (2017) Are rodent models of Parkinson's disease behaving as they should? *Behav. Brain Res.*, **In press**.

Wang, C.-T., Mao, C.-J., Zhang, X.-Q., Zhang, C.-Y., Lv, D.-J., Yang, Y.-P., Xia, K.-L., Liu, J.-Y., Wang, F., Hu, L.-F., Xu, G.-Y., & Liu, C.-F. (2017) Attenuation of hyperalgesia responses via the modulation of 5-hydroxytryptamine signalings in the rostral ventromedial medulla and spinal cord in a 6-hydroxydopamine-induced rat model of Parkinson's disease. *Mol. Pain*, **13**, 1744806917691525.

White, N.M. (1997) Mnemonic functions of the basal ganglia. *Curr. Opin. Neurobiol.*, **7**, 164–169.

White, N.M. & McDonald, R.J. (2002) Multiple parallel memory systems in the brain of the rat. *Neurobiol. Learn. Mem.*, **77**, 125–184.

Yalcin, I., Charlet, A., Freund-Mercier, M.-J., Barrot, M., & Poisbeau, P. (2009) Differentiating Thermal Allodynia and Hyperalgesia Using Dynamic Hot and Cold Plate in Rodents. *J. Pain*, **10**, 767–773.

Zengin-Toktas, Y., Ferrier, J., Durif, F., Llorca, P.-M., & Authier, N. (2013) Bilateral lesions of the nigrostriatal pathways are associated with chronic mechanical pain hypersensitivity in rats. *Neurosci. Res.*, **76**, 261–264.

FIGURE LEGENDS

FIG. 1. Motor performance in the rotarod task after bilateral SNc and/or tVTA lesion. Animal underwent SNc lesion (6-OHDA) and/or tVTA excitotoxic lesion (ibotenic acid). 7 to 10 days after the lesion, motor performance was tested in the rotarod test. (A) Histological evidence for bilateral SNc and tVTA lesion with TH and NeuN immunostaining. Scale bars, TH images = 1 mm; NeuN images = 200 µm. (B) Latency to fall is modified in animals with SNc or tVTA lesion but not in animals with concomitant bilateral SNc/tVTA lesion. (C) Distribution of latency to fall for the third test day. Values are presented as mean ± SEM. (*, $P<0.05$; **, $P<0.01$; ***, $P<0.005$). The number of animals is given between brackets. Scatter plots indicate individual data points. Abbreviation: NeuN = Neuronal Nuclei; SNc = Substantia nigra *pars compacta*; TH = Tyrosine hydroxylase; tVTA = tail of the ventral tegmental area.

FIG. 2. Effect of bilateral SNc lesion with 6-hydroxydopamine (6-OHDA) on motor and non-motor symptoms in rats. Animals underwent SNc lesion (6-OHDA) and consequences were tested on motor (rotarod) and non-motor symptoms (body weight, digital forceps, tail flick, hot plate, dynamic hot plate and sucrose preference). (A) A bilateral partial lesion of the SNc led to a partial lesion of the striatum. Scale bars, 1 mm. (B) SNc lesioned animals displayed motor deficits at the highest speed in the rotarod task. (C) The body weight of SNc lesioned animals remained lower than sham animals along the experiment. (D) SNc lesioned animals had a lower mechanical nociceptive threshold in a digital forceps test. (E) SNc lesioned animals showed a slowdown of the withdrawal response in the tail flick test but not in the classical hot plate test (F). (G) In a dynamic hot plate test, SNc lesion animals respond to lower temperature than sham animals at 5 and 14 weeks post-surgery (left panel). Likewise, lesion animals have higher number of nociceptive responses at normally non-nociceptive temperatures than control animals (right panel). (H) In a two-bottle-choice paradigm, lesioned animals showed a lower preference to sucrose solution (1%) compared to sham animals at 4 and 13 weeks after surgery (left panel). They also showed a decrease in sucrose consumption volume at 3, 5 and 13 weeks (middle panel) but not in water volume (right panel). The number of animals is given between brackets. Values are presented as mean ± SEM. (*, $P < 0.05$; **, $P < 0.01$; ***; $P < 0.005$).

FIG. 3. Effect of bilateral tVTA lesion on non-motor symptoms in a model of Parkinson's disease. Animal underwent SNc lesion (6-OHDA) and/or tVTA excitotoxic lesion (ibotenic acid). The impact was studied on body weight, on nociceptive response to digital forceps and

in the sucrose preference test. (A) The body weight of SNc lesioned animals remained lower than other groups along the experiment. Animal with SNc and tVTA lesions showed similar body weight as control animals. (B) SNc lesioned animals showed lower mechanical nociceptive thresholds in the digital forceps test at all considered time points, which was compensated by concomitant lesion of the tVTA. (C) SNc lesioned animals showed a lower preference to sucrose compared to sham animals at 5 weeks after surgery (left panel), and a tendency to decreased overall sucrose (middle panel) but not water (right panel) consumption. As for other modalities, the tVTA bilateral lesion compensated sucrose preference in 6-OHDA lesioned animals. The number of animals is given between brackets. Values are presented as mean ± SEM. (*, $P < 0.05$; **, $P < 0.01$; ***; $P < 0.005$).

FIG. 1.

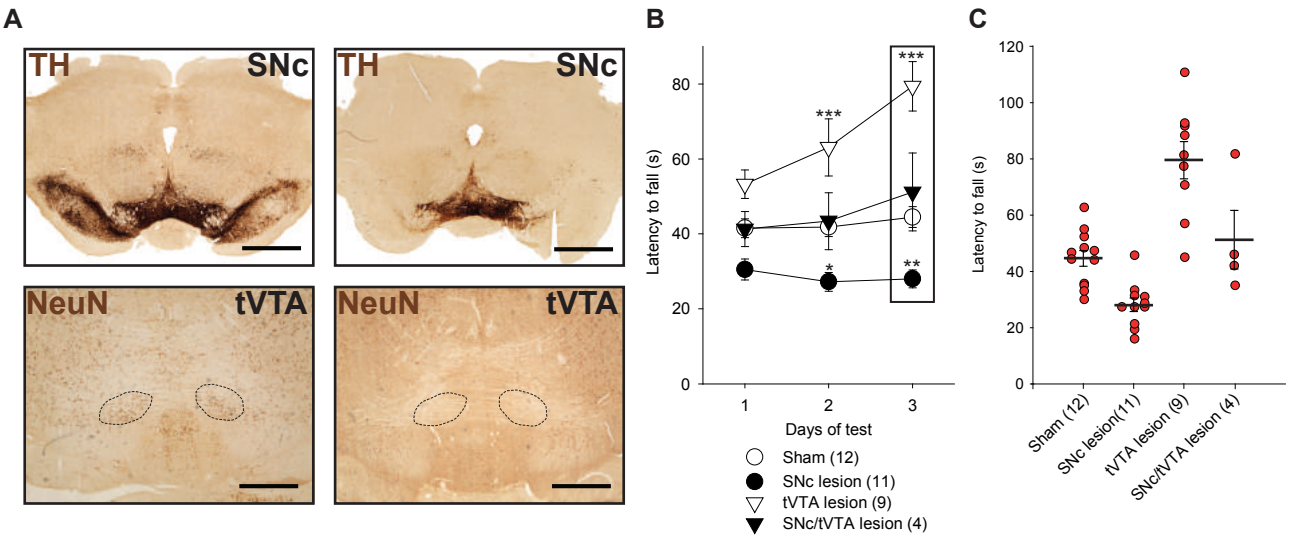
A
TH
SNc
TH
SNc
NeuN
tVTA
NeuN
tVTA
B
Latency to fall (s)
0
20
40
60
80
***
***
*
**
1
2
3
Days of test
Sham (12)
SNc lesion (11)
tVTA lesion (9)
SNc/tVTA lesion (4)
C
Latency to fall (s)
0
20
40
60
80
100
120
Sham (12)
SNc lesion(11)
tVTA lesion (9)
SNc/tVTA lesion (4)

FIG. 2.

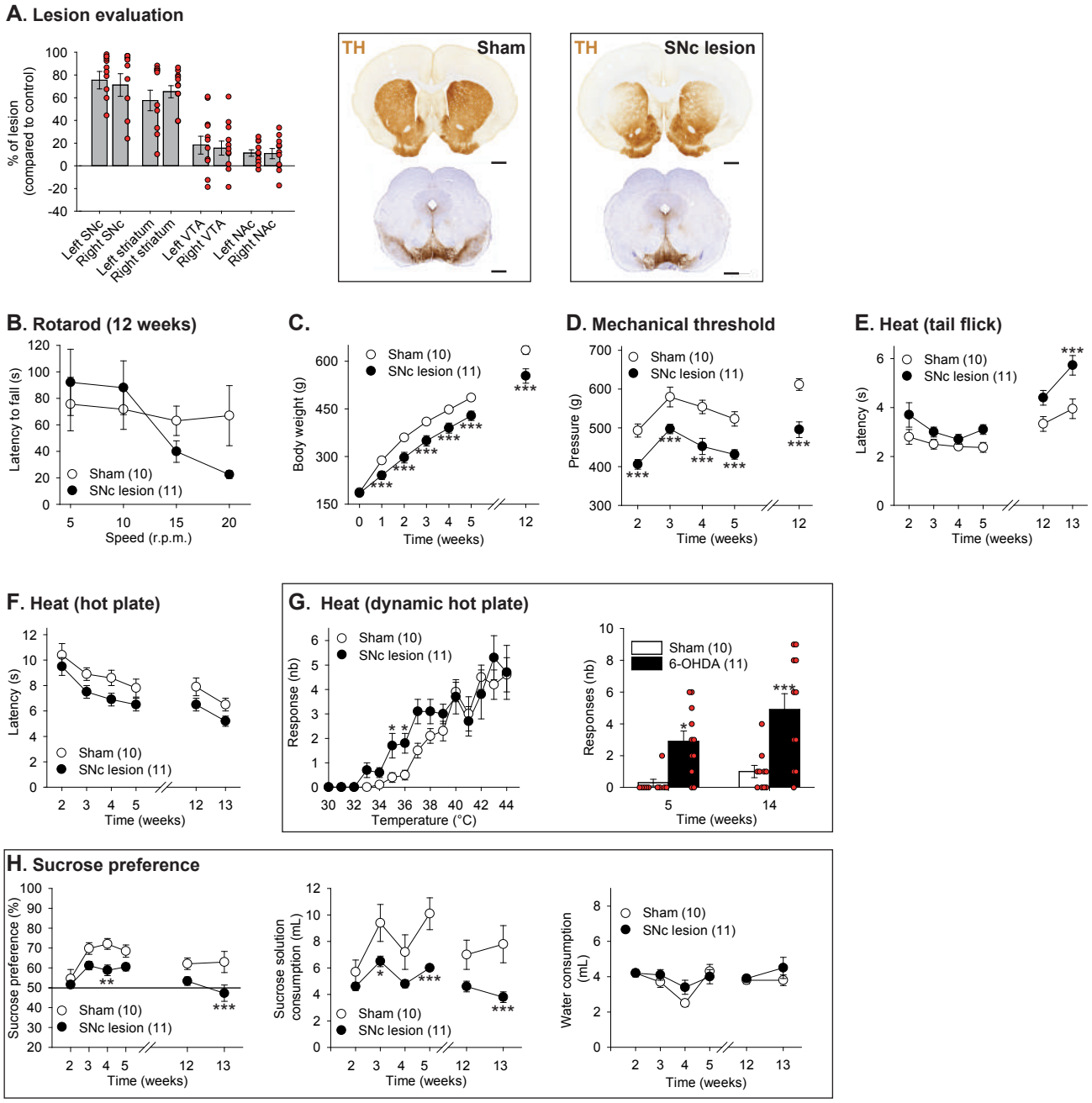
A. Lesion evaluation
% of lesion (compared to control)
Left SNc
Right SNc
Left striatum
Right striatum
Left VTA
Right VTA
Left NAc
Right NAc
TH
Sham
SNc lesion
B. Rotarod (12 weeks)
Latency to fall (s)
Speed (r.p.m.)
Sham (10)
SNc lesion (11)
C.
Body weight (g)
Time (weeks)
D. Mechanical threshold
Pressure (g)
E. Heat (tail flick)
Latency (s)
F. Heat (hot plate)
G. Heat (dynamic hot plate)
Response (nb)
Temperature (°C)
6-OHDA (11)
Responses (nb)
H. Sucrose preference
Sucrose preference (%)
Sucrose solution consumption (mL)
Water consumption (mL)

FIG. 3

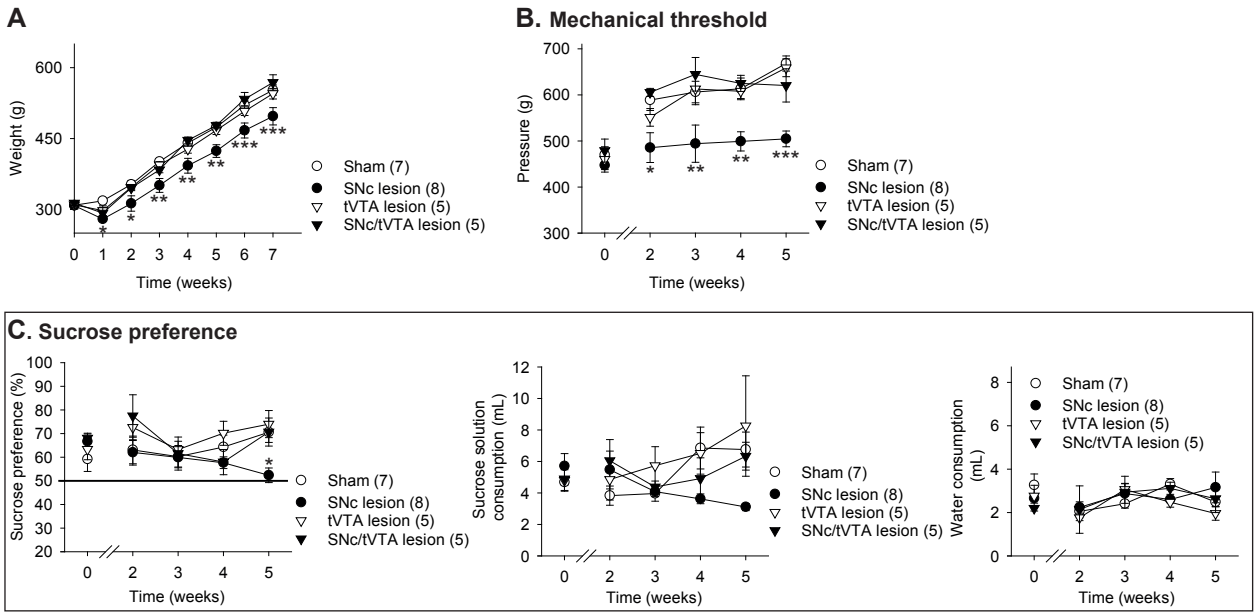
A
Weight (g)
600
450
300
0 1 2 3 4 5 6 7
Time (weeks)
Sham (7)
SNc lesion (8)
tVTA lesion (5)
SNc/tVTA lesion (5)
B. Mechanical threshold
Pressure (g)
700
600
500
400
300
0 2 3 4 5
Time (weeks)
Sham (7)
SNc lesion (8)
tVTA lesion (5)
SNc/tVTA lesion (5)
C. Sucrose preference
Sucrose preference (%)
100 90 80 70 60 50 40 30 20
0 2 3 4 5
Time (weeks)
Sham (7)
SNc lesion (8)
tVTA lesion (5)
SNc/tVTA lesion (5)
Sucrose solution consumption (mL)
12 10 8 6 4 2 0
0 2 3 4 5
Time (weeks)
Sham (7)
SNc lesion (8)
tVTA lesion (5)
SNc/tVTA lesion (5)
Water consumption (mL)
8 6 4 2 0
0 2 3 4 5
Time (weeks)
Sham (7)
SNc lesion (8)
tVTA lesion (5)
SNc/tVTA lesion (5)

DISCUSSION GENERALE

Les travaux réalisés durant cette thèse nous ont tout d'abord permis de vérifier que les différentes définitions de la tVTA utilisées dans la littérature désignaient bien une seule et même structure. Ainsi la définition neurochimique se fondant sur les marquages NeuN, Fos, GAD et MOPR montre une structure de forme et de localisation identique dans la zone mésencéphalo-pontique. Cette définition neurochimique et la définition hodologique fondée sur les connexions de la LHb avec la tVTA ne sont pas totalement concordantes, les fibres issues de la LHb étant divisées en deux zones, une zone riche en fibres et une zone avec une densité de fibres plus faible. Enfin, l'étude de séquençage d'ARN nous a permis de mettre en évidence une population de gènes enrichis dans cette structure et donc de fournir une première définition génomique de la tVTA.

D'un point de vue fonctionnel, l'étude de la réponse de la tVTA à une grande variété de stimuli aversifs, tant chimiques que physiques, nous a permis de déterminer que la tVTA n'était pas indispensable à la réponse à tous ces stimuli aversifs.

Enfin, la dernière étude présentée dans cette thèse a permis de montrer qu'une co-lésion de la tVTA dans un modèle de maladie de Parkinson entraînait un rétablissement des performances motrices, un retour des seuils nociceptifs à un niveau basal et une diminution des symptômes de type dépressifs.

Certains aspects des résultats sont discutés dans les articles présentés avant, nous ne reviendrons donc pas dessus dans cette discussion générale. Nous reprendrons ici trois grandes questions laissées en suspens : 1) comment peut-on définir une structure et donc comment peut-on définir la tVTA, 2) l'approche lésionnelle utilisée dans notre étude sur l'influence de la tVTA dans les symptômes de la maladie de Parkinson est-elle la meilleure approche ? et enfin 3) la place de la tVTA dans l'évolution et sa découverte chez l'Homme. A l'issue de cette discussion, nous dégagerons les perspectives ouvertes par nos travaux.

A. Définition cytoarchitecturale

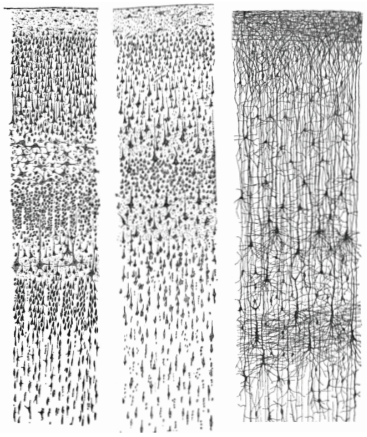

B. Définition neurochimique

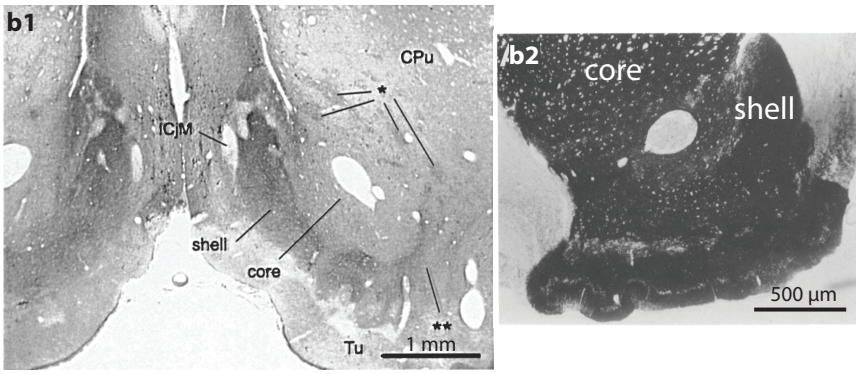

C. Définition neurochimique et hodologique

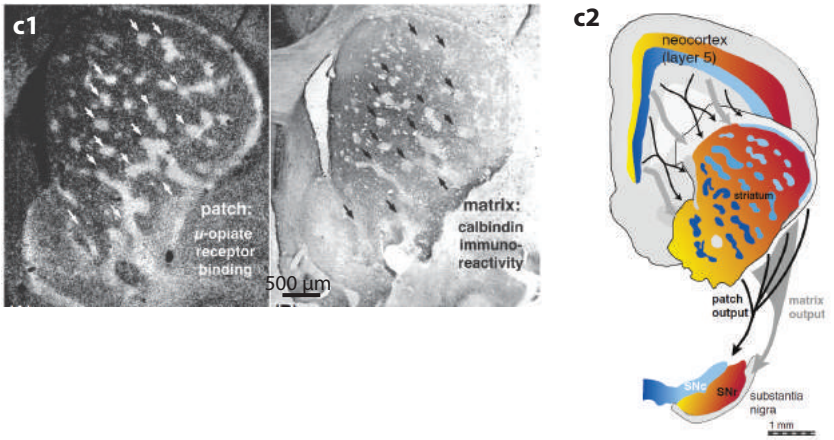

D. Définition fonctionnelle

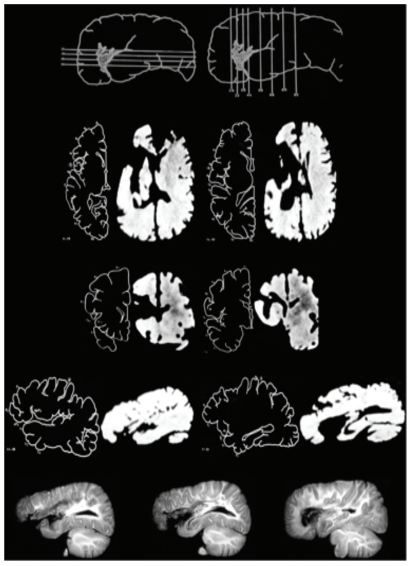

Figure 12. Comment définir une structure ? (A) Représentation des couches du cortex cérébral par Ramon-Y-Cajal après visualisation des neurones par la méthode de Golgi (Ramon-Y-Cajal, 1909). (B) Séparation du coeur et de la coquille du noyau accumbens par leur composition neurochimique. Ainsi, la coquille du noyau accumbens exprime plus fortement la calrétinine (b1) (Zahm, 1999) et l'acétylcholinestérase (b2) (adaptée de Zaborszky et al., 1985) que le coeur. (C) Les patchs ou striosomes du noyau accumbens sont riches en récepteur μ des opioïdes (image en couleurs inversées) alors que la matrice exprime plus fortement la calbindine (c1). Les patchs reçoivent des afférences de la couche 5 du cortex prélimbique et projettent à la substance noire compacte alors que la matrice reçoit des afférences des aires corticales sensorielle et motrice et projette à la substance noire réticulée (c2) (Dudman et Gerfen, 2015). (D) Images radiologiques du cerveau de Leborgne, le patient aphasique observé par Broca. Ce patient présentait une lésion du lobe frontal gauche, s'étendant également médialement, affectant le ganglion basal gauche et l'insula (Dronkers et al., 2007).

A. Quelle définition pour la tVTA ?

a1. Comment peut-on définir une structure ?

Il n'existe pas de vrai consensus quant à la façon de définir une structure cérébrale. Ainsi, une structure peut avoir une définition fondée sur la morphologie de ses cellules et leur organisation au sein de la structure (cytoarchitecture), sur la nature des protéines ou neuromessagers qu'elle contient (neurochimie), les ARNm qu'elle exprime (génomique), sur son origine développementale, sur sa connectivité ou encore sur les fonctions qu'elle exerce. Ainsi, avant de donner une définition de la tVTA, il me paraît important de montrer l'apport de ces différentes définitions en neuroanatomie.

Une des premières possibilités utilisées pour définir une structure est sa **cytoarchitecture**. La cytoarchitecture désigne la composition cellulaire d'un tissu cérébral mais aussi son organisation cellulaire (couches, densité, granulosité). Historiquement, c'est par des méthodes cytoarchitecturales que la morphologie des neurones a été mise en évidence pour la première fois. La coloration argentique dite de Golgi, découverte en 1873, est une méthode se basant sur l'imprégnation du tissu par un bain de nitrate d'argent (Pannese, 1999). Ainsi, la coloration de Golgi a permis à Ramón y Cajal de suivre un neurone et ses projections mais également de visualiser des types neuronaux différents (Ramon-y-Cajal, 1909; Pannese, 1999). Un des inconvénients majeurs de cette méthode est qu'elle est peu reproductible et ne met en évidence qu'une partie des neurones (Kang et al., 2017). Une autre méthode permettant d'étudier la morphologie neuronale est la méthode de coloration de Nissl. Cette méthode consiste à utiliser des colorants basiques, tels que le bleu de méthylène ou plus communément le crésyl violet, qui vont interagir avec les acides nucléiques présents notamment dans le réticulum endoplasmique des neurones (Kádár et al., 2009). Ces diverses méthodes, encore utilisées aujourd'hui, ont permis d'introduire des révolutions majeures en matière de composition et d'organisation neuronales. Ainsi, la description du cortex cérébral et de son organisation en couche a été rendu possible grâce à ces méthodes (Brodmann, 1909; von Economo and Koskinas, 1925) et les atlas utilisent encore la coloration de Nissl afin de visualiser les différentes structures cérébrales (Paxinos and Watson, 2014) (Figure 12A).

Une deuxième façon de définir une structure consiste à la définir en fonction de sa **neurochimie** c'est-à-dire en fonction de marqueurs que la structure exprime tels que, entre autre, des neurotransmetteurs. Par exemple, la notion de cœur (« core ») et coquille (« shell ») du noyau accumbens a émergée à la suite de l'observation de différences morphologiques et

neurochimiques entre ces deux zones du noyau accumbens (Herkenham et al., 1984; Záborszky et al., 1985). Ainsi le « shell » montre une immunoréactivité plus importante que le « core » pour le récepteur 5-HT_4 de la sérotonine, le récepteur D3 de la dopamine, la calrétinine (Zahm, 1999) ou encore l'acétylcholinestérase (Herkenham et al., 1984; Záborszky et al., 1985). A l'inverse, le « core » exprime plus fortement la calbindine-D 28 kDa, l'enképhaline, la cholécystokinine (CCK8) et des sous-unités du récepteur GABA-A (Záborszky et al., 1985; Zahm, 1999) (Figure 12B).

Avec le développement des méthodes de traçage neuronal, la **connectivité** a également été utilisée pour définir des structures, souvent en complément de la neurochimie. Ainsi, la notion de patch/matrice du striatum a été mise en évidence via sa connectivité parallèlement à sa neurochimie. En se basant sur les données neurochimiques, il a été montré que les récepteurs µ des opioïdes se situent préférentiellement dans des îlots nommés patchs ou striosomes (Herkenham and Pert, 1981) alors que la matrice, pauvre en récepteur µ des opioïdes, montre une forte activité de l'acetylcholinestérase (Graybiel and Ragsdale, 1978; Herkenham and Pert, 1981). L'étude hodologique a ensuite montré que ces patchs reçoivent des informations préférentiellement de la couche 5 du cortex prélimbique et projettent à la substance noire *pars compacta* alors que la matrice reçoit des afférences des aires corticales sensorielle et motrice et projette à la substance noire *pars reticulata*, (Gerfen, 1984, 1985; Jiménez-Castellanos and Graybiel, 1989; Dudman and Gerfen, 2015) montrant ainsi deux compartiments bien distincts en terme de neurochimie et de connectivité (Figure 12C).

Il apparait évident aujourd'hui qu'une autre définition de structures peut être en lien avec la **fonction** qu'elle exerce. Cette association structure/fonction est très ancienne comme le montre la découverte des fonctions des différentes régions corticales. Ainsi, c'est en 1861 que Paul Broca a mis en évidence une « aire du langage » dite aire de Broca, dans le lobe frontal d'un patient atteint d'aphasie (pour revue: Dronkers et al., 2007) (Figure 12D). Durant la même période, Fritsch et Hitzig ont montré qu'une stimulation électrique du cortex cérébral du chien entrainait la production d'un mouvement, mettant ainsi en évidence l'existence d'un cortex moteur (Gross, 2007). C'est par ces études princeps que la notion d'aire corticale associée à une fonction a été découverte.

Enfin, il apparaît également évident que l'aspect **génomique** est important pour affiner la définition d'une structure cérébrale. Ainsi l'Allen Brain Atlas permet de visualiser l'expression d'ARNm dans des structures cérébrales particulières tant sur un cerveau mature que lors de son développement (http://www.brain-map.org/).

Ces diverses études mènent donc à envisager une structure par différentes caractéristiques mais il est important de noter qu'une structure n'est pas uniquement définie par une seule de ses définitions mais que c'est bien en les considérant toutes dans leur ensemble qu'une vision globale de la structure pourra être donnée.

a2. De la définition de la VTA à la découverte de la tVTA

La première définition connue de la VTA est une définition **cytoarchitecturale**, montrant par coloration de Nissl et de Golgi un groupe de cellules nommé « nucleus tegmenti ventralis », groupe auparavant décrit comme appartenant à la substance noire (Tsai, 1925; Oades and Halliday, 1987). Cette structure est composée de cellules fusiformes comme celles de la substance noire mais plus petites et anatomiquement séparées de celle-ci (Tsai, 1925). Cette distinction entre la VTA et la substance noire est également bien visible au regard des **aspects développementaux et génomiques** puisque les neurones dopaminergiques de la VTA et de la SNc montrent une différence d'expression de certains précurseurs. C'est le cas par exemple du facteur de transcription OTX2 (orthodenticle homeobox 2) exprimé spécifiquement dans une sous-population postéro-médiale de la VTA, ou encore de la ALDH1A1 (une aldéhyde deshydrogénase) exprimée uniquement dans les neurones de la SNc (Subramaniam and Roeper, 2016). C'est aussi le cas du facteur de transcription *Pitx3*, exprimé exclusivement dans les neurones dopaminergiques du mésencéphale et conduisant à leur différenciation et leur survie, dont la quantité est 6 fois plus importante dans la VTA que dans la SNc (Korotkova et al., 2005). D'un autre côté, ce sont des études de traçage réalisées notamment par Nauta qui ont permis de montrer que la VTA n'était pas une sous-structure de la substance noire mais bien une structure à part entière, présentant des **connexions** qui lui sont propres (Nauta, 1958; Ikemoto, 2007). D'un point de vue **neurochimique**, la VTA est souvent considérée comme correspondant à l'aire A10 dopaminergique. Cette aire, identifiée à l'aide de la technique d'histofluorescence au formaldéhyde, a été définie comme étant riche en catécholamines (Dahlström and Fuxe, 1964). L'introduction des études immunohistochimiques quelques années plus tard permettra de préciser la nature des neurones constituant cette aire A10 en montrant l'enrichissement en tyrosine hydroxylase (Björklund and Dunnett, 2007). La VTA contient au moins trois types neuronaux différents : des neurones dopaminergiques (≈ 65%) (Yetnikoff et al., 2014), très hétérogènes des points de vue électrophysiologiques (Morales and Margolis, 2017) et fonctionnels (Bromberg-Martin et al., 2010) ; des neurones GABAergiques

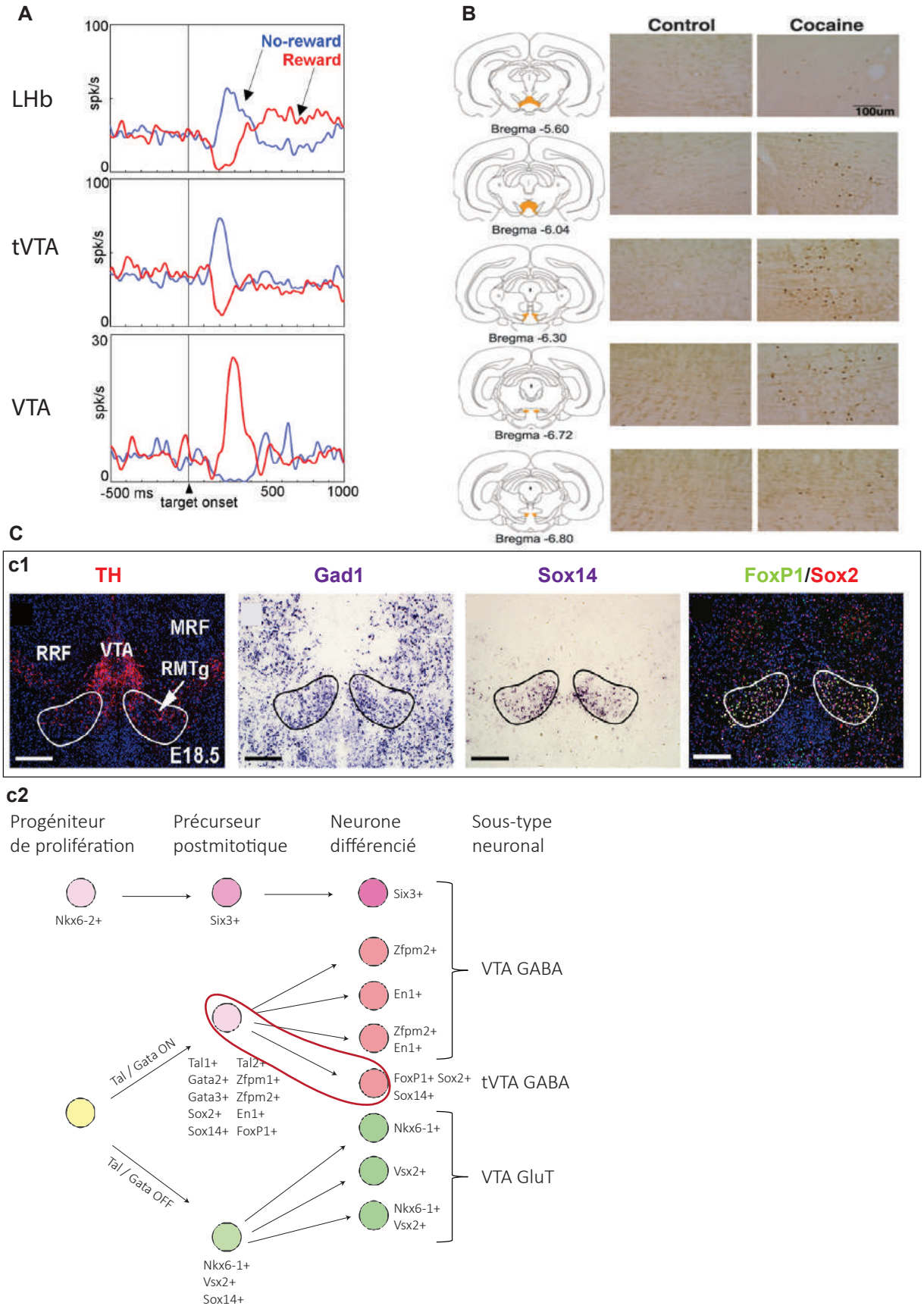

Figure 13. La tVTA, une structure à part entière. (A) Les neurones de la LHb et de la tVTA sont activés après la présentation d'un signal prédisant une absence de récompense (bleu) et sont inhibés par un signal prédisant l'arrivée d'une récompense (rouge). A l'inverse, les neurones de la VTA présentent des réponses opposées (Hong et al., 2011). (B) La tVTA est recrutée après une injection de cocaïne alors que la VTA ne présente que peu de marquage (Perrotti et al., 2015). (C) Lors du développement, les neurones qui formeront la tVTA expriment Gad1, Sox 14, Sox 2 et FoxP1 (c1). De plus, les précurseurs neuronaux des neurones GABAergiques de la tVTA et ceux de la VTA ne sont pas issus des mêmes précurseurs (entourés en rouge) (c2) (Lahti et al., 2016).

(≈ 30%) dont la composition est également hétérogène (Yetnikoff et al., 2014; Morales and Margolis, 2017) et des neurones glutamatergiques (≈ 5%) (Yetnikoff et al., 2014) exprimant des ARN messagers codant pour le transporteur du glutamate VGLUT2 (Hnasko et al., 2012; Morales and Root, 2014; Morales and Margolis, 2017). Enfin, la VTA est définie, d'un point de vue **fonctionnel**, comme une structure clé dans les comportements adaptatifs, motivés, de récompense, dans l'humeur mais aussi dans de nombreuses pathologies psychiatriques (Bromberg-Martin et al., 2010).

La VTA présente une forte hétérogénéité selon son axe antéro-postérieur, tant d'un point de vue fonctionnel (dans la réponse à certaines drogues par exemple) (Olson et al., 2005; Sanchez-Catalan et al., 2014) que neurochimique, les neurones dopaminergiques étant majoritaires dans le tiers médian de la VTA (Olson et al., 2005). Ces différences ont ainsi permis de définir deux compartiments dans la VTA : la VTA antérieure ou rostrale (aVTA) et la VTA postérieure ou caudale (pVTA). La limite entre ces deux sous-régions, définie entre autre selon qu'elle entraîne ou non un conditionnement de place après administration de cocaïne, se situe à environ -5.5 mm du bregma chez le rat (Olson et al., 2005).

La distinction de la tVTA comme une structure à part entière a longtemps été ignorée. Ainsi, nous pouvons considérer que la première définition de la tVTA, bien qu'encore intégrée à la VTA, a été fournie par des **études fonctionnelles**. En effet, ces études ont montré que la tVTA était préférentiellement recrutée lors de l'administration de drogues psychostimulantes (Scammell et al., 2000; Perrotti et al., 2005). Dans une vue antéro-postérieure, l'apparition de FosB/ΔFosB dans une région directement postérieure à la pVTA a permis de nommer cette structure tVTA. De plus, les études de traçage des afférences de la LHb par Herkenham et Nauta (1979) avaient déjà mis en évidence une région dont nous savons aujourd'hui qu'elle correspond pour partie à la tVTA.

La question restant à élucider était de savoir si la tVTA était bien une structure à part entière ou bien une sous-région de la VTA. L'analyse des afférences de la tVTA montrent que celles-ci sont issues des mêmes régions que celles de la VTA (Kaufling et al., 2009), mais que les efférences sont bien différentes (Kaufling et al., 2010a). De plus, bien qu'une projection directe de la LHb vers la VTA ait été confirmée (Herkenham and Nauta, 1979; Araki et al., 1988; Kim, 2009), il parait désormais évident que la tVTA est un relai majeur entre la LHb et la VTA, comme le montre le parallélisme de réponse de la LHb et de la tVTA dans le traitement des erreurs de prédiction de récompense (Matsumoto and Hikosaka, 2007; Hong et al., 2011; Tian et al., 2016) (Figure 13A). Le deuxième argument tendant à montrer que la tVTA est bien une

structure à part entière est son activation après l'administration de drogues psychostimulantes. En effet, une injection de cocaïne induit l'apparition de Fos dans la tVTA sans activation de la VTA (Perrotti et al., 2005; Kaufling et al., 2010a, 2010b) (Figure 13B). Enfin le dernier argument permettant de montrer que les définitions de la tVTA et de la VTA sont bien distinctes est la définition développementale de ces structures. Il a en effet été récemment montré que les neurones GABAergiques de la VTA et ceux de la tVTA sont issus de progéniteurs bien distincts (Lahti et al., 2016) (Figure 13C).

a3. Vers une définition universelle de la tVTA ?

Avec la multiplication des études concernant la tVTA, il est maintenant important de donner une définition de cette structure qui pourra servir de référence dans les études à venir et permettra enfin d'inclure cette structure dans les atlas de référence. En effet, la tVTA n'est pas encore répertoriée dans ces atlas mais pourrait, en partie postérieure, correspondre au noyau interstitiel de la décussation du pédoncule cérebelleux supérieur (planches 89 à 92 de l'atlas de Paxinos et Watson *(*Paxinos and Watson, 2014)). Dans ce paragraphe, je vais donc donner différents arguments qui m'ont permis de forger une définition de la tVTA. Chez le rat, la **définition neurochimique** de la tVTA, en premier lieu, semble permettre de bien la distinguer des structures avoisinantes. Ainsi, la tVTA est une structure majoritairement GABAergique et dont de nombreux neurones expriment également le récepteur μ des opioïdes (Olson and Nestler, 2007; Jhou et al., 2009a, 2009b, Kaufling et al., 2009, 2010a; Jalabert et al., 2011; Jhou et al., 2012; Kaufling and Aston-Jones, 2015; Yetnikoff et al., 2015; Wasserman et al., 2016). De plus, elle est souvent définie comme le frein inhibiteur majeur des neurones dopaminergiques du mésencéphale, la **connectivité** entre la tVTA et la VTA/SNc semblant donc être un deuxième point permettant d'en obtenir une bonne définition (Kaufling et al., 2010a; Balcita-Pedicino et al., 2011; Bourdy et al., 2014). La connexion de la LHb avec la tVTA peut également être un bon moyen de définir la tVTA. Il faudra néanmoins considérer cette définition avec prudence au vu des résultats de notre étude montrant une différence de densité de fibres dans la zone de la tVTA telle que définie par l'induction des protéines Fos. Considérer la voie LHb-tVTA-VTA, et donc utiliser des approches de traçage réciproques, pourrait néanmoins aboutir à une définition assez précise de la tVTA et pourrait être utilisé dans d'autres espèces de laboratoire comme la souris par exemple. Enfin, les récentes découvertes concernant l'**aspect développemental** de cette structure laissent à penser qu'une définition

précise de la tVTA pourrait être obtenue à l'aide du marqueur Sox14, déjà défini dans la littérature comme étant un précurseur spécifique des neurones GABA de la tVTA chez la souris (Lahti et al., 2016) et apparaissant comme très enrichi par rapport au cerveau complet dans notre étude de séquençage d'ARN. Les études futures en RNAscope nous permettront de vérifier ce résultat et de l'utiliser pour définir la tVTA dans d'autres espèces animales.

Bien que les facteurs de transcription de la famille Fos et donc **l'aspect fonctionnel**, mettent en évidence de façon nette les contours de la tVTA chez le rat, le fait que cette induction n'apparaisse pas (Barrot et al., 2016) ou peu (Lahti et al., 2016) chez la souris n'en fait, selon moi, pas une définition suffisamment universelle pour être étendue à d'autres espèces. Enfin, au vu des nombreuses fonctions que la littérature attribue à la tVTA (réponse aux drogues psychostimulantes, réponse aux stimuli aversifs, erreurs de prédiction de récompense, contrôle moteur et enfin sommeil), la **définition fonctionnelle** de la tVTA semble trop complexe et vaste pour permettre d'en faire une donnée universelle.

Un dernier point à aborder dans cette définition doit nécessairement passer par la dénomination de cette structure. La tVTA est également connu sous le nom de noyau rostromédial du tegmentum (RMTg). Nous savons aujourd'hui que ces deux noms rapportent à la même structure au regard de la neurochimie et de la connectivité (Jhou et al., 2009b; Kaufling et al., 2009). La notion de tVTA réfère à la particularité de cette structure d'être en partie insérée dans la VTA et propose donc une vue antéro-postérieure de la structure. D'un autre côté, la notion de RMTg réfère au fait que la dernière partie de la tVTA s'étends vers le noyau pédonculopontin et présentent des homologies avec les structures tegmentales, proposant donc une vision plus postérieure de la tVTA (Bourdy and Barrot, 2012). Même si les deux définitions se valent, il semblerait que la notion de RMTg soit désormais adoptée dans les publications récentes concernant cette structure.

En conclusion, il semblerait que la meilleure définition de la tVTA et d'une structure cérébrale en générale, nécessite de prendre en compte, non pas une, mais plusieurs caractéristiques de cette structure.

B. La lésion de la tVTA, un bon modèle ?

b1. La lésion, une méthode irréversible

Dans notre étude, nous avons évalué l'influence d'une lésion bilatérale de la tVTA sur les symptômes de la maladie de Parkinson. Une des premières méthodes utilisées pour réaliser une lésion d'une structure cérébrale est la lésion électrolytique. Elle consiste en l'introduction d'une électrode dans la structure d'intérêt et en la destruction du tissu cérébral au niveau de la pointe de l'électrode (Olds and Olds, 1969). Cependant, pour la tVTA, cette méthode ne serait pas appropriée au vu de la présence des fibres de passage de la décussation du pédoncule cérébelleux supérieur. La lésion de la tVTA par l'acide iboténique semblait alors être une approche intéressante puisqu'elle évite la destruction des fibres de passage et avait déjà été menée dans l'équipe pour montrer l'implication de la tVTA dans le contrôle des neurones de la voie nigrostriée (Bourdy et al., 2014). L'injection intra-cérébrale d'acide iboténique entraîne la destruction des corps cellulaires des neurones (Schwarcz et al., 1979) par un mécanisme d'excitotoxicité, c'est-à-dire causé par l'activation des récepteurs des acides aminés excitateurs (Beal, 1992). L'injection d'acide iboténique, comme celle des acides kainique ou quinolinique, entraine l'activation excessive des récepteurs du glutamate, conduisant à la nécrose ou l'apoptose des cellules neuronales (Döbrössy et al., 2011). Mais cette méthode possède de nombreux inconvénients. Tout d'abord, elle est irréversible, empêchant son utilisation dans un potentiel modèle thérapeutique. Deuxièmement, elle reste peu spécifique puisqu'elle concerne potentiellement tous les neurones possédant des récepteurs du glutamate. Ainsi, la VTA risque par sa grande proximité avec la tVTA d'être également fortement lésée. Une étude a utilisé la dermorphine-saporine pour léser la tVTA (Fu et al., 2016). La dermorphine-saporine est une protéine chimérique obtenue à partir de la fusion de la dermorphine, un agoniste du récepteur μ des opioïdes, et de la saporine, une toxine issue de la plante *Saponaria officinalis*, permettant ainsi une destruction spécifique des neurones exprimant le récepteur μ des opioïdes. Cependant et comme lors de l'utilisation de l'acide iboténique, cette méthode reste irréversible et peut entrainer la destruction de neurones de la VTA, contenant eux aussi des récepteurs μ des opioïdes dans les neurones GABAergiques des noyaux parabrachial pigmentosus et paranigral (Sesack and Pickel, 1995; Garzón and Pickel, 2002).

b2. Vers une méthode réversible

De nombreuses méthodes permettent aujourd'hui d'obtenir une inhibition réversible d'une structure. Une première méthode consiste à diminuer localement la température de la structure. La « cryoloop » est une des méthodes utilisées pour inhiber une structure par le froid. Elle nécessite l'utilisation d'un tube hypodermique en acier inoxydable rempli de méthanol permettant ainsi de réduire la température de la structure jusqu'à 20°C ou moins, induisant la complète inhibition de celle-ci (Lomber et al., 1999; Long and Fee, 2008; Coomber et al., 2011). Ces méthodes utilisant le froid sont réversibles, peuvent être contrôlées et ont une fenêtre d'inactivation de l'ordre de quelques minutes (Lomber, 1999). Néanmoins, cette méthode, très utilisée pour l'étude de structures corticales, semblent peu appropriée pour l'étude de structures plus profondes puisqu'elle nécessite l'introduction d'un tube dont le refroidissement se fait de manière constante sur toute sa longueur et sera donc peu spécifique.

Une autre méthode très utilisée consiste à réaliser une inactivation réversible à l'aide de substances chimiques comme la lidocaïne ou à l'aide d'agonistes des récepteurs GABA-A et GABA-B, le baclofen et le muscimol respectivement (Lomber, 1999). La complète récupération suivant cette méthode peut prendre de 15 minutes à plusieurs heures selon le protocole d'administration (Lomber, 1999). L'inhibition par le muscimol a souvent été utilisée pour l'étude de la tVTA (Jalabert et al., 2011; Stopper et al., 2014; Huff and LaLumiere, 2015; Kaufling and Aston-Jones, 2015) mais garde l'inconvénient majeur d'être peu sélective au vu de la possible diffusion de ces agents dans les structures voisines de la tVTA et notamment la VTA. Concernant l'utilisation de lidocaïne, son action sur les canaux ioniques pourrait entraîner des inhibitions aspécifiques, notamment des fibres de passage du pédoncule cérébelleux supérieur et reste donc peu adaptée aux études concernant la tVTA.

L'optogénétique est une méthode plus récente basée sur l'introduction de vecteurs viraux contenant des gènes codant pour des opsines, protéines sensibles à la lumière et capables d'exciter ou d'inhiber les neurones dans lesquels elle sont exprimées (Aston-Jones and Deisseroth, 2013). L'archéorhodopsine et l'archéorhodopsine T répondent à un pulse de lumière jaune ou vert en pompant des protons en dehors de la cellule, entraînant une hyperpolarisation de la cellule ainsi qu'une modification de son pH cellulaire (El-Gaby et al., 2016). L'halorodospine, quant à elle, répond à un pulse de lumière jaune et laisse alors passer les ions Cl^-, entraînant une hyperpolarisation de la cellule qui l'exprime et donc son inhibition (Aston-Jones and Deisseroth, 2013) (Figure 14A). Cette méthode a déjà fait ses preuves dans

A. Méthode optogénétique

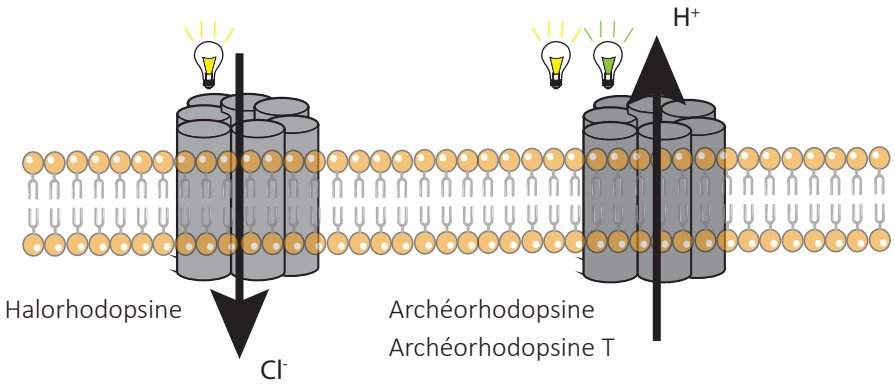

B. DREADD & κ-DREADDκ-DREADD

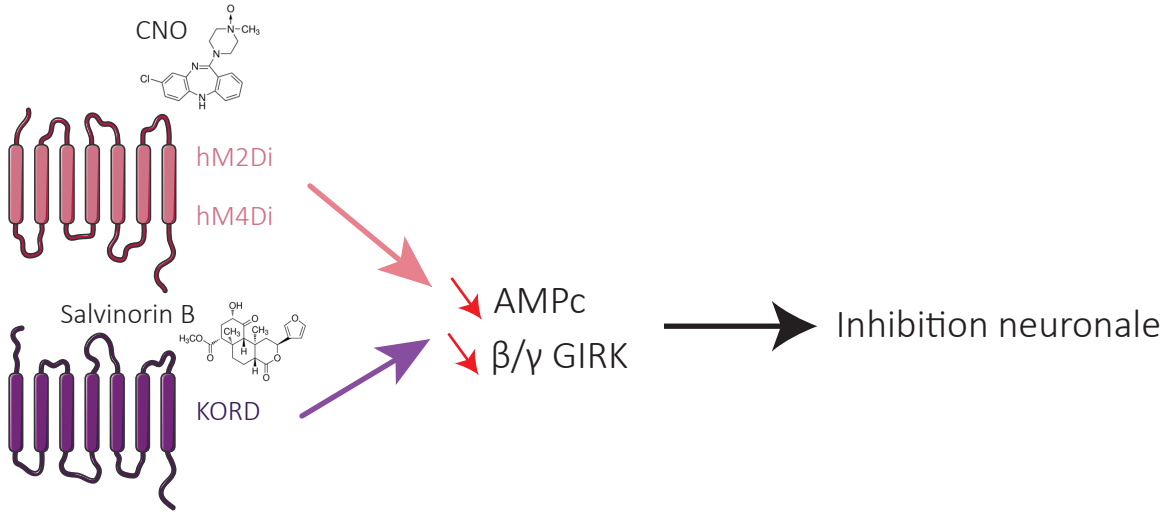

C. Stimulation cérébrale profonde

c1

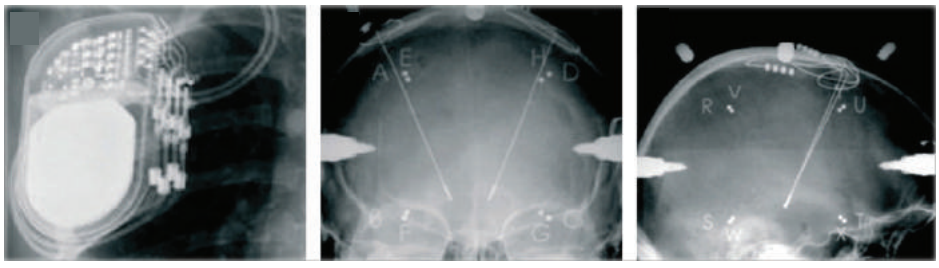

c2

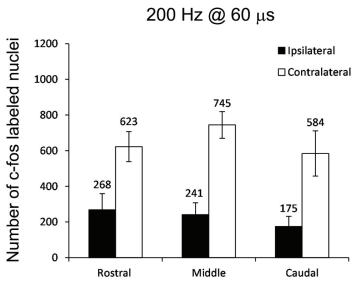

Figure 14. Vers une méthode d'inhibition réversible ? (A) L'optogénétique permet, après introduction de gènes codant pour l'halorhodopsine ou l'archéorhodopsine qui sont des canaux transmembranaires sensibles à la lumière, d'inhiber la cellule qui l'exprime (adapté de Aston-Jones & Deisseroth, 2013). (B) Le DREADD pour Designer Receptor Exclusively Activated by Designer Drug est une méthode d'inhibition utilisant des récépteurs muscariniques modifiés activables uniquement par la fixation de la Clozapine-N-Oxyde, un composé inerte et non présent dans l'organisme. Le κ-DREADD utilise, quant à lui, des récepteurs κ des opioïdes modifiés et activables uniquement par l'administration de Salvinorine B. Ces deux méthodes entraîne une inhibition du neurone qui exprime ces récepteurs (adapté de Roth, 2016). (C) La stimulation cérébrale profonde est utilisée chez l'homme pour traiter les symptômes moteurs de la maladie de Parkinson. (c1) Des électrodes sont implantées dans les noyaux sous-thalamiques et la stimulation à une fréquence de 130 Hz permet l'inhibition de ces noyaux (Benabid et al., 2009). (c2) Chez le rat, la stimulation cérébrale profonde des noyaux sous-thalamique à 200 Hz pendant 60 µs diminue la production de Fos localement (Shehab et al., 2018).

l'étude des fonctions de la tVTA (Jhou et al., 2013; Vento et al., 2017). Il est néanmoins important de prendre en compte que cette méthode ne peut être utilisée que pour de brèves inactivations et qu'elle nécessite une forte illumination, pouvant modifier le volume des structures cérébrales dus au risque de surchauffe et de lésions qu'entraine l'utilisation des lasers (Wiegert et al., 2017). De plus, comme précédemment, la situation anatomique de la tVTA rend difficile la transfection de cette structure.

La technique chemogénétique du DREADD *pour Designer Receptor Exclusively Activated by Designer Drug* utilise des récepteurs muscariniques humains modifiés (hMR), non activés par l'acetylcholine (*i.e.* leur ligand endogène) mais activés par un composé pharmacologiquement inactif et non présent *in vivo*, la clozapine-N-oxide (CNO) (Armbruster et al., 2007). Les récepteurs muscariniques, de la famille des récepteurs couplés aux protéines G (GPCR), peuvent être couplés à des protéines G activatrices (Gq) ou inhibitrices (Gi), résultant en une activation ou une inhibition neuronale après administration de CNO (Armbruster et al., 2007; Roth, 2016). La fixation du CNO sur les récepteurs modifiés hM2Di et hM4Di entraine une hyperpolarisation du neurone et donc son inhibition (Roth, 2016) (Figure 14B). Néanmoins, des études récentes ont montré que le CNO ne passait pas la barrière hématoencéphalique, pouvait se fixer sur d'autres récepteurs que les récepteurs muscariniques modifiés et était converti en clozapine, induisant de nombreux effets secondaires (Gomez et al., 2017; Manvich et al., 2018). Afin de s'affranchir des problèmes liés à l'utilisation du CNO, un autre modèle de DREADD peut être utilisé : le κ-DREADD. En utilisant un récepteur κ des opioïdes modifié (KORD), Vardy et collaborateurs ont ainsi créé un nouveau récepteur inhibiteur activé uniquement par la salvinorine B, un composé inerte *in vivo* (Vardy et al., 2015) et permettant de réaliser des études comportementales comme la mesure de l'activité locomotrice (Marchant et al., 2016) (Figure 14B). J'ai tenté de mettre en place cette méthode durant ma thèse, sans résultat concluant. En effet et comme pour toutes les méthodes citées précédemment et nécessitant une transfection virale, la première difficulté a été de transfecter spécifiquement la tVTA. La deuxième difficulté concernait l'administration de salvinorine-B puisque cette molécule, insoluble dans le NaCl, a dû être diluée dans du DMSO à forte concentration et a entraîné des nécroses au niveau des sites d'injection sous-cutanés. Cependant, nous savons aujourd'hui qu'il est possible d'administrer la salvinorine-B par eau de boisson et nous pourrions donc envisager un nouvel essai en κ-DREADD.

La stimulation cérébrale profonde (DBS pour *deep brain stimulation* en anglais) est une technique très utilisée dans le traitement des symptômes moteurs de la maladie de Parkinson.

Elle consiste, le plus souvent, en la stimulation du noyau sous-thalamique à une fréquence très élevée (130 Hz) conduisant à l'inhibition de ce noyau et résultant en une récupération motrice identique à celle observée lors de l'ablation de ce noyau dans des modèles précliniques (Miller and DeLong, 1987; Bergman et al., 1990; Filion and Tremblay, 1991; Benabid et al., 1994; Limousin et al., 1995) (Figure 14C). Nous pourrions imaginer implémenter cette méthode dans notre modèle pour inhiber la tVTA. Cette méthode, bien caractérisée chez le rat (Shehab et al., 2018) et ayant déjà été utilisée dans une étude sur la tVTA (Melse et al., 2016) (Figure 14C), aurait l'avantage de s'affranchir d'une injection dans la tVTA et donc d'éviter les risques de contamination discutés précédemment, même si le problème des fibres du pédoncule cérebelleux supérieur reste toujours présent. Cette méthode réversible ne nécessite aucun traitement particulier afin d'être activée et permet une étude comparative sur le même animal, réduisant également le besoin en animaux.

En conclusion, nous pouvons dire qu'il n'existe actuellement aucune méthode ne présentant que des avantages. Une perspective à plus long terme serait d'utiliser les résultats que nous avons obtenus lors de notre étude de séquençage d'ARN et donc de créer une lignée de rats transgéniques en utilisant le marqueur *Sox14*. En utilisant le système de la CRE recombinase, nous pourrions créer un modèle de knock-out conditionnel pour le marqueur Sox14 et donc inhiber spécifiquement une population neuronale de la tVTA. Nous aurions alors une méthode plus spécifique.

C. Place de la tVTA dans l'évolution

L'étude de l'évolution des structures cérébrales est compliquée. En effet, l'absence d'accès aux données fossiles, aux ancêtres et aux différentes étapes évolutives fait que l'analyse de l'évolution des structures cérébrales n'est fondée que sur des déductions faites à partir des espèces vivantes actuelles. Comme je l'ai indiqué dans la première partie de cette discussion, les structures cérébrales peuvent être définies par leur neurochimie et par leur connectivité. Dans le cadre de l'étude de leur évolution, il est néanmoins difficile de se baser sur les données neurochimiques tant celles-ci sont susceptibles de varier à travers les espèces et donc à travers l'évolution. Le but de l'étude de l'évolution d'une structure cérébrale étant plutôt de rechercher des fonctions communes, le critère le plus souvent utilisé est donc celui de la connectivité. Ainsi, pour étudier l'évolution, nous allons rechercher chez des espèces actuelles les structures ayant une connectivité similaire et une localisation proche afin de formuler des hypothèses quant à leur homologie.

La VTA est souvent décrite, en accord avec la nomenclature de Dahlstrom and Fuxe (1964), comme appartenant au groupe A10 dopaminergique diencéphalo-mésencéphalique. Les études portant sur l'évolution de la VTA à travers les espèces se fondent sur la connectivité spécifique de cette structure avec le noyau accumbens afin de trouver des homologies (Yamamoto and Vernier, 2011). Ainsi la VTA telle que décrite chez les rongeurs se retrouve chez d'autres membres de la classe des synapsides comme les primates non-humain et l'Homme (Oades and Halliday, 1987). La VTA se retrouve également avec une configuration similaire chez les oiseaux et les reptiles appartenant à la classe des sauropsides (Oades and Halliday, 1987; Yamamoto and Vernier, 2011) (Figure 15A). Chez les amphibiens, un équivalent de la voie mésolimbique des amniotes (*i.e.* de la VTA au noyau accumbens) a été identifié mais avec une localisation un peu différente. En effet, ce groupe de neurones dopaminergiques présente une localisation plus rostrale, la plupart étant localisés dans des régions diencéphaliques (Yamamoto and Vernier, 2011). Concernant les téléostéens et la lamproie, considérée comme le vertébré actuel le plus basal, des différences dans la localisation et la dénomination de la VTA apparaissent. En effet, le terme de VTA ou d'aire A10 dopaminergique n'existe pas chez ces espèces (Yamamoto and Vernier, 2011). En revanche, on retrouve une structure analogue aux aires A9/A10 dopaminergiques au niveau du noyau du tubercule postérieur (Reiner et al., 1998; Pérez-Fernández et al., 2014) (Figure 15B), lui-même constitué de deux populations neuronales différentes : l'aire tegmentale localisée en avant du noyau interpédonculaire, et un noyau présentant des homologies avec la substance noire et situé autour du noyau rouge (Yamamoto and Vernier, 2011). Cette analogie du noyau du tubercule postérieur avec les aires A9 et A10 des mammifères se fonde sur des études hodologiques et des études développementales montrant une ontogénie similaire du noyau du tubercule postérieur avec celle du tegmentum chez les amniotes (Reiner et al., 1998) (Figure 15C). Ainsi il semblerait que la VTA soit une synapomorphie (*i.e.* un caractère dérivé) des vertébrés qui a été conservée dans l'ensemble du clade, de la lamproie à l'Homme. Il me parait donc possible d'imaginer que si la VTA est un caractère partagé par toutes ces espèces, alors la tVTA, structure contrôlant l'activité de ces neurones dopaminergiques, pourrait également être partagée par ces différents groupes évolutifs.

Cette hypothèse semble être confirmée par la littérature actuelle. Le groupe de Grillner a ainsi montré en 2012 que la région mamillaire dorsale (dMAM) de la lamproie présentait de fortes homologies avec la tVTA telle que nous la connaissons. En effet, la dMAM est composée en majorité par des neurones GABAergiques (Figure 16A), reçoit des projections issues des

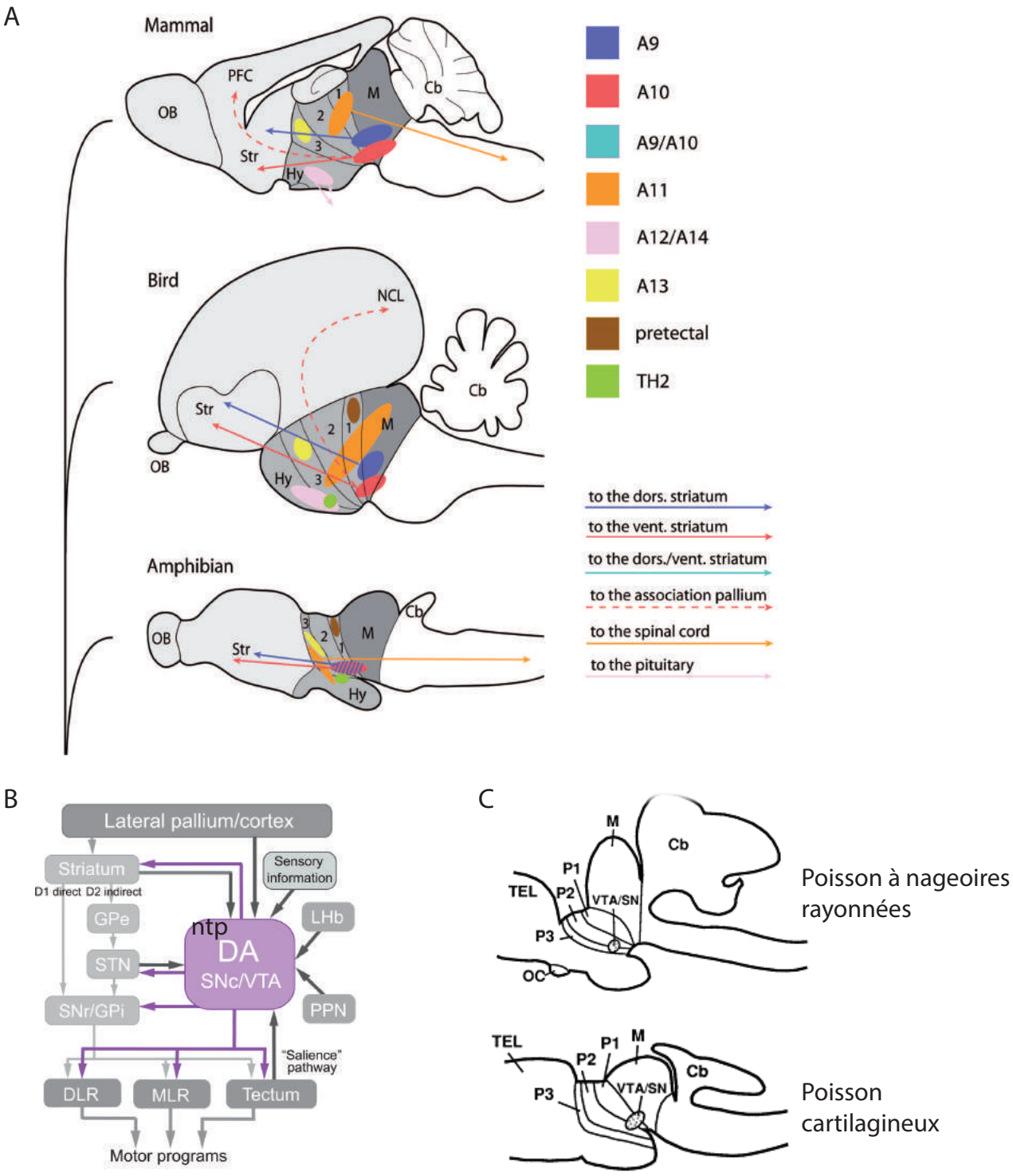

Figure 15. Les neurones dopaminergiques durant l'évolution. (A) La vue sagittale d'un cerveau de mammifère (souris), d'oiseau (poulet) et d'amphibien (grenouille) permet de mettre en évidence des concordances dans la localisation et la connectivité des neurones des aires A9 (SNc) et A10 (VTA) dopaminergiques (Yamamoto & Vernier, 2011). (B) Chez la lamproie, présentée comme le vertébré le plus ancien, il n'existe pas de réelle concordance avec les aires A9 et A10 présentes chez les autres espèces (Yamamoto &Vernier, 2011). Néanmoins, des études de connectivité ont montré une équivalence entre le noyau du tubercule postérieur et la VTA/SNc (Pérez-Fernandez et al., 2014). (C) Evidence de la présence de structures analogues à la VTA/SNc chez deux classes d'anamniotes, les poissons à nageoires rayonnées (poissons osseux) et les poissons cartilagineux (requin) (Reiner et al., 1998).

noyaux dorsal droit et ventral droit de l'habénula, analogues de la LHb (Figure 16B); et projette au noyau du tubercule postérieur (Figure 16C). L'homologie se situe même au niveau de la localisation de la dMAM, puisque chez la lamproie cette région présente une localisation homologue à la localisation connue de la tVTA le rat, c'est-à-dire juste à côté des neurones dopaminergiques (Stephenson-Jones et al., 2012; Robertson et al., 2014). Concernant les mammifères, il semblerait que la tVTA présente une certaine stabilité neurochimique, hodologique et fonctionnelle. C'est ainsi le cas pour la souris, puisque de nombreuses études montrent une neurochimie (Maroteaux and Mameli, 2012), une connectivité (Quina et al., 2015; Tooley et al., 2018) et des aspects fonctionnels (Stamatakis and Stuber, 2012; Wasserman et al., 2016; Steidl et al., 2017) identiques à ceux définis chez le rat bien que la tVTA de la souris ne semble pas présenter la même sensibilité aux psychostimulants que celle du rat. De même, chez le macaque rhésus, la tVTA putative présente une homologie de localisation et de fonction avec la tVTA telle que définie chez le rat (Hong et al., 2011). Ces similarités de la tVTA à travers des espèces très proches d'un point de vue évolutif laissent ainsi penser que la tVTA est une structure présentant une stabilité à travers les vertébrés. Toutefois, ses contours restent encore à définir dans l'ensemble de ces espèces.

Cette présence de la tVTA depuis le vertébré le plus basal jusqu'au primate non-humain nous fait nous questionner sur la présence de la tVTA chez l'Homme. Une étude d'imagerie fonctionnelle n'a pas permis de mettre en évidence un groupe de cellules répondant aux erreurs de prédiction de récompense et pouvant ainsi correspondre à la tVTA (Ide and Li, 2011). Cependant, la tVTA étant en premier lieu connue comme intervenant dans la réponse aux drogues psychostimulantes, des expériences pourraient être imaginées pour vérifier sa présence chez l'Homme. Le modafinil est un médicament prescrit pour le traitement de la somnolence dans les états de narcolepsie chez l'Homme. Son administration chez le rat entraine l'expression de Fos localement (Scammell et al., 2000), reflétant ainsi le recrutement de la tVTA. Nous pourrions donc imaginer un protocole d'IRM fonctionnelle dans lequel nous comparerions l'activité cérébrale d'individus contrôles et d'individus narcoleptiques sous traitement afin de mettre en évidence des structures répondant aux traitements et ayant des caractéristiques proches de la tVTA chez le rat. Une deuxième possibilité serait de se baser sur les résultats de notre étude génomique. L'analyse en séquençage d'ARN nous a permis de mettre en évidence un certain nombre de gènes assez spécifiques de cette structure. Ainsi, le gène *Sox14* est enrichi dans la tVTA chez le rat et a été montré dans la littérature comme présent chez la souris (Lahti et al., 2016). Il pourrait donc nous servir afin de rechercher la présence de la tVTA chez diverses

A. Les neurones de la dMAM sont en majorité GABAergiques

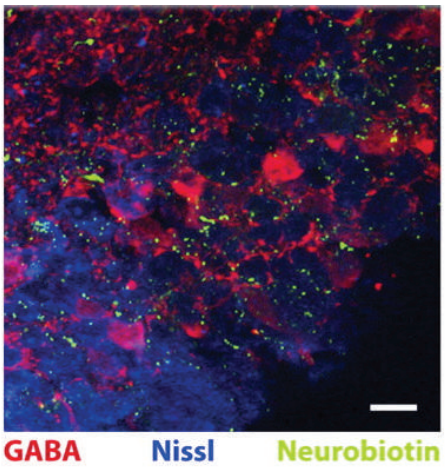

B. Projections des noyaux dorsaux et ventraux droits de l'habénula vers la dMAM

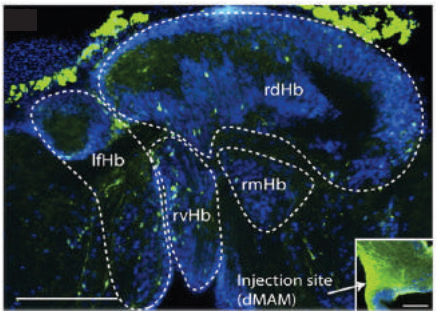

B. Projections de la dMAM vers le tubercule postérieur

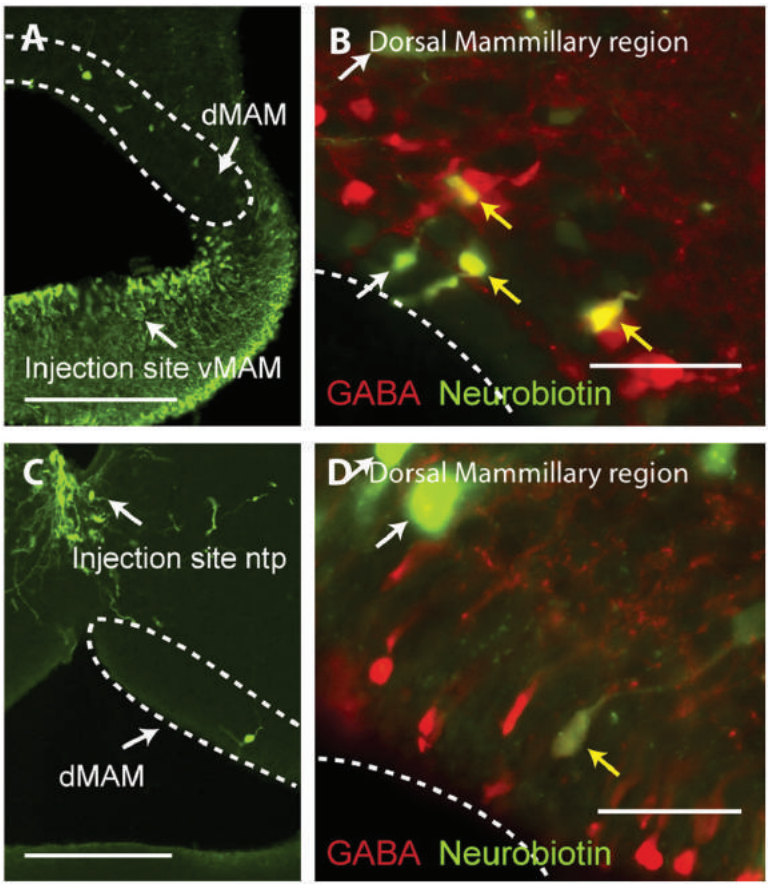

Figure 16. Evidence d'une homologie entre la région mammilaire dorsale (dMAM) des lamproies et la tVTA chez le rongeur. (A) La dMAM, comme la tVTA, est constituée en majorité par des neurones GABAergiques. (B) Elle reçoit des afférences des noyaux dorsaux et ventraux droits de l'habénula, analogues de la LHb chez les amniotes. (C) La dMAM projette aux neurones dopaminergiques du tubercule postérieur, homologue de la VTA/SNc chez les amniotes (Stephenson-Jones et al., 2012).

espèces animales et également sur des cerveaux *post-mortem* humains. De même, FoxP1 semble aussi être un candidat intéressant pour réaliser une analyse ontogénique de la tVTA. En effet, des données récentes de la littérature ont montré qu'il était présent chez la souris durant le développement de cette structure (Lahti et al., 2016; Polter et al., 2018). Il reste donc encore de nombreuses interrogations concernant la place de la tVTA à travers l'ontogénie et la phylogénie. Un des grands enjeux sera de mettre en place des méthodes pour aboutir à une caractérisation de la tVTA à travers différentes espèces de mammifères et jusqu'à l'Homme.

BIBLIOGRAPHIE

Araki M, McGeer PL, Kimura H (1988) The efferent projections of the rat lateral habenular nucleus revealed by the PHA-L anterograde tracing method. Brain Res 441:319–330.

Armbruster BN, Li X, Pausch MH, Herlitze S, Roth BL (2007) Evolving the lock to fit the key to create a family of G protein-coupled receptors potently activated by an inert ligand. Proc Natl Acad Sci U S A 104:5163–5168.

Aston-Jones G, Deisseroth K (2013) Recent advances in optogenetics and pharmacogenetics. Brain Res 1511:1–5.

Balcita-Pedicino JJ, Omelchenko N, Bell R, Sesack SR (2011) The inhibitory influence of the lateral habenula on midbrain dopamine cells: ultrastructural evidence for indirect mediation via the rostromedial mesopontine tegmental nucleus. J Comp Neurol 519:1143–1164.

Barrot M, Georges F, Veinante P (2016) Chapter25. The Tail of the Ventral Tegmental Area/ Rostromedial Tegmental Nucleus: A Modulator of Midbrain Dopamine Systems. In: Handbook of Basal Ganglia Structure and Function, pp 495–511. Academic Press.

Barrot M, Sesack SR, Georges F, Pistis M, Hong S, Jhou TC (2012) Braking dopamine systems: a new GABA master structure for mesolimbic and nigrostriatal functions. J Neurosci 32:14094–14101.

Beal MF (1992) Mechanisms of excitotoxicity in neurologic diseases. FASEB J Off Publ Fed Am Soc Exp Biol 6:3338–3344.

Benabid AL, Chabardes S, Mitrofanis J, Pollak P (2009) Deep brain stimulation of the subthalamic nucleus for the treatment of Parkinson’s disease. Lancet Neurol 8:67–81.

Benabid AL, Pollak P, Gross C, Hoffmann D, Benazzouz A, Gao DM, Laurent A, Gentil M, Perret J (1994) Acute and long-term effects of subthalamic nucleus stimulation in Parkinson’s disease. Stereotact Funct Neurosurg 62:76–84.

Bergman H, Wichmann T, DeLong MR (1990) Reversal of experimental parkinsonism by lesions of the subthalamic nucleus. Science 249:1436–1438.

Björklund A, Dunnett SB (2007) Dopamine neuron systems in the brain: an update. Trends Neurosci 30:194–202.

Bourdy R, Barrot M (2012) A new control center for dopaminergic systems: pulling the VTA by the tail. Trends Neurosci 35:681–690.

Bourdy R, Sánchez-Catalán M-J, Kaufling J, Balcita-Pedicino JJ, Freund-Mercier M-J, Veinante P, Sesack SR, Georges F, Barrot M (2014) Control of the nigrostriatal dopamine neuron activity and motor function by the tail of the ventral tegmental area. Neuropsychopharmacology 39:2788–2798.

Brodmann K (1909) Vergleichende Lokalisationslehre der Großhirnrinde in ihren Prinzipien dargestellt auf Grund des Zellenbaues.

Bromberg-Martin ES, Matsumoto M, Hikosaka O (2010) Dopamine in motivational control: rewarding, aversive, and alerting. Neuron 68:815–834.

Broms J, Antolin-Fontes B, Tingström A, Ibañez-Tallon I (2015) Conserved expression of the GPR151 receptor in habenular axonal projections of vertebrates. J Comp Neurol 523:359–380.

Brown PL, Shepard PD (2013) Lesions of the fasciculus retroflexus alter footshock-induced cFos expression in the mesopontine rostromedial tegmental area of rats. PloS One 8:e60678.

Chaudhuri KR, Healy DG, Schapira AHV, National Institute for Clinical Excellence (2006) Non-motor symptoms of Parkinson's disease: diagnosis and management. Lancet Neurol 5:235–245.

Colussi-Mas J, Geisler S, Zimmer L, Zahm DS, Bérod A (2007) Activation of afferents to the ventral tegmental area in response to acute amphetamine: a double-labelling study. Eur J Neurosci 26:1011–1025.

Coomber B, Edwards D, Jones SJ, Shackleton TM, Goldschmidt J, Wallace MN, Palmer AR (2011) Cortical inactivation by cooling in small animals. Front Syst Neurosci 5:53.

Dahlström A, Fuxe K (1964) Localization of monoamines in the lower brain stem. Experientia 20:398–399.

Döbrössy MD, Büchele F, Nikkhah G (2011) Excitotoxic Lesions of the Rodent Striatum. In: Animal Models of Movement Disorders, pp 21–35 Neuromethods. Available at: https://link.springer.com/protocol/10.1007/978-1-61779-301-1_2.

Dronkers NF, Plaisant O, Iba-Zizen MT, Cabanis EA (2007) Paul Broca's historic cases: high resolution MR imaging of the brains of Leborgne and Lelong. Brain J Neurol 130:1432–1441.

Dudman JT, Gerfen CR (2015) Chapter 17. The Basal Ganglia. In: The Rat Nervous System, 4th ed., pp 391–440.

El-Gaby M, Zhang Y, Wolf K, Schwiening CJ, Paulsen O, Shipton OA (2016) Archaerhodopsin Selectively and Reversibly Silences Synaptic Transmission through Altered pH. Cell Rep 16:2259–2268.

Filion M, Tremblay L (1991) Abnormal spontaneous activity of globus pallidus neurons in monkeys with MPTP-induced parkinsonism. Brain Res 547:142–151.

Fu R, Chen X, Zuo W, Li J, Kang S, Zhou L-H, Siegel A, Bekker A, Ye J-H (2016) Ablation of μ opioid receptor-expressing GABA neurons in rostromedial tegmental nucleus increases

ethanol consumption and regulates ethanol-related behaviors. Neuropharmacology 107:58–67.

Garzón M, Pickel VM (2002) Ultrastructural localization of enkephalin and mu-opioid receptors in the rat ventral tegmental area. Neuroscience 114:461–474.

Geisler S, Marinelli M, Degarmo B, Becker ML, Freiman AJ, Beales M, Meredith GE, Zahm DS (2008) Prominent activation of brainstem and pallidal afferents of the ventral tegmental area by cocaine. Neuropsychopharmacology 33:2688–2700.

Gerfen CR (1984) The neostriatal mosaic: compartmentalization of corticostriatal input and striatonigral output systems. Nature 311:461–464.

Gerfen CR (1985) The neostriatal mosaic. I. Compartmental organization of projections from the striatum to the substantia nigra in the rat. J Comp Neurol 236:454–476.

Gomez JL, Bonaventura J, Lesniak W, Mathews WB, Sysa-Shah P, Rodriguez LA, Ellis RJ, Richie CT, Harvey BK, Dannals RF, Pomper MG, Bonci A, Michaelides M (2017) Chemogenetics revealed: DREADD occupancy and activation via converted clozapine. Science 357:503–507.

Graybiel AM, Ragsdale CW (1978) Histochemically distinct compartments in the striatum of human, monkeys, and cat demonstrated by acetylthiocholinesterase staining. Proc Natl Acad Sci U S A 75:5723–5726.

Gross CG (2007) The discovery of motor cortex and its background. J Hist Neurosci 16:320–331.

Herkenham M, Edley SM, Stuart J (1984) Cell clusters in the nucleus accumbens of the rat, and the mosaic relationship of opiate receptors, acetylcholinesterase and subcortical afferent terminations. Neuroscience 11:561–593.

Herkenham M, Nauta WJ (1979) Efferent connections of the habenular nuclei in the rat. J Comp Neurol 187:19–47.

Herkenham M, Pert CB (1981) Mosaic distribution of opiate receptors, parafascicular projections and acetylcholinesterase in rat striatum. Nature 291:415–418.

Hnasko TS, Hjelmstad GO, Fields HL, Edwards RH (2012) Ventral tegmental area glutamate neurons: electrophysiological properties and projections. J Neurosci 32:15076–15085.

Hong S, Jhou TC, Smith M, Saleem KS, Hikosaka O (2011) Negative reward signals from the lateral habenula to dopamine neurons are mediated by rostromedial tegmental nucleus in primates. J Neurosci 31:11457–11471.

Huff ML, LaLumiere RT (2015) The rostromedial tegmental nucleus modulates behavioral inhibition following cocaine self-administration in rats. Neuropsychopharmacology 40:861–873.

Ide JS, Li C-SR (2011) Error-related functional connectivity of the habenula in humans. Front Hum Neurosci 5:25.

Ikemoto S (2007) Dopamine reward circuitry: two projection systems from the ventral midbrain to the nucleus accumbens-olfactory tubercle complex. Brain Res Rev 56:27–78.

Jalabert M, Bourdy R, Courtin J, Veinante P, Manzoni OJ, Barrot M, Georges F (2011) Neuronal circuits underlying acute morphine action on dopamine neurons. Proc Natl Acad Sci U S A 108:16446–16450.

Jhou T (2005) Neural mechanisms of freezing and passive aversive behaviors. J Comp Neurol 493:111–114.

Jhou TC, Fields HL, Baxter MG, Saper CB, Holland PC (2009a) The rostromedial tegmental nucleus (RMTg), a GABAergic afferent to midbrain dopamine neurons, encodes aversive stimuli and inhibits motor responses. Neuron 61:786–800.

Jhou TC, Geisler S, Marinelli M, Degarmo BA, Zahm DS (2009b) The mesopontine rostromedial tegmental nucleus: A structure targeted by the lateral habenula that projects to the ventral tegmental area of Tsai and substantia nigra compacta. J Comp Neurol 513:566–596.

Jhou TC, Good CH, Rowley CS, Xu S-P, Wang H, Burnham NW, Hoffman AF, Lupica CR, Ikemoto S (2013) Cocaine drives aversive conditioning via delayed activation of dopamine-responsive habenular and midbrain pathways. J Neurosci 33:7501–7512.

Jhou TC, Xu S-P, Lee MR, Gallen CL, Ikemoto S (2012) Mapping of reinforcing and analgesic effects of the mu opioid agonist endomorphin-1 in the ventral midbrain of the rat. Psychopharmacology (Berl) 224:303–312.

Jiménez-Castellanos J, Graybiel AM (1989) Compartmental origins of striatal efferent projections in the cat. Neuroscience 32:297–321.

Kádár A, Wittmann G, Liposits Z, Fekete C (2009) Improved method for combination of immunocytochemistry and Nissl staining. J Neurosci Methods 184:115–118.

Kang HW, Kim HK, Moon BH, Lee SJ, Lee SJ, Rhyu IJ (2017) Comprehensive Review of Golgi Staining Methods for Nervous Tissue. Appl Microsc 47:63–69.

Kaufling J, Aston-Jones G (2015) Persistent Adaptations in Afferents to Ventral Tegmental Dopamine Neurons after Opiate Withdrawal. J Neurosci 35:10290–10303.

Kaufling J, Veinante P, Pawlowski SA, Freund-Mercier M-J, Barrot M (2009) Afferents to the GABAergic tail of the ventral tegmental area in the rat. J Comp Neurol 513:597–621.

Kaufling J, Veinante P, Pawlowski SA, Freund-Mercier M-J, Barrot M (2010a) gamma-Aminobutyric acid cells with cocaine-induced DeltaFosB in the ventral tegmental area innervate mesolimbic neurons. Biol Psychiatry 67:88–92.

Kaufling J, Waltisperger E, Bourdy R, Valera A, Veinante P, Freund-Mercier M-J, Barrot M (2010b) Pharmacological recruitment of the GABAergic tail of the ventral tegmental area by acute drug exposure. Br J Pharmacol 161:1677–1691.

Kim U (2009) Topographic commissural and descending projections of the habenula in the rat. J Comp Neurol 513:173–187.

Korotkova TM, Ponomarenko AA, Haas HL, Sergeeva OA (2005) Differential expression of the homeobox gene Pitx3 in midbrain dopaminergic neurons. Eur J Neurosci 22:1287–1293.

Lahti L, Haugas M, Tikker L, Airavaara M, Voutilainen MH, Anttila J, Kumar S, Inkinen C, Salminen M, Partanen J (2016) Differentiation and molecular heterogeneity of inhibitory and excitatory neurons associated with midbrain dopaminergic nuclei. Dev Camb Engl 143:516–529.

Lecca S, Melis M, Luchicchi A, Ennas MG, Castelli MP, Muntoni AL, Pistis M (2011) Effects of drugs of abuse on putative rostromedial tegmental neurons, inhibitory afferents to midbrain dopamine cells. Neuropsychopharmacology 36:589–602.

Lecca S, Melis M, Luchicchi A, Muntoni AL, Pistis M (2012) Inhibitory inputs from rostromedial tegmental neurons regulate spontaneous activity of midbrain dopamine cells and their responses to drugs of abuse. Neuropsychopharmacology 37:1164–1176.

Limousin P, Pollak P, Benazzouz A, Hoffmann D, Le Bas JF, Broussolle E, Perret JE, Benabid AL (1995) Effect of parkinsonian signs and symptoms of bilateral subthalamic nucleus stimulation. Lancet Lond Engl 345:91–95.

Lomber SG (1999) The advantages and limitations of permanent or reversible deactivation techniques in the assessment of neural function. J Neurosci Methods 86:109–117.

Lomber SG, Payne BR, Horel JA (1999) The cryoloop: an adaptable reversible cooling deactivation method for behavioral or electrophysiological assessment of neural function. J Neurosci Methods 86:179–194.

Long MA, Fee MS (2008) Using temperature to analyse temporal dynamics in the songbird motor pathway. Nature 456:189–194.

Manvich DF, Webster KA, Foster SL, Farrell MS, Ritchie JC, Porter JH, Weinshenker D (2018) The DREADD agonist clozapine N-oxide (CNO) is reverse-metabolized to clozapine and produces clozapine-like interoceptive stimulus effects in rats and mice. Sci Rep 8:3840.

Marchant NJ, Whitaker LR, Bossert JM, Harvey BK, Hope BT, Kaganovsky K, Adhikary S, Prisinzano TE, Vardy E, Roth BL, Shaham Y (2016) Behavioral and Physiological Effects of a Novel Kappa-Opioid Receptor-Based DREADD in Rats. Neuropsychopharmacology 41:402–409.

Maroteaux M, Mameli M (2012) Cocaine evokes projection-specific synaptic plasticity of lateral habenula neurons. J Neurosci 32:12641–12646.

Matsumoto M, Hikosaka O (2007) Lateral habenula as a source of negative reward signals in dopamine neurons. Nature 447:1111–1115.

Melis M, Sagheddu C, De Felice M, Casti A, Madeddu C, Spiga S, Muntoni AL, Mackie K, Marsicano G, Colombo G, Castelli MP, Pistis M (2014) Enhanced endocannabinoid-mediated modulation of rostromedial tegmental nucleus drive onto dopamine neurons in Sardinian alcohol-preferring rats. J Neurosci 34:12716–12724.

Melse M, Temel Y, Tan SK, Jahanshahi A (2016) Deep brain stimulation of the rostromedial tegmental nucleus: An unanticipated, selective effect on food intake. Brain Res Bull 127:23–28.

Miller WC, DeLong MR (1987) Altered Tonic Activity of Neurons in the Globus Pallidus and Subthalamic Nucleus in the Primate MPTP Model of Parkinsonism. In: The Basal Ganglia II, pp 415–427 Advances in Behavioral Biology. Springer, Boston, MA. Available at: https://link.springer.com/chapter/10.1007/978-1-4684-5347-8_29.

Morales M, Margolis EB (2017) Ventral tegmental area: cellular heterogeneity, connectivity and behaviour. Nat Rev Neurosci 18:73–85.

Morales M, Root DH (2014) Glutamate neurons within the midbrain dopamine regions. Neuroscience 282:60–68.

Nauta WJH (1958) Hippocampal Projections and Related Neural Pathways to the Mid-Brain in the Cat. In: Neuroanatomy, pp 117–139 Contemporary Neuroscientists. Birkhäuser, Boston, MA. Available at: https://link.springer.com/chapter/10.1007/978-1-4684-7920-1_9.

Nestler EJ, Barrot M, Self DW (2001) DeltaFosB: a sustained molecular switch for addiction. Proc Natl Acad Sci U S A 98:11042–11046.

Oades RD, Halliday GM (1987) Ventral tegmental (A10) system: neurobiology. 1. Anatomy and connectivity. Brain Res 434:117–165.

Olds ME, Olds J (1969) Effects of lesions in medial forebrain bundle on self-stimulation behavior. Am J Physiol 217:1253–1264.

Olson VG, Nestler EJ (2007) Topographical organization of GABAergic neurons within the ventral tegmental area of the rat. Synap N Y N 61:87–95.

Olson VG, Zabetian CP, Bolanos CA, Edwards S, Barrot M, Eisch AJ, Hughes T, Self DW, Neve RL, Nestler EJ (2005) Regulation of drug reward by cAMP response element-binding protein: evidence for two functionally distinct subregions of the ventral tegmental area. J Neurosci 25:5553–5562.

Pang Y, Kiba H, Jayaraman A (1993) Acute nicotine injections induce c-fos mostly in non-dopaminergic neurons of the midbrain of the rat. Brain Res Mol Brain Res 20:162–170.

Pannese E (1999) The Golgi Stain: invention, diffusion and impact on neurosciences. J Hist Neurosci 8:132–140.

Park A, Stacy M (2009) Non-motor symptoms in Parkinson's disease. J Neurol 256 Suppl 3:293–298.

Paxinos G, Watson C (2014) The Rat Brain in Stereotaxic Coordinates. Academic Press.

Pérez-Fernández J, Stephenson-Jones M, Suryanarayana SM, Robertson B, Grillner S (2014) Evolutionarily conserved organization of the dopaminergic system in lamprey: SNc/VTA afferent and efferent connectivity and D2 receptor expression. J Comp Neurol 522:3775–3794.

Perrotti LI, Bolaños CA, Choi K-H, Russo SJ, Edwards S, Ulery PG, Wallace DL, Self DW, Nestler EJ, Barrot M (2005) DeltaFosB accumulates in a GABAergic cell population in the posterior tail of the ventral tegmental area after psychostimulant treatment. Eur J Neurosci 21:2817–2824.

Polter AM, Barcomb K, Tsuda AC, Kauer JA (2018) Synaptic function and plasticity in identified inhibitory inputs onto VTA dopamine neurons. Eur J Neurosci In press.

Quina LA, Tempest L, Ng L, Harris JA, Ferguson S, Jhou TC, Turner EE (2015) Efferent pathways of the mouse lateral habenula. J Comp Neurol 523:32–60.

Ramon-Y-Cajal S (1909) Histologie du système nerveux de l'homme et des vertébrés.

Reiner A, Medina L, Veenman CL (1998) Structural and functional evolution of the basal ganglia in vertebrates. Brain Res Brain Res Rev 28:235–285.

Robertson B, Kardamakis A, Capantini L, Pérez-Fernández J, Suryanarayana SM, Wallén P, Stephenson-Jones M, Grillner S (2014) The lamprey blueprint of the mammalian nervous system. Prog Brain Res 212:337–349.

Roth BL (2016) DREADDs for Neuroscientists. Neuron 89:683–694.

Sánchez-Catalán M-J, Faivre F, Yalcin I, Muller M-A, Massotte D, Majchrzak M, Barrot M (2017) Response of the Tail of the Ventral Tegmental Area to Aversive Stimuli. Neuropsychopharmacology 42:638–648.

Sanchez-Catalan MJ, Kaufling J, Georges F, Veinante P, Barrot M (2014) The antero-posterior heterogeneity of the ventral tegmental area. Neuroscience 282:198–216.

Scammell TE, Estabrooke IV, McCarthy MT, Chemelli RM, Yanagisawa M, Miller MS, Saper CB (2000) Hypothalamic arousal regions are activated during modafinil-induced wakefulness. J Neurosci 20:8620–8628.

Schwarcz R, Hökfelt T, Fuxe K, Jonsson G, Goldstein M, Terenius L (1979) Ibotenic acid-induced neuronal degeneration: a morphological and neurochemical study. Exp Brain Res 37:199–216.

Sesack SR, Pickel VM (1995) Ultrastructural relationships between terminals immunoreactive for enkephalin, GABA, or both transmitters in the rat ventral tegmental area. Brain Res 672:261–275.

Shehab S, D'souza C, Ljubisavljevic M, Redgrave P (2018) Activation of the subthalamic nucleus suppressed by high frequency stimulation: A c-Fos immunohistochemical study. Brain Res 1685:42–50.

Stamatakis AM, Stuber GD (2012) Activation of lateral habenula inputs to the ventral midbrain promotes behavioral avoidance. Nat Neurosci 15:1105–1107.

Steidl S, Dhillon ES, Sharma N, Ludwig J (2017) Muscarinic cholinergic receptor antagonists in the VTA and RMTg have opposite effects on morphine-induced locomotion in mice. Behav Brain Res 323:111–116.

Stephenson-Jones M, Floros O, Robertson B, Grillner S (2012) Evolutionary conservation of the habenular nuclei and their circuitry controlling the dopamine and 5-hydroxytryptophan (5-HT) systems. Proc Natl Acad Sci U S A 109:E164-173.

Stopper CM, Tse MTL, Montes DR, Wiedman CR, Floresco SB (2014) Overriding phasic dopamine signals redirects action selection during risk/reward decision making. Neuron 84:177–189.

Subramaniam M, Roeper J (2016) Chapter 16. Subtypes of Midbrain Dopamine Neurons. In: Handbook of Basal Ganglia Structure and Function, pp 317–334. Academic Press.

Tian J, Huang R, Cohen JY, Osakada F, Kobak D, Machens CK, Callaway EM, Uchida N, Watabe-Uchida M (2016) Distributed and Mixed Information in Monosynaptic Inputs to Dopamine Neurons. Neuron 91:1374–1389.

Tooley J, Marconi L, Alipio JB, Matikainen-Ankney B, Georgiou P, Kravitz AV, Creed MC (2018) Glutamatergic Ventral Pallidal Neurons Modulate Activity of the Habenula-Tegmental Circuitry and Constrain Reward Seeking. Biol Psychiatry 83:1012–1023.

Tsai C (1925) The optic tracts and centers of the opossum. Didelphis virginiana. J Comp Neurol 39:173–216.

Vardy E et al. (2015) A New DREADD Facilitates the Multiplexed Chemogenetic Interrogation of Behavior. Neuron 86:936–946.

Vento PJ, Burnham NW, Rowley CS, Jhou TC (2017) Learning From One's Mistakes: A Dual Role for the Rostromedial Tegmental Nucleus in the Encoding and Expression of Punished Reward Seeking. Biol Psychiatry 81:1041–1049.

von Economo C, Koskinas GND (1925) Die Cytoarchitektonik der Hirnrinde des erwachsenen Menschen.

Wasserman DI, Tan JMJ, Kim JC, Yeomans JS (2016) Muscarinic control of rostromedial tegmental nucleus GABA neurons and morphine-induced locomotion. Eur J Neurosci 44:1761–1770.

Wiegert JS, Mahn M, Prigge M, Printz Y, Yizhar O (2017) Silencing Neurons: Tools, Applications, and Experimental Constraints. Neuron 95:504–529.

Yamamoto K, Vernier P (2011) The evolution of dopamine systems in chordates. Front Neuroanat 5:21.

Yetnikoff L, Cheng AY, Lavezzi HN, Parsley KP, Zahm DS (2015) Sources of input to the rostromedial tegmental nucleus, ventral tegmental area, and lateral habenula compared: A study in rat. J Comp Neurol 523:2426–2456.

Yetnikoff L, Lavezzi HN, Reichard RA, Zahm DS (2014) An update on the connections of the ventral mesencephalic dopaminergic complex. Neuroscience 282:23–48.

Záborszky L, Alheid GF, Beinfeld MC, Eiden LE, Heimer L, Palkovits M (1985) Cholecystokinin innervation of the ventral striatum: a morphological and radioimmunological study. Neuroscience 14:427–453.

Zahm DS (1999) Functional-anatomical implications of the nucleus accumbens core and shell subterritories. Ann N Y Acad Sci 877:113–128.

Fanny FAIVRE

La queue de l'aire tegmentale ventrale : définition anatomo-moléculaire, implication dans la réponse aux stimuli aversifs et influence sur la voie nigrostriée

Résumé

La queue de l'aire tegmentale ventrale (tVTA) est le principal contrôle inhibiteur des neurones dopaminergiques du mésencéphale. Cette structure, bien qu'aujourd'hui très étudiée, n'est cependant pas encore référencée dans les atlas stéréotaxiques. Anatomiquement, nous avons pu apporter une définition de référence de la tVTA, à travers son analyse neurochimique, stéréologique, hodologique et génomique. Fonctionnellement, nous avons montré son rôle dans la réponse à des expériences émotionnelles aversives et nous avons testé son influence sur les symptômes moteurs et non-moteurs de la maladie de Parkinson. Nous avons ainsi montré qu'une co-lésion de la tVTA dans un modèle murin de la maladie permet une amélioration des performances motrices, des seuils nociceptifs et des symptômes de type dépressifs. Ce travail a ainsi participé au progrès de nos connaissances sur la tVTA et ouvre de nouvelles pistes d'exploration quant à son implication fonctionnelle.

Mots-clés : queue de l'aire tegmentale ventrale, neuroanatomie, aversion, voie nigrostriée, maladie de Parkinson

Abstract

The tail of the ventral tegmental area (tVTA) is the major brake of the midbrain dopamine neurons. This structure although studied, is not yet referenced in stereotaxic atlases. Anatomically, this work allowed to obtain a reference definition of the tVTA through its neurochemical, stereological, connectivity-based and genomic analyses. Functionally, we studied its role for the response of aversive stimuli and we tested its influence on motor and non-motor symptoms of Parkinson's disease. We observed that a co-lesion of the tVTA in a rodent model of this disease induces improvements of motor, nociceptive and depressive-like symptoms. This work has thus contributed to the progress of our knowledge on the tVTA and opens new explorative tracks for its functional implication.

Keywords: tail of the ventral tegmental area, neuroanatomy, aversion, nigrostriatal pathway, Parkinson's disease